# Fuzzy Logic Controller for an Artificial Heart

by

**Vinay Menon**

A thesis submitted to
the Faculty of Graduate Studies and Research
in partial fulfilment of
the requirements for the degree of
**Masters of Engineering**

Ottawa-Carleton Institute for
Mechanical and Aerospace Engineering

Department of
Mechanical and Aerospace Engineering
Carleton University
Ottawa, Ontario
May $12^{th}$, 1998

# Abstract

To provide fixed rate control of an artificial heart a Fuzzy Logic Controller (FLC) was designed with the aid of a mock circulatory system model [1] to test and simulate the controller. The model was ported to Simulink, a three element aorta segment was added and the systemic parameters were tuned to provide better simulation results (transient simulation). The controller is a FLC of the form Single Input and Single Output (SISO) and was designed to maintain pump output at a desired value preset by the user. The controller uses systolic force as a control variable which is determined from the feedback of estimated pump output. The control maintains the pump output during changes in model peripheral resistance ($R_p$) by changing the systolic force acting during systolic phase. To provide non-invasive measurement of volume an estimator was designed, it uses the pressure gradients across the inlet and outlet valves to provide estimates of End Diastolic Volume (EDV) and End Systolic Volume (ESV) on a beat by beat basis with an Adaptive Neuro Fuzzy Inference System (ANFIS). These volumes were used to estimate cardiac output for the FLC. An increase or descrease in pump output was able to be corrected by the FLC. The system was observed to attain a steady state within the first minute. The controller was also seen to behave well during sensitivity studies, but changes to the artificial heart parameters altered the trained ANFIS and hence produced errors in the estimator for pump output. The ANFIS estimator is shown to provide a good estimate of the EDV and ESV for changing pump output. The FLC was found to be able to maintain control of pump output by altering the systolic force on a beat by beat basis.

# Contents

# List of Tables

# List of Figures

# List of Symbols

| | |
|---|---|
| $\emptyset$ | Empty Set |
| $\langle\rangle$ | Domain containg all Real values between limits |
| $\wedge$ | A fuzzy T-norm operator (Intersection) |
| $\vee$ | A fuzzy T-conorm operator (Union) |
| $A \subset B$ | A is a subset of B |
| $\Re$ | Set of all Real Numbers |
| $A$ | Piston Effective Area |
| $A^c$ | Complement of A |
| AH | Artificial Heart |
| ANFIS | Adaptive Neuro Fuzzy Inference System |
| AOP | Mean Aortic Pressure |
| bpm | Beats per Minute |
| $C_{at}$ | Arterial Compliance |
| $C_{ht}$ | Artificial Heart Compliance |
| $C_{vn}$ | Venous Compliance |
| CO | Cardiac Output (Natural heart output interchangable with PO) |
| $\Delta P_{in}$ | Pressure gradient across Inlet Valve |
| $\Delta P_{out}$ | Pressure gradient across Outlet Valve |
| $\Delta F_{sys}$ | Change In Ststolic Force |
| DOM | Degree of Memebership |
| DOF | Degree Of Firing |
| ECG | ElectroCardiogram |
| EDV | End Diastolic Volume |
| ESV | End Systolic Volume |
| FFFE | Full Fill Full Eject |
| FLC | Fuzzy Logic Controller |

| | |
|---|---|
| $F_{dia}$ | Diatolic Force |
| $F_{sys}$ | Systolic Force |
| HR | Heart Rate |
| $I_{ao}$ | Aorta Inertance |
| $I_{cnin}$ | Inlet Cannulae Inertance |
| $I_{cnot}$ | Outlet Cannulae Inertance |
| $I_{ht}$ | Artificial Heart Inertance |
| $I_{pe}$ | Periperal Inertance |
| $\lambda$ | Classical Characteristic Function |
| MAP | Mean Arterial Pressure |
| $O_2U$ | $O_2$-Utilization |
| PO | Pump Output |
| $R_{ao}$ | Aorta Resistance |
| $R_{in}$ | Inlet valve Resistance |
| $R_{ou}$ | Outlet valve Resistance |
| $R_{ht}$ | Artificial Heart Resistance |
| $R_{inm}$ | Inlet Valve Dynamic Resistance |
| $R_{otm}$ | Outlet Valve Dynamic Resistance |
| $R_{pe}$ | Periperial Resistance |
| $R_{cnin}$ | Inlet Cannulae Resistance |
| $R_{cnot}$ | Outlet Cannulae Resistance |
| SV | Stroke Volume |
| $SvO_2$ | Venous Oxygen Saturation |
| $SaO_2$ | Arterial Oxygen Saturation |
| $\tau_i$ | Degree of firing or rule $i$ |
| t | Seconds |
| $t_{dia_i}$ | Time of diastole at beat $i$ |
| $t_{sys_i}$ | Time of systole at beat $i$ |

| | |
|---|---|
| $t_{dia_{i-1}}$ | Time of diastole at beat $i-1$ |
| $t_{sys_{i-1}}$ | Time of systole at beat $i-1$ |
| TAH | Total Arfificial Heart |
| $\mu$ | Fuzzy Characteristic Function |
| VAD | Ventricular Assist Device |
| $v$ | Volume |

# Chapter 1

# Introduction

The number of deaths due to dysfunction of the human cardiovascular system has always been high. The statistics on cardiovascular disease show that more than a million people suffer from cardiovascular dysfunction in North America alone. These people require coronary bypass procedures, heart valve replacement, pacemakers, replacement of the natural heart and sometimes an assist to ventricular performance. Today, due to advances in medical technology and bioengineering, we have begun to explore the possibilities of integrating mechanical hardware into biological systems. This has been possible due to the development of enhanced bio-materials which have little or no rejection problems [2, 3].

There are two existing classes of artificial hearts. They are Total Artificial Hearts (TAH) and Ventricular Assist Devices (VAD). Their main functions are the same, however the latter one is attached in parrallel or in series to a damaged ventricle when low cardiac output is detected. The ventricular assist device helps in assisting the pumping of blood to either the lungs (Right Ventricle) or the aorta (Left Ventricle) [2]. The use of an assist device reduces cost, material implantation and amount of space required in the human body for implantation. The decrease in implanted material also reduces the risk of rejection and other complications. Total artificial

hearts are used when assisted pumping (VAD) is not sufficient (severe myocardial dysfunction) and where replacement of the entire natural heart is necessary to remedy the situation [4]. At present, the method used during surgical procedures is a fixed rate method of control [5]. At postsurgical situtations a Full Fill-Full Eject (FFFE) method is used for normal operation [5]. The use of active control may be required to regulate left and right ventricular pressures and stroke volumes [6] for rapid changing of peripheral/vascular resistance due to metabolic changes, medication or exercise. A fuzzy logic controller is proposed to provide better control during surgical situations as an alternative to the fixed rate method of control to compensate for changing requirements. It may also be used as a monitoring device for an artificial heart [7].

## 1.1 Simulation Study

The mathematical model of the circulatory system was simulated with the aid of MATLAB and Simulink and is further discussed in Chapter 5. The control of the artificial heart model and the pump output estimator was implemented with the aid of the Fuzzy Logic Toolbox. The simulated response and effect of the control action to changes in the circulatory model was studied.

## 1.2 Cardiovascular model

The cardiovascular model [1] was used to test and evaluate the proposed controller. The circulatory model was represented by 12 first order differential equations generated from a bond graph shown in Figure 5.1. The equations define 12 state variables as described in Chapter 5. The model is divided into an aorta, lumped arterial, peripheral, venous, inlet/outlet cannulae and the artificial heart. The artificial heart is modeled by a generic model represented by a cylinderical chamber with a piston [1]. The ordinary differential equations were then integrated with the 4th order Runge-Kutta routine to generate time response values. The model was simulated with a fixed rate of 1 beat per second. Some modifications were made to the previous

model to improve performance during control. These improvements were made to the system model where the artificial device was attached to the human circulatory system. The improvements include a three element aorta segment, changes in inlet/outlet cannula compliance and inclusion of resistance elements on the inlet and outlet cannulae.

## 1.3 Controller Design

The goal of this study was to enable an artificial heart system to provide the required pump output during changes to system. This was carried out using fuzzy logic. The concept of fuzzy logic provides us with a way of describing known processes in complex systems whose behaviour is understood by experience and comprehension of the system dynamics by specialists. The dynamics and behaviours were then modelled with the aid of fuzzy logic and empirical rules. The controller designed for the circulatory model provide the required change in systolic force based on the estimated pump output on a beat by beat basis. The pump output was modelled in two stages with an Adaptive Neuro Fuzzy Inference System (ANFIS) which estimates the End Diastolic Volume and the End Systolic Volume on a beat by beat basis. The estimated pump output was then used in a Mamdani fuzzy logic control model. The Mamdani fuzzy logic controller controls the systolic force on the modeled piston during the systolic phase to maintain the desired pump output when changes in physiological conditions occur.

## 1.4 Controller Evaluation

The controller was evaluated by altering the circulatory model peripheral resistance ($R_{pe}$) and the initial conditions while observing the system and controller responses to correct the pump output. Also Pressure-Volume loops and ejection fractions were used to confirm the performance of the controller and artificial heart which is explained further in Sections 6.11 and 6.12.

## 1.5 Sensitivity Study for Controller

A sensitivity study was conducted after the controller design was implemented to test the controller's domain of sensitivity in the simulation due to changes in selected model parameters. The effect of each parameter is discussed in detail and shown graphically in Chapter 6.

# Chapter 2

# Literture Review

## 2.1 General Artificial Heart

The artificial heart was developed as a temporary solution for patients waiting for donor hearts [4, 8] and as a support for patients who have been denied the transplant option with a mechanical assist [9]. The artificial heart was first used clinically after the second world war and was first reported in use by Gibbson in 1954 [10] who used a heart-lung device. Assist devices have become of major interests for various research groups since the 1960s. Increases in bioengineering and medical device development have generated much research in developing the first commercial artificial heart and assist device.

### 2.1.1 Types of Artificial Hearts

There are two main types of artificial hearts: the total artificial heart and the ventricular assist device. The main function of ventricular assist devices and total artificial hearts is to provide blood flow at an acceptable rate (pump output) to maintain the patient's health and the proper function of internal organs and tissues.

#### Total Artificial Heart

The goal of the total artificial heart is to provide a replacement for a patient's natural heart [11]. The replacement involves the removal of the left and right ventricle.

Generally the right artificial ventricle is attached to the right atrium or vena cava via an inlet cannula and the outlet cannula is attached to the pulmonary artery. Similarly the left artificial ventricle is attached via the left atrium by an inlet cannula and the outlet is connected to the ascending or descending aorta. In some cases the entire natural heart is removed and replaced by a TAH [8]. These devices are generally an extention of an assist device with a much more complex control scheme.

#### Assist Devices

These devices are pumps designed to provide assistance to the natural heart. The pump device is generally able to be implanted internally. The device consists of an input cannula, a pump mechanism and an output cannula segment with a power source. The device's input is generally from the left atrium or from the apex of the left ventricle (left ventricle assist) and the output is connected to the ascending aorta or the descending aorta. A similar type of device can be used in the case of right ventricle failure and the input cannula is attached to the right atrium or the right ventricle apex and the output cannula is attached to the pulmonary artery.

### 2.1.2 Human Circulatory Requirements

The artificial heart is used to provide circulatory requirements that the natural heart can no longer provide on its own or cannot provide at all. This consists of providing blood flow at the required flow rate to adequately provide nutrients, temperature control for organs, oxygen for tissues and organs and waste removal from cells and tissues [12]. All these functions can be regulated by maintaining one of the most important parameters in the circulatory system which is the known as cardiac output or pump output for artificial hearts.

## 2.2 Circulatory Model Elements

The present model of the human circulatory system uses various elements to develop the computer model. These elements are described below mathematically and are

used later in the thesis to explain the behaviour of the simulation.

An element commonly used is the compliance element which is the pressure volume relationship of any vessel segment [1]. When volume is increased in a segment its pressure also increases. The relation which defines the amount of increase or decrease in pressure for a unit increase or decrease in volume is given by:

$$C = \frac{\Delta V}{\Delta P} \tag{2.1}$$

The flow resistance is the resistance encountered by the blood flowing through any segment in the human body [13]. The flow resistance of a tube is given by the difference in the pressure across two reference points and the mean flow rate between the reference points.

$$R = \frac{\Delta P \text{ across segment}}{\text{Mean Flow Rate in segment}} \tag{2.2}$$

The blood inertance defines the inertia of the blood in a segment [1, 13]. The blood density is assumed constant and equal to that of water since blood is composed of about 80% water [13]. When the geometry of a segment is known the inertance can be calculated. If the Interance, is given by:

$$I = \frac{\rho L}{A} \tag{2.3}$$

Where $A$ is the cross sectional area of the segment, $L$ is the length of the cannula segment and $\rho$ is the density of blood.

## 2.3 Measurement Of Circulatory Parameters

When artificial hearts are implanted in the human body, sensors are also implanted to record and diagnose the performance of the artificial heart. Such sensors are usually implanted with the artificial heart. Generally, pressure sensors, oxygen sensors, flowrate meters and hall effect sensors are examples of typical sensors that can may be implanted to provide a method of diagnosis of the artficial heart state [6, 8]. In

order to provide a suitable control certain heart parameters have to be observed and from that information a plausible method of control can be derived.

### 2.3.1 Estimators

The use of sensors causes various problems when they are implanted in the human body. Some of these problems are related to material implantation and others due to the location of the implanted sensor. Many sensors are implanted in the flow stream of the blood which is generally the case for flow rate readings. These sensors tend to drift due to accumulation of blood and tissue on the sensor probe causing maintenance difficulties after implantation [6].

A method which is more effective is to produce models using simple sensors that are less invasive to the human circulatory system. These sensors are used to produce a calculated estimate of the required parameters under study. Thus, avoiding harmful implantation of sensors and the difficulties of maintaining such sensors.

An estimator is used to provide an estimated value of the volume of blood in the artificial heart at various times during a beat. These estimates are derived from assumed implantation of pressure sensors at the inlet and outlet of the artificial heart. The estimator provides a calculated pump output which is used as the controller input.

## 2.4 Methods of Control

The physiological system is a very complex system that uses pressure, hormonal, neural and chemical reaction to control the stroke volume, preload, arterial pressure, blood flow rate, heart rate and oxgyen content in blood of a human circulatory system. These systems have cross coupling between variables which can cause difficulty in designing controllers. The model discussed in this thesis is a generic model of a human circulatory system. The following are various control parameters and

how they effect the cardiovascular system. This is usefull in understanding the physiological relationships between control and the systems response [14].

## 2.5 Heart Parameters

When physiological parameters are altered they change the system point of equilibrium. These effects in turn produce observable pressures and flow rates that can be used to provide infomation on the circulatory system's behaviour with the aid of sensors. These pressures and flow rates can then be used as an input signal to the control logic to provide a control action to maintain stable physiological function.

### 2.5.1 Preload Pressure

An important parameter for the heart is the preload pressure. The preload pressure is the pressure outside the inlet valve of the artificial heart. This pressure influences the End Diastolic Volume. The end diastolic volume is the volume of blood in the heart after the inlet valve is closed and just before ejection begins. The preload pressure affects the difference in pressure across the inlet valve and hence the flow rate through the inlet valve. When the preload pressure is increased the flow rate into the artificial heart is in turn increased and end diastolic volume is increased. Hence the use of preload pressure can indirectly be used to control cardiac output. There are no realistic, simple means of changing preload. Some procedures to change the preload pressure would be to introduce drugs to induce a higher pressure at the inlet side of the heart [15]. In artificial hearts control might be accomplished by changing the properties of the inlet cannula temporarily which would involve a complex design of a variable compliance chamber or changing the inlet cannula resistance. A simple procedure known as the intrathoratic balloon is used on the aorta to relieve left ventricular loading. A similar device can be used on the inlet to provide control of EDV [2].

### 2.5.2 Ejection Phase

The ejection phase is the phase were the blood is pushed out of the heart. It is also known as the systolic phase. The amount of blood ejected during systole is known as stroke volume. During systole the outlet valve is open and the inlet valve is closed. The pressure gradient across the outlet is important and changes the ejection time. The volume in the heart after the outlet valve is closed and just before the inlet valve is open is known as the End Systolic Volume (ESV). The stroke volume can then be calculated for the beat by the difference in the EDV and ESV as in Equation (2.4).

$$SV = EDV - ESV \tag{2.4}$$

### 2.5.3 Heart Rate and Pump Output

The heart rate is the number of heart beats per minute ($\frac{beats}{min}$). Each beat consists of a filling (diastolic) phase followed by ejection (systolic) phase. The heart rate is made up of these two processes: the diastolic and systolic phases. The sum of these two time periods produces a single beat in the cardiac cycle. When oxygen consumption is increased the human body responds by increasing the heart rate or increasing the filling pressure (preload) as one method of stablizing the system. This provides increased blood flow by increasing cardiac output as shown in Equation (2.5). This effect is known as the Starling-effect [2, 13, 16].

$$PO = SV \times HR \tag{2.5}$$

The duration of the diastolic (filling) process is known as diastolic time and denoted by $t_{dia}$. By altering the time of diastole the end diastolic volume can be changed in the artificial heart. When $t_{dia}$ is decreased the end diastolic volume is lower and when increased the end diastolic volume is higher. This increase/decrease also depends on the preload pressure and hence the flow rate through the inlet valve. Since the valves are passive the activation of the valve is a function of the pressure gradient over the valve. The duration of the systolic process is known as systolic time and denoted by $t_{sys}$. Figure 2.1 shows the driving force in the artificial heart

and the period over which the force is sustained.

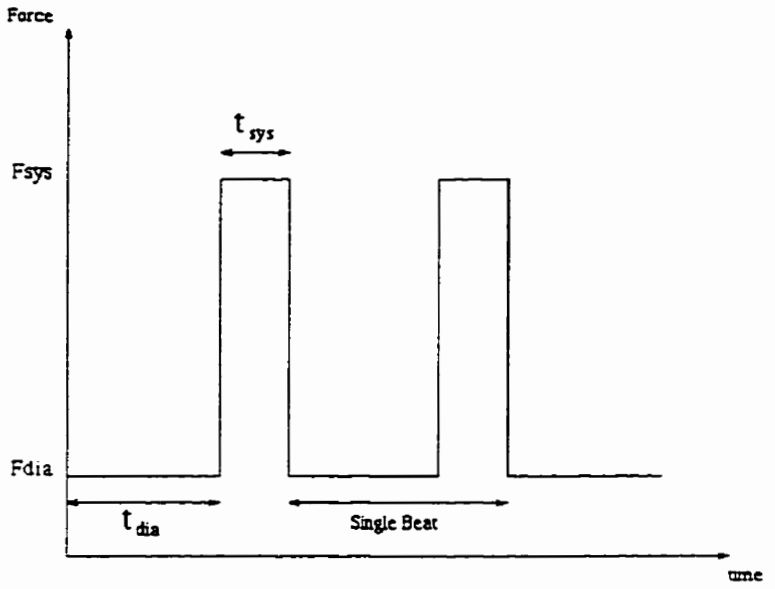


**Figure 2.1:** Artificial Heart beat time for systole ($t_{sys}$) and diastole ($t_{dia}$). Also shows the operating force waveform ($F_{sys}$ and $F_{dia}$). The beat is defined as diastole followed by a systolic process.

The systolic and diastolic times when reduced will increase the heart rate, since a single beat will begin and end faster. This has implications for the end diastolic volume and the end systolic volume in the heart. The systolic phase timing is generally constant and studies have shown that systolic time changes are very small as compared to diastolic timing changes [14].

The increase in pump output is brought about by increasing the heart rate or by increasing the stroke volume. The pump output can be broken down and expressed by the product of stroke volume (SV) and heart rate as in Equation (2.5). This shows that the pump output can be increased either by increasing the heart rate or the stroke volume.

### 2.5.4 Driving Force

The natural heart, during the systolic phase, ejects blood by contracting the myocradial muscles until the internal heart pressure exceeds that of the aorta pressure. Similarly during diastolic phase the internal heart pressure is lower than the venous pressure (depending on connection) which causes the inlet valve to open and blood to flow into the heart. A similar behaviour is found in the artificial heart. The artificial heart, during the systolic phase applies a force ($F_{sys}$ to increase the internal pressure shown in Figure 2.1) on the artificial heart chamber which increases the internal camber pressure to exceed the pressure outside the heart output valve (output cannula pressure). This pressure gradient causes the output valve to open and thus ejects the blood in the artificial heart into the output cannula. The flow rate from the artifical heart is a function of the pressure difference across the output valve and its resistance [17].

During the diastolic phase the artificial heart applies a reduced (possibly negative) force ($F_{dia}$). This diastolic force will result in a drop in internal artificial heart pressure, allowing the pressure in the venous system (inlet cannula) to cause blood to flow into the heart. This drop in pressure may cause the venous segment to collapse [18, 19, 20]. The present model does not model the venous as a collapsable segment and is recommended for future work. The Figure 2.1 shows again the forces and the timing for a generic artificial heart (Input waveform).

## 2.6 Control Of Artificial Hearts

The main aspect in this research on artificial hearts is to provide methods of control that meet the human circulatory requirements under varying circumstances by monitoring a few physiological parameters with the aid of sensors. A model of the circulatory system is used to represent the human circulatory system and the parameters are altered to simulate changing physiological conditions.

### 2.6.1 Fixed Rate

A fixed rate control of an artificial heart is commonly in use today in surgical situations. During these cases changes in circulatory parameters can be large. The method of fixed control uses a fixed systolic and diastolic timing which is set to a preassigned value. The systolic and diastolic driving force is also fixed during the control processes. The values of the timing and force have to be manually preset by a doctor or an artificial heart technician. if the patients metabolism changes [8].

The model presently in use for this study operates on a fixed rate method [1]. The systolic and diastolic times are held at 0.3 secs and 0.7 secs respectively. The systolic force during nominal steady state conditions is set at a value of 41.8 N and the diastolic force is set to a value of 0 N.

### 2.6.2 Full Fill Full Eject

Another method of control in popular use is called full fill full eject. The artificial heart is controlled by observing the artificial heart volume. When the blood volume in the heart during diastole reaches a certain threshold the diastolic phase is switched to a systolic phase to eject the blood until the heart is empty. This enables the systolic time and diastolic time to vary depending on the preload pressure. This provides the artificial heart with the ability to passively vary its response to the human physiological state [1, 8].

### 2.6.3 Knowledge-Based Control

The use of knowledge based control is a new type of control proposed for complex and coupled systems. The control can be defined by knowledge of the system and its ability to handle vague data to determine a control action. Breaking down complex systems into simpler subsystems is possible [21, 22, 23].

## 2.7 Fuzzy Logic Control

The new area of research is the development of a new way to describe ill-defined or complex interaction between systems. The biological system is one of the most complex systems known to mankind. Its interactions contain chemical, hormonal and electrical coupled reactions. Fuzzy logic controllers solve non-linear, time varying and time delay control problems based on logic [24]. Many scientific institutions are presently studying this newly developed theory known as fuzzy logic control and knowledge based systems to design physiological models, monitoring systems or to control such complex systems [25, 24]. Fuzzy logic is presently used in aircraft flight control [26, 27], decision making and reasoning [28], medical monitoring [7, 29], drug administration [24, 30] and medical diagonsis [28]. Fuzzy logic can also be found in various consumer products like air conditioners, washing machines, microwaves, and televisions [31].

# Chapter 3

# Fuzzy Set Theory

In this chapter we introduce some of the basic ideas of classical logic and fuzzy logic which are used to develop the rule base for the input/output domain. It also provides the basic terminology and mathematical relationships used to develop fuzzy logic models and controllers. For more detailed information see A. Kaufmann or R. Yager and D. P. Filev [32, 33].

## 3.1 Classical sets

A set is a collection of objects. Let $X$ be a set known as the Universe of Discourse. If $x$ is an element (object or member) of a set $X$. We denote it by,

$$x \epsilon X \tag{3.1}$$

If $x$ is not an element in $X$, we denote it by,

$$x \notin X \tag{3.2}$$

Let $A$ be a set such that whenever $a \epsilon A$ then $a \epsilon X$, then $A$ is called a subset of $X$ and usually denoted by,

$$A \subseteq X \tag{3.3}$$

If $A \subseteq X$ and $X \subseteq A$ then we write

$$A = X \tag{3.4}$$

If $A \subseteq X$, but $A \neq X$, then we write

$$A \subset X \tag{3.5}$$

A set $\emptyset$ which contains no elements at all is called an empty set. We always consider $\emptyset$ and $X$ as subsets of $X$.

## 3.2 Set Operators

If $A$ and $B$ are two subsets of a set $X$, then we define the symbol $\cup$ to represent union of two subsets and is defined by equation 3.6. While the $\cap$ symbol is the intersection of two sets defined by equation 3.7. The complement of a set is denoted by a bar over the top of the character representing the set and is defined in equation 3.8.

$$A \cup B = \{x \mid x \epsilon A \ \underline{or} \ x \epsilon B\} \tag{3.6}$$

The set of all elements $x$ such that either $x \epsilon A$ or $x \epsilon B$. Clearly,

$$A \cap B = \{x \mid x \epsilon A \ \underline{and} \ x \epsilon B\} \tag{3.7}$$

$$\bar{A} = \{x \mid x \notin A\} \tag{3.8}$$

### 3.2.1 Classical Carestian Product

The cartesian product of $A$ and $B$ (written as $A \times B$) is defined by

$$A \times B = \{(a, b) \mid a \epsilon A, b \epsilon B\} \tag{3.9}$$

In other words $A \times B$ is the set of all elements $(a, b)$ such that, $a \epsilon A$, $b \epsilon B$. Here the order of the elements are important. The first element always comes from $A$ and only from set $A$. The second element always from set $B$ and only from set $B$.

### 3.2.2 Transformation

A subset $C$ of $A \times B$ is called a relation. *Example:* $(a_2, b_1), (a_4, b_2)$ is a relation, since these 2-form tuplets are subsets of $A \times B$. A function $f$ on a set $A$ to a set $B$ assigns to each element $a \epsilon A$ an element $f(a) \epsilon B$.

The set $A$ is called domain and the set of all elements $f(a)$, for each $a \epsilon A$ is called a codomain.

$$f : A \longrightarrow B \tag{3.10}$$

The arrow indicates that $f$ is a function with domain $A$ and range $B$. A function is often called a mapping or transformation.

### 3.2.3 Characteristic Function (Classical)

A subset $A$ of a set $X$ can be defined with the help of a function $\lambda_A$, where

$$\lambda_A : X = \{0, 1\} \tag{3.11}$$

$$\lambda_A(x) = \begin{cases} 0 & \text{for } x \notin A \\ 1 & \text{for } x \epsilon A \end{cases} \tag{3.12}$$

The above is called a characteristic function [34].

In classical set theory two important properties known as the *Law of the excluded middle* and *Law of non contradiction* are true. These laws are equivalent to the two conditions below.

$$A \cup \bar{A} = X \tag{3.13}$$

$$A \cap \bar{A} = \emptyset \tag{3.14}$$

From here onwords, subsets of the classical set will be refered to as *Crisp Subsets* and the universal classical set will be refered to as *Crisp Set*. This helps us to distinguish between classical subsets and fuzzy subsets.

## 3.3 Fuzzy Set Theory

In classical set theory, we speak of an element either completely in $A$ or not in $A$. In 1965, Zadeh gave a new generalization of the concept of an element belonging to a set $A$ [35]. He introduced the idea of degree of membership of an element ($a \in A$). A fuzzy set is a class of objects such that each object has a degree of membership. Such a set can be defined with the help of a characteristic function or transformation $\mu$ which assigns to each element of the set a degree of membership ranging from zero to one. Hence when the value of $\mu_A(x)$ is near to unity then the degree of the membership of $x$ in the set is also higher [33, 34].

$$\begin{aligned} a \text{ is completely in } A \quad & \mu_A(x) = 1 \\ a \text{ is almost (conditional) in } A \quad & 0 < \mu_A(x) < 1 \\ a \text{ does not belong in } A \quad & \mu_A(x) = 0 \end{aligned}$$

This can be defined with the help of a characteristic function $\mu_A$.

$$\mu_A : X \longrightarrow [0, 1] \tag{3.15}$$

where $[0, 1]$ is a closed set containing all the possible real numbers from 0 to 1 including 0 and 1.

### Fuzzy Subsets

A subset $A \subseteq X$ with a characteristic function $\mu_A$.

$$\mu_A : X \longrightarrow [0, 1] \tag{3.16}$$

is called a fuzzy subset.

## Equality of Fuzzy sets

Two fuzzy subsets $A$ and $B$ are said to be equal ($A = B$) if and only if

$$\mu_A(x) = \mu_B(x), \ \forall x \epsilon X \tag{3.17}$$

## Fuzzy Union and Intersection

We define union and intersection of fuzzy subsets $A$ and $B$ as follows

$$\mu_{A \cup B}(x) = max(\mu_A(x), \mu_B(x)), \ \forall x \epsilon X \tag{3.18}$$

$$\mu_{A \cap B}(x) = min(\mu_A(x), \mu_B(x)), \ \forall x \epsilon X \tag{3.19}$$

The max and min operators are known as special cases of T-norm and T-conorm operators.

## Complement of A

The complement of $A$ (written as $A^c$) is defined by,

$$\mu_{A^c}(x) = 1 - \mu_A(x), \ \forall x \epsilon X \tag{3.20}$$

It can be shown from equation 3.13 and equation 3.14 that the *Law of the excluded middle* and the *Law of Non-contradiction* are not valid for fuzzy subsets.

$$A \cup A^c \neq X \tag{3.21}$$

$$A \cap A^c \neq \emptyset \tag{3.22}$$

## Containment

A fuzzy subset $A$ is said to be included in a fuzzy subset $B$ (Denoted by $A \subseteq B$) if and only if,

$$\mu_A(x) \leq \mu_B(x),\ \forall x \epsilon X \tag{3.23}$$

Now we extend the idea of relations, cartesian product, mapping of classical set theory to fuzzy subsets.

### $\alpha$-cuts

Let $A$ be a fuzzy set. The $\alpha$-cut of the set $A$, denoted by $A_\alpha$, is defined by,

$$A_\alpha(x) = \{x \epsilon X \mid \mu_A(x) \geq \alpha\},\ \forall x \epsilon X \tag{3.24}$$

When $\alpha \epsilon [0,1]$, then clearly $A_\alpha$ contains all points $x \epsilon X$ with a membership value $(\mu_A(x))$ of at least $\alpha$. The $A_\alpha$,

$$A_\alpha(x) = \{x \epsilon X \mid \mu_A(x) > \alpha\},\ \forall x \epsilon X \tag{3.25}$$

is called the strict $\alpha$-cut of $A$. The family of all $\alpha$-cuts, $\alpha \epsilon [0,1]$ gives all the information of the fuzzy set $A$.

## 3.4 Fuzzy Cartesian Product

Any fuzzy subset of the cartesian product $X \times Y$ is called a fuzzy relationship. Let $A$ and $B$ be two fuzzy subsets of $X$ and $Y$ respectively. The cartesian product of $A$ and $B$ is a fuzzy relationship on the set $X \times Y$, denoted by $T = A \times B$ where,

$$T(a,b) = min(\mu_A(a), \mu_B(b)) \tag{3.26}$$

More generally if $A_1 \times A_2 \times A_3 ..... \times A_k$ are fuzzy subsets of $X_1 \times X_2 \times X_3 .....X_k$ respectively, then their cartesian product $T = A_1 \times A_2 \times A_3 ..... \times A_k$ is defined by,

$$T(a_1, a_2, ..... a_k) = min(\mu_{A_1}(a_1), ..... \mu_{A_k}(a_k)) \tag{3.27}$$

Now we introduce a special case of the above cartesian product of fuzzy subsets.

## 3.5 Cylindrical Extension

Let $X$ and $Y$ be two crisp sets. Let $A$ be a fuzzy subset of $X$. The cylindrical extension of the fuzzy subset $A$ to $X \times Y$ is the fuzzy cross product.

$$\begin{aligned} \tilde{A} &= A \times Y \\ \text{where } \tilde{A}(x,y) &= min(\mu_A(x), \mu_Y(y)) \\ &= \mu_A(x) \end{aligned} \tag{3.28}$$

## 3.6 Fuzzy Operators: T-norm and T-conorm

Now we consider the cartesian product of the closed sets $[0,1]$. Let $T$ be a mapping (or an operator) from the cartesian product $[0,1] \times [0,1]$ to the closed set $[0,1]$ which is denoted as.

$$T : [0,1] \times [0,1] \longrightarrow [0,1] \tag{3.29}$$

The operator $T$ is called a **T-norm** operator if the following conditions are satisfied.

$$T(a,b) = T(b,a) \tag{3.30}$$

$$T(a,T(b,c)) = T(T(a,b),c) \tag{3.31}$$

$$T(a,b) \geq T(c,d) \text{if } a \geq c \text{ and } b \geq d \tag{3.32}$$

$$T(a,1) = a \tag{3.33}$$

One simple example for the T-norm is the intersection of ordinary subsets of any set. Another important example is the *min* operator which we have already defined for fuzzy subsets.

In a similar manner we define a **T-conorm** as.

$$S : [0,1] \times [0,1] \longrightarrow [0,1] \tag{3.34}$$

Such that the operator $S$ satisfied the following conditions.

$$S(a.b) = S(b.a) \tag{3.35}$$

$$S(a.S(b.c)) = S(S(a.b).c) \tag{3.36}$$

$$S(a.b) \geq S(c.d) \text{if } a \geq c \text{ and } b \geq d \tag{3.37}$$

$$S(a.0) = a \tag{3.38}$$

We see that ($max$) property which we have defined for fuzzy subsets is an example of a T-conorm. We also see that the only distinction between the two operators T-norm and T-conorm is the fourth condition which is.

$$T(a.1) = a \tag{3.39}$$

$$S(a.0) = a \tag{3.40}$$

All other conditions are the same for both operators. The T-norm ($min$) and T-conorm ($max$) are the minimum and maximum of all possible T-norms and T-conorms that satisy the conditions stipulated above. Another special pair of T-norm and T-conorm are the product operator ($ab$) and the probabilistic sum operator ($a + b - ab$) respectively.

We can generate other relationships for operators. This can be done by adding other properties to the above four which makes up the other forms of fuzzy operators like T-norm and T-conorm.

# Chapter 4

# Fuzzy Logic Controller and Models

The principles of control theory are based on mathematical methods, although feedback control has been used in ancient times with the aid of experience, intuition and a solid understanding of the system to be controlled [33]. There are two main types of fuzzy logic controllers. These are known as Mamdani and Takagi-Sugeno-Kang (TSK) [33, 36, 37]. Also a derived adaptive fuzzy inference system was developed from the TSK with the aid of a neural network known as Adaptive Neural Fuzzy Inference System (ANFIS) [33, 38].

## 4.1 Mamdani Type Controller

The control law is described by a knowledge-based system which consists of IF-THEN rules with vague predicates and a Fuzzy Inference System (FIS). The rule base of IF-THEN statements describes the relationship between inputs and the outputs of the controller. The control action is brought about by an incremental change in the controllers output [21, 22, 33].

We describe an input to a hypothetical controller as the error ($\epsilon$) between a desired value ($d_1$) and the actual value ($a_1$) as in Equation (4.1). $\epsilon$ will be an element of the universe of discourse which is given by $X_1$.

$$\epsilon(k) = d_1(k) - a_1(k) \tag{4.1}$$

We define a second input as the change in error ($\Delta\epsilon$) which is defined as the direction of the growth of error (change in error) which is given by Equation (4.2) and its universe of discourse is given by $X_2$.

$$\Delta\epsilon(k) = \epsilon(k) - \epsilon(k-1) \tag{4.2}$$

We denote the output or control variable with ($v$) and its universe of discourse with ($Y$), where $v$ will be the crisp output from the controller. Therefore the control is given by Equation (4.3).

$$v(k) = f(\epsilon(k), \Delta\epsilon(k)) \tag{4.3}$$

### 4.1.1 Universe of Discourses

The error ($\epsilon$) has a universe of discourse which is selected from the universe of real numbers ($\epsilon\epsilon\Re$). This range $X_1$, is chosen based on experience of the system or from simulation to detemine a possible range for the error ($X_1 \subset \Re$). This range can be changed to fit any desired range required, but the larger the error domain the larger number of reference fuzzy sets required to define the domain. This causes an explosion of dimensionality which increases computational time. The range of error values are fit with reference fuzzy sets (membership functions) with labels known as LOW, NORMAL, and HIGH or any other linguistic terms which describes the domain. A typical example of linguistic terms ($\epsilon$, $\Delta\epsilon$ and $v$) and their membership functions is shown in Figure 4.2.

Similarly the change in error variable ($\Delta\epsilon$) is chosen to satisfy the change in error range were $X_2 \subset \Re$. This domain is also divided into linguistic labels defined by various membership functions and is typically similar to Figure 4.2 with a different domain set.

The variable for control ($v$) has the universe $Y$, where $Y \subset \Re$. This universe of discourse is divided into linguistic labels also and defined by membership functions

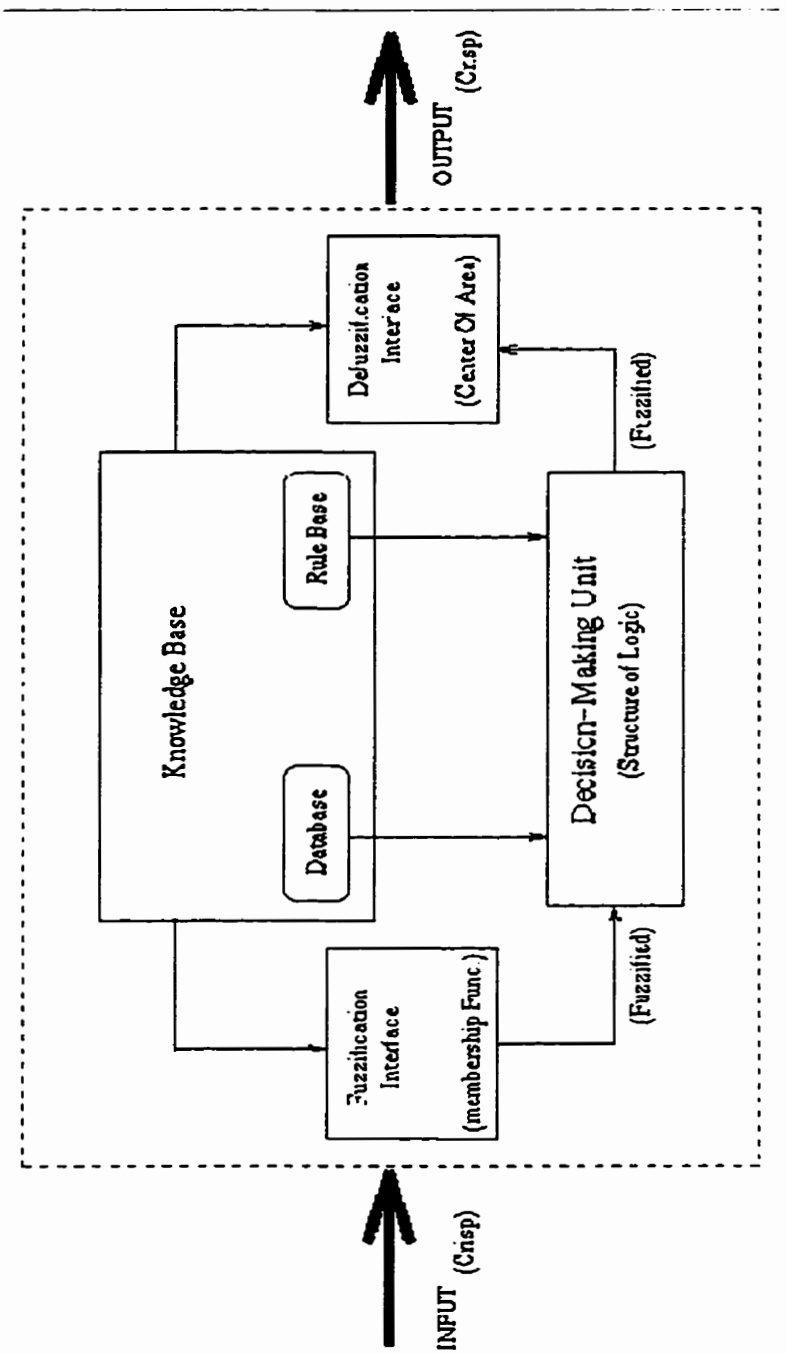


**Figure 4.1:** Schematic diagram of a Mamdani fuzzy controller showing the stages of input, output, fuzzification, decision logic unit, knowledge base and defuzzification. The internal logic can be altered to fit the dynamics to be controlled. But the structure is generally the same.

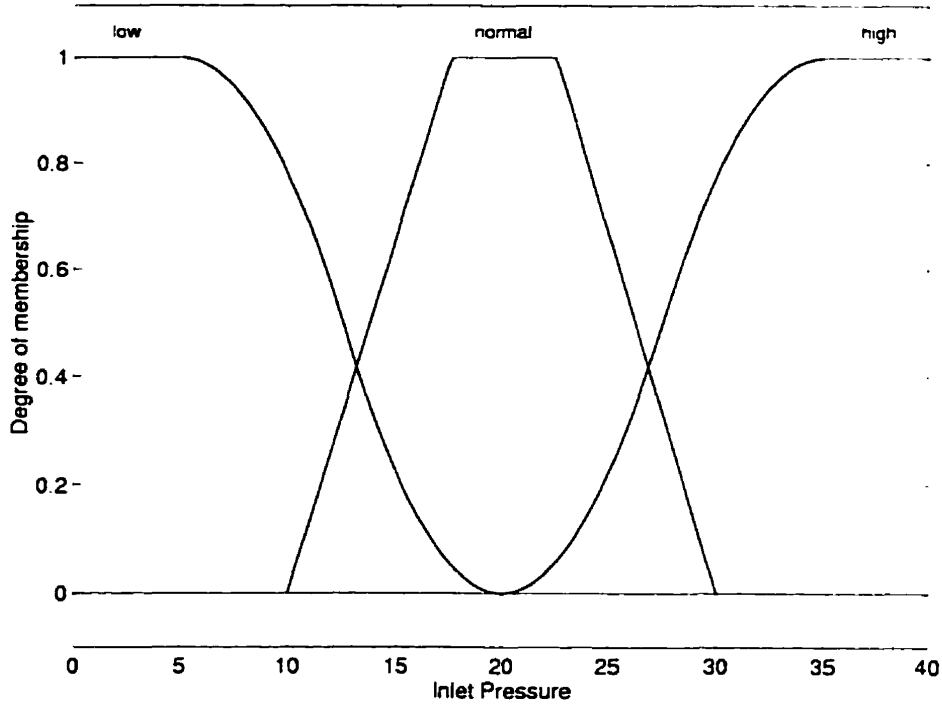


**Figure 4.2:** A typical set with reference fuzzy sets with labeled linguistic terms Low, Medium and High for the example inputs and output ($e$, $\Delta e$ and $c$).

also similar to Figure 4.2 with a different domain set.

### 4.1.2 Reference Fuzzy Sets

The membership funtions are used to describe the reference fuzzy sets which are made up of mathematical functions. These functions can be monotonic or non-monotonic functions. The Figure 4.2 linguistic terms are defined by Equations (4.4)-(4.6). The values of the variables $a_1, c_1, a_2, b_2, c_2, d_2, a_3, c_3$ in the equations are determined by analytical and manual tuning to provide adequate expected response of the system in question.

$$LOW: f(x:(a_1,c_1)) = \frac{1}{1+e^{-a_1(x-c_1)}} \tag{4.4}$$

$$NORMAL: f(x:(a_2,b_2,c_2,d_2)) = \begin{cases} 0 & \text{for } x \le a_2 \\ \frac{x-a_2}{b_2-a_2} & \text{for } a_2 \le x \le b_2 \\ 1 & \text{for } b_2 \le x \le c_2 \\ \frac{d_2-x}{d_2-c_2} & \text{for } c_2 \le x \le d_2 \\ 0 & \text{for } d_2 \le x \end{cases} \tag{4.5}$$

$$HIGH: f(x:(a_3,c_3)) = \frac{1}{1+e^{-a_3(x-c_3)}} \tag{4.6}$$

## 4.2 Rule Base

The rule base is created such that it defines the input's relationship to the output. The rule base of a fuzzy logic controller is made up of two parts the IF part which is known as the antecedent and the THEN part which is known as the consequent of a rule. A set of five rules are shown below which is typical for a simple controller based on the Proportional-Derivative (PD) type. The maximum number of rules that can be generated from two input's and one output which are divided in 3 linguistic variables each is 9 rules ($3 \times 3$). But a lower or higher number of rules can be used to describe the input/output relationship. These rules are generated from intuitive knowledge, experience and an understanding of the system being controlled or modeled. The rule base of the example system described here is made up of 5 rules. Figure 4.3 shows the graphical implementation of these rules for a given set of input values $x_1^*$ and $x_2^*$.

IF ($e(k)$ is HIGH) and ($\Delta e(k)$ is Norm) THEN ($v(k)$ is HIGH) (4.7)

IF ($e(k)$ is LOW) and ($\Delta e(k)$ is Norm) THEN ($v(k)$ is LOW) (4.8)

IF ($e(k)$ is Norm) and ($\Delta e(k)$ is Norm) THEN ($v(k)$ is Norm) (4.9)

IF ($e(k)$ is Norm) and ($\Delta e(k)$ is HIGH) THEN ($v(k)$ is HIGH) (4.10)

IF ($e(k)$ is Norm) and ($\Delta e(k)$ is LOW) THEN ($v(k)$ is LOW) (4.11)

## 4.3 Degree of Firing of Antecedent

The degree of firing of each rule is based on the level of satisfaction of the input antecedents. Let a crisp value of the input error $\epsilon$ be $x_1^*$, $x_1^* \varepsilon X_1$ and a crisp value of the input change in error $\Delta\epsilon$ as $x_2^*$, $x_2^* \varepsilon X_2$, where the input variables $x_1^*$ and $x_2^*$ are measured or estimated from the system to be controlled. All the rules are evaluated for a given set of input values. The rule 4.7 will be evaluated as the degree to which antecedent $\epsilon(x_1^*)$ satisfies the membership function of the linguistic label HIGH. This produces a value between [0, 1]. The degree to which antecedent $\Delta\epsilon(x_2^*)$ satisfies the membership function of the linguistic label Norm also is between [0, 1] as shown in Figure 4.3. The outcome of these antecedents are ANDed (T-norm) together to produce a single value as described by Equation (4.12). This value is known as the Degree of Firing (DOF). Also rule gains can be given to each rule which is also known as the weighted rules and is sometimes used to provide weighted output from each rule.

$$\tau_i = (\epsilon(x_1^*) \text{ is HIGH}) \wedge (\Delta\epsilon(x_2^*) \text{ is Norm}) \tag{4.12}$$

where ($\wedge$) symbolizes a T-norm operator which is the minimum operator (AND) in the Mamdani controller. $\tau_i$ is known as the degree of firing (DOF) of rule $i$. The DOF is characterized as the truthfulness of the antecedents part of rules input's. A DOF is attained for each rule in the rule base, hence five DOF's will be evaluated for the above rules described. Figure 4.3 shows three rules evaluated for a specific input, while the other two DOF's are zero.

## 4.4 Fuzzy Implication

We now take the degree of firing of the antecedents of each rule and relate it to the consequent of each rule. The relation between antecedent and consequent is carried out by another T-norm operator which is a minimum operator (AND) (for a Mamdani controller). The minimum operator extracts the minimum of both the

DOF and the consequent of each rule as described by Equation (4.13). In the case of rule 4.7 above the consequent is HIGH. The output of each rule in the fuzzy implication is a function which is defined over the output space ($v$). hence $F_i(y) \epsilon Y$. This is known as fuzzy implication. The fuzzy implication is carried out for each rule which yields 5 functions defined in the domain $Y$. The Figure 4.3 shows three non zeros rules.

$$F_i(y) = \tau_i \wedge D_i(y) \tag{4.13}$$

Where $D_i(y)$ is the function defining the consequent of the rule $i$ being evaluated and $\tau_i$ is the degree of firing of the antecedents.

## 4.5 Rule Aggregation

All the fuzzy implications of the rules are combined by a T-conorm operator (denoted by $\vee$) which is an ORing operator for the Mamdani controller. This takes all the functions defined for each rule on $Y$ and evaluates them into a single function defined on $Y$ which is given by Equation (4.14) and known as rule aggregation shown as the right most graph in Figure 4.3.

$$F(y) = \vee_i F_i(y),\ i\epsilon\ 1.2.3..5 \tag{4.14}$$

This method of reasoning is known as the constructive approach of reasoning which is used in the Mamdani type of control. The constructive approach basically overlaps all the fuzzy implications and traces the outline hence constructing the output.

## 4.6 Defuzzfication

The output at this point is a single function that exists on $Y$ output space. A crisp value must be infered from the output. There are several methods for defuzzification

of the fuzzy output on the output universe. Mean of Maxima (MOM) and Center of Area (COA) are two of the popular methods for defuzzification.

### 4.6.1 Center Of Area

A single crisp control action can be calculated from the fuzzy function on the output universe of discourse by Equation (4.15). The output using the center of area method produces a moving continuous output, unlike the Mean of Maxima method. The output $y^*$ is crisp and is an element belonging to $Y$, $y^* \varepsilon Y$. Figure 4.3 shows the Mamdani type control evaluation of the set of inputs.

$$y^* = \frac{\int_Y yF(y)dy}{\int_Y F(y)dy} \tag{4.15}$$

## 4.7 Takagi-Seguno-Kang Type Controller

The Takagi-Seguno-Kang type of controller was derived from the Mamdani model to provide a more tuneable model as in Figure 4.4. The general layout is similar to the Mamdani model with a modification of the defuzzification stage which is not present. Instead, the fuzzy rule base consequents are replaced by a defined function as shown in Equation (4.16).

$$\text{IF } (u_1^* \text{ is } B_{11}) \text{ and } (u_2^* \text{ is } B_{12}) \text{ THEN } y_1^* = p_1 u_1^* + q_1 u_2^* + r_1 \tag{4.16}$$

.....

$$\text{IF } (u_1^* \text{ is } B_{i1}) \text{ and } (u_2^* \text{ is } B_{i2}) \text{ THEN } y_i^* = p_i u_1^* + q_i u_2^* + r_i \tag{4.17}$$

where $i$ is the number of rules in the rule base. The above is a two input and single output system. The functions are linear with crisp inputs $u_1^*$ and $u_2^*$. While the output $y_i^*$ of each rule is a crisp value also. The crisp output is aggregated with an average weight by each rules degree of firing which is given more clearly by Equation (4.18). In general, nonlinear functions can be used as the consequent rather than linear functions.

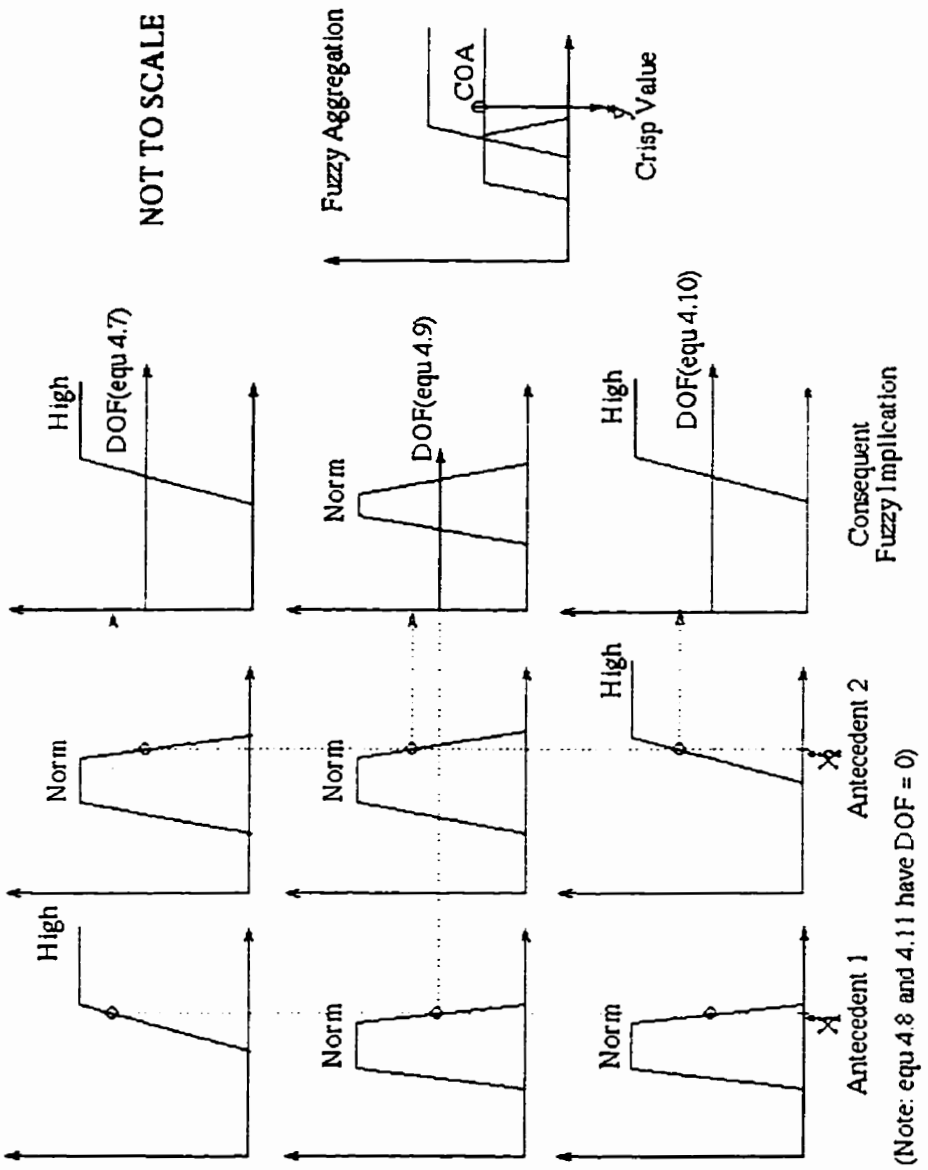


**Figure 4.3:** Graphical representation of reasoning for a Mamdani type fuzzy controller. All five rules are evaluated, but two rules are omitted because one of the antecedents was evaluated to be zero for the given inputs (DOF = 0). The figure shows the DOF, Fuzzy implication, Fuzzy aggregation and Defuzzification.

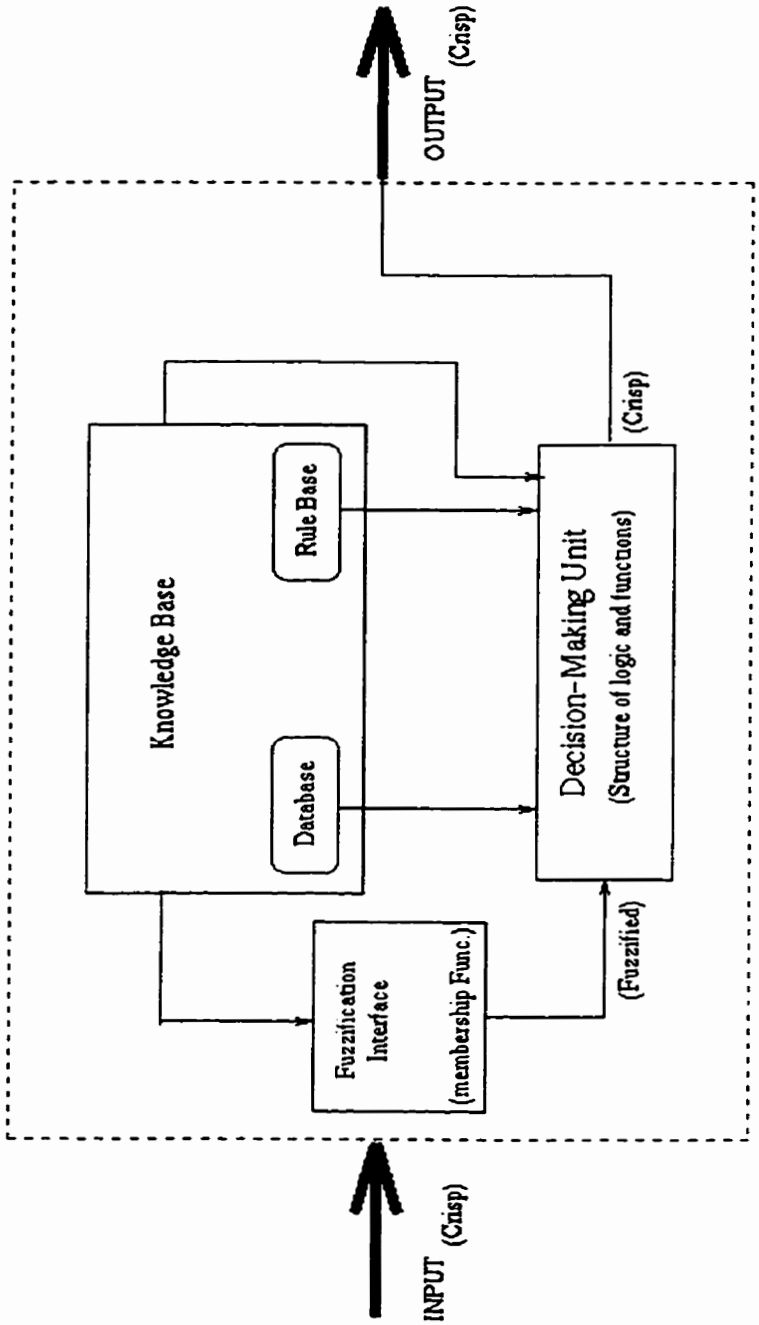


**Figure 4.4:** Schematic diagram of TSK type Fuzzy Controller. The figure shows the stages that differ from the mamdani method above. There is no Defuzzification stage which is replaced by a linear or Non linear function.

$$y^* = \sum_{j=1}^{i} \frac{\tau_j}{\tau_1 + \tau_2 + ... + \tau_i} y_j \tag{4.18}$$

This type of method of fuzzy reasoning is useful in describing complex systems by decomposing them into simple subsystems represented by linear/nonlinear functions. This method of reasoning helps in realistic modeling and control since subsystem region boundaries and piecewise nature of the knowledge bases makes it hard to produce a single crisp value without fuzzy reasoning.

## 4.8 Adaptive Neuro Fuzzy Inference System

In Chapter 6 we make use of ANFIS to generate an esitimator for EDV and ESV to predict the stroke volume and hence cardiac ouput of the artificial heart during a single beat. The fuzzy inference system considered here will have two input's and a single output. The fuzzy inference system is of the Takagi-Seguno-Kang (TSK) type which was briefly discussed above. The inputs are denoted by $x$ and $y$ whose universe of discourse are denoted by $X$ and $Y$ respectively. The output variable is denoted by $z$ and the universe of discourse by $Z$ [38, 39].

### 4.8.1 Layer 1

The first layer of nodes in Figure 4.5 is denoted by square boxes to indicate that these nodes have an adaptive structure. The number of square boxes on each input variable is dependent on the number of membership functions that the variables universe of discourse is divided into. At present we assume each input variable universe of discourse is divided by two reference fuzzy sets with linguistic labels Low and High. Each node in this level is denoted by Equation (4.19). $O_i^1$ is the degree to which the input $x$ satisfies membership function $A_i$.

$$O_i^1 = \mu_{A_i}(x) \tag{4.19}$$

where $O_i^1$ denotes nodal layer 1 and node element $i$. $A_i$ is the linguistic variable of the membership which can be Low or High. We usually chose the membership

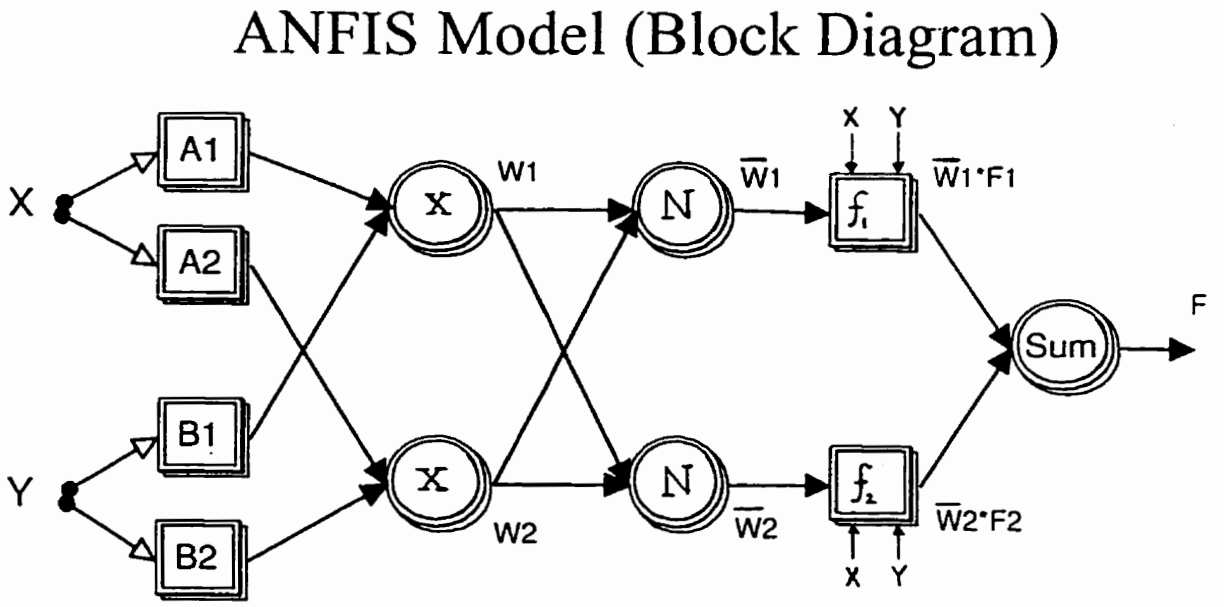


**Figure 4.5:** Block Diagram of an Adaptive Neuro Fuzzy Inference System showing the various layers of the network to produce a trained set of values for the linear functions in the rule consequence.

function $\mu_{A_i}(x)$ to be a bell shaped function which is defined by Equation (4.20).

$$\mu_{A_i}(x) = \frac{1}{1 + b_i[\frac{x-c_i}{a_i}]^2} \tag{4.20}$$

where $a_i, b_i, c_i$ are the variable parameter set for node $i$. When these parameters are changed we change the degree that $x$ satisfies the linguistic terms $A_i$, hence changing $O_i^1$. By altering these parameters we can change the degree of firing of the antecedents of each rule.

### 4.8.2 Layer 2

The layer 2 is symbolized with using circles in Figure 4.5. A T-norm is used to carry out an arithmetric process on the input values of the node. The input variables are multiplied together as shown in Equation (4.21).

$$\tau_i = \mu_{A_i}(x) \times \mu_{B_i}(y),\ i = 1, 2. \tag{4.21}$$

The inputs to this node are based on the structure of the rule base. Other T-norm's maybe used instead of the product operator, one such T-norm, discussed earlier, is the AND T-norm. The output from this node is again the firing strength known as Degree Of Firing ($\tau$) (DOF) of the antcedents.

### 4.8.3 Layer 3

The next set of nodes in layer 3 are symbolized with circles and labeled with N this indicates that the previous firing strength is normalized with respect to the other rule's firing strengths in the rule base. The normalized firing strength is attained by Equation (4.22).

$$\bar{\tau}_i = \frac{\tau_i}{\tau_1 + \tau_2} \tag{4.22}$$

### 4.8.4 Layer 4

All the nodes are denoted by square boxes signifing an adaptive layer of nodes. These nodes are made up of a function that is weighted by the input of normalized firing strength from the previous layer 3. A linear function is used as the nodal function which is multiplied by the normalized firing strength as shown in Equation (4.23). when a nonlinear function is used, training becomes increasingly difficult.

$$O_i^4 = \bar{\tau}_i f_i = \bar{\tau}_i(p_i x + q_i y + r_i) \tag{4.23}$$

where $p_i, q_i, r_i$ are the variable parameter set. Each rule produces its final value from a node in this layer. Each node function is mutiplied by its normalized firing strength. The node function can also be seen to be a function of the crisp inputs $x$ and $y$ as shown in figure 4.5.

### 4.8.5 Layer 5

This layer is shown with a circle also meaning it is a fixed node and has no variable parameter set. The node contains a $\sum$ symbol. All the rules are inputs into this final node. Each rule value is added together to produce the final crisp output value. The summation function is shown in Equation (4.24).

$$O_i^5 = \sum_i \bar{r}_i f_i \tag{4.24}$$

# Chapter 5

# Cardiovascular Model

## 5.1 The Cardiovascular Model

The bond graph [40] in Figure 5.1 produces first order differential equations (5.1)-(5.12). Each equation defines a state variable of the cardiovascular model as shown in Table 5.1. The pressure volume functions are defined in Table 5.2. The equations were implemented in Matlab and coded in the file called *frlad.m* as shown in the appendix A [16, 41, 42].

$$\dot{p_2} = F_{in} - \left(\frac{R_h t}{I_{ht}}\right) p_2 - A\, P_{ht}(x_6) \tag{5.1}$$

$$\begin{aligned} \dot{x_6} &= \left(\frac{A}{I_{ht}}\right) p_2 - \left(\frac{1}{R_{in}} + \frac{1}{R_{ot}}\right) P_{ht}(x_6) \\ &+ \left(\frac{1}{R_{ot}}\right) P_{blo}(x_{10}) + \left(\frac{1}{R_{in}}\right) P_{bli}(x_{23}) \end{aligned} \tag{5.2}$$

$$\dot{x_{10}} = \left(\frac{1}{R_{ot}}\right) P_{ht}(x_6) - \left(\frac{1}{R_{ot}}\right) P_{blo}(x_{10}) - \left(\frac{1}{I_{cnot}}\right) p_{12} \tag{5.3}$$

$$\dot{p_{12}} = P_{blo}(x_{10}) - P_{ao}(x_{29}) - \left(\frac{R_{cnot}}{I_{cnot}}\right) p_{12} \tag{5.4}$$

$$\dot{x_{29}} = \left(\frac{1}{I_{cnot}}\right) p_{12} - \left(\frac{1}{I_{ao}}\right) p_{31} \tag{5.5}$$

$$\dot{p_{31}} = -P_{at}(x_{14}) + P_{ao}(x_{29}) - \left(\frac{R_{ao}}{I_{ao}}\right) p_{31} + P cos(wt) \tag{5.6}$$

$$\dot{x_{14}} = -\left(\frac{1}{I_{pe}}\right) p_{17} + \left(\frac{1}{I_{ao}}\right) p_{31} \tag{5.7}$$

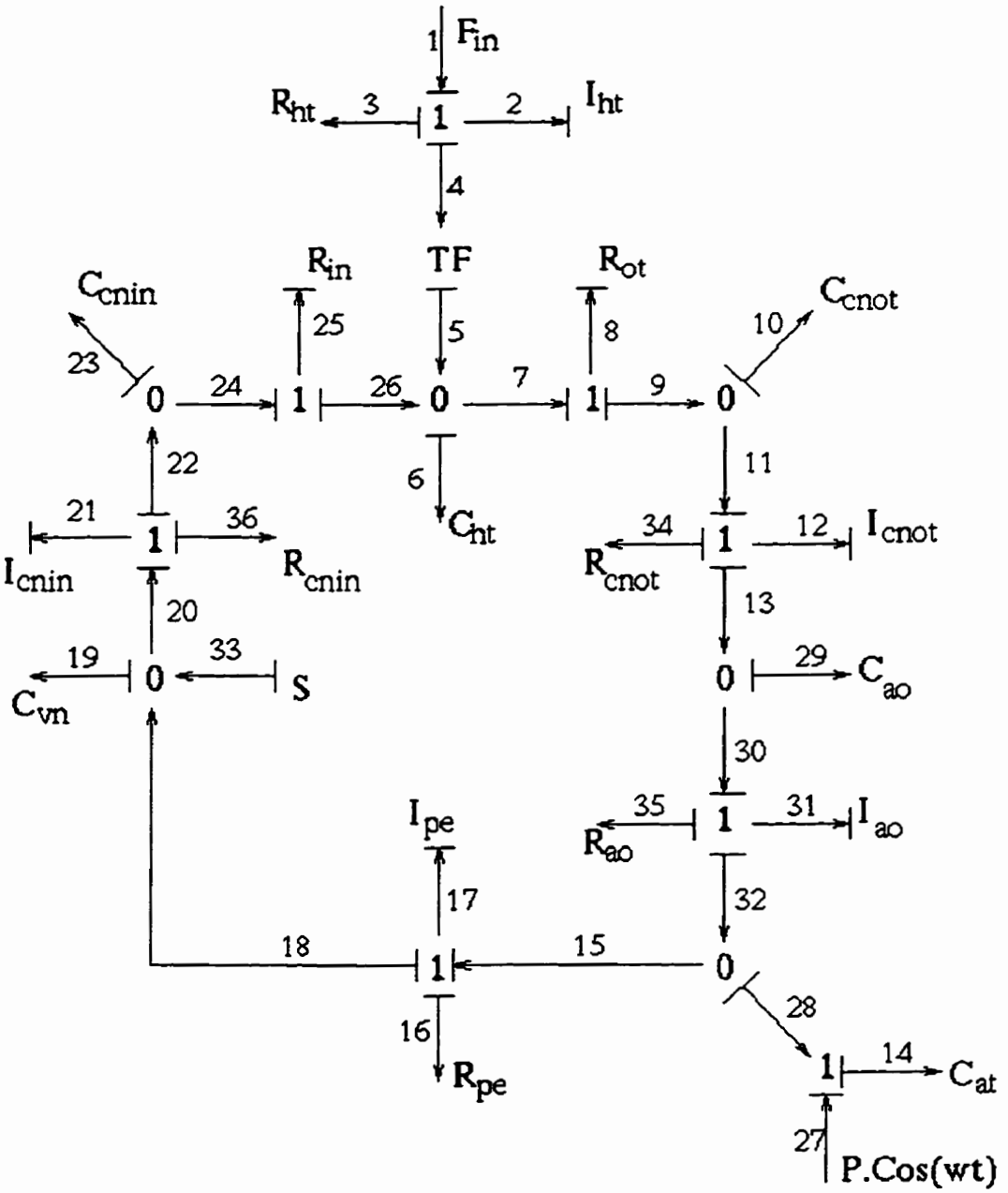


**Figure 5.1:** Bond graph diagram of the mathematical circulatory model with a generic artificial heart (R-resistance, C-compliance, I-inertance, F-force). The model consists of a Artificial heart, Outlet cannula segment, Aorta segment, Arterial segment, Peripheral, Venous segment and Inlet cannula segment.

| Circulatory Model States | | |
|---|---|---|
| **State** | **Description** | **State Units** |
| $p_2$ | Piston Momentum | $Ns$ |
| $x_6$ | Artificial Heart Volume | $cm^3$ |
| $x_{10}$ | Output cannula Volume | $cm^3$ |
| $p_{12}$ | Outlet Cannula Momentum | $\frac{Ns}{cm^2}$ |
| $x_{29}$ | Aorta Volume | $cm^3$ |
| $p_{31}$ | Aorta Segment Momentum | $\frac{Ns}{cm^2}$ |
| $x_{14}$ | Arterial Volume | $cm^3$ |
| $p_{17}$ | Peripheral Momentum | $\frac{Ns}{cm^2}$ |
| $x_{19}$ | Venous Volume | $cm^3$ |
| $p_{21}$ | Inlet Cannula Momentum | $\frac{Ns}{cm^2}$ |
| $x_{23}$ | Input Cannula Volume | $cm^3$ |
| $x_1$ | Piston Position | $cm$ |

**Table 5.1:** State variables, units and description of the Bond graph circulatory model in Figure 5.1

| Compliance Pressure-Volume functions | | | |
|---|---|---|---|
| **Function** | **Input $cm^3$** | **Output $\frac{N}{cm^2}$** | **Filename** |
| $P_{ht}$ | $x_6$ | Heart Pressure | *heartwoff.m* |
| $P_{blo}$ | $x_{10}$ | Output cannula Pressure | *outputcanwoff.m* |
| $P_{bli}$ | $x_{23}$ | Input cannula Pressure | *inputcanwoff.m* |
| $P_{ao}$ | $x_{29}$ | Aorta Pressure (Cubic) | *aortaPVe.m* |
| $P_{ao}$ | $x_{29}$ | Aorta Pressure (Linear) | *aortaLin.m* |
| $P_{vn}$ | $x_{19}$ | Venous Pressure | *venouswoff.m* |
| $P_{at}$ | $x_{14}$ | Arterial Pressure | *arterialwof.m* |

**Table 5.2:** Compliance functions defined for the Simulation model segments and their respective filenames.

$$\dot{p_{17}} = P_{at}(x_{14}) - \left(\frac{R_{pe}}{I_{pe}}\right) p_{17} - P_{vn}(x_{19}) - Pcos(wt) \tag{5.8}$$

$$\dot{x_{19}} = \left(\frac{1}{I_{pe}}\right) p_{17} - \left(\frac{1}{I_{cnin}}\right) p_{21} + S \tag{5.9}$$

$$\dot{p_{21}} = P_{vn}(x_{19}) - P_{bli}(x_{23}) - \left(\frac{R_{cnin}}{I_{cnin}}\right) p_{21} \tag{5.10}$$

$$\dot{x_{23}} = \left(\frac{1}{R_{in}}\right) P_{ht}(x_6) + \left(\frac{1}{I_{cnin}}\right) p_{21} - \left(\frac{1}{R_{in}}\right) P_{bli}(x_{23}) \tag{5.11}$$

$$\dot{x_1} = \frac{p_2}{I_{ht}} \tag{5.12}$$

## 5.2 Model Improvements

A few improvements were made to the previous cardiovascular model [1] to simulate a real human cardiovascular system. One of the changes split the lumped arteries into an aorta component ($P_{ao}(v)$) and the rest of the arteries into a single compliance $C_{at}$. The aorta model is based on experimental pressure-volume data [18, 43, 44].

### 5.2.1 Arterial Compliance

Arterial compliance is the term given to the volume response of the arteries to pressure changes which is defined by equaton 2.1. The blood pumped from the left ventricle is pushed into the outlet cannula which is connected to the aorta. The aorta is cylinderical in shape and is made up of three layers of tissues. These tissues help in smoothing out the pulsatile flow from the ventricle (Windkessel effect). The aorta connects to arteries, arterioles, capillaries, venules, veins and then the blood is pumped back into the heart through the vena cava.

The previous model was made up of a single compliance element ($C_{at}$). The compliance was assumed to be constant at a value of $100\frac{cm^5}{N}$ with a standard deviation of $\pm 2\frac{cm^5}{N}$ which was determined from a study conducted on 10 patients to determine the total systemic arterial compliance [45]. The arterial pressure-volume relationship was modeled with a linear equation as shown in Equation (5.13). The offset of the pressure was chosen to fit physiological human pressures in the arterial system [1]. The offset was chosen to be $-4.13\frac{N}{cm^2}$. The paramter $v$ is the volume ($cm^3$) in the arteries which is a state variable and governed by Equation (5.5).

$$P(v) = C_{Sys}(v) = \frac{v}{100} - 4.13 \ [\frac{N}{cm^2}] \tag{5.13}$$

Recent research on the actual pressure-volume relationship in the human aorta have shown through experiments that the elastic properties of the aorta and arterial tissues are nonlinear and age dependent [43]. As one ages, studies have shown that the arteries tend to become less elastic. Their main function to suppress large pressure spikes from the left ventricule is still carried out. The lower compliance results in an increased nominal aortic pressure and lower efficiency of the aorta.

A recently published study on a comparison of non-linear models of the pressure-volume relationship in the arterial system with a linear model showed that the linear compliance tends to underestimate the end-diastolic pressure (lowest arterial pressure during filling) and overestimates the peak systolic pressure (maximum arterial

pressure during ejection) [44]. The linear compliance model tends to behave well only about the mean arterial pressure. When the volume of blood extends out of the nominal range, the pressures predicted from the linear model are poor.

## 5.3 The Models

The new aorta model is made up of three elements as shown in Figure 5.2. The elements are a resistance, compliance and an inertance. The model is know as a Three Elemental Arterial Model (TEAM). The Single compliance (previous model) is known as the Single Compliance Arterial Model (SCAM) and is also shown in Figure 5.2.

The artifical heart is attached to the aorta by an outlet cannula whose compliance is usually quite low (output cannula is modeled as $C_{blo} = 32\frac{cm^5}{N}$). Therefore the local accelerations and pressure increases due to blood ejection during systole are promient in the aorta. During control actions the blood volume in the aorta can vary causing changes in cardiac output. A similar effect is observed when vascular resistance changes also. When vascular resistance is increased aorta blood volume is observed to increase [46, 47]. Therefore modeling the aorta as an independent element is important since aorta pressures would determine the feasability of the controller during various physiological conditions which effect blood volume distribution. The use of a non-linear model of the aorta also produces a slightly smoother pressure wave [18]. The pressure wave in the aorta will yield similar wave shapes to natural pressure shapes in humans.

## 5.4 Cubic Aorta Model

The aorta model was based on a pressure volume relationship which is found with the aid of experimental human data. There are many studies showing pressure-volume in the aorta [43, 44]. Since heart disease is most common about the age of 36 to 52, the aorta compliance is chosen to match the age group of 47-52 years from the data

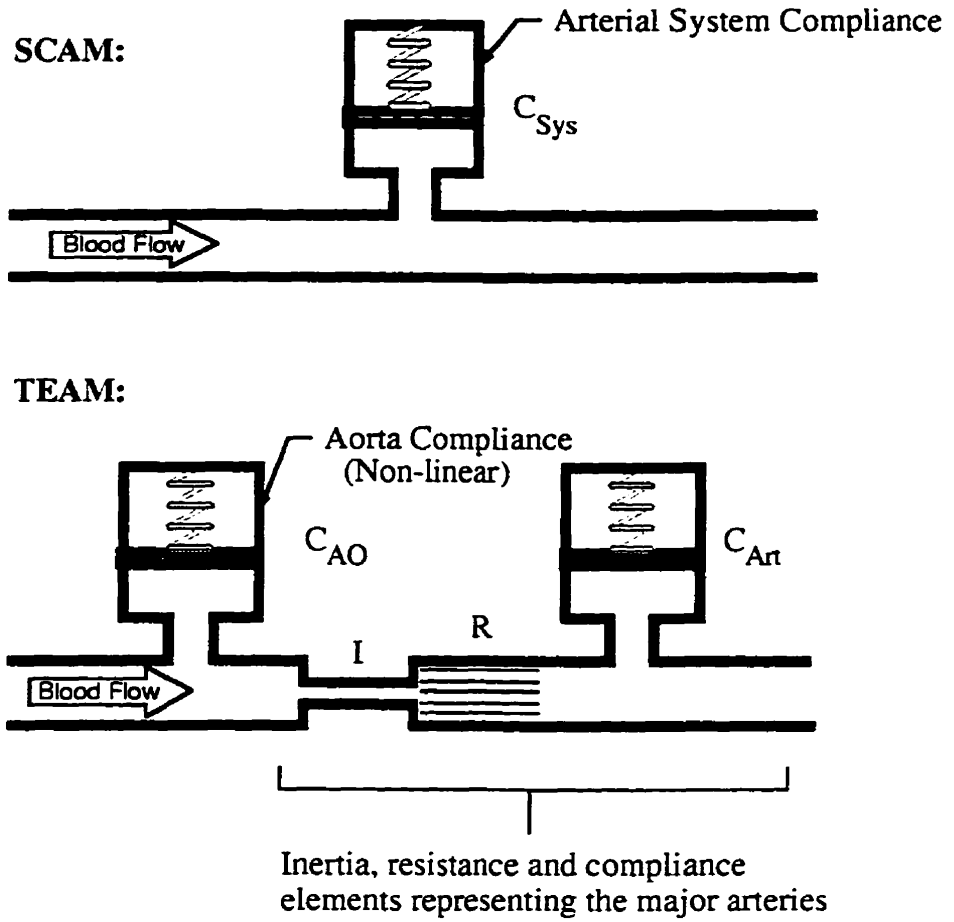


**Figure 5.2:** Schematic representation of the SCAM and TEAM configuration.

stated in [43]. The data was obtained from the graph. The Table 5.3 shows the data points taken from the graph [43] and used to attain the cubic approximation. The points represent pressure in a human aorta segment in terms of volume per unit length ($\frac{cm^3}{cmofaorta}$).

The data is from a disected human cadaver aorta which was closed at one end and a longitude restriction was also applied to prevent the segment from bending [43]. A volume of measured saline solution was then pumped into the segment and the pressure was measured. This relationship is then used to model human aortic behaviour. Although these tests are carried out in-vitro, we assume the behaviour to be applicable to in-vivo also. This trend is not entirely true since disected arteries or

| Aorta P-V data for curve fitting | |
|---|---|
| **Pressure (mm Hg)** | **Volume** $\frac{cm^3}{cm of Aorta}$ |
| 0 | 0 |
| 12.5 | 1.350 |
| 25 | 1.525 |
| 37.5 | 1.725 |
| 50 | 1.975 |
| 62.5 | 2.20 |
| 75 | 2.375 |
| 87.5 | 2.5 |
| 100 | 2.65 |
| 112.5 | 2.75 |
| 125 | 2.850 |
| 137.5 | 2.95 |
| 150 | 3.025 |
| 162.5 | 3.1 |
| 175 | 3.175 |
| 187.5 | 3.225 |
| 200 | 3.275 |
| 212.5 | 3.315 |
| 225 | 3.34 |

**Table 5.3:** The Pressure-Volume data taken to fit cubic function for aorta

tissues tend to lose their internal residual stress and elongation of the segment is also known to take place if very carefull experimental procedures are not undertaken [13].

The Table 5.3 shows volume as a function of length of aorta. The aorta segment used for modeling the ascending aorta which is usually where the outlet cannula is attached. Its length was determined to be approximately about 15 cm. The data was fitted to a cubic function with the aid of a least squares method by minimizing the error between the function and the data points in Table 5.3. The function and code used are listed in the appendix A. where detailed comments and notes are included. The polynomial is shown in Equation (5.14).

$$P(v) = 0.0105v^3 - 0.2543v^2 + 3.1069v + 1.4208 \tag{5.14}$$

The curve was fitted to pressure as a function of volume, since blood volume in the aorta is a state varaible from the bond graph Equation (5.5). The fitted data and the data points from the Table 5.3 are shown in Figure 5.3. When Figure 5.3 is closely observed it can be seen that the data of the pressure-volume relationship is linear to approximatly about 100 mm Hg after which the pressure-volume relationship becomes non-linear [46]. The published value of arterial compliance from Liu in 1990 shows a best fitted curve with an exponential function for the aortic arch segment which is shown in Equation (5.15) [44].

$$V = -44.5e^{-0.0131P} + 39.3 \tag{5.15}$$

The function fit shows that the aorta becomes stiffer at higher pressures. This is due to the middle layer of smooth muscle which when extended to its maximum length becomes more rigid. Simlarly for reduced pressures in the aorta the smooth muscle contracts to its minimum length becoming stiffer until the artery collapses. The collapse of the aortic segment is not simulated at present. This is the actual characteristic of an aortic tube or an elastic vessel.

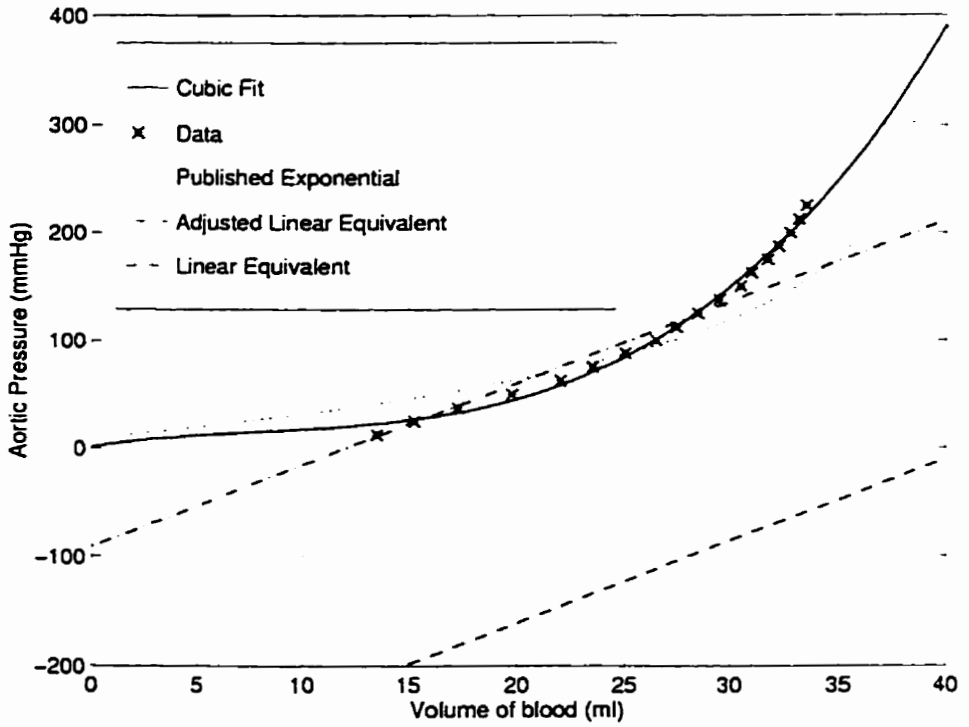


**Figure 5.3:** Aorta Pressure-Volume models simulated and ploted for a typical human. Data taken from King [43] for age group of 36-42 years

The nominal average pressure in the aorta is about 100 mm Hg for a full beat. The simulation shows an aorta average pressure of about 108 mm Hg. The maximum of 120 mm Hg during systolic phase and 80 mm Hg during the diastolic phase.

To determine the rest of the lumped artery parameters the fitted curve of the aorta was approximated as a linear best fit to find an approximate compliance value of the aorta. This is shown in Figure 5.3 as the dashed-dotted line. The linear fit of the cubic function yielded an aortic compliance of approximately $10\frac{cm^5}{N}$ from determining the slope of the dashed-dotted line. This value of aortic compliance was subtracted from the total systemic arterial compliance of $100\frac{cm^5}{N}$ to produce the value of $C_{at}$ to be $90\frac{cm^5}{N}$. The offset of $C_{at}$ was set to be $-4.13\frac{N}{cm^2}$ because little or no variation was observed in the arterial pressure range. The lumped arterial system was modeled as a linear system as shown in Equation (5.16).

$$P_{at}(v) = \frac{v}{90} - 4.13\ [\frac{N}{cm^2}] \tag{5.16}$$

### 5.4.1 Resistance Element

The model was simulated without the aid of the resistance element to show the oscillations produced from the change in compliance value of the outlet cannula and the aorta segment. The oscillations produced overide the shape and also distort the maximum and minimum pressures in the aorta. The outlet cannula oscillations also are seen to be higher without the aortic resistance. The oscillations produced between the outlet cannula and aorta can be damped by the addition of a resistive element [48, 49]. Figure 5.4 shows the simulated model at nominal conditions with the resistive element $R_{ao}$ set to zero.

The oscillations can also be seen to be apparent in the arterial segment as in Figure 5.5. This is seen as the changes in the pressure caused from the large amplitude of the pressure wave in the outlet cannula. The aorta is seen to be more sensitive

to changes in blood volume than the arterial segment due to the cubic modeling.

The resistance element was tuned to provide a smooth pressure wave form and a more accurate flow wave shape as compared to [13]. This was done by observing the change in aorta flow and also the the pressure while changing the resistance value. The final resistance value selected yielded aorta pressures and flow rate similar to the human circulatory system. The Figure 5.6 shows the aorta parameters with the resistance element set to $R_{ao} = 0.0011 \frac{Ns}{cm^5}$. It shows that the pressure waveform is smoother and also the dicrotic notch can be seen. The dicrotic notch is a visible phenomenon in human physiology which occurs when the output valve is shut and a sharp pressure drop is seen briefly. Then a slight rise in pressure is generally seen due to the elasticity of the valve (which is not seen here since valves are not modeled as elastic membranes).

### 5.4.2 Inertance element

The inertance element was added to create dynamically decoupled states for the aorta and the arterial segment. The inertance allows the state $x_5$, which is the volume in the aorta, and the state $x_7$, the volume in the arterial segment excluding the aorta, to be independent of each other.

#### Estimation of Aorta inertance

The value of $I_{ao}$ was selected based on typical length and cross sectional area estimates and Equation (2.3). The cross sectional area of the aorta was attained from [50] which was 1.33 inches in diameter. The density of blood is assumed to be approimately the same as water. Then with the aid of Equation (2.3) we attain a inertance value of $1.705 \times 10^{-5} \frac{Ns^2}{cm^5}$. This was compared with a different models published values from [51] and found to be within a satisfactory range.

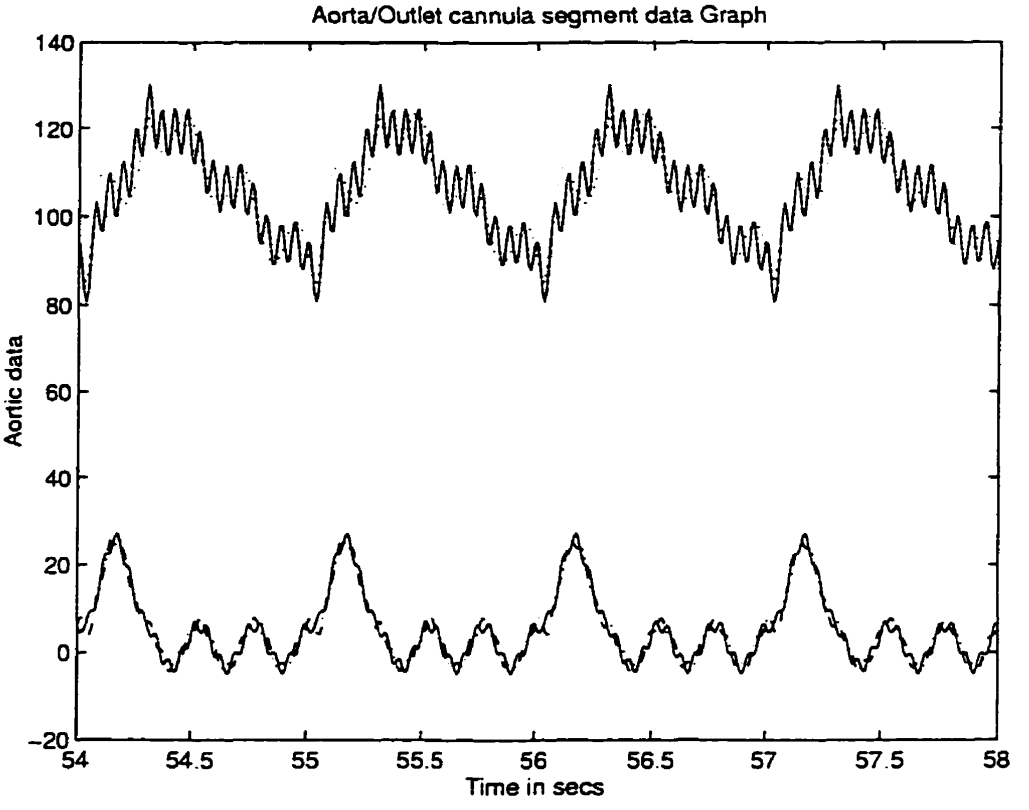


**Figure 5.4:** Simulated Aorta parameters for $R_{ao} = 0\frac{Ns}{cm^5}$ at steady state (- Aorta pressures [mm Hg], .. Outlet cannula pressure [mm Hg], -.- aorta flow rate $[\frac{L}{min}]$, - outlet cannula flow rate (lower line) $[\frac{L}{min}]$)

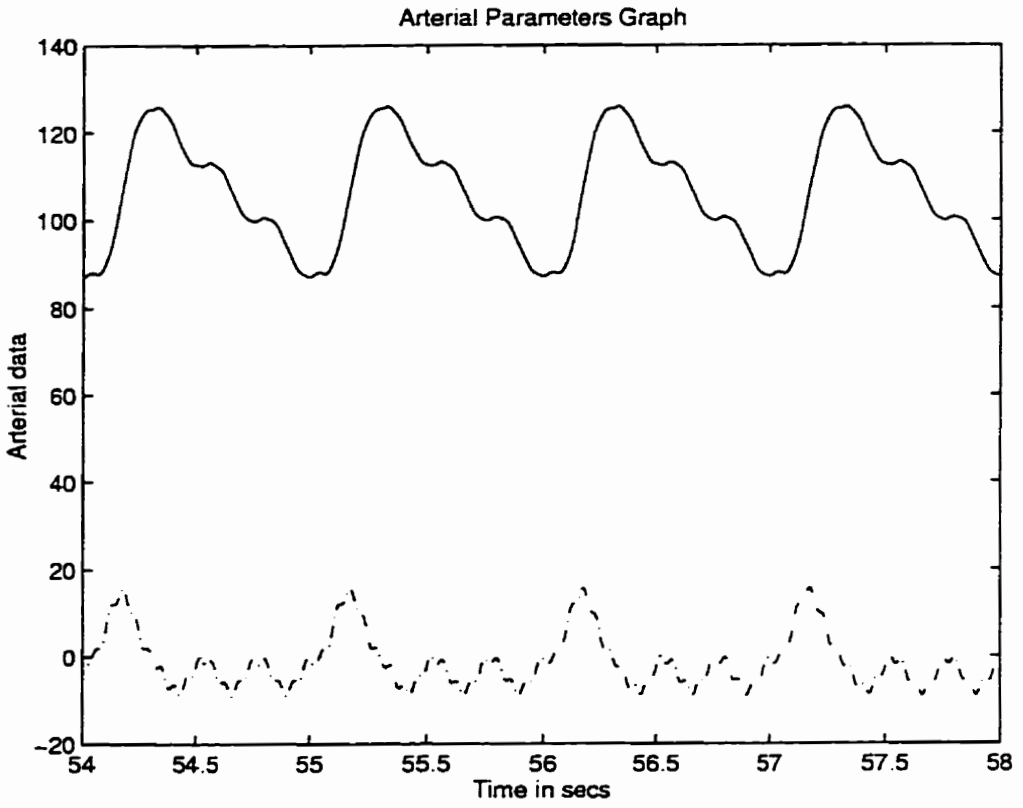


**Figure 5.5:** Simulated Arterial parameters for $R_{ao} = 0\frac{Ns}{cm^5}$ at steady state (- Arterial pressures [mm Hg], -.- arterial flow rate $[\frac{L}{min}]$)

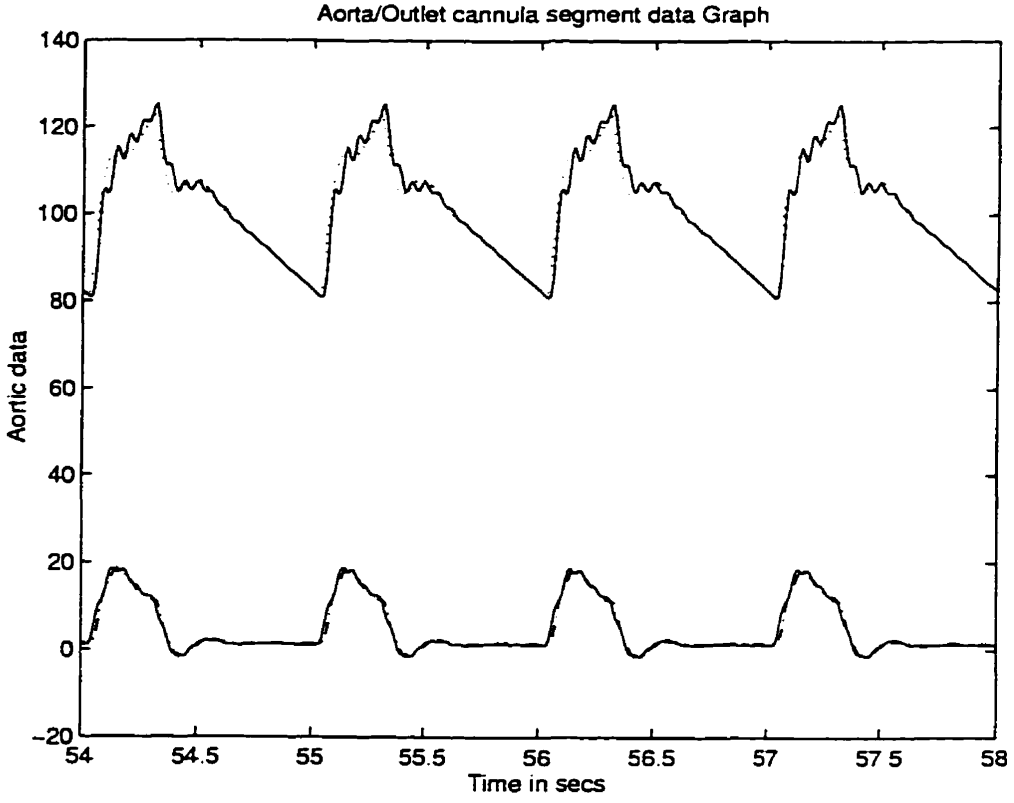


**Figure 5.6:** Simulated Aorta/outlet cannula segment data for $R_{ao} = 0.0011 \frac{Ns}{cm^5}$ at steady state (- Aorta pressures [mm Hg], .. Outlet cannula pressure [mm Hg], -.- aorta flow rate $[\frac{L}{min}]$, - outlet cannula flow rate (lower line) $[\frac{L}{min}]$)

## 5.5 Comparison of Aorta models

Since the SCAM model cannot be directly compared to the TEAM model, the SCAM model compliance was split as shown in Figure 5.7 and labeled as $C_2$ into two compliance elements as shown in Figure 5.8, while maintaining the overall arterial compliance as was determined in the SCAM model in Equation (5.16).

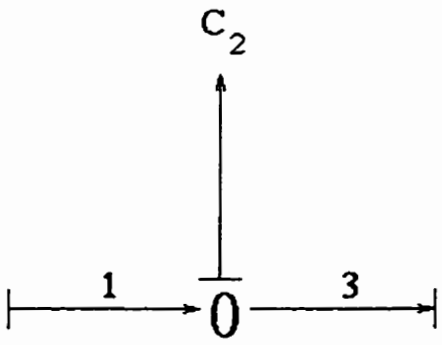


**Figure 5.7:** Single Element Compliance model

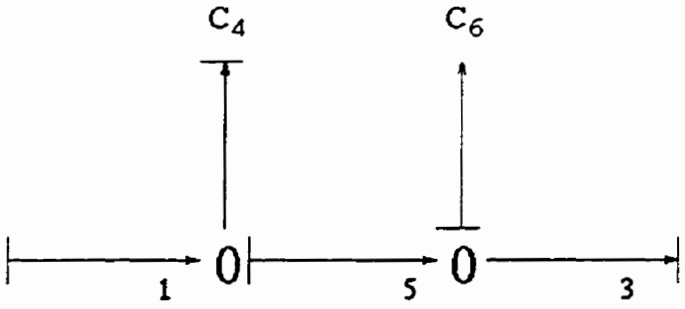


**Figure 5.8:** Equivalent split Compliance model

The equivalent model in Figure 5.8 is shown to be split into two compliance, one representing the aorta ($C_4$) the other compliance representing the rest of the lumped arterial compliance ($C_6$). The $C_4$ element is not a state variable and is therefore a function of state variable of element $C_6$. The bond graphs in Figure 5.7 and Figure 5.8 with their respective compliance offsets $A_1..A_4$ and $A_6$ were solved individually which yielded SCAM Equation (5.17) and an equivalent SCAM model in Equation (5.18).

$$e_1 = \frac{1}{C_2}(q_1 - q_3) + A_2 \tag{5.17}$$

$$e_1 = \frac{1}{C_4 + C_6}[(q_1 - q_3) + (A_6C_6 + C_4A_4)] \tag{5.18}$$

The equations were then equated since the boundary conditions must be the same for both models. The two equations were solved simultaneously yielding a compliance Equation (5.19) and an offset Equation (5.20).

$$C_4 = C_2 - C_6 \tag{5.19}$$

$$A_4 = \frac{1}{C_4}[A_2(C_6 + C_4) - C_6A_6] \tag{5.20}$$

The value of $C_2$ is $100\frac{cm^5}{N}$ as stated earlier from published values. The value of $C_6$ was maintained at $90\frac{cm^5}{N}$ as in the TEAM model presently been used. Therefore with the aid of Equation (5.19) we can calculate $C_4$ to be $10\frac{cm^5}{N}$.

Similarly, we know the offset of $A_6$ to be $-4.13\frac{N}{cm^2}$ which was used in the TEAM model Equation (5.16). The value of $A_2$ was initially given to be $-4.13\frac{N}{cm^2}$ also. Using Equation (5.20) we solve for $A_4$ which is $-4.13\frac{N}{cm^2}$.

The function given in Equation (5.21) is the equivalent aortic model and it was plotted in Figure 5.3 as the dashed line. The equivalent linear aorta model of the SCAM can be seen to be poor when compared to the TEAM aorta model and data points of a real aorta. The linear approximation can be made to better fit the aorta data by changing the calculated offset $A_4$.

$$P_{ao}^{Linear}(v) = \frac{v}{10} - 4.13 \tag{5.21}$$

The offset $A_4$ was changed to $-1.21\frac{N}{cm^2}$ by visual inspection for a better fit of the data. The offset Equation (5.20) was observed to be very sensitive to changes in the

offset value of $A_6$. This can be shown if we assume $A_6 = A_2 + \Delta\epsilon$. Then substituting $A_6$ using Equation (5.20) and solving for $A_4$ which results in Equation (5.22).

$$A_4 = A_2 - [\frac{C_6}{C_2}]\Delta\epsilon \tag{5.22}$$

Since $C_6$ and $C_2$ are known values from above and the fraction $\frac{C_6}{C_2} = 9$. a small change in the value of $A_6$ implies a large change in $A_4$. Since the corrected aorta linear model offset is $-1.21\frac{N}{cm^2}$. the value of $A_6$ can be calculated to be $-1.44\frac{N}{cm^2}$ from Equation (5.22). This is a difference of $-0.31\frac{N}{cm^2}$ between the previous value of $A_6$ and its present value. When the TEAM total arterial compliance offset is changed to $-4.45\frac{N}{cm^2}$ the aorta SCAM offset attained would be $-1.2\frac{N}{cm^2}$ which is shown in Equation (5.23).

$$P_{ao}^{SCAM}(v) = \frac{v}{10} - 1.2. \tag{5.23}$$

The split SCAM and TEAM models were then simulated to show their differences. The TEAM produces two pressure outputs which are the aorta pressure and the total arterial pressure. while the SCAM and the equivalent TEAM produce a single output because the states are not independent. In the equivalent TEAM model the aorta volume is a function of the arterial volume. These are shown for the nominal condition in Figure 5.9.

The Figure 5.9 shows the TEAM pressures. during systole the pressures rise to maximum of about 120 mm Hg and during diastole the pressure drops to a minimum of 80 mm Hg. The dicrotic notch is also visible. This visible trait is mainly due to the resistive element which dampens out the oscillations produced by the cannula.

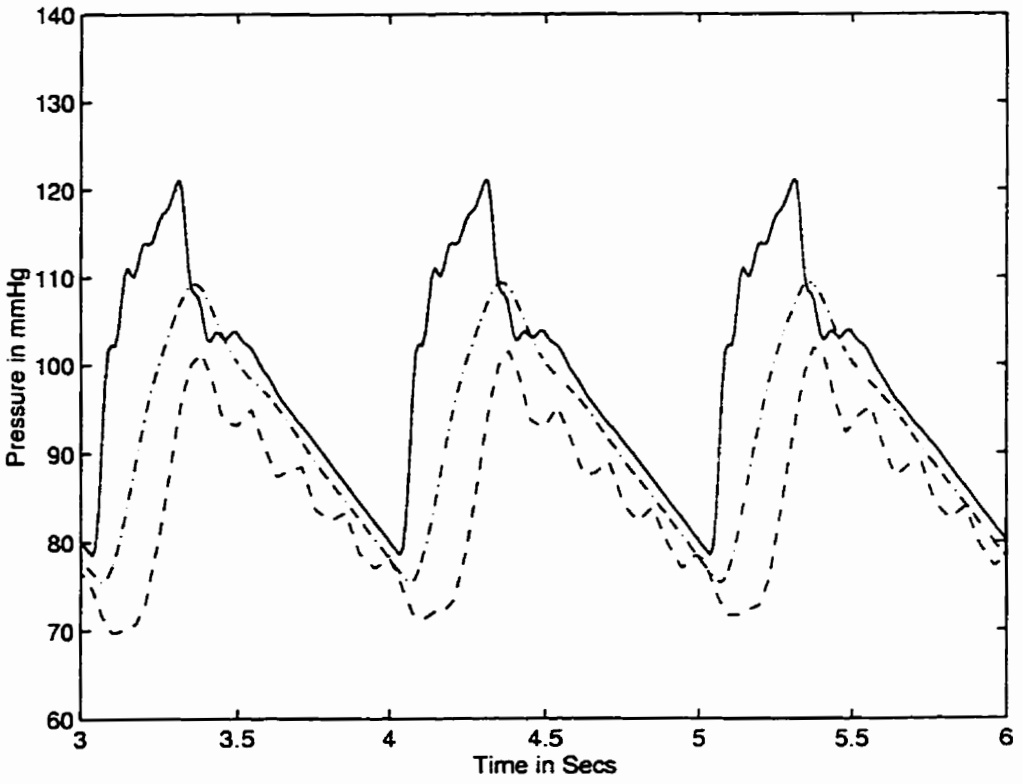


**Figure 5.9:** The simulated pressures for the TEAM and SCAM for nominal conditions(- aorta pressures TEAM [mm Hg]. -.- arterial pressures TEAM [mm Hg], - SCAM Simulated pressures [mm Hg])

## 5.6 Comparsion of Physiological values

The models were simulated for various aorta blood volumes. This was done by changing the peripheral resistance. When peripheral resistance is increased the blood tends to pool in the aorta and hence increase the steady state aorta blood volume. When peripheral resistance is decreased aorta blood volume is also decreased.

When blood volume deviates from its nominal value (mean blood volume) in the aorta the pressure also varies. In the best linear fit case the pressure-volume relationship is expressed by the Equation (5.23) which is used to simulate the performance of the aorta model. This is compared to the cubic aorta TEAM model in Equation (5.14). The Figure 5.10 shows that for a decrease in the peripherial resistance the aorta volume also decreases. The cubic aorta pressure is seen to reach a maximum of about 103 mm Hg at systole and at diastole it reach a minimum pressure of 60 mm Hg. While for the same change in perpherial resistance, the Figure 5.11 shows the result of the pressures in the aorta segment for the linear Equation (5.23). The systolic maximum pressure is seen to be about 110 mm Hg and diastolic minimum is about 77 mm Hg. When Figure 5.3 is used as an aid it can be seen that when blood volume is decreased in the aorta the linear and cubic P-V functions deviate. The cubic is seen to produce a lower pressure than the linear. At lower volumes we see very little difference between the linear and cubic estimates of aortic pressure due to the linear relationship at pressures lower than 100 mm Hg.

When the peripherial resistance is increased, the blood volume in the aorta segment is increased. This was again simulated for both the cubic and the linear aorta functions to show the differences. The Figure 5.12 shows Equation (5.14) when simulated for an increase in blood volume. The pressure yielded by the cubic shows the maximum systolic pressure of 153 mm Hg and for the minimum diastolic pressure of 110 mm Hg. The Figure 5.13 shows the linear functions maximum pressure at systolic to be 137 mm Hg and the minimum diastolic pressure to be 115 mm Hg.

The difference between the linear and cubic model is quite large. This can again be seen in Figure 5.3 by noticing that at higher blood volumes the cubic and the linear function deviate strongly, where the cubic function increases steeply as compared to the linear function as blood volume increases.

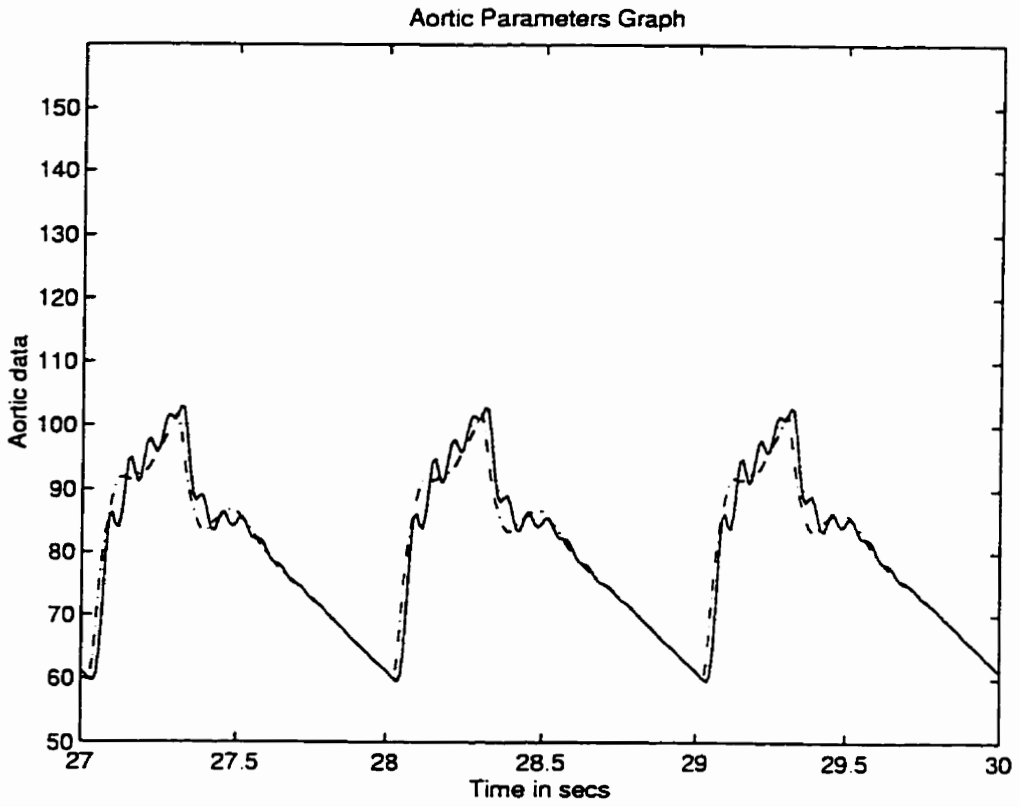


**Figure 5.10:** Simulated aorta pressures for cubic aorta model for decreased peripherial resistance ($R_{pe} = nominal \times 0.7$). (- aorta pressures [mm Hg], -.- outlet cannula pressure [mm Hg])

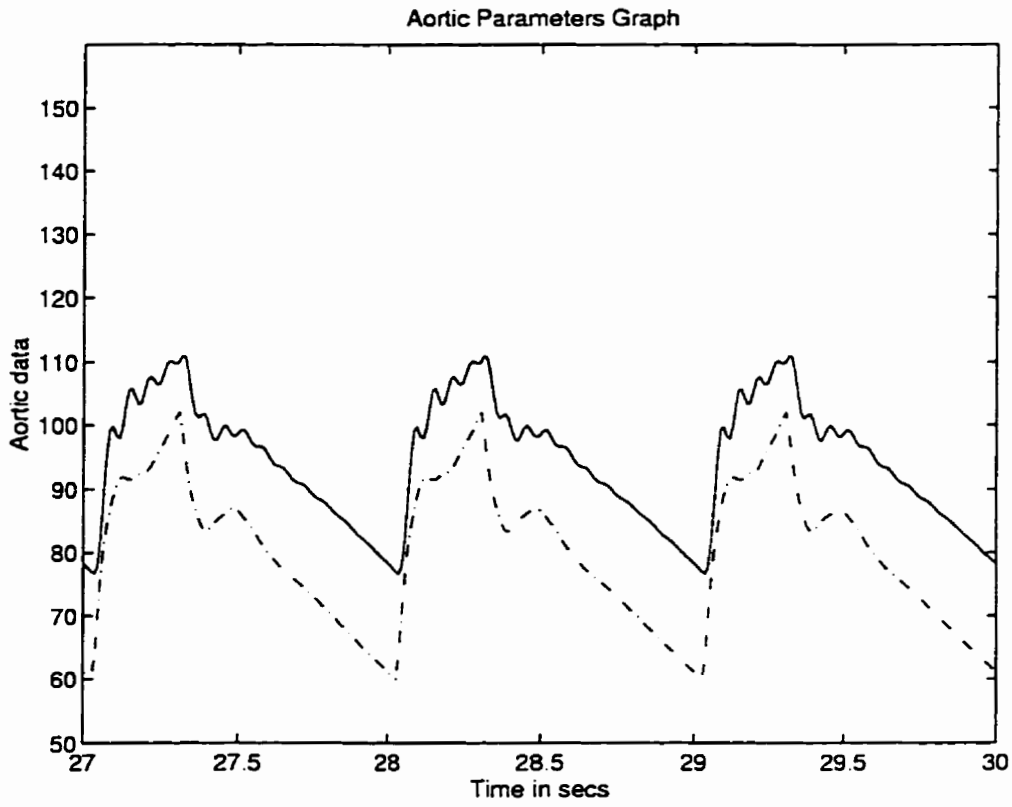


**Figure 5.11:** Simulated aorta pressures for linear aorta model for decreased peripherial resistance ($R_{pe} = nominal \times 0.7$). (- aorta pressures [mm Hg]. -.- outlet cannula pressure [mm Hg])

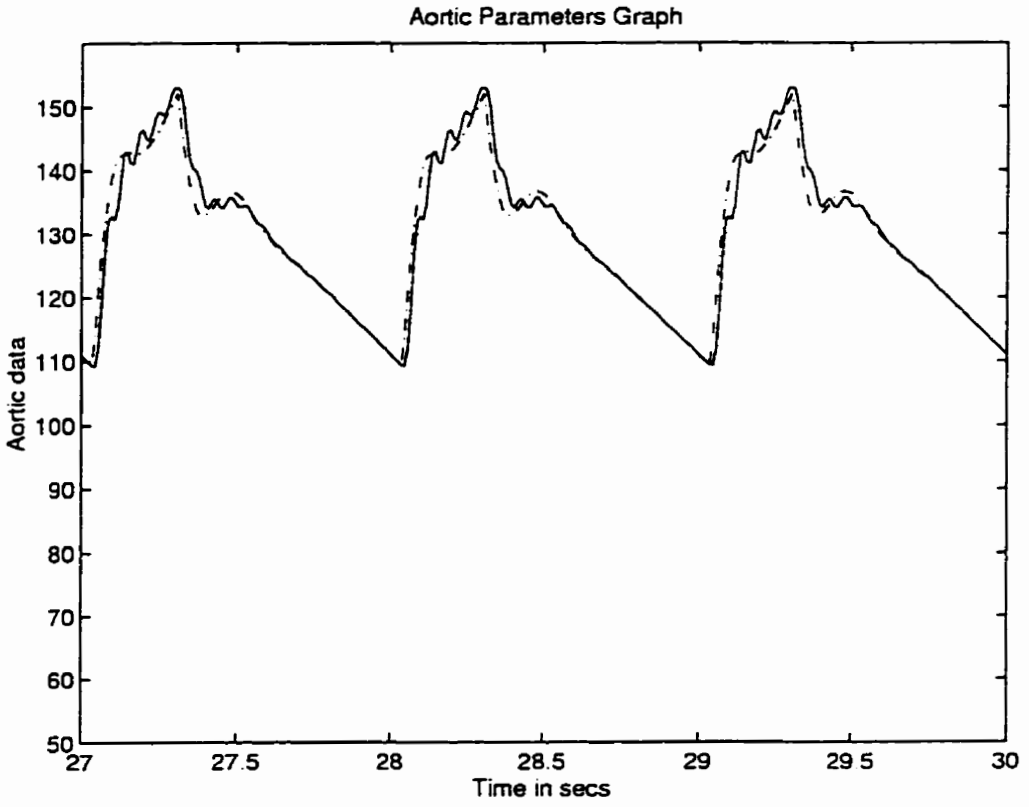


**Figure 5.12:** Simulated aorta pressures for cubic aorta model for increased peripherial resistance ($R_{pe} = nominal \times 1.4$). (- aorta pressures [mm Hg]. -.- outlet cannula pressure [mm Hg])

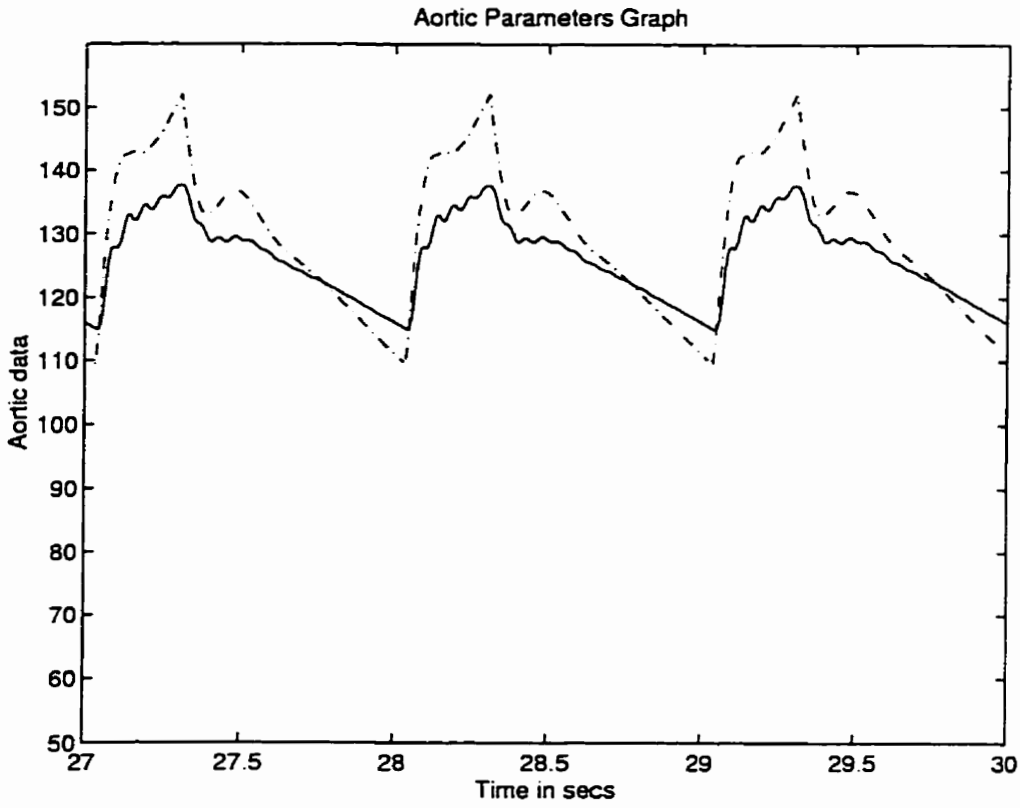


**Figure 5.13:** Simulated aorta pressures for linear aorta model for increased peripherial resistance ($R_{pe} = nominal \times 1.4$). (- aorta pressures [mm Hg]. -.- outlet cannula pressure [mm Hg])

| Elements of Circulatory Model | | | |
|---|---|---|---|
| **Description** | **Variable** | **Value** | **Units** |
| Artificial Heart Resistance | $R_{ht}$ | 0.47 | $\frac{Ns}{cm^5}$ |
| Artificial Heart Inertance | $I_{ht}$ | 0.0038 | $\times 100kg$ |
| Outlet Cannula Inertance | $I_{cnot}$ | 0.0000263 | $\frac{Ns^2}{cm^5}$ |
| Inlet Cannula Inertance | $I_{cnin}$ | 0.0000132 | $\frac{Ns^2}{cm^5}$ |
| Inlet Valve Resistance | $R_{in}$ | 0.0008 | $\frac{Ns}{cm^5}$ |
| Outlet Valve Resistance | $R_{ot}$ | 0.0008 | $\frac{Ns}{cm^5}$ |
| Aorta Inertance | $I_{ao}$ | 0.00003401 | $\frac{Ns^2}{cm^5}$ |
| Aorta Resistance | $R_{ao}$ | 0.0011 | $\frac{Ns}{cm^5}$ |
| Periperial Resistance | $R_{pe}$ | 0.0125 | $\frac{Ns}{cm^5}$ |
| Periperial Inertance | $I_{pe}$ | 0.0275 | $\frac{Ns^2}{cm^5}$ |
| Outlet Cannula Resistance | $R_{cnot}$ | 0.0 | $\frac{Ns}{cm^5}$ |
| Intlet Cannula Resistance | $R_{cnin}$ | 0.0 | $\frac{Ns}{cm^5}$ |

**Table 5.4:** Nominal circulatory parameter values for compliance, inertance and resistance elements with units

## 5.7 Nominal Circulatory Simulation

The nominal system was setup with the parameter values for simulation from Table 5.4 and 5.5. The controller is active during this process and its response is minimal, since the circulatory system is at steady state from initial conditions.

The simulation is conducted for 60 seconds on a SGI work station. The initial conditions of the simulation are given in the file *fxlvad.m*. Most values are taken from the Master's thesis work of Tan, 1996 [1].

### 5.7.1 Simulated results

When the circulatory model was run under nominal conditions, the following results were obtained and graphed with the aid of function *pdata_fixed.m*. In Figure 5.15

| Segments of Circulatory System | | | |
|---|---|---|---|
| **Segment** | **Variable** | **Compliance** $\frac{cm^5}{N}$ | **Offset** $\frac{N}{cm^2}$ |
| Artificial Heart Chamber | $C_{ht}$ | 28 | -0.178 |
| Outlet Cannula | $C_{cnot}$ | 32 | -5.24 |
| Arterial | $C_{at}$ | 90 | -4.13 |
| Venous | $C_{vn}$ | 3500 | -0.4 |
| Inlet Cannula | $C_{cnin}$ | 32 | -2.62 |

**Table 5.5:** Nominal circulatory compliance function values and offsets

the pressures across the output valve have a positive gradient during the systolic phase and a negative gradient during the diastolic phase. When the pressure gradient is favourable (positive) the output valve is opened (passive unidirectional valves depend on the pressure gradient). When the pressure gradient across the valve is negative the outlet valve is closed shut until the pressure gradient is favourable again. The nominal circulation produces a 20 mm Hg difference in pressure across the output valve during systole and -95 mm Hg during diastole.

Figure 5.16 shows the data for the aorta segment of the model. The simulation model shows a value of 80 mm Hg for end diastole and 120 mm Hg at peak systole pressure. The pressure in the outlet cannula is seen to be very close to the pressure values of the aorta. The outlet cannula has lower pressure oscillations because it has a higher compliance than the aorta segment. The resistance element in the aorta also dampens out the oscillations. The average pressure in the outlet cannula is 111.6 mm Hg during systolic process. The flow rate can be seen to peak at systolic phase of the beat to a value of about $19\frac{L}{min}$ while the diastole process the flow rate is maintained at a constant rate at about $2\frac{L}{min}$ which is a result of the Windkessel effect of the aorta.

Figure 5.17 shows the arterial segment data for the circulatory system. The arterial pressures can be seen to be linear and very litttle oscillations can be seen in the

waveform from the outlet cannula or the aorta segment. The lumped arterial pressures are 75 mm Hg at end diastole and 115 mm Hg at peak systole pressure. The flow rate is negative because the flow rate represented here is the flow into and out of the compliance element $C_{at}$ and hence can have a negative value which is shown schematically in Figure 5.14. The waveform shape of the flow rate is very similar to the aorta flow rate because it is a continuous system. Also, close examination of the arterial pressure shows that there is a time delay between the start of the aorta pressure rise and the arterial pressure due to the length of the cannula and aorta segments.

Figure 5.18 shows the peripheral flow through the system. The data is the same as the cardiac output from the heart which is required to be held constant by the FLC at a value preset at $4.7\frac{L}{min}$. This is the flow rate seen by the physiological system during control. This parameter is the most important parameter for maintaing the function of the body organs and cells. If this parameter drops too low for an extended period of time it can cause permanent damage to tissues and brain cells which may lead to death or other severe complcations [52].

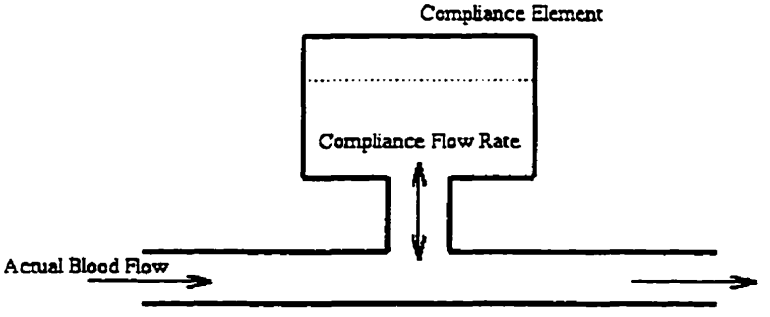


**Figure 5.14:** Flow rate of a compliance element

Figure 5.19 shows the venous and inlet cannula segment data. The venous segment pressure in nominally about 18 mm Hg with a very low frequency of oscillation produced by the pumping of the heart. Hence the oscillation frequency is based on the

beat rate. This pressure is slightly high because we have included the right side of the heart in the model of the venous segment. Hence the pressure value is actually the pressure seen in the left atrium of the heart. since it is this pressure that will activate the inlet valve for the artificial heart device. The pressure in the veins can easily be changed by changing the compliance relationship in the venous segment shown in Table 5.5. The inlet cannula pressure is very oscillatory because no resistance was included. The high frequency of oscillation is observed briefly during the systolic phase because the inlet valve to the artificial heart is closed and hence the pressure is reflected back into the system. This causes oscillations in the inlet cannula known as the water hammer effect. An increase in these oscillation can cause failure or wearing (cyclic loading) of the inlet value after prolonged use. Once the inlet valve opens it is observed that the oscillations dampen out until the valve closes again for systole. The average value of the cannula pressure is about the same as for the venous segment at 19.6 mm Hg during diastole. The blood flow rate oscillates because of the oscillations in pressure in the inlet cannula. The blood flow and the cannula oscillations can be dampened with the addition of a small resistance to the element $R_{cnin}$. set at $0.002\frac{cm^5}{\lambda}$ which was tuned from simulation and observation of the venous parameters.

Figure 5.20 shows the pressure difference between the inlet cannula and the artificial heart. The pressure shows that it is positive during the diastole at a value of about 8 mm Hg and a negative gradient for the systole at a value of -115 mm Hg. The large dip seen in the negative gradient is generated from the high oscillatory pressures in the inlet cannula. The average pressure difference in the inlet cannula pressure during diastole is 7.565 mm Hg.

The Figure 5.21 shows the artificial heart states. During systole the average pressure in the heart raises to 128.7 mm Hg and during diastole an average pressure of 12.04 mm Hg. The peaking of the pressure during systole is due to the piston momentum which is still moving when both inlet and outlet values are closed for a brief period as seen in Figure 5.22 by the gap between systolic flow and diastolic flow.

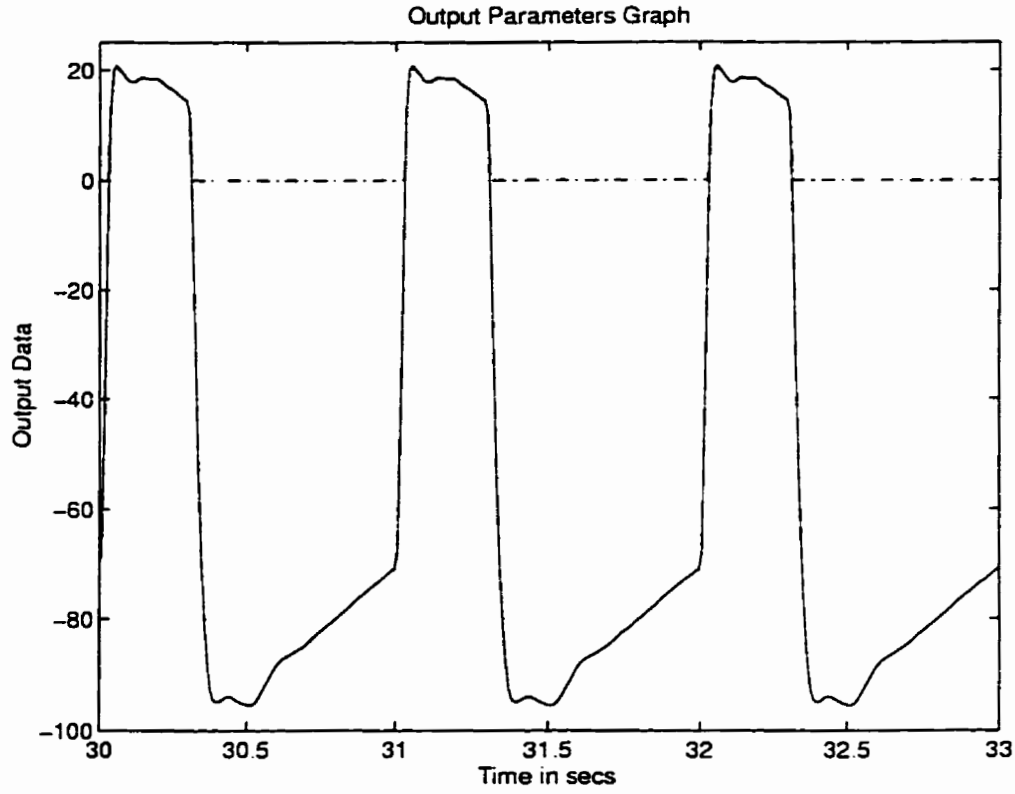


**Figure 5.15:** Nominal condition output valve data ( - Pressure graient across outlet valve [mm Hg], -.- Flow rate across outlet valve $[\frac{L}{min}]$)

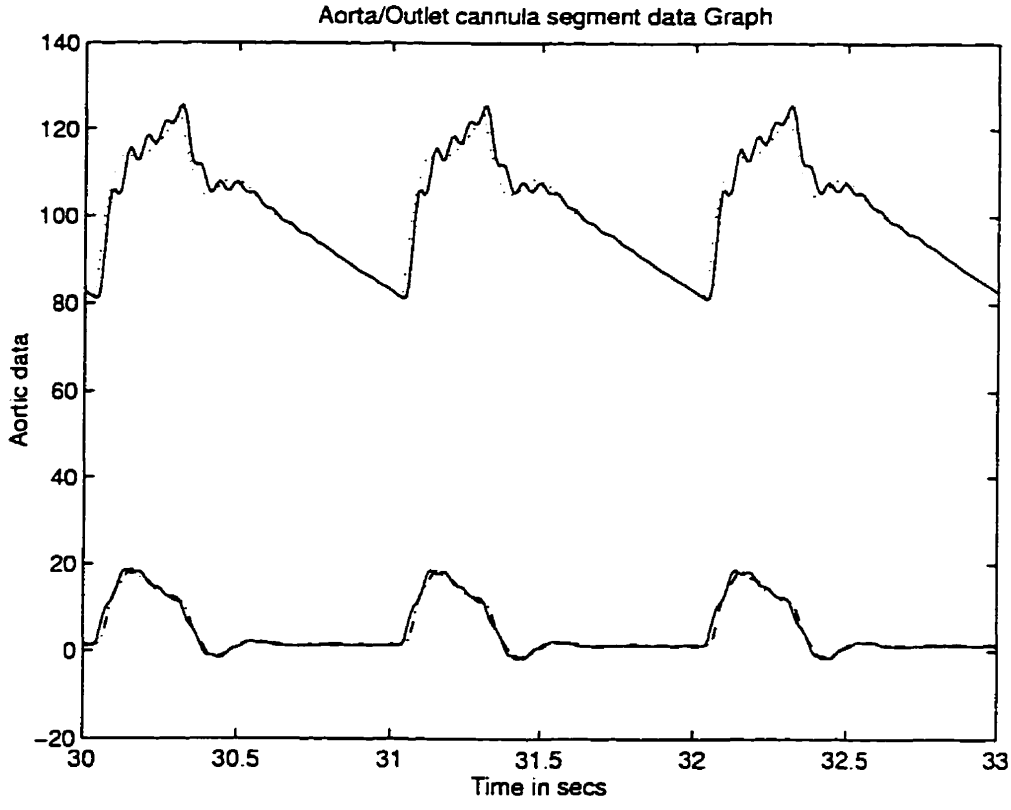


**Figure 5.16:** Nominal condition aorta/outlet cannula segment data ( - aorta pressure [mm Hg], .. outlet cannula pressure [mm Hg], -.- aorta flow rate $[\frac{L}{min}]$, - outlet cannula flow rate (lower line) $[\frac{L}{min}]$)

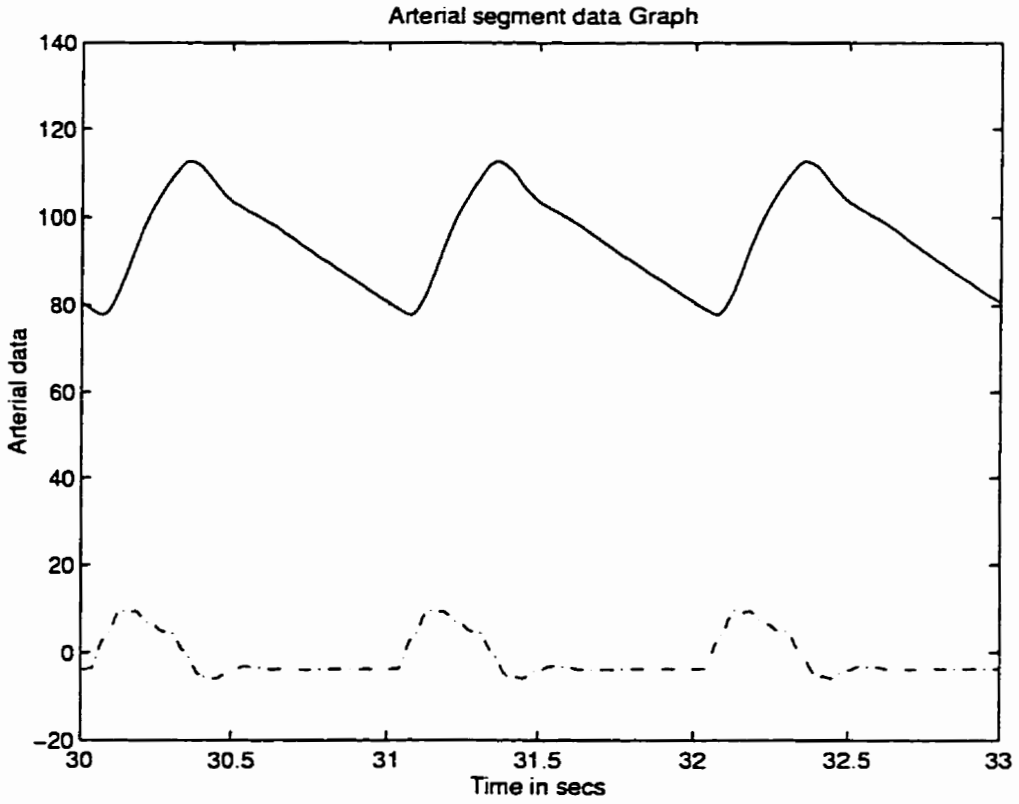


**Figure 5.17:** Nominal condition arterial segment data ( -.- arterial pressure [mm Hg], -.- arterial flow rate $[\frac{L}{min}]$)

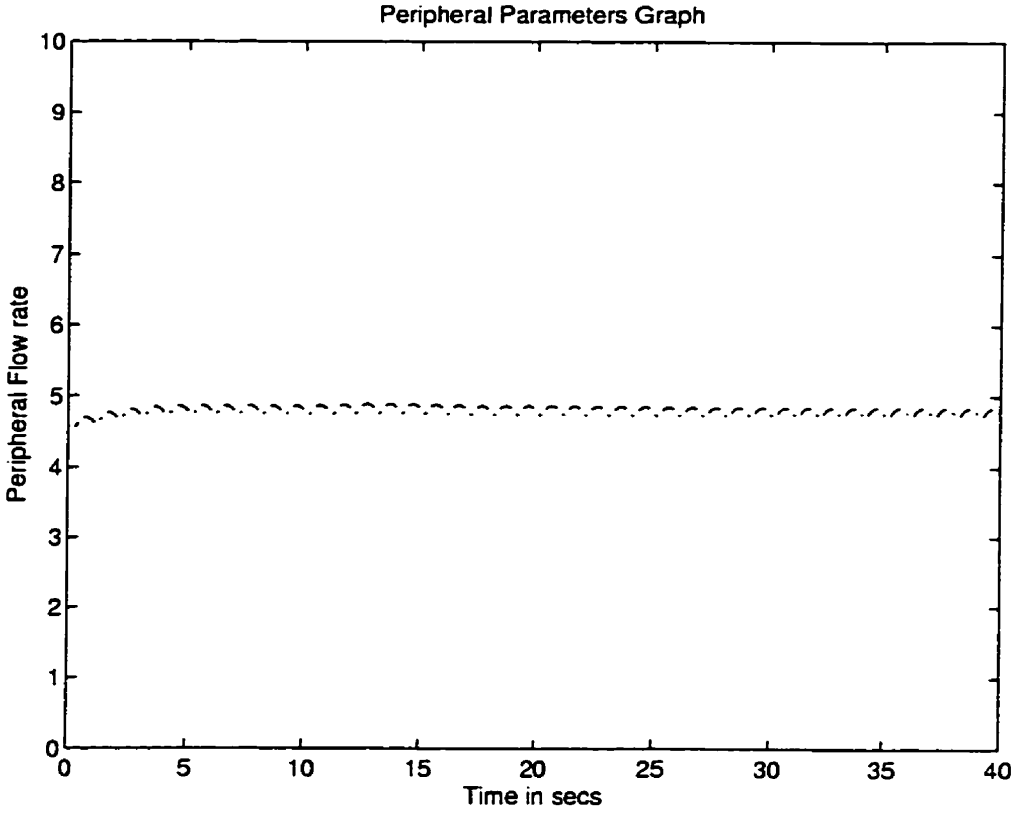


**Figure 5.18:** Nominal Peripheral flow ( - peripheral flow rate $[\frac{L}{min}]$)

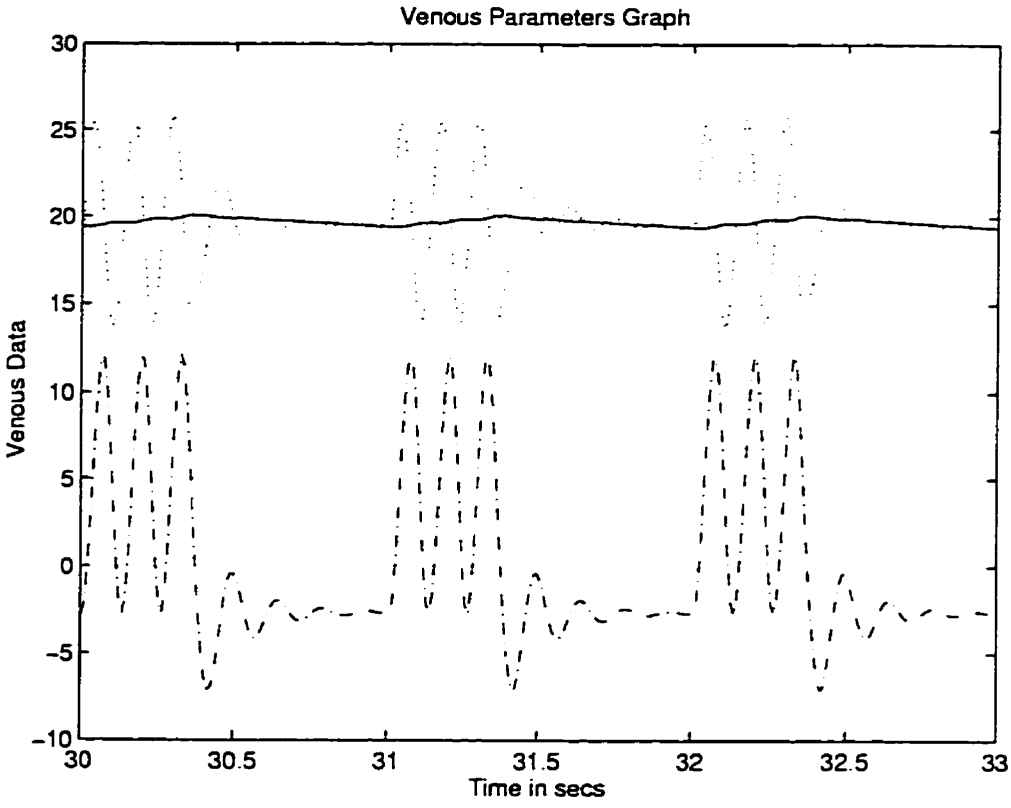


**Figure 5.19:** Nominal condition venous/inlet cannula segment data ( - venous pressure [mm Hg], .. inlet cannula pressure [mm Hg]. -.- inlet cannula flow rate $[\frac{L}{min}]$)

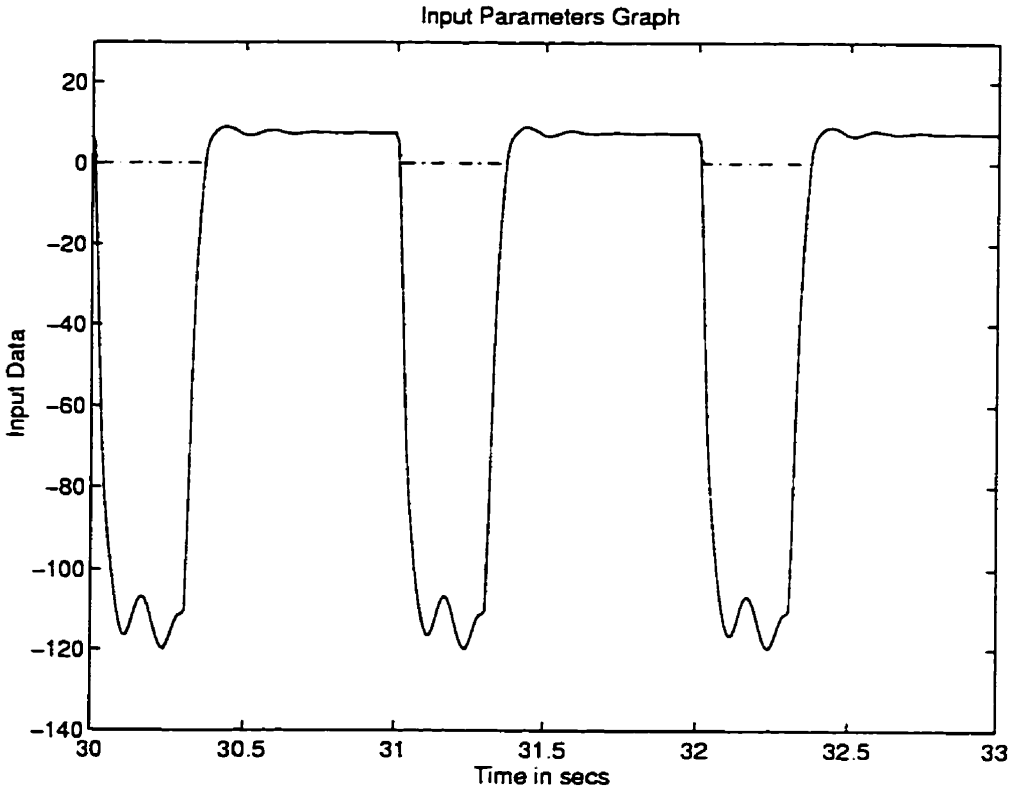


**Figure 5.20:** Nominal condition inlet valve data data ( - pressure gradient across inlet valve [mm Hg], flow rate across inlet valve $[\frac{L}{min}]$)

Figure 5.23 shows the artificial heart volume of blood. The volume of blood in the heart is measured in $ml$ and is seen to oscillate with a range of 75-80 ml. The volume is seen to be slowly decreasing. This is because of the slight error that is produced between the estimated pump output and the actual pump output since the controller is active during this simulation. This volume can be shifted by adjustment of the compliance of the heart ($C_{ht}$). diastolic timing or the diastolic force $F_{dia}$. The piston position at start is selected arbitrarily. hence the reference start position and volume can be set at any prefered value. Therefore the offset in blood volume can be raised by changing the reference piston position. The small drift seen in the nominal condition is because the starting force was set to 41.13 N. The controller shows that at steady state this value is slightly higher at 41.21 N due to the estimated pump output. The same information from this figure can be viewed in the Pressure-Volume Loop of Figure 5.24

Figure 5.22 shows the flow rates into and out of the artificial heart. The flow rate from the heart during systole which is about $18\frac{L}{min}$ after peak ejection. The flow rate during the diastole phase which has a nominal value $7.5\frac{L}{min}$. There is a visible period when both the inlet and outlet valves are closed. This also results in a pressure increase in the artificial heart parameters during the end of systole. The Figure 5.24 shows the pressure volume loop of the heart which shows the pressures in the heart and the volume of blood during every beat of the simulation.

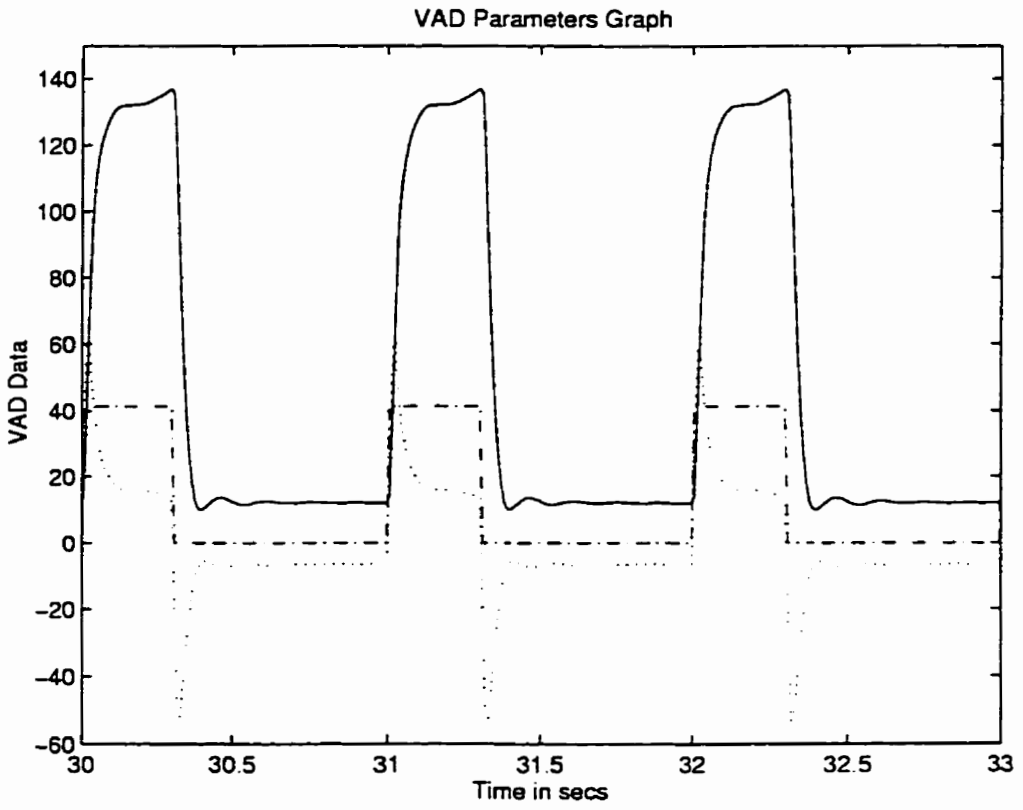


**Figure 5.21:** Nominal condition artificial heart data ( - internal artificial heart pressure [mm Hg]. -.- Force acting on the artificial heart [N]. .. velocity of artificial heart piston $[\frac{cm}{s}]$)

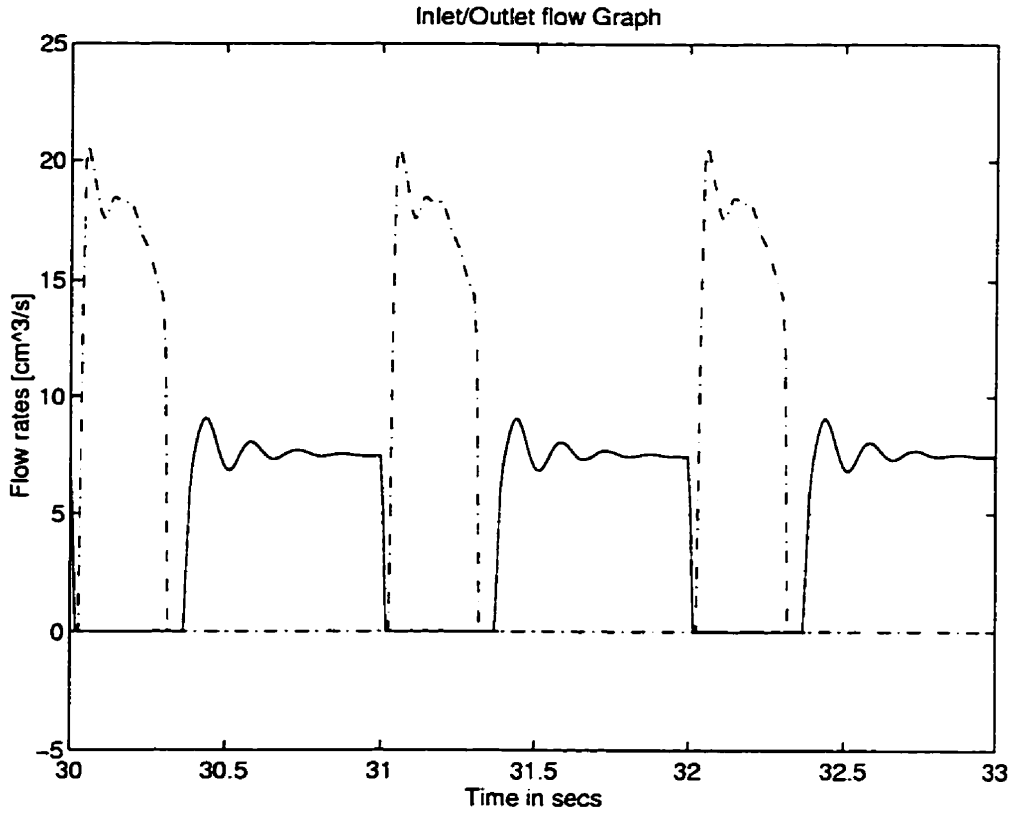


**Figure 5.22:** Nominal condition artificial heart inlet/outlet flow data ( -.- systolic flow rate from artificial heart $[\frac{L}{min}]$, - diastolic flow rate into artificial heart $[\frac{L}{min}]$)

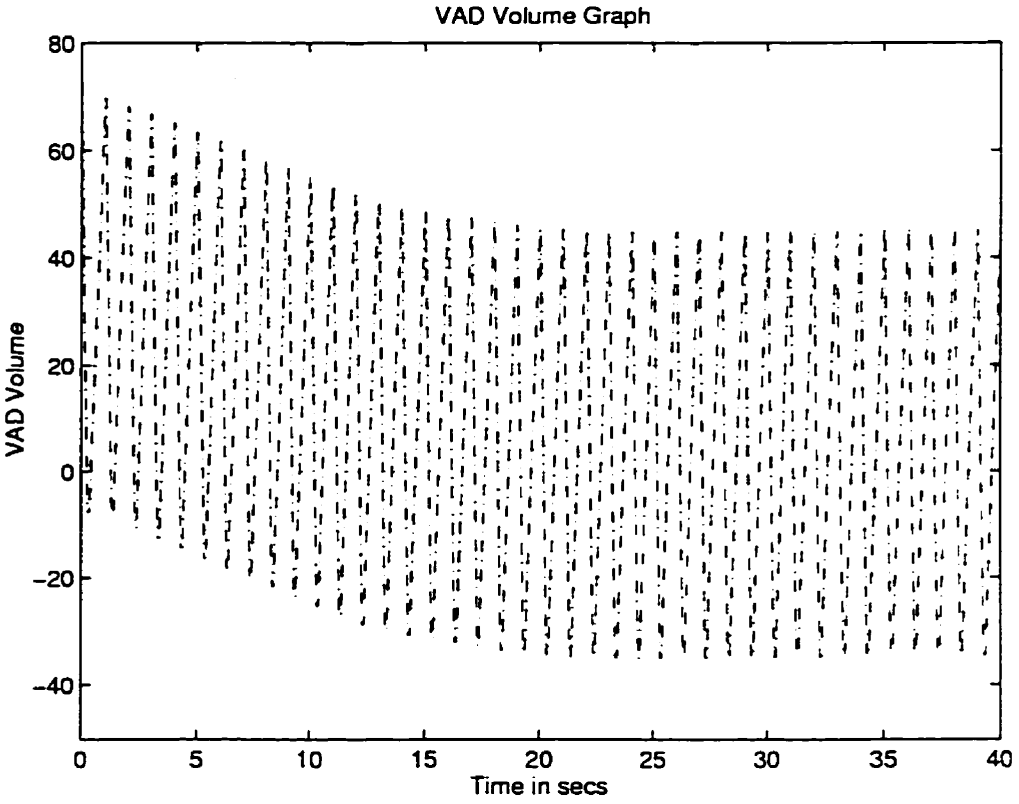


**Figure 5.23:** Nominal condition artificial heart blood volume ( -.- blood volume in artificial heart [ml])

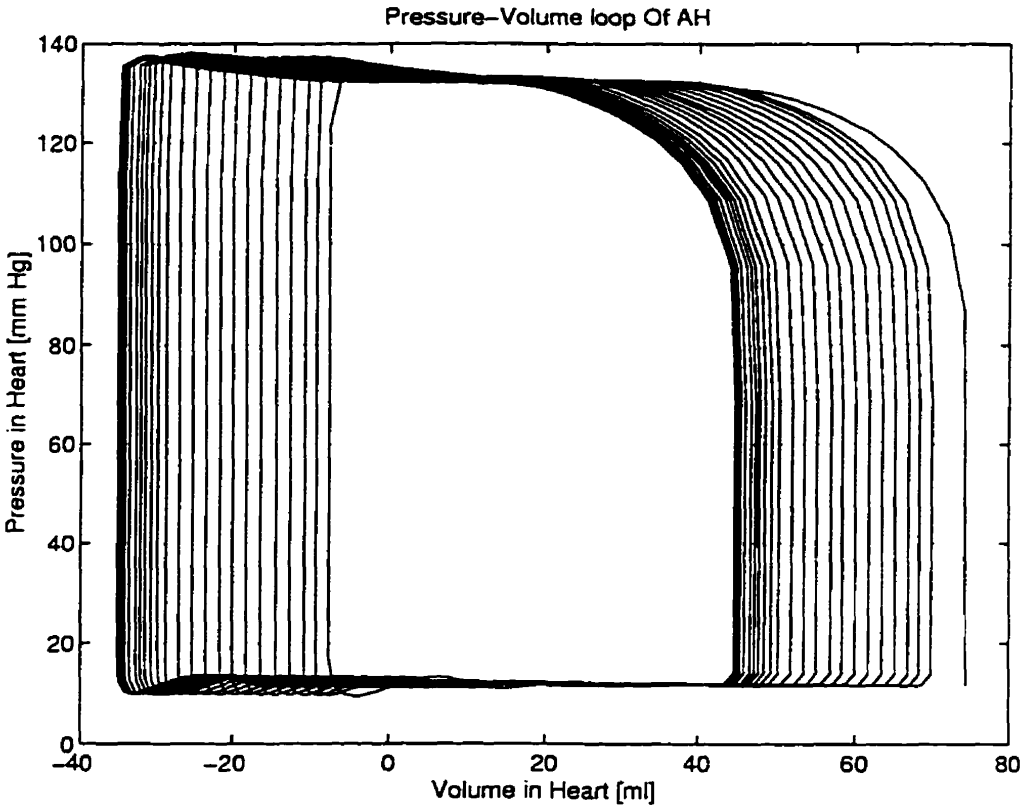


**Figure 5.24:** Nominal condition artificial heart pressure-volume loop data (- pressure-volume loop [ml])

# Chapter 6

# Design of Fuzzy Controller

## 6.1 Supervisory Controller

A supervisory controller provides control actions on a beat by beat basis when the system deviates from its nominal steady state which is determined by its pump output. The controller design must be robust and able to adapt to changes in the physiological system while maintaining the normal functions of the cardiovascular system. The controller is evaulated once for each beat and during the beat the controller is in an open loop configuration. Hence at the end of every beat the supervisory controller determines if the present control action needs to be updated or not.

## 6.2 Control Parameters

There are two main types of control parameters that are able to be modified to provide adequate control. These are the forces applied on the artificial heart diaphragm and the timing of systole and diastole. The model under study is in the fixed mode of operation. The present control scheme is to present an improvement to the fixed rate mode of the control scheme by including a feedback loop and the use of a rule base to describe the dynamic process required for control.

### 6.2.1 Diaphragm Forces

The diaphragm force is the force exerted on the piston during the systolic and diastolic phase. The diastolic phase force is maintained at a value of zero ($F_{dia} = 0$ Nor 12 mm Hg). Hence the diastolic filling phase is a passive filling process. Since no collapsable venous segment has presently been modeled into the circulatory system the diastolic force was maintained at zero. The force applied during the systolic phase was set as a varibale determined on a beat by beat basis. The controller sets the required force based on the pump output to maintain nominal function. The nominal value of the systolic force at steady state was observed from simulation to be 41.8 N or 120 mm Hg.

### 6.2.2 Valve Timings

The systolic and diastolic timings are fixed during the simulation to maintain the fixed mode control. The systolic duration is set to $t_{sys} = 0.3$ secs and the diastolic duration is set to $t_{dia} = 0.7$ secs. The switching of the force on the diaphragm is preset by the valve timings. Hence after the diastolic duration is complete the force on the diaphragm is switched to systole. For future design varying of the diastolic and systolic timings may be desirable.

The detection of timing of the ejection time ($t_{sys}$) and filling time ($t_{dia}$) are determined by finding the change in the input (driving) forces systolic force ($F_{sys}$) and diastolic force ($F_{dia}$) acting on the artificial heart. The algorithm to determine the duration of diastolic timing therefore detects the sudden change in the force from systole to diastole to reveal the begining of the diastolic phase (filling) and marks it as $t_{sys_{t-1}}$ which is the end of the previous beat. The next switch from diastole to systole marked as $t_{dia_t}$ and is subtracted from the previous time to provide the duration of the diastole process which is shown in Figure 6.1 and Equation (6.1).

$$t_{dia} = t_{dia_t} - t_{sys_{t-1}} \tag{6.1}$$

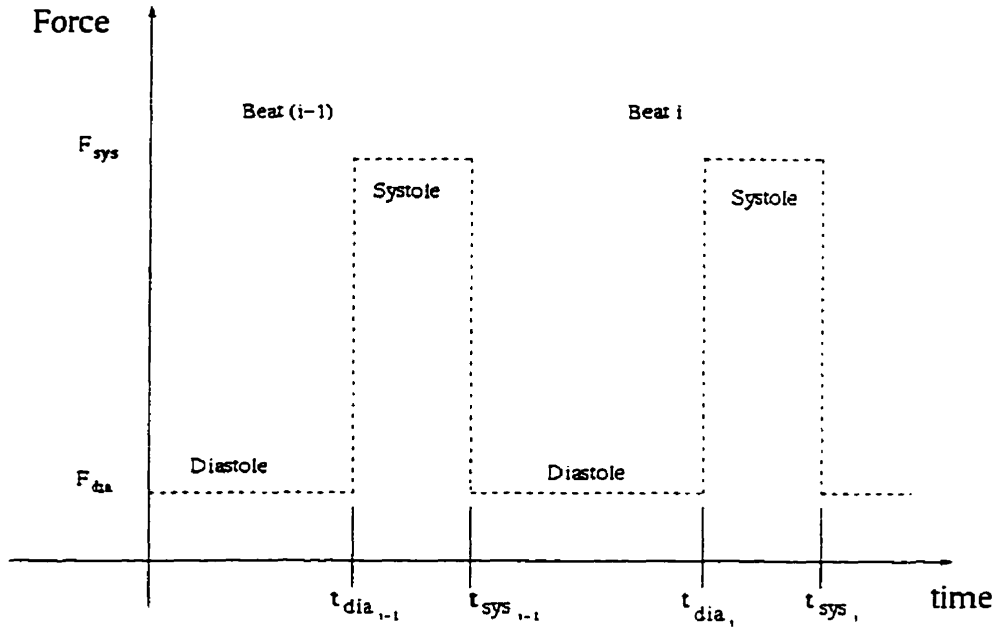


**Figure 6.1:** Artificial heart diastolic and systolic duration ( $i$ denotes present beat. $i-1$ denotes previous beat. $t_{dia_i}$ and $t_{sys_i}$ denotes diastole and systole end time for present beat $i$ [sec]. $F_{sys}$ is the systolic force [N]. $F_{dia}$ is the diastolic force [N])

The next switch from systole to diastole is again marked as $t_{sys_i}$ and is then subtracted from the time of $t_{dia_i}$ to yield the duration of the systolic process also shown in Figure 6.1 and Equation (6.2). The integration routines in Matlab tend to have varying time steps due to the set tolerance value and minimum step size chosen. An accurate $t_{dia}$ and $t_{sys}$ are required for the averaged data used in training the EDV and ESV. A dual search for two sequencial equal force values is done before a valid switch is done to avoid detection of more than a single beat due to tolerance switch failure (chattering). Also it has been observed that the minimum step size on the simulation makes a large impact on the systole and diastole timing which in turn effects the averaging values of diastolic and systolic pressures used in the estimators

for end diastolic volume and end systolic volume.

$$t_{sys} = t_{sys_i} - t_{dia_i} \tag{6.2}$$

## 6.3 Controller Goals

The main controller goal is to provide oxygen and blood flow to organs and tissues to maintain adequate human physiological function by improving the fixed rate mode of control presently used. These requirements can all be combined to a single variable known as the pump output. Therefore pump output is used as a feedback variable to the controller.

## 6.4 Problem Statement

The cardiac output from literature shows that a normal average human requires a cardiac output of about $4.7\frac{L}{min}$ when at rest [13]. The required cardiac output is also shown to increase when metabolic and physical activity is increased [53, 54, 55]. Hence pump output was selected as the feedback variable. In order to provide feedback control we need to measure the pump output. This can be done by direct measurement of system variables of flow rate and timing. But this method was not considered due to its intrusive method of measurement of the circulatory system. The measurement of stroke volume would require the placement of flow sensors directly into the blood stream. Instead, the use of already implanted senors are used to provide an estimate of the pump output. Pressure transducers are usually a very commonly implanted sensor in most artificial hearts and are assumed to be available in this simulation [8, 56, 57, 51]. It is assumed that such a sensor is implanted for the purposes of this study. They are used to monitor heart behaviour and for diagnostics. These sensors are planned to be used to provide an estimate of the pump output on a beat by beat basis. The pump output shown in Equation (2.5) is made up of two elements the heart rate which is fixed at $60\frac{beats}{min}$ and the stroke

volume. The stroke volume varies with changes with physiological parameters from beat to beat.

## 6.5 Estimation of Stroke Volume

The stroke volume is defined by Equation (2.4) which is made up of the end diastolic volume and the end systolic volume. When physiological parameters and external loads are applied to the system it is seen in simulation that the end diastolic and end systolic volume changes from beat to beat. This causes the stroke volume to change. These changes in artificial heart stroke volume are attributed to the changes in pressure across the inlet, outlet valves and the duration the valves are open.

Therefore the problem of determining stroke volume was broken up into two parts. The estimation of the End Diastolic Volume (EDV) and End Systolic Volume (ESV) were done seperately to determine the overall estimate of stroke volume for each beat.

## 6.6 Estimation of End Diastolic Volume

### 6.6.1 Structure of EDV model

The End Diastolic Volume is based on the Adaptive Neuro Fuzzy Inference System shown in Chapter 4. The model consists of two inputs and a single output. The end diastolic volume determined in this simulation is the amount of blood volume that entered the artificial heart during the present beat. Therefore the EDV determined is the volume in the heart from the present beat which is expressed by Equation (6.3) and Figure 6.1.

$$EDV = [\text{Blood Volume at } t_{dia_t}] - [\text{Blood Volume at } t_{sys_{t-1}}] \qquad (6.3)$$

Where $t_{dia_t}$ is the time when the force of the diaphragm switches from diastole to systole. The $t_{sys_{t-1}}$ is the time of the end of the systolic process of the previous beat. Using Equation (5.2) for time $t_{dia_t}$ and $t_{sys_{t-1}}$ and intergrating within the time

domain results in the volume known as EDV. Equation 6.4 is the volume in the artificial heart for any beat $i$ when the above times are substituted in Equation (6.3).

$$EDV = [\frac{A}{I_{ht}}]\int_{t_i}^{t_f} e_2(t)\,dt - [\frac{1}{R_{ot}}]\int_{t_i}^{t_f} \Delta P_{out}(t)\,dt + [\frac{1}{R_{in}}]\int_{t_i}^{t_f} \Delta P_{in}(t)\,dt \quad (6.4)$$

In Equation (6.4) we see that EDV is a function of the difference in pressure across the inlet value and difference in pressure across outlet valve and the piston momentum. During the process of diastolic filling in the artificial heart the outlet valve is closed and is simulated by a large resistance value of the output valve $R_{ot}$ in the order of $10^6$ in magnitude. Hence the second term in Equation (6.4) can be neglected. The remaining terms make up the EDV on a beat by beat basis, hence piston momentum and inlet pressure gradient are the variable parameters. The piston momentum is small compared to the third term on pressure gradient since $F_{dia} = 0$ N.

Therefore the inputs used in the ANFIS estimate model were chosen to be time averaged $\Delta P_{in}$ during diastole and $t_{dia}$. The $t_{dia}$ was chosen because it was a second term that can be used to alter the EDV for control purposes in the future. The value of $t_{dia}$ at present is set to a constant value of 0.7 sec for a 1 sec beat period (fixed rate) function of the heart.

The first input parameter was selected to be the inlet pressure gradient averaged over diastole ($\Delta P_{in}$). The universe of discourse ($X_1$) was chosen to fit the possible range of inlet pressure gradient. The domain $X_1$ is a set of real numbers ($X_1 \subset \Re$). The domain $X_1$ was determined from the operational range determined to be $\Delta P_{in} = \langle 5, 9.5 \rangle$ mm Hg by examining simulation results for a range of model peripheral resistance values. The peripheral resistance ($R_{pe}$) was varied from 2 times to 0.5 its nominal value.

The second input parameter was set as the diastolic timing. Its universe of discourse ($X_2$) was held constant at 0.7 sec due to the present fixed rate mode operation.

Its domain was also selected from the set of real numbers ($X_2 \subset \Re$). Since the duration of diastole is determined from integration, small errors of $\pm 0.02sec$ are observed. The universe of discourses operational range was determined to be $t_{dia} = (0.6974, 0.7)$ secs. This variation in the diastolic time can be fixed by running the simulation and obtaining training data for a much smaller integration step size ($\leq 0.001$). This causes the simulation to be computationally slow, although stand alone complied C code may speed it up. A version of the program was also written in Matlab without the aid of simulink toolbox to improve computability. This showed an improvement in performance of the simulation time, but still is highly computational for attaining a very accurate diastolic or systolic duration for training purposes.

### 6.6.2 Training EDV model

The training data of the ANFIS was attained for various pressure gradients across the inlet valve and observing the EDV at such pressures. The pressure gradient across the inlet valve was attained by varying the model peripherial resistance of the circulatory model. Hence determining the behaviour of the volume filling the artificial heart is required to estimate stroke volume from beat to beat.

When the model peripherial resistance is increased it causes the pressure gradient across the inlet valve to decrease. This is because the increase in model peripheral resistance constricts blood flow through the peripherial which results in a lower inlet cannula blood volume and hence a lower pressure in the inlet cannula. Similarly a decrease in the model peripherial resistence will result in an increase in the blood volume in the inlet cannula and hence an increase in pressure across the inlet valve. The data taken for the training phase of the simulation is shown in the Table 6.1. The simulation was run for steady state which was observed to be approximately 60 beats under worst cases. The odd sets of data where used to train the EDV model.

The data used in the training of the EDV is stored in the file *dat_edv.m*. The

| Training data for EDV ANFIS | | | |
|---|---|---|---|
| Steady State $\Delta P_{in}$mm Hg | $R_{pe}$ $\frac{cm^5}{N}$ | Simulation time $Secs$ | No of points |
| 9.7 | $R_{pe} * 0.5$ | 60 secs | 30 |
| 9.1 | $R_{pe} * 0.6$ | 60 secs | 30 |
| 8.6 | $R_{pe} * 0.7$ | 60 secs | 30 |
| 8.3 | $R_{pe} * 0.75$ | 60 secs | 30 |
| 8.2 | $R_{pe} * 0.8$ | 60 secs | 30 |
| 7.8 | $R_{pe} * 0.9$ | 60 secs | 30 |
| 7.4 | $R_{pe}$ | 60 secs | 30 |
| 6.7 | $R_{pe} * 1.2$ | 60 secs | 30 |
| 6.2 | $R_{pe} * 1.4$ | 60 secs | 30 |
| 5.8 | $R_{pe} * 1.6$ | 60 secs | 30 |
| 5.4 | $R_{pe} * 1.8$ | 60 secs | 30 |
| 5.0 | $R_{pe} * 2.0$ | 60 secs | 30 |

**Table 6.1:** Training data collected for EDV ANFIS model. Odd beat data are taken from a 60 beat simulation for training the ANFIS. The pressure gradient across the inlet valve is averaged over the diastolic process.

presented data was arranged into a martrix and processed by the training program in file *train_edv.m* which is given in Appendix A. The initial reference fuzzy set functions was generated with Equation (6.5) for all the linguistic terms.

$$f(x, a, c) = \frac{1}{1 + e^{-a(x-c)}} \tag{6.5}$$

The input domain $\Delta P_{in}$ was divided into five reference fuzzy sets. The reference fuzzy sets defined by Equation (6.5) were equally divided into the domain of $\Delta P_{in}$ which is $\langle 5.10 \rangle$ mm Hg. The second input domain $t_{dia}$ was divided into three reference fuzzy sets. The three reference fuzzy sets was chosen because of the small error in diastolic duration due to integration as previously discussed. The three reference fuzzy sets were divided equally into the domain $\langle 0.6974, 0.7 \rangle$ secs. After training the results are shown in Figure 6.2 and Figure 6.3 which shows the final reference fuzzy sets on the two input domains. The $t_{dia}$ is seen to have only two reference fuzzy sets after training because one of the reference fuzzy set was set to zero.

The data was trained for 100 batch training. The terms of the Equation (6.5) for each of the reference fuzzy sets and the consequent Equation (4.23) variables for the rules are adjusted as to best fit the data provided from Table 6.1 with the aid of a neural net.

### 6.6.3 EDV estimator

There were two sets of input/output data used. A training data set and a checking data set. The training data was used to train the ANFIS and the checking data was used to determine the estimator's accuracy. Figure 6.4 shows the error between the training data and the checking data. The error is known as the RMSE which is the Root Mean Squared Error given by Equation (6.6) [58]. The training data slows a gradual decrease in the RMSE for each epoch. The training data RSME reaches a steady error at about the $70^{th}$ epoch. The training data used shows a lower RMSE than of the checking data for each epoch as shown in Figure 6.4.

$$RMSE = \frac{|\text{training data - training result}|}{\sqrt{[\text{Number of training data}]}} \tag{6.6}$$

Figure 6.5 shows the surface plot of the input and the outputs shown on a 3 dimensional plot. The surface shows the behaviour of $\Delta P_{in}$, $t_{dia}$ and EDV. The figure shows that an increase in inlet pressure gradient results in an increased EDV. The relationship is seen to be very linear for a fixed diastolic timing of 0.7 sec. But when diastole duration ($t_{dia}$) is increased it was observed and can be speculated that the EDV would increase for any inlet pressure gradient. The large dip shown at a diastolic time of 0.698 sec is because no training data for that region above 6.5 mm Hg for inlet pressure gradient and a diastolic timing of about 0.9985 sec was used.

Another conclusion that can be drawn from Figure 6.5 is that the EDV can be approximated by a linear function of pressure gradient across inlet.

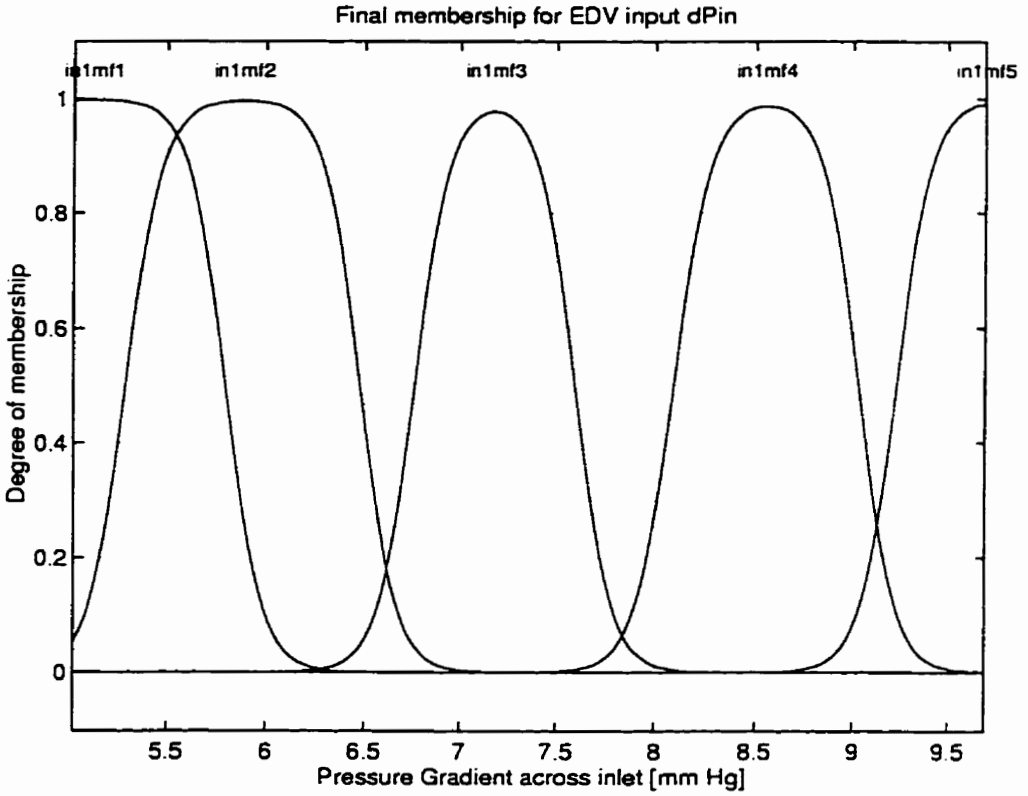


**Figure 6.2:** Final EDV membership functions after training for $\Delta P_{in}$ (Pressure gradient across in the inlet valve). The figure shows the five linguistic varibales in1mf1 to in1mf5. The parameteric values of the memberships can be found in *Est_neu_EDV.fis*

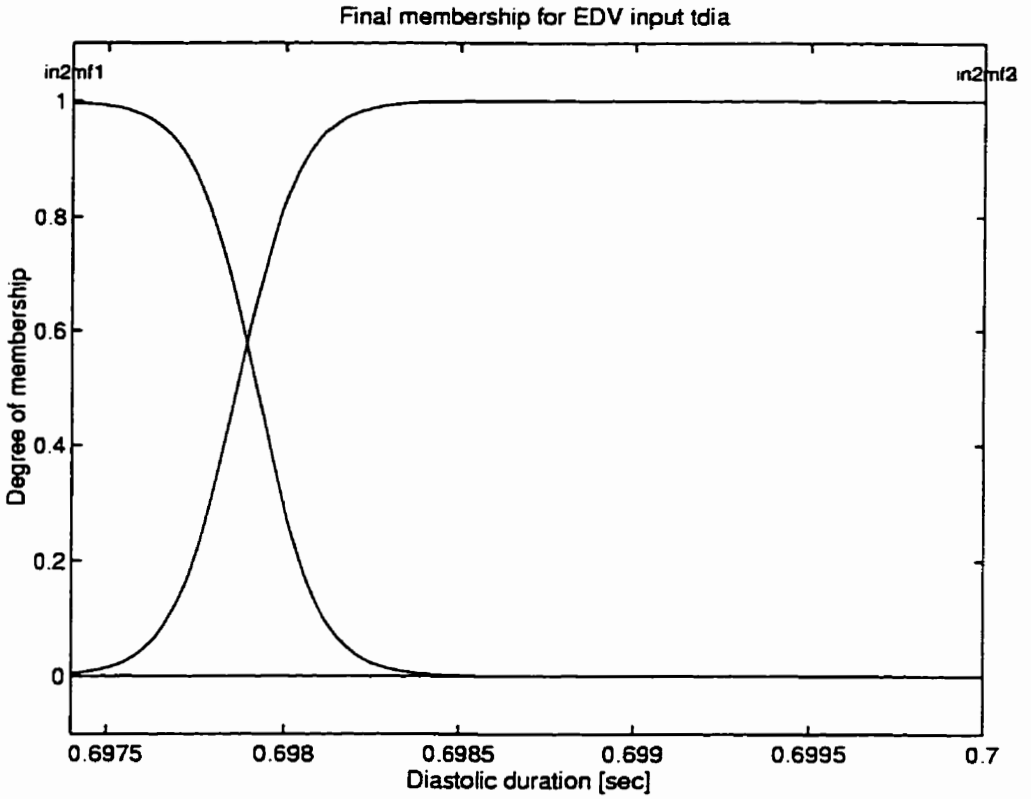


**Figure 6.3:** Final EDV membership functions after training for $t_{dia}$ (Diastolic duration). The parameteric values of the memberships can be found in *Est_neu_EDV.fis*

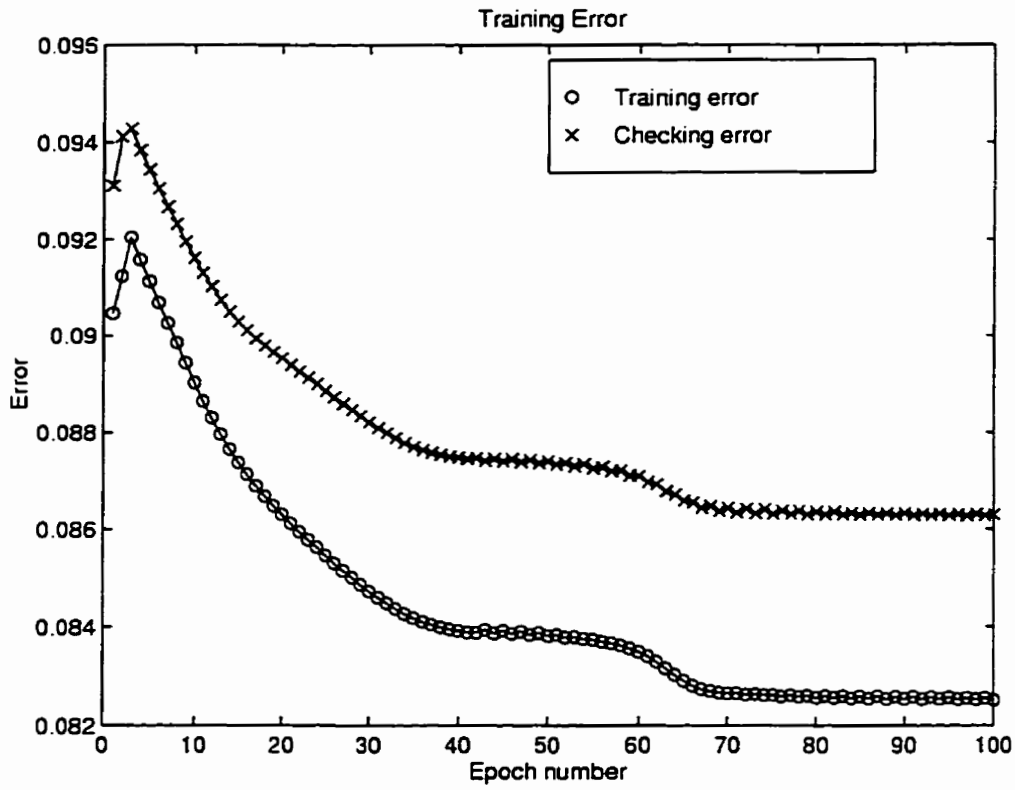


**Figure 6.4:** Error on the training process for EDV showing the convergence between the training data and the checking data using Equation (6.6)

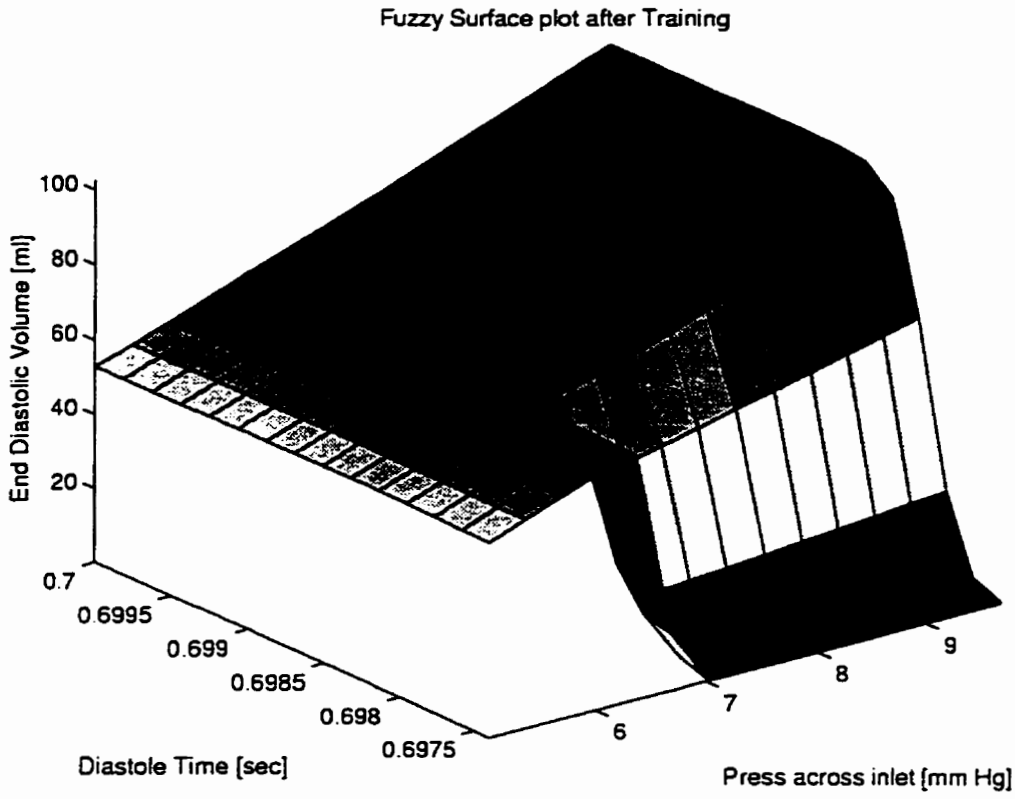


**Figure 6.5:** A contour plot of the EDV estimators domain showing the relationship between inputs and outputs of the ANFIS on a 3-D plot. The plots shows that the relationship is approximatly linear. The sharp drop i the surface is due to lack of training data for the region.

## 6.7 Estimation of End Systolic Volume

### 6.7.1 Structure of the ESV Model

The End Systolic Volume (ESV) is also estimated with the Adaptive Neuro Fuzzy Inference System as used in the determination of EDV. The ESV is the volume of blood in the heart at the end of systole relative to the previous end systolic volume: that is, the net change in volume during the previous beat. The ESV is therefore defined by Equation (6.7)

$$ESV = [\text{Blood Volume at } t_{sys_{i-1}}] - [\text{Blood Volume at } t_{sys_i}] \tag{6.7}$$

Where $t_{sys_{i-1}}$ is the end of the systolic phase of the beat $i-1$ and $t_{sys_i}$ is the end of systolic phase of the present beat $i$. The difference yields a value of the blood remaining in the heart after the present beat known as ESV. As in EDV we determine the ESV by intergrating Equation (5.2) for time $t_{sys_{i-1}}$ and $t_{sys_i}$.

$$ESV = [\frac{A}{I_{ht}}]\int_{t_i}^{t_f} \epsilon_2(t)\ dt - [\frac{1}{R_{ot}}]\int_{t_i}^{t_f} \Delta P_{out}(t)\ dt + [\frac{1}{R_{in}}]\int_{t_i}^{t_f} \Delta P_{in}(t)\ dt \tag{6.8}$$

Using the ESV Equation (6.8) some terms in the equation can be rejected. The third term can be seen to disappear when the artificial heart is in the ejection phase. The input valve is closed and hence has a high resistance. This makes the third term small in comparision to the other terms in the equation.

Equation (6.8) shows the only main terms are 1 and 2. But in a closed system where the blood volume can vary from one element to another it is hard to determine the systems state from measurement of only the outlet pressure gardient. The inlet pressure gradient can be used as a reference mark to aid in predicting the systems position is a non-steady state transient. Therefore the two inputs used in the ANFIS were inlet pressure gradient across artificial heart inlet valve and outlet pressure

gradient across the artificial heart outlet valve. These two terms enable us to give us a picture of the artificial heart volumes present state in any transient.

The universe of discourse for the pressure gradient ranges for input and output valves $X_1$ and $X_2$ respectively, where $X_1 \subset \Re$ and $X_2 \subset \Re$. The inlet pressure gradient range was set to $\Delta P_{in} = \langle 3, 12 \rangle$ mm Hg ($X_1$). While the outlet pressure gradient $\Delta P_{out} = \langle 8, 27 \rangle$ mm Hg ($X_2$). These data ranges were attained for simulated values of $R_{pe}$ from values of 0.1 to 3.2 times its nominal value. A larger $\Delta P_{in}$ and $\Delta P_{out}$ range are required for the ESV estimate becuase of the active force $F_{sys}$ which can increase the outlet pressure gradient. The ESV universe of discourse which was set from observed values when $R_{pe}$ was changed to be $\langle -40, 30 \rangle$ ml. The universe of discourse of ESV is denoted by ($Y$). The negative value of ESV signifies insufficient volume was in the heart at that particular beat.

The negative value can be changed or corrected by increasing the EDV by either using a negative diastole force, diastolic duration ($t_{dia}$) longer or changing the reference piston stroke length which was chosen arbitrarily as described earlier.

### 6.7.2 Training ESV Model

As in the case of the EDV estimator the training data was attained by observing the changes in $\Delta P_{in}$, $\Delta P_{out}$, and ESV for a change in $R_{pe}$, which effects the pressure gradient across the inlet and outlet valve. The $\Delta P_{in}$ is time averaged over the diastolic period as in the EDV estimator. While $\Delta P_{out}$ is time averaged over the systolic period. The $R_{pe}$ was varied from 0.2 to 3.2 times its nominal value in increments of 0.1.

When $R_{pe}$ is increased this causes an increase in blood volume in the outlet cannula, aorta and arteries and hence an increase in pressure in the elements respectively. Similarly a decrease in $R_{pe}$ would produce a decrease of blood volume in outlet cannula, aorta and arteries which causes a lower pressure in the elements. The parameter values for $R_{pe}$ are used for training are shown in Table 6.2. The data used

are avalable in file it dat_ESV.m and the training procedure is in file *train_ESV.m* which is given in the Appendix A.

The input domain $\Delta P_{in}$ was divided into five reference fuzzy sets. The five membership are divided equally into the domain of (3, 12) mm Hg of $\Delta P_{in}$. The second input was also made up of five reference fuzzy sets which were initially divided equally into its domain (8.5, 28.7) mm Hg for $\Delta P_{out}$. The output universe of discourse was divided into 25 linear equations which span a domain of (-38.5, 28) ml given by Equation (4.23). The reference fuzzy sets were then trained by 100 batch learning job. The final trained memberships for the $\Delta P_{in}$ and $\Delta P_{in}$ are shown in Figure 6.6 and Figure 6.7 respectively. The reference fuzzy set functions for the linguisitic terms are defined by the same Equation (6.5) as in the EDV ANFIS model.

### 6.7.3 ESV estimator

The Figure 6.8 shows the RMSE between the training data and the checking data using Equation (6.6). The initial batch can be seen to show a large error. The difference between the checking and training data are small. The errors drop sharply as the number of training epochs increases and is seen to attain steady state at about 90 epochs.

Figure 6.9 shows the relationship between the input and output variables on a three axis graph. The figure shows a surface plot of the $\Delta P_{in}$, $\Delta P_{out}$ and ESV. The contour shows the flat regions and large dips. These large dips are mainly due because no training data is applicable to the region. Clearly a single function cannot define the complete domain as in the case of EDV, but the use of multiple linear functions (other than ANFIS) or the use of a contour fit over the surface may provide a similar defintion of the input/output relationship.

| Training data for ESV ANFIS | | | | |
|---|---|---|---|---|
| SS $\Delta P_{in}$ | SS $\Delta P_{out}$ | $R_{pe}$ $\frac{cm^5}{N}$ | Simulation time *Secs* | No of points |
| 12.0 | 26.6 | $R_{pe} * 0.2$ | 60 secs | 30 |
| 11.2 | 24.7 | $R_{pe} * 0.3$ | 60 secs | 30 |
| 10.4 | 23.1 | $R_{pe} * 0.4$ | 60 secs | 30 |
| 9.7 | 21.9 | $R_{pe} * 0.5$ | 60 secs | 30 |
| 9.1 | 20.6 | $R_{pe} * 0.6$ | 60 secs | 30 |
| 8.6 | 19.4 | $R_{pe} * 0.7$ | 60 secs | 30 |
| 8.5 | 18.5 | $R_{pe} * 0.8$ | 60 secs | 30 |
| 7.8 | 17.7 | $R_{pe} * 0.9$ | 60 secs | 30 |
| 7.4 | 17.1 | $R_{pe}$ | 60 secs | 30 |
| 6.7 | 15.6 | $R_{pe} * 1.2$ | 60 secs | 30 |
| 6.2 | 14.5 | $R_{pe} * 1.4$ | 60 secs | 30 |
| 5.8 | 13.5 | $R_{pe} * 1.6$ | 60 secs | 30 |
| 5.4 | 12.7 | $R_{pe} * 1.8$ | 60 secs | 30 |
| 5.0 | 12.0 | $R_{pe} * 2.0$ | 60 secs | 30 |
| 4.7 | 11.3 | $R_{pe} * 2.2$ | 60 secs | 30 |
| 4.5 | 10.7 | $R_{pe} * 2.4$ | 60 secs | 30 |
| 4.2 | 10.1 | $R_{pe} * 2.6$ | 60 secs | 30 |
| 4.1 | 9.7 | $R_{pe} * 2.8$ | 60 secs | 30 |
| 3.9 | 9.2 | $R_{pe} * 3.0$ | 60 secs | 30 |
| 3.7 | 8.9 | $R_{pe} * 3.2$ | 60 secs | 30 |

**Table 6.2:** Training data collected for ESV ANFIS model. Odd beat data are taken from a 60 beat simulation for training the ANFIS. The pressure gradient across the inlet valve is averaged over the diastolic process and the pressure gradient across the outlet valve is averaged over the systolic process.

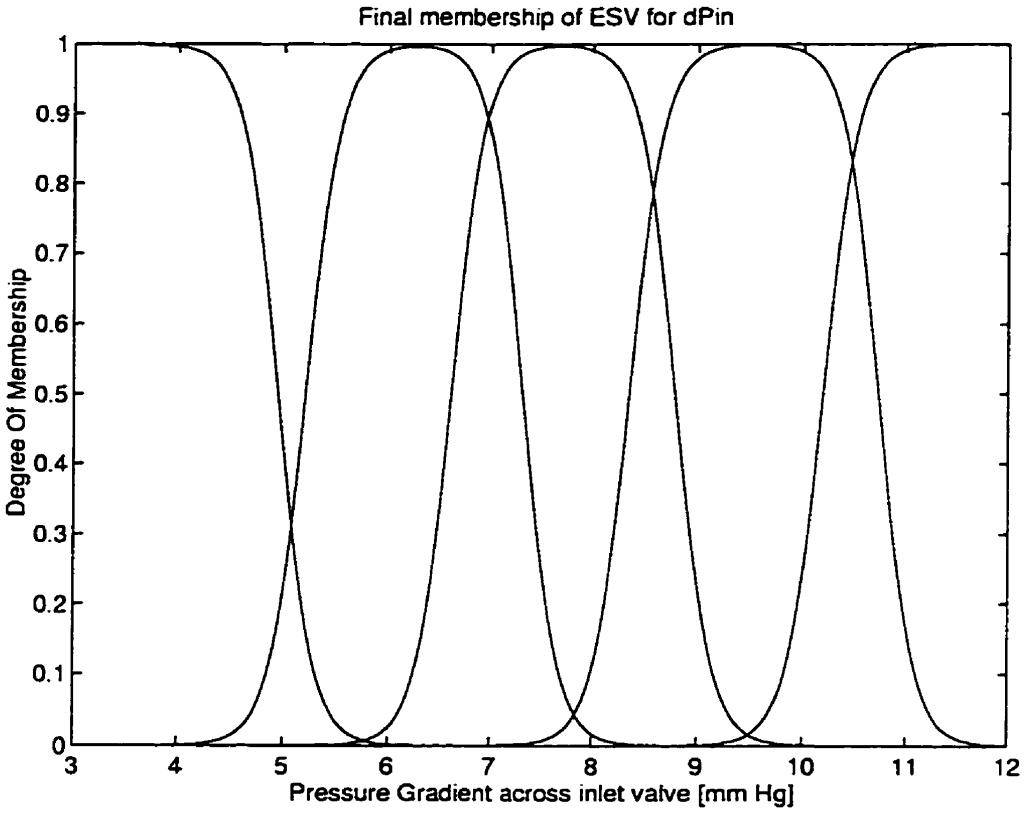


**Figure 6.6:** Final ESV membership functions after training for $\Delta P_{in}$ (Pressure gradient across the inlet valve). The parameteric values of the memberships can be found in *Est_neu_ESV.fis*

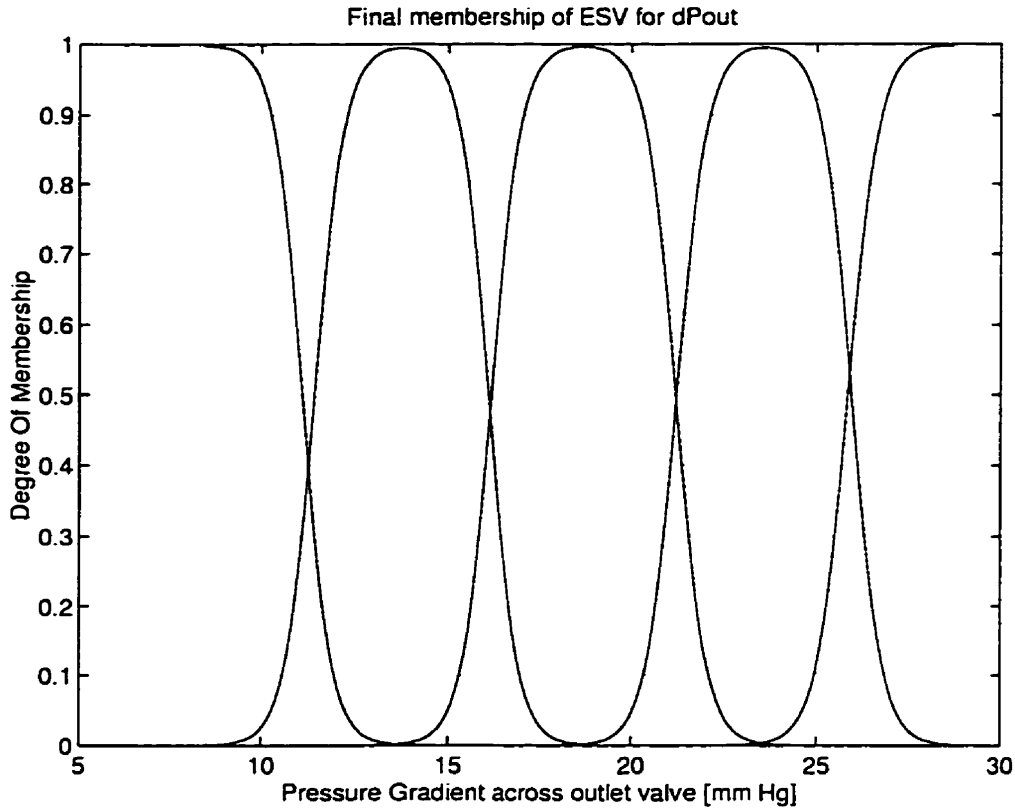


**Figure 6.7:** Final ESV membership functions after training for $\Delta P_{out}$ (Pressure gradient across the outlet valve). The parameteric values of the memberships can be found in *Est_neu_ESV.fis*

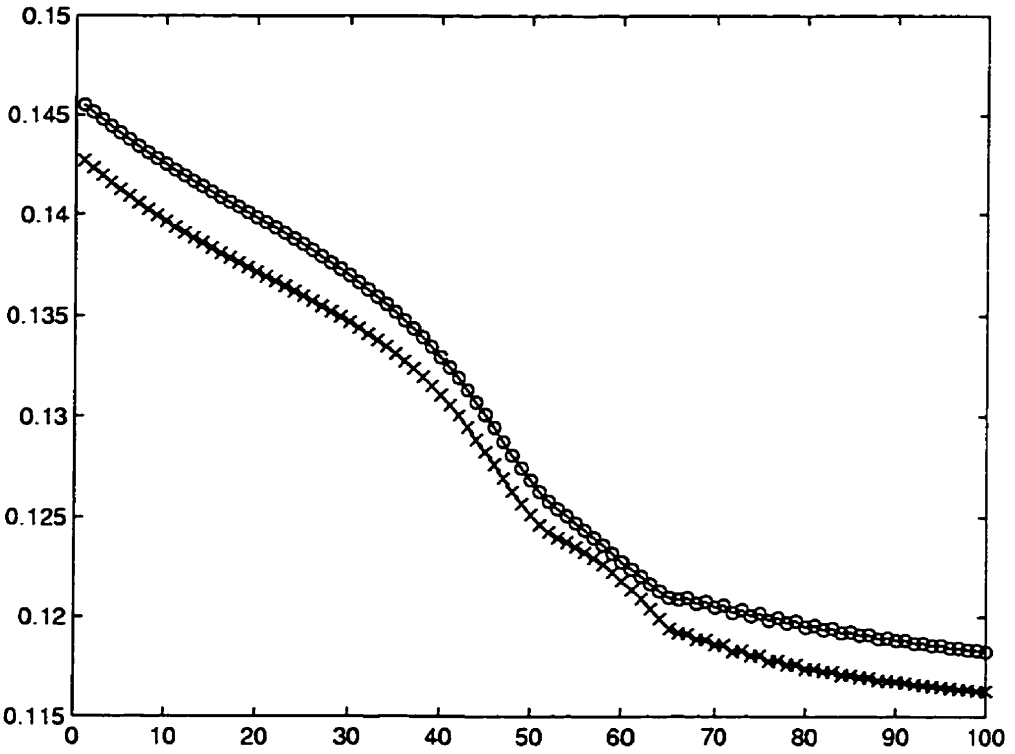


**Figure 6.8:** Error on the training process for ESV showing the convergence between the training data and the checking data using Equation (6.6)

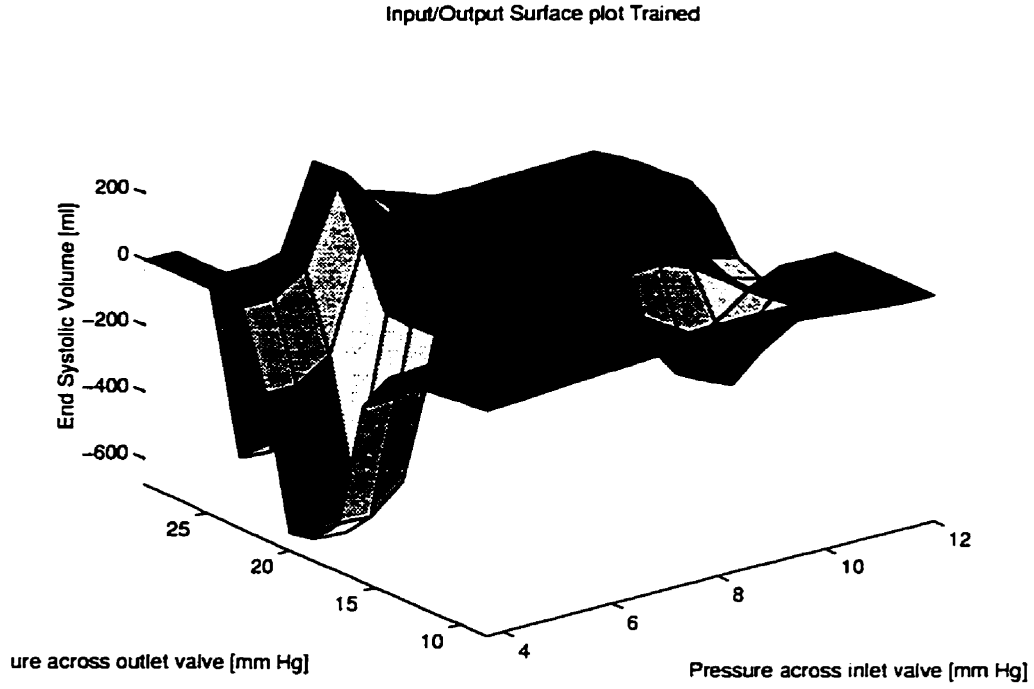


**Figure 6.9:** A contour plot of the ESV estimators domain showing the relationship between inputs and outputs of the ANFIS on a 3-D plot. The estimator data are mainly confined to the middle flat section of the plot.

## 6.8 Estimation of pump Output

The pump output is estimated on a beat by beat basis. The duration of diastole and systole are recorded from the change in driving force and used to attain a value of the heart rate in terms of beats per minute which is fixed in this simulation at approximatly $60\frac{beats}{min}$ with slight variation due to integration. The stroke volume is determined by Equation (6.9).

An increase in outlet cannula pressure causes the ESV value to be positive since the pressure gradient across the outlet is lower and therefore a lower volume of blood is ejected on each systolic beat. This causes in drop of stroke volume which causes a lower pump output. This is proposed to be corrected by a fuzzy logic controller. The reverse is true for a decrease in the outlet cannula pressure which can cause an increase in the pump output with a lower blood volume remaining in the artificial heart. In an increased case of pump output the controller is to try to maintain a preset value of pump output.

$$PO_{est}(beat) = (EDV_{est} - ESV_{est}) * \mathrm{HR} \tag{6.9}$$

## 6.9 Fuzzy Logic Controller

The fuzzy logic controller is designed to use the estimated pump output as a feedback parameter to determine the change in force required during systolic ejection. The control is to maintain the specified pump output set by a user or by a desired pump output monitor. The controller is simple to maintain robustness. The controller is Single Input and Single Output (SISO) and uses a Mamdani logic structure discussed in chapter 4.

### 6.9.1 Inputs to FLC

The input into the Mamdani fuzzy controller was chosen to be the estimated pump output from Equation (6.9). The pump output is measured in $\frac{L}{min}$. The Universe of

discourse of the input variable pump output was determined to be twice the desired value of pump output for normal human at rest. The desired value of pump output was selected for a normal human to be $4.7\frac{L}{min}$ [13]. Hence the universe of discourse ($X$) was set to $(0.9.4)\frac{L}{min}$ where $X \subset \Re$. The reference fuzzy set functions were based on Equation (6.10) known as Gaussian bell function. The input variables of the universe of discoures were divided into 5 reference fuzzy sets with linguistic terms VLow, MLow, Norm, MHigh and VHigh. The values of a,b and c for each of the linguistic terms of the functions are given in the file *HardCntrl.fis* given in the appendix A. The linguistic variable for each term were attained by careful tuning of the controllers response.

$$f(x : a, b, c) = \frac{1}{1 + [\frac{x-c}{a}]^{2b}} \tag{6.10}$$

The linguistic term VLow implies Very Low pump output, MLow implies Medium Low pump output, Norm implies normal pump output, MHigh implies Medium High pump output and VHigh implies Very High pump output. When the pump output is less than $\leq 3\frac{L}{min}$ it was selected to be Very Low pump output with a degree of membership equal to 1 which would mean immediate increase in pump output is required. While a value of $\geq 6\frac{L}{min}$ was considered a Very High pump output also with a degree of membership equal to 1 would mean an immediate decrease in pump output is required. The Medium Low and Medium High were selected to provide control when the system was approaching the desired pump output by decreasing the effect of the controller. The Normal range was considered a small range about the nominal desired pump output to prevent small numerical oscillations about the desired value of pump output.

A value of pump output is attained during simulation from the estimator at the end of a beat. The degree that the output satisfies to each lingusitic term is calculated for a Degree of Membership (DOM) from Figure 6.10. Hence a nominal value of cardaic output will result in the DOM of the linguistic label *Norm* to be higher than the rest of the linguistic lables DOM's. These DOM values are used to evaluate the

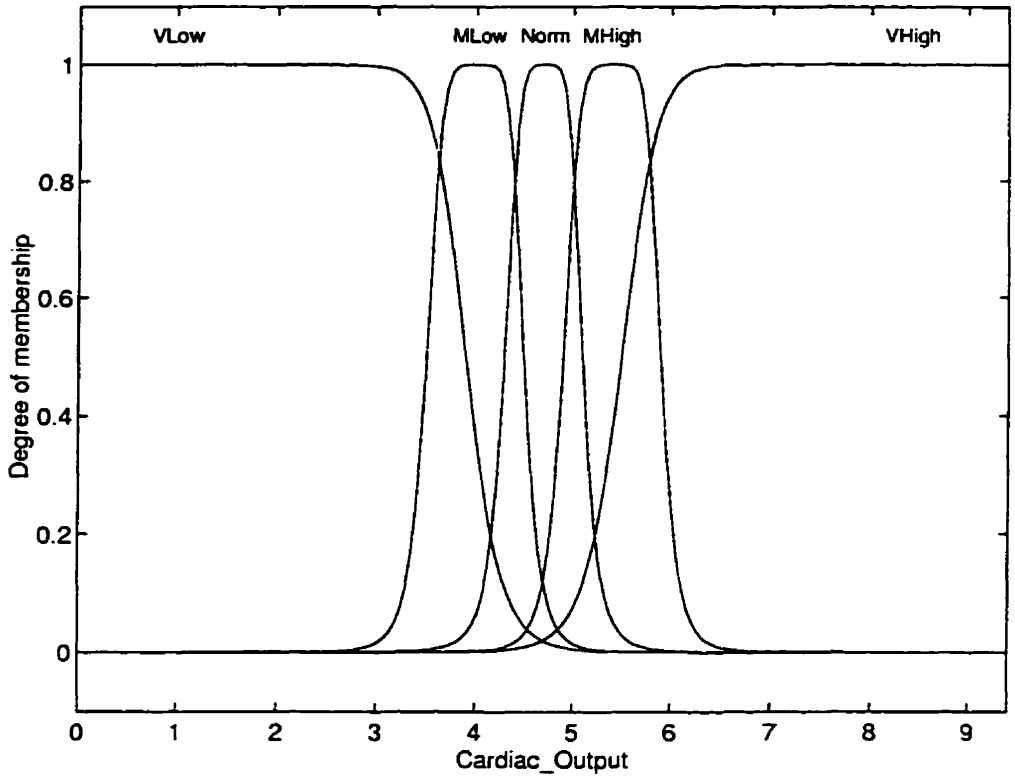


**Figure 6.10:** Fuzzy logic controller showing membership functions of the input (pump output $\frac{L}{min}$). The parameteric values of the FLC are given in *HardCntrl.fis*

rules of antecedents of the rule base.

## 6.9.2 Rule Base

The design of the rule base was constructed on intutive knowledge of the circulatory system and its behaviour. When a drop in pump output was detected it meant that the flow rate from the artificial heart is lower due to a drop in the pressure gradient across the outlet valve. Therefore to increase the flow rate from the heart an increase in the pressure gradient across the outlet value is required. The way such an increase can be attained is by increasing the systolic stroke force ($F_{sys}$). This would increase the artificial heart pressure during systole while increasing the overall

pressure gradient across the outlet valve. A side effect of the increase in the systolic force is the increase in the average outlet cannula pressure during systole and an increase in the operating pressure of the artificial heart during systole. When the pressure gradient is favourable and outlet valve is open. The artificial heart systolic pressure influences the outlet cannula pressure. The following rules are derived to provide such an increase in systolic force by incrementally changing the nominal systolic force by $\Delta F_{sys}$ with the aid of a pump output feedback loop hence adapting to the changes in the system. A similar logic is used to correct an increase in pump output from the nominal values. An increase in pump output would mean that the pressure gradient across the outlet is higher. Therefore a decrease in the systolic force will reduce the amount of blood ejected per stroke.

IF (CO(beat) is LOW) THEN ($\Delta F_{sys}$(beat) is HIGH) (6.11)

IF (CO(beat) is Norm) THEN ($\Delta F_{sys}$(beat) is Norm) (6.12)

IF (CO(beat) is HIGH) THEN ($\Delta F_{sys}$(beat) is LOW) (6.13)

Once the basic rules were selected the output universe of discourse is selected. The main criteria was to maintain low number of rules for the controller to operate on a beat by beat basis to reduce computational overhead. Hence three rules were selected to provide adequate control of the system.

### 6.9.3 Output of FLC

The output variable was selected to be an incremental change in the systolic force denoted as ($\Delta F_{sys}$). This provided a way of preventing a bad estimate from either the EDV or the ESV from an adverse effecting the control or causing damage to the system being controlled by predicting a large systolic force $F_{sys}$. The universe of discourse ($Y$) was selected to be (-10, 10 ) N, where $Y \subset \Re$. The universe of discourse was divided into 5 reference fuzzy sets again Nega, MNega, Norm, MPosi and Posi as shown in Figure 6.11.

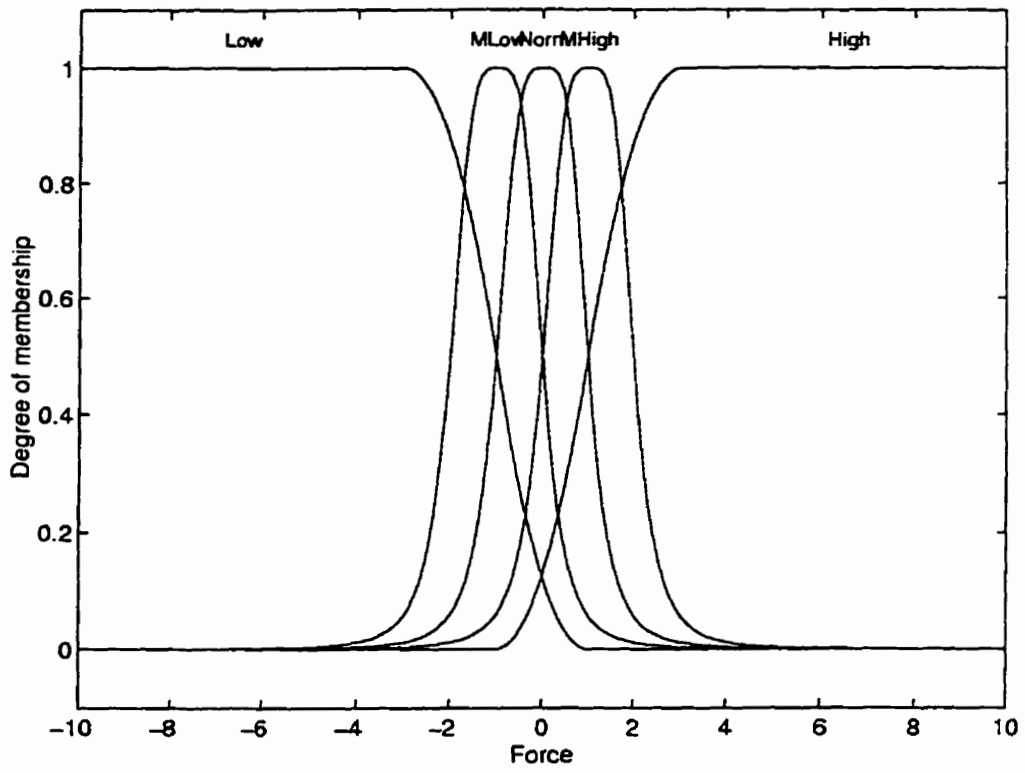


**Figure 6.11:** Change in systolic force membership functions ($\Delta F_{sys}$) [N]

Where Nega implies Negative change in force and hence a step down from the present systolic force. MNega implies a medium negative drop in present systolic force. Norm implies a normal systolic force with little or no change to the current value. MPosi implies a medium increase in the systolic force and finally Posi implies a large increase in systolic force. As before the reference fuzzy set functions are defined by Equation (6.10). The parameters a,b and c are used to tune the DOM values of the terms and there relation to each other to provide adequate control.

### 6.9.4 Controller Tuning

The final input and output memberships. shown in Figure 6.10 and Figure 6.11 were attained after numerous tuning to provide the best possible control of the system. The tuning was to provide minimal overshoot and attain a quick steady state during

a step change in the model peripheral resistance.

The tuning process was done by adjusting the membership shapes and their crossover DOM values between linguistic terms. Also weighted rules were tried to provide a better control response as described briefly in section 4.2. The weighted method for the rules was found not to be very effective due to the small rule base at present. A larger rule base was used with weighted rules which provided some improvement in response, but at an increase in computation due to the larger number of reference fuzzy sets to be tuned. The tuning was done by simulation of the system under different model peripheral resistance levels and observing the response and correcting the parameters on the membership functions to adjust the control. The task was tedious and very time consuming.

A problem encountered with the above rules was that the controller tended to overshoot and cause chattering when simulated for some values of $R_{pe}$. Initially to overcome this problem a method of intelligent controller switching was attempted. Where two FLC controllers were setup with different sensitivity to the feedback variable pump output, the controller would switch to a "Hard-controller" if the desired and actual pump output was vastly different by a preset hard controller threshold value. When the desired and actual values are below a certain threshold the controller algorithm switches to a "Soft-controller". This technique was abandoned because of the complexity of the control. Since a simple control algorithm is less likely to fail and is easier to design, to solve the problem of the overshoot with the aid of a single controller two extra rules were added. The rules are shown below and are counter intuative. These rules are opposite to the intutive knowledge or logic of the system being controlled. This provides higher sensitivity of the controller when pump output is about nominal by distributing the center of the area (defuzzification) to the opposite side of the control action.

IF (CO(beat) is MLow) THEN ($\Delta F_{sys}$(beat) is MLow) (6.14)

IF (CO(beat) is Mhigh) THEN ($\Delta F_{sys}$(beat) is MHigh) (6.15)

The chatter problem was controlled by adding a cut-off value for the change in systolic force. When the proposed change in force from the controller is below a certain set threshold which is presently set at 0.05 N in the file *frbtbybt.m* the change in force is not applied to the system. Hence only a change in force above the threshold is implimented by the controller. This value of set threshold can be altered to provide less sensitivity or can actively be controlled depending on the systems response. Also during tuning increased membership functions were attempted in each input and output universe of discourse and in so doing the computation also increased as well as the number or rules required to describe the system. But an increase in the number of membership functions provided a better control of the control space to a much finer degree. The number of extra rules that were added also made computation time longer but provided a better control over the control space.

### 6.9.5 Defuzzification

The method used to defuzzify the output function in the output universe of discourse is described in Equation (4.15) in chapter 4. The fuzzy inference system for the hybrid controller is in file *Hardcntrl* and is shown in the Appendix A.

### 6.9.6 Analysis of Control Space

Figure 6.12 shows the control space. In this case the control space is only 2-D due to the SISO system. The figure shows that at high pump output in the order of $\geq 6\frac{L}{min}$ the control action is to reduce the nominal force acting on the heart by a large value of about -5.5 N. When pump output is very low $\leq 3\frac{L}{min}$ the controller increases the value of nominal of systolic force by a larger increment of 5.5 N. This shows that although the output universe of discourse is defined as (-10. 10) N its actual effective control space is approximately (-5.5. 5.5) N. When pump output is about nominal the control relationship is seen to be a linear function. The slope of

the linear function can be altered by changing the DOM value of either the output or the input. Also addition of more membership functions can produce more accurate control over different regions of pump output ranges.

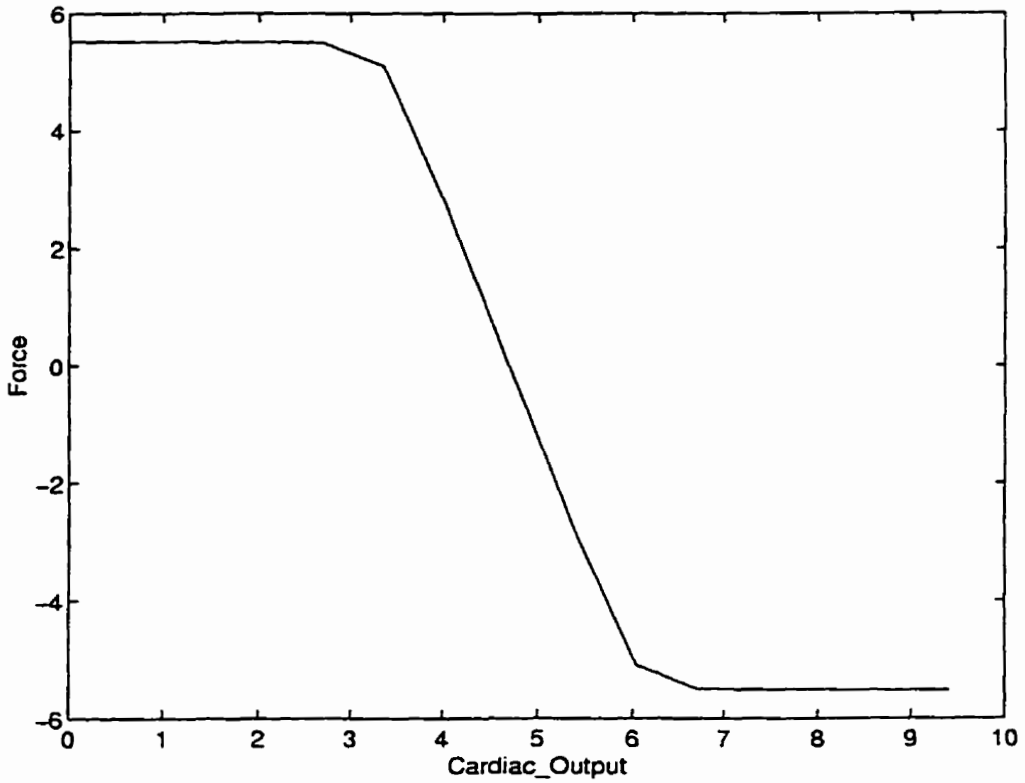


**Figure 6.12:** The FLC plot showing the relationship between pump output and the change in systolic force ($\Delta F_{sys}$)

## 6.10 Variablity of the pump Output

At present the controller is designed to maintain a fixed pump output which is based on the normal resting human pump output. Studies have shown that the use of the difference in venous and arterial oxyhemoglobin to determine the pump output required would be an effective method of estimating the body requirement of oxygen when metabolism and external factors change [6, 12].

The controller can be modified very simply to provide control for a varied input of pump output (desired pump output). This was the purpose for maintaining the input set $X$ at 0 to 2 times the nominal value. The modification is that the nominal value can be made to be a gain value and the input space divided into a universe of discourse of a domain $(0, 2)$ which is non-dimensional. The gain value can be varied depending on the required pump output to maintain proper function of the circulatory system. The control corrections will be made based on the desired value set by the required pump output estimate.

## 6.11 Pressure-Volume Loops

The Pressure-Volume loops show the pressure and volume data of the artificial heart all displayed on a single graph. A typical pressure-volume loop of the nominal function of the artificial heart is shown in Figure 6.13.

The pressure-volume curve shows the filling, isovolumic contraction, ejection and isovolumic relaxation which are illustrated counterclockwise from the left bottom end. The top width of the loop during any single beat is known as the stroke volume which is given by $EDV - ESV$ (Systole), and the bottom width is known as the filling phase (Diastole). The pressure-volume loop moves left or right depending on the blood volume in the heart. These pressure-volume loops vary depending on the characteristics of the artificial heart. In natural hearts these loops move in constrained passive and active elastic curves known as diastolic elastance and systolic elastance (inverse of compliance function) respectively. The pressure-volume loops can move left, right, upwards, and downwards. These curves act as boundaries of the natural heart to provide a maximum and minimum [2, 9].

## 6.12 Ejection Performance

The ejection fraction is a mathematical value which rates the performance of the artificial heart or natural heart with its filling and pumping of blood from the heart

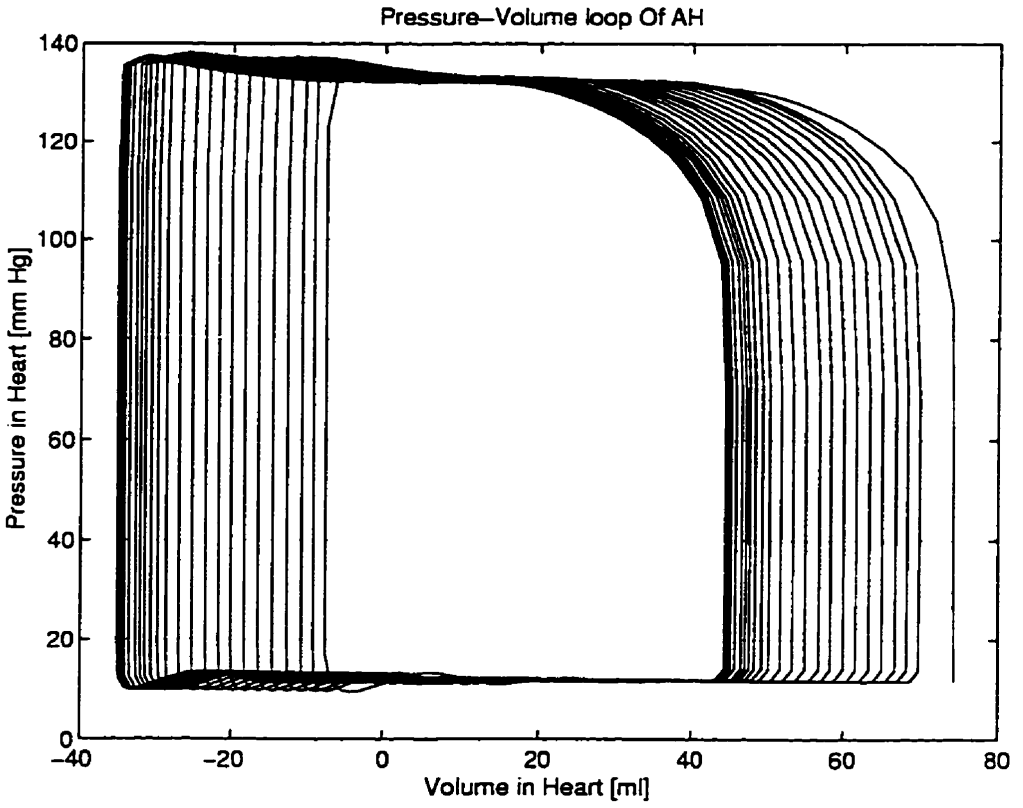


**Figure 6.13:** Nominal condition showing the pressure-volume loop. The plot shows the pressures during systolic and diastolic phases and also the blood volume volume in the heart. Every beat makes a single loop and the loop trends shows the transient of the artificial heart ( - pressure volume loop).

given by Equation (6.16). The parameter is dimensionless. A typical ejection fraction is shown in Figure 6.14 which shows a unity ejection fraction implying that the stroke volume is equal to the end Diastolic Volume (EDV) at about the 40th beat. An increase is seen in the ejection fraction during the initial phase which implies that the stroke volume is larger than the EDV for the first few beats in the simulation.

$$EJ = \frac{\text{Stroke Volume}}{\text{End Diastolic Volume}} \tag{6.16}$$

The ejection fraction is an output of the simulation on a beat by beat bases as shown in the code *frbtbybt.m*.

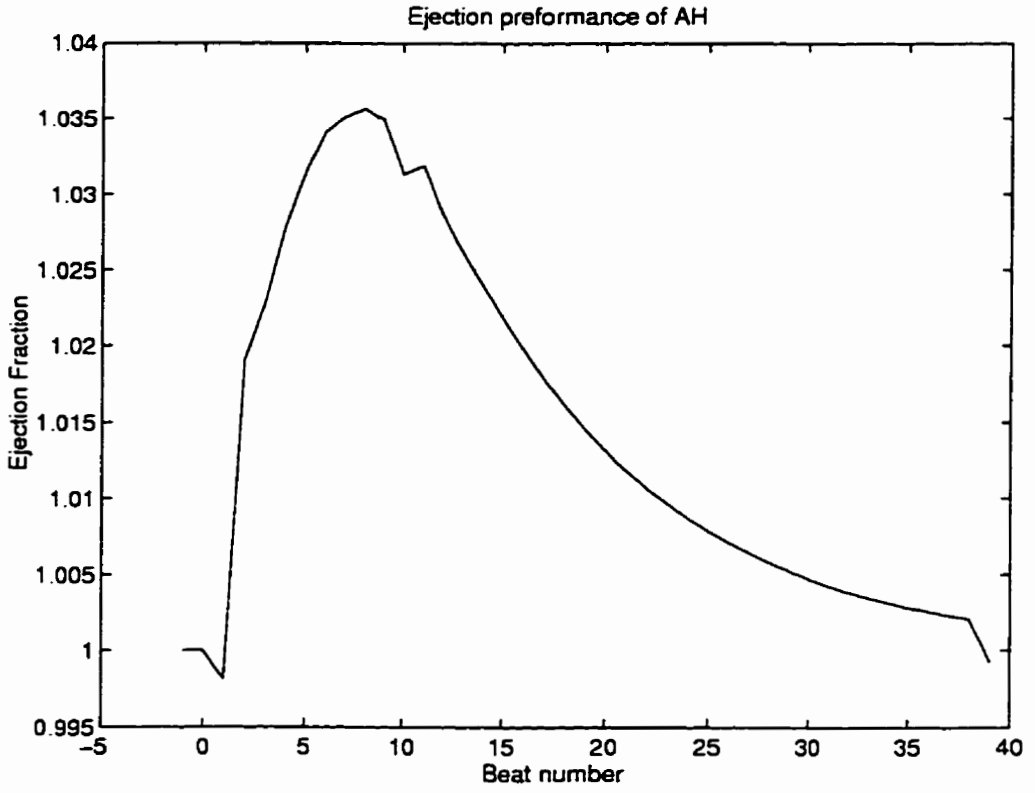


**Figure 6.14:** Ejection fraction showing the filling and ejection of the artificial heart. The sharp edges show generally bad estimates on the stroke volume which causes sudden changes in systolic force from the FLC.

| Peripheral Resistance Simulation | | | |
|---|---|---|---|
| **Effect** | **Multiplers** | **Failure Value** | **Failure Mode** |
| Increase | 1.2, 1.25, 1.5, 1.75, 2, 4, 8, 10 | > 10 | ESV Failure (range) |
| Decrease | 0.9, 0.75, 0.5, 0.25, 0.1 | < 0.1 | ESV Faliure (range) |

**Table 6.3:** Periperhal Resistance FLC Simulation

## 6.13 Peripheral Resistance And Control

The change in peripheral resistance is a common way the human body responds to external stimuli. When an individual is exposed to hot or cold climates their peripheral vascular resistance changes to control their body temperature. Similarly when an individual is sick their peripheral vascular resistance varies depending on the amount of oxygen required by the body. Therefore control of pump output during such periods is the key to attain a good controller for an artificial heart. At present the controller is fixed to maintain a desired pump output which is fixed at $4.7\frac{L}{min}$. An increase or decrease in peripheral resistance is simulated and controlled with the FLC. The Table 6.3 shows the range of values used in peripheral vascular resistance simulation and a summary of the failure observed.

### 6.13.1 Increase in $R_{pe}$

When peripheral resistance is increased we see that the aorta pressure rises as shown in Figure 6.15. At two times the nominal peripheral resistance of the blood flowing through the peripheral is constricted and hence increasing the volume of blood in the arterial, aorta and outlet cannula segments. Similarly a lower blood volume is seen in the venous segment of the circulatory system. The increase in volume causes an increase in pressure which lowers the flow rate from the artificial heart causing low pump output. The peripheral flow is seen to dip in the begining due to the increase in resistance and rises after the first few beats due to the control action of the fuzzy logic control as shown in Figure 6.16. We assume that when a drop in peripheral flow falls below $3\frac{L}{min}$ for a very brief period of less than 5 beats it will

not cause damage to internal organs or tissues. The pressure volume loop shown in Figure 6.17 shows that the loop is seen to shift towards the left and the artificial heart systolic pressure is seen to gradually increase due to the increase in the systolic force.

### 6.13.2 Control Response

The Figure 6.18 shows the control force $\Delta F_{sys}$ and $F_{sys}$ as a function of beat number. The systolic force is seen to rise quickly in the first 10 beats of control to make up the drop in pump output. The pump output shown in Figure 6.19 initially drops showing a low pump output. The change in force rises the pump output to a value of about $4.7\frac{L}{min}$ in less than 10 beats. Due to the small error between the estimated pump output and actual pump output the actual pump output is slightly lower than the desired pump output as shown in Figure 6.19. The sharp corners on the pump output Figure 6.19 is due to the changes in the systolic force and the averaging calculation of pump output for a beat by beat numerical estimate. The steady state systolic force is about 58.41 N to maintain required pump output at the desired value. The outlet cannula pressure is seen to rise as a consequence of the rise in systolic force and the increase in steady state blood volume in the outlet cannula in Figure 6.20. The steady state outlet cannula pressure is about 178.9 mm Hg which is quite high and would depend on mechanical design constraints of the outlet cannula stress tolerance and the effect of such high pressures on outlet valves. Although such high pressures are seen in acute patients suffering high blood pressure [52] and is not a adverse problem to the patient.

Figure 6.21 and Figure 6.22 show the EDV and ESV estimates respectively. The estimated EDV is seen to be steady. The actual EDV is seen to decrease initially due to the increased peripheral resistance and lower inlet cannula presure. The control brings back the EDV gradually. The ESV is seen to rise positively initially due to the decreased outlet pressure gradient which is corrected by the controllers increase in systolic force. The EDV is within expected errors as shown in Figure 6.23 with

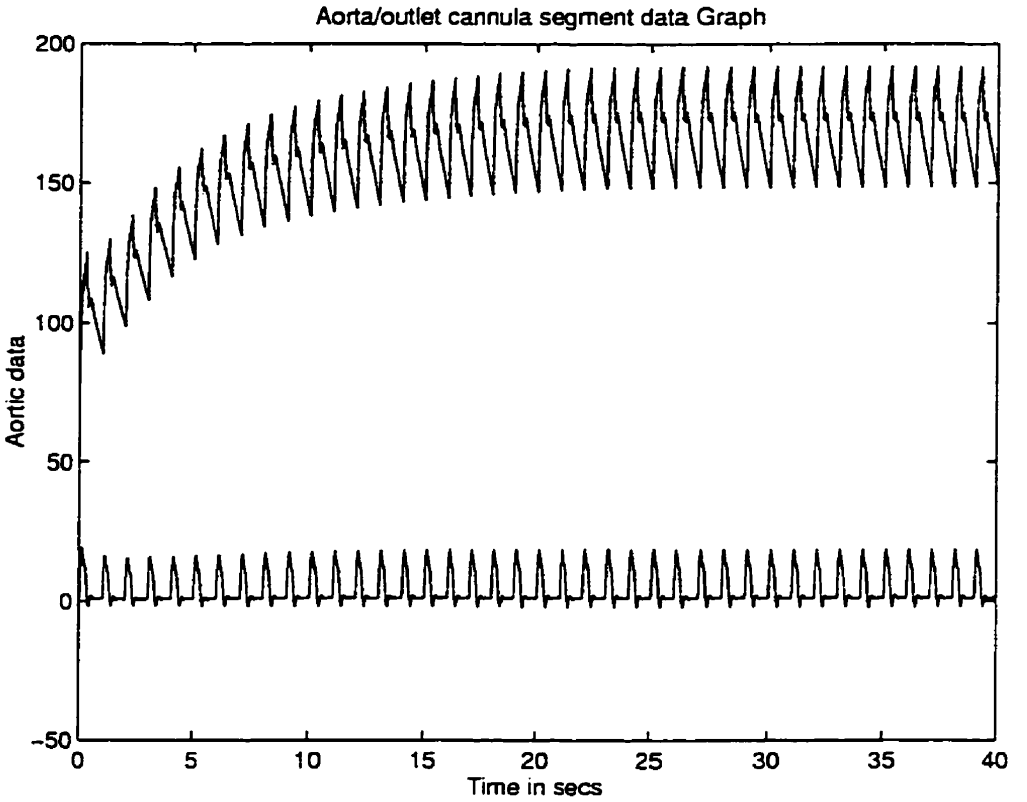


**Figure 6.15:** aorta/outlet cannula segment data for an increase in peripherial resistance ($R_{pe} \times 2$) ( - aorta pressure [mm Hg], .. outlet cannula pressure [mm Hg], -.- aorta flow rate $[\frac{L}{min}]$, - outlet cannula flow rate (lower line) $[\frac{L}{min}]$)

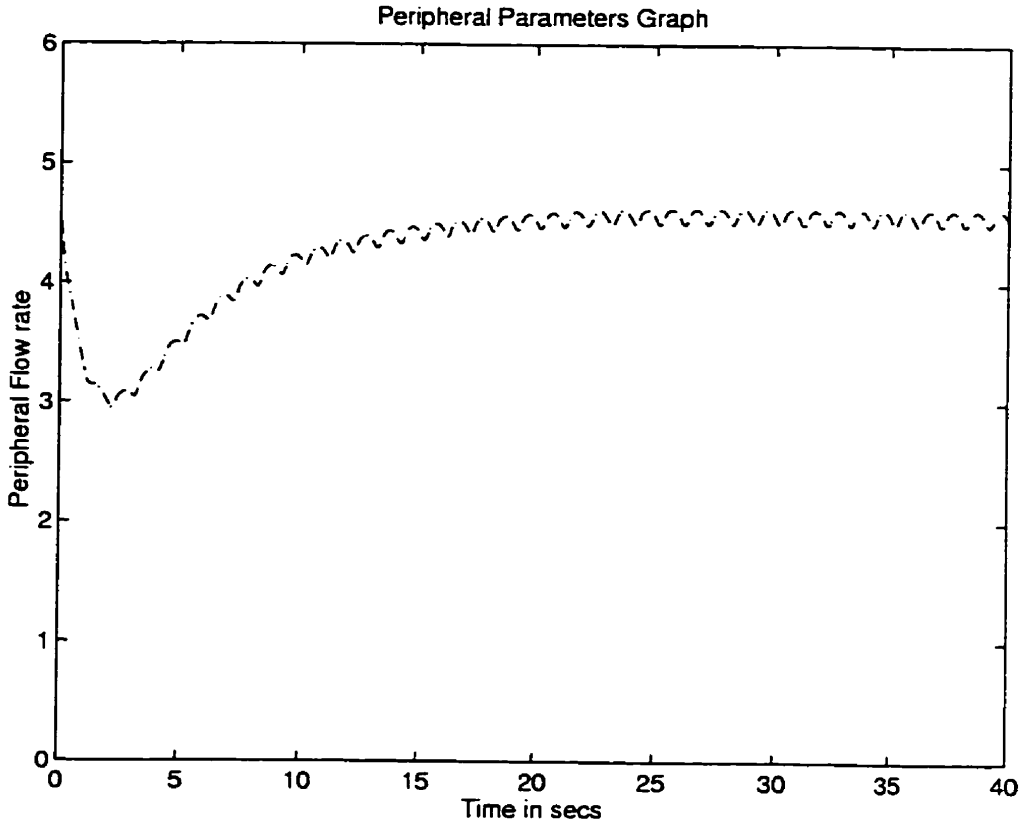


**Figure 6.16:** Peripheral flow $[\frac{L}{min}]$ for an increase in peripherial resistance ($R_{pe} \times$ 2)

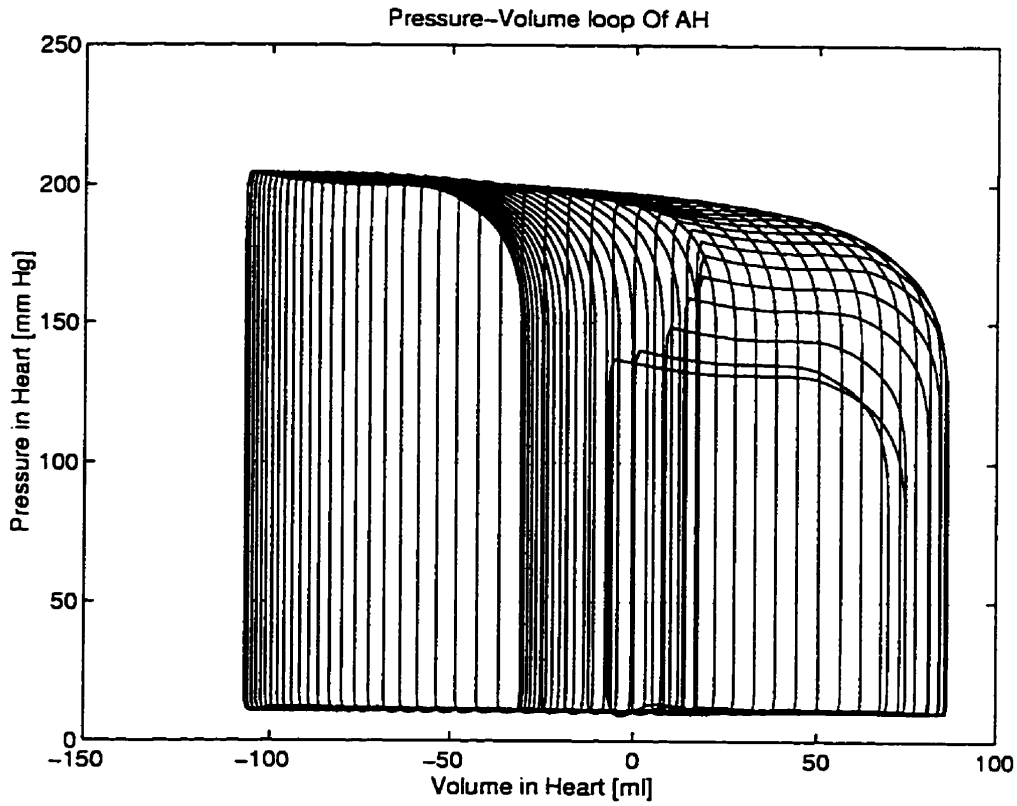


**Figure 6.17:** Pressure Volume Loop for an increase in peripherial resistance ($R_{pe} \times 2$)

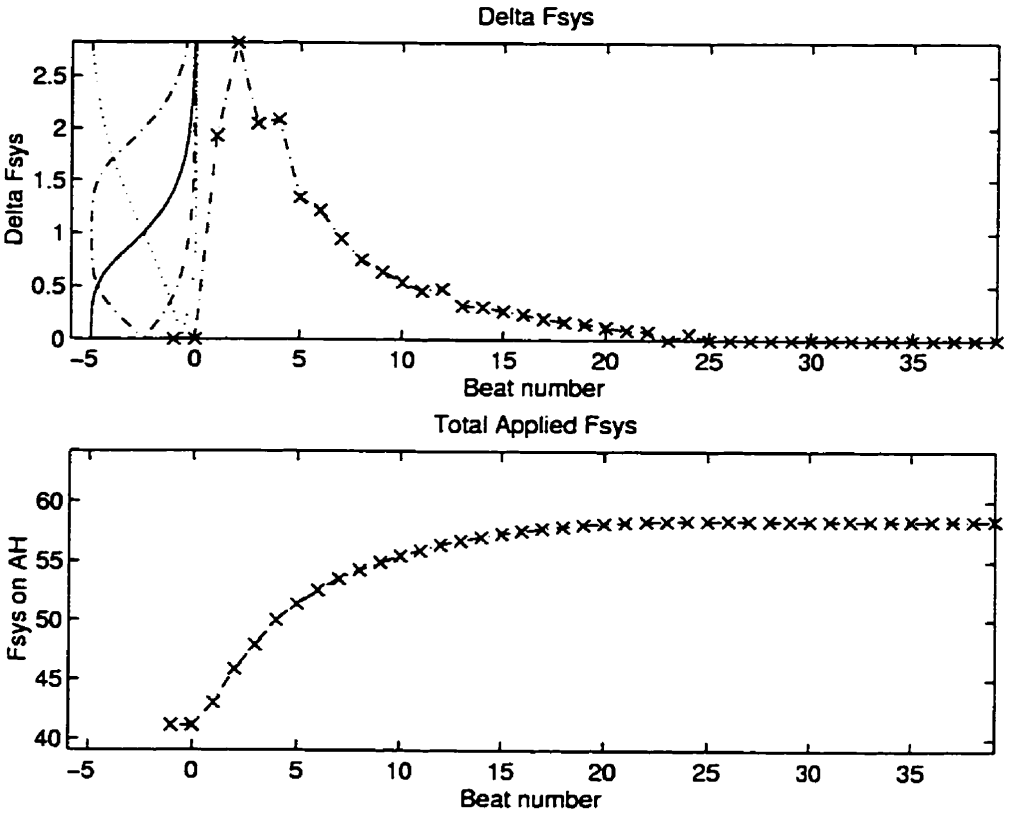


**Figure 6.18:** Control changes for an increase in peripherial resistance ($R_{pe} \times 2$). Top: change in systolic force for each beat [N]. Bottom: The systolic force acting on the artificial heart from beat to beat [N]

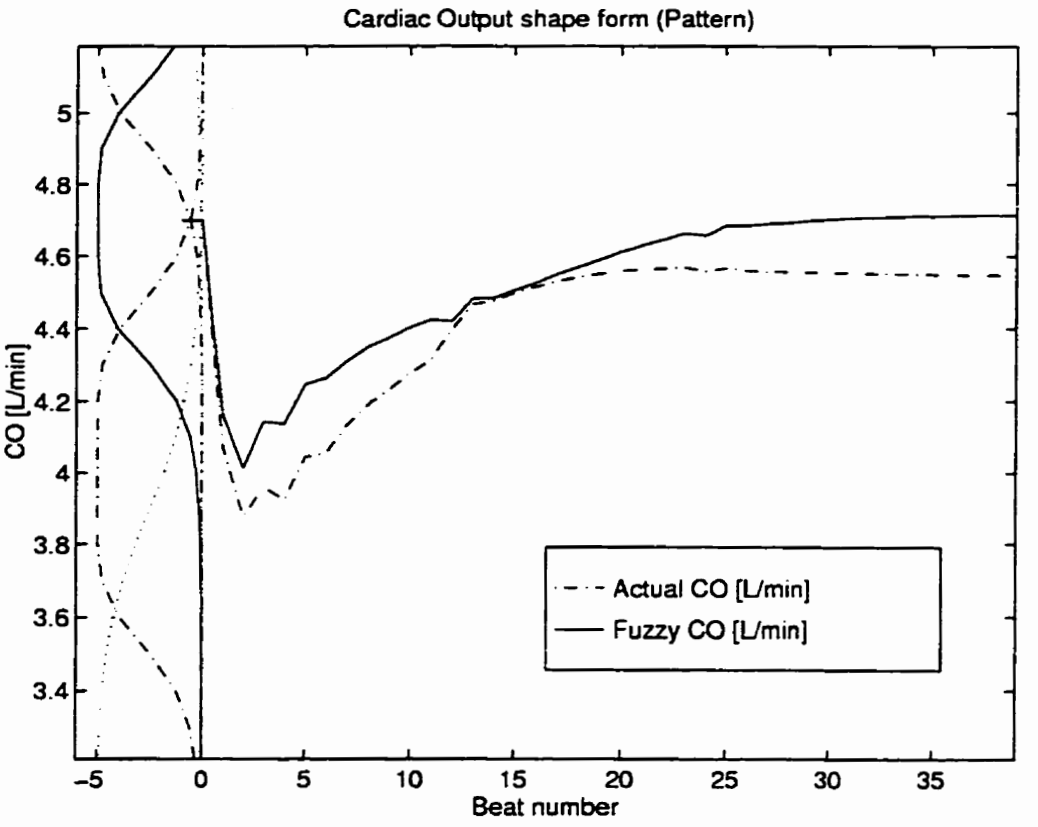


**Figure 6.19:** pump output for an increase in peripherial resistance ($R_{pe} \times 2$). ( - Fuzzy infered pump output $[\frac{L}{min}]$, -.- Actual pump output $[\frac{L}{min}]$).

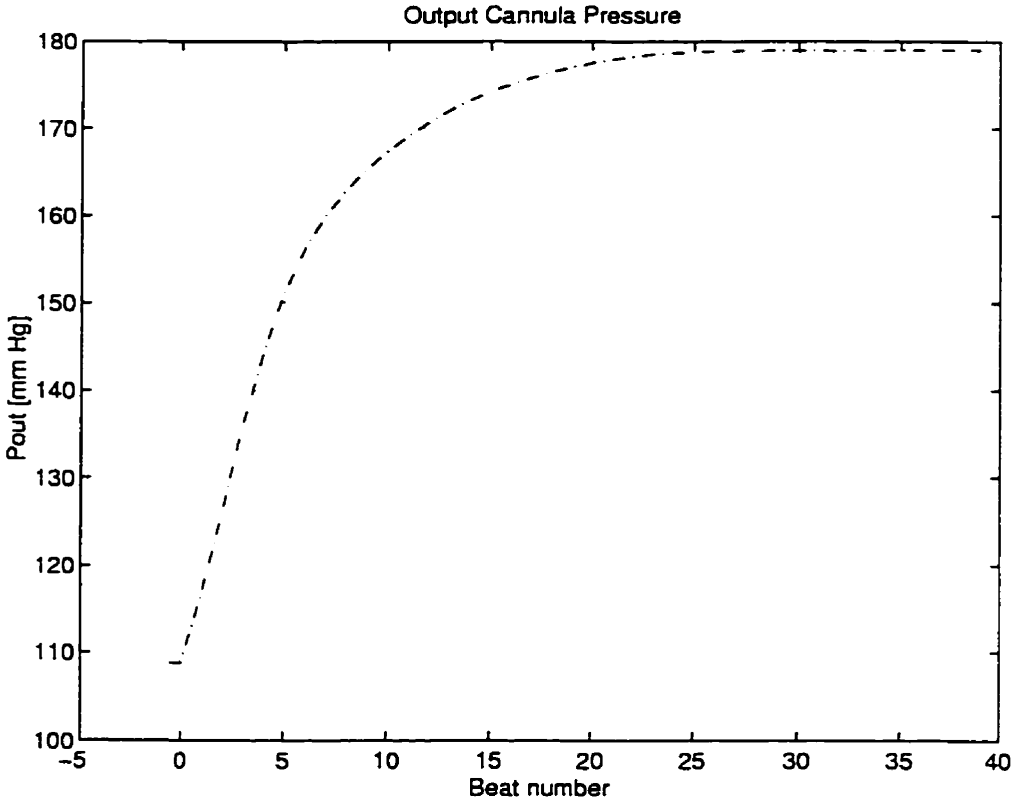


**Figure 6.20:** Average outlet cannula pressure over the systolic phase for an increase in peripherial resistance ($R_{pe} \times 2$). ( -.- Output cannula pressure [mm Hg])

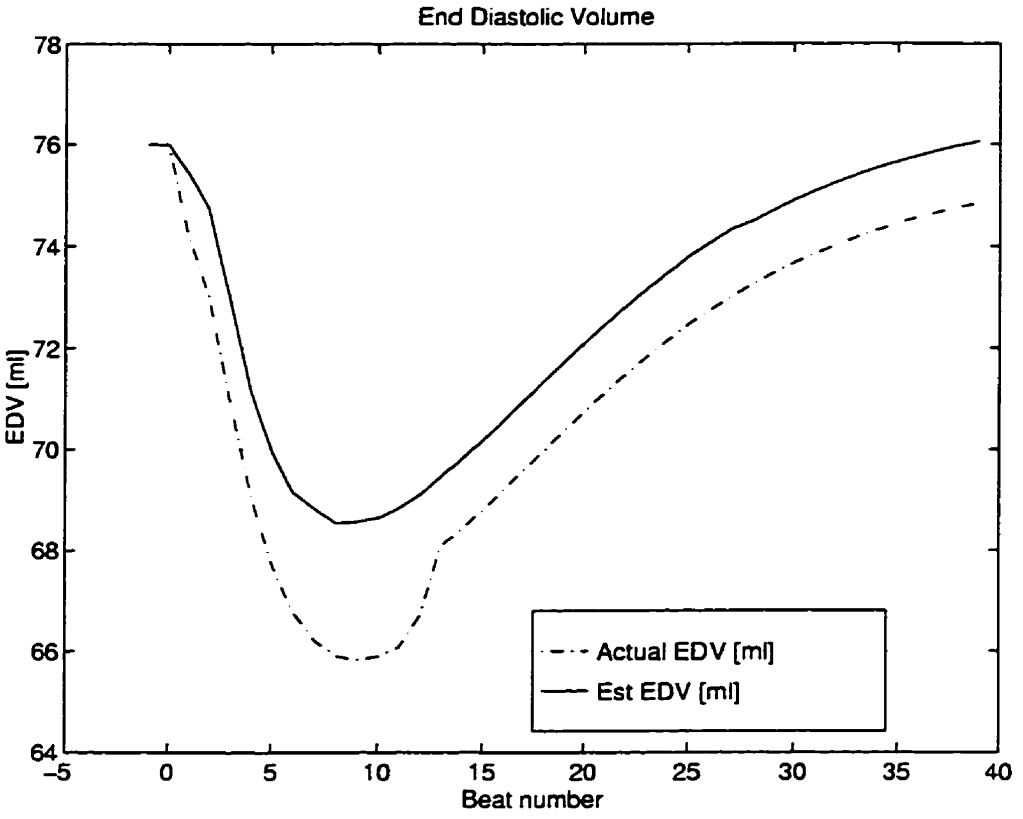


**Figure 6.21:** End diastolic volume for an increase in peripherial resistance ($R_{pe} \times 2$). ( - Fuzzy infered EDV [ml], -.- Actual EDV [ml])

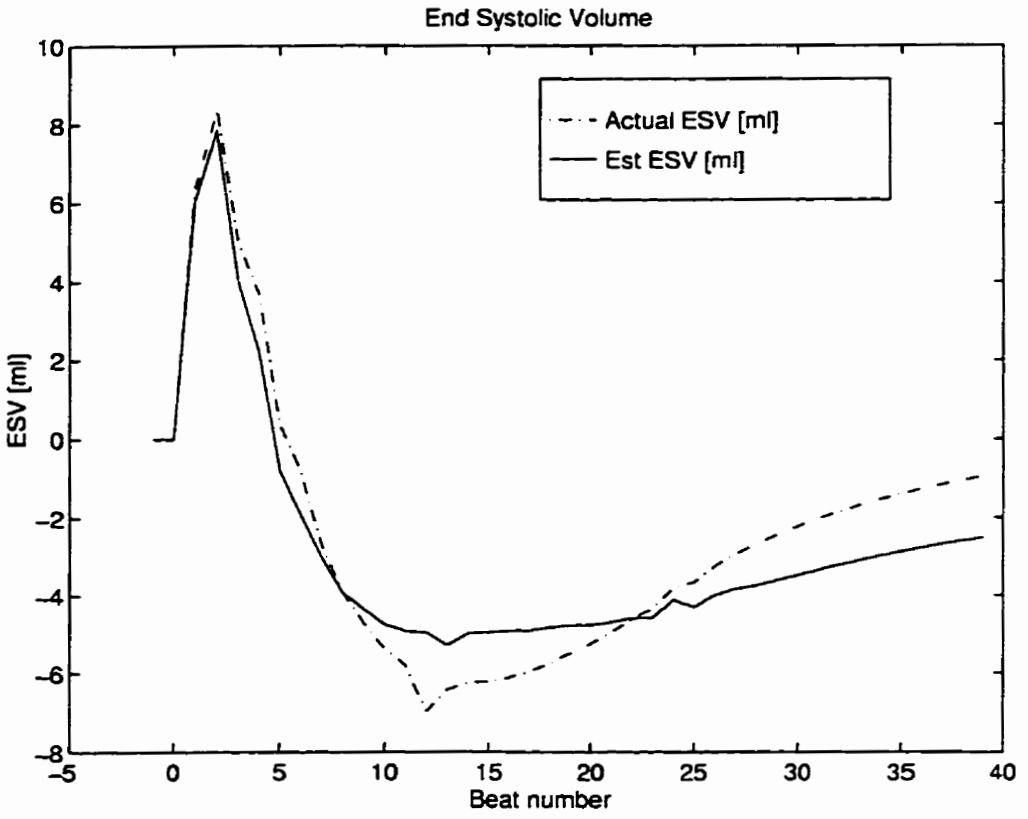


**Figure 6.22:** End systolic volume for an increase in peripherial resistance ($R_{pe} \times 2$). ( - Fuzzy infered ESV [ml], -.- Actual ESV [ml])

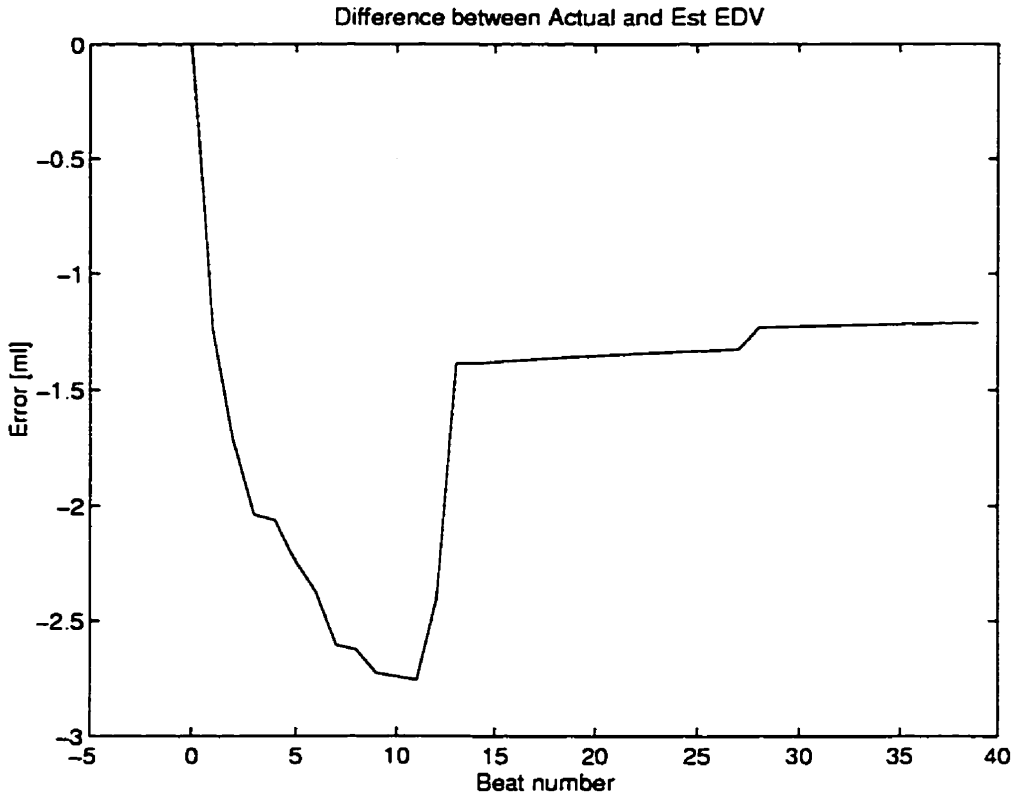


**Figure 6.23:** End diastolic volume [ml] error for an increase in peripherial resistance ($R_{pe} \times 2$).

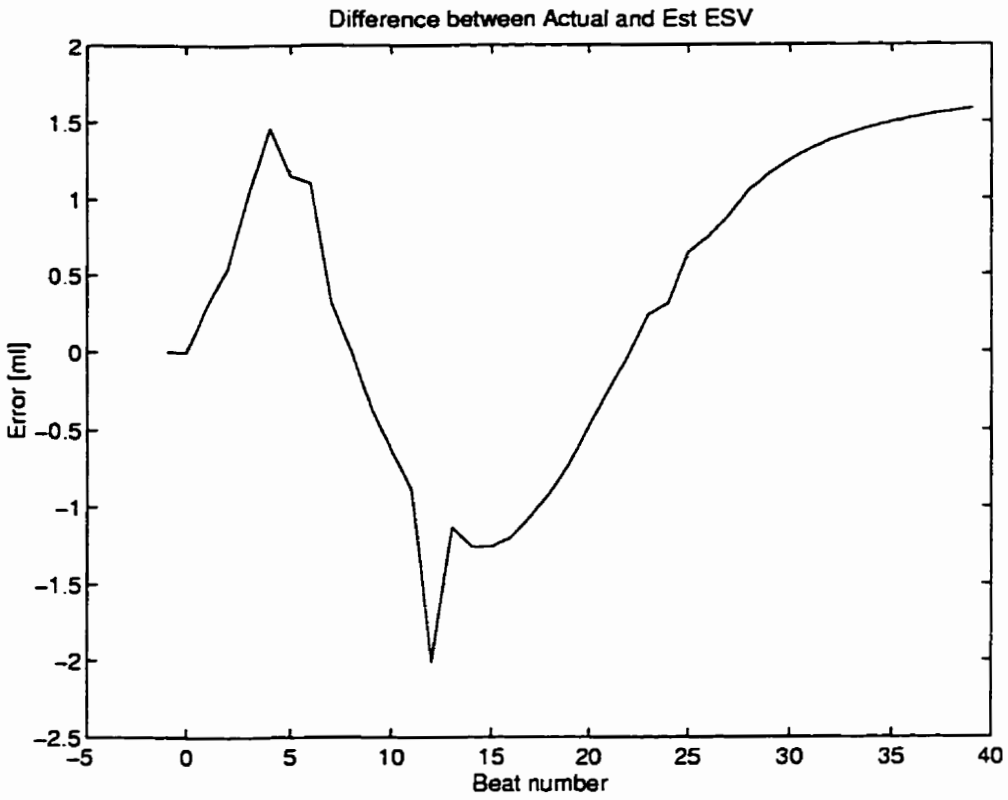


**Figure 6.24:** End systolic volume [ml] error for an increase in peripherial resistance ($R_{pe} \times 2$).

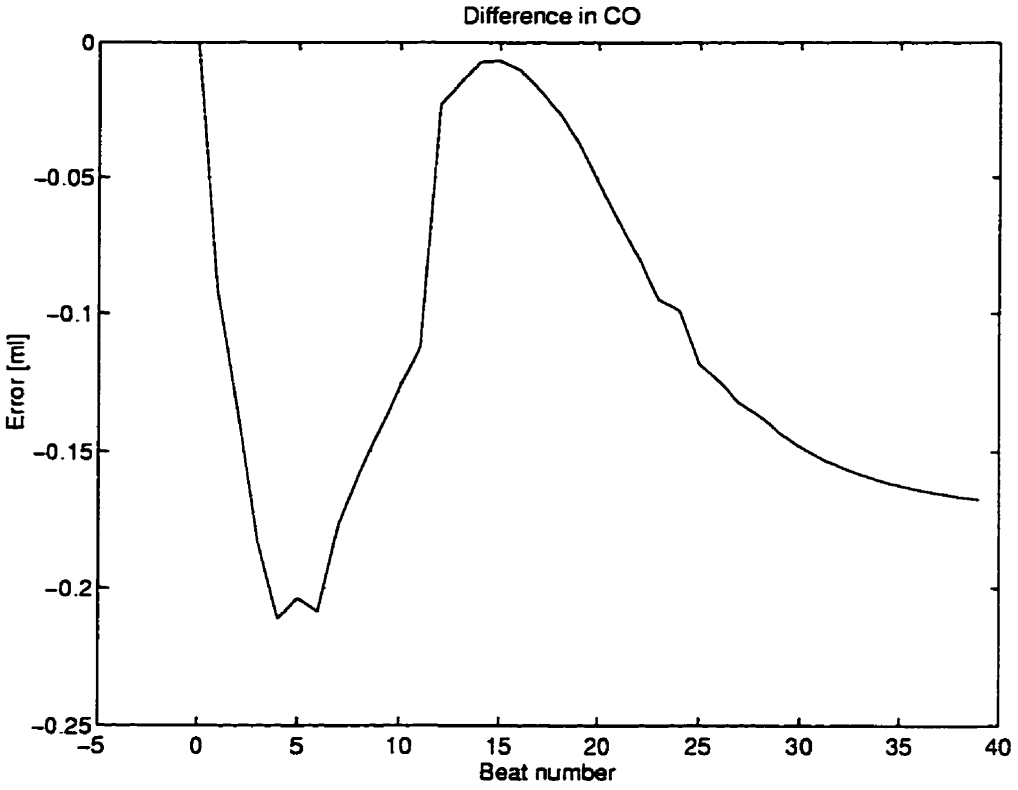


**Figure 6.25:** pump output $[\frac{L}{min}]$ error for an increase in peripherial resistance ($R_{pe} \times 2$).

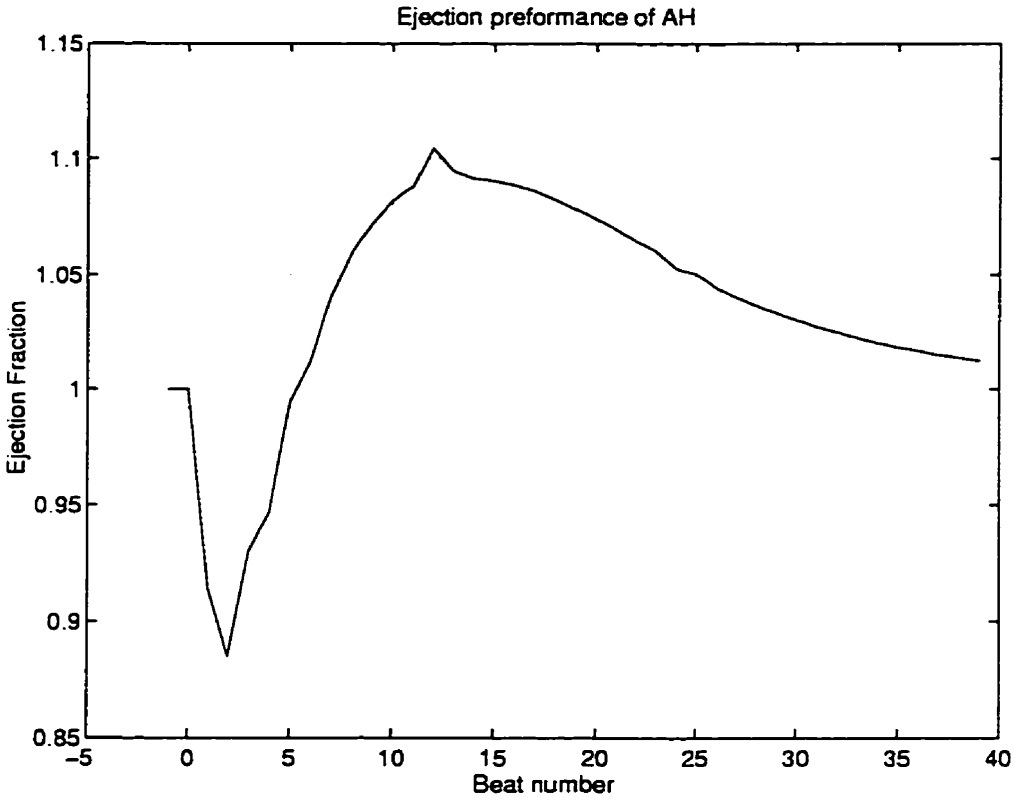


**Figure 6.26:** Ejection fraction for an increase in peripherial resistance ($R_{pe} \times 2$).

### 6.13.3 Decrease in $R_{pe}$

A decrease in peripheral vascular resistance shows that aortic pressure has dropped significantly from their nominal values to about 90 mm Hg at peak systolic pressures and 45 mm Hg at minimum diastole shown in Figure 6.27. The trend in aortic pressures is seen to oscillate due to the changes in control force (overshoot/undershoot). The peripheral flow in Figure 6.28 shows the oscillations in the peripheral flow rate seen by the circulatory system. The peripheral flow does not drop below $4\frac{L}{min}$ and steady state is reached in 20 beats. The peripheral flow shows an oscillatory motion with a large time period. The overshoot of pump output is seen during initial control to be about $6.5\frac{L}{min}$. The pressure-volume loop in Figure 6.29 shows that an increase in stroke volume moves the loop towards the left. As the artificial heart pressure gradually drops from the fuzzy logic controllers overestimate, the pressure-volume loop moves towards the right. The systolic pressure in the heart is also seen to increase to a value of about 135 mm Hg at steady state from the increase in the systolic force.

### 6.13.4 Control Response

Figure 6.30 shows the control action taken by the controller for a decrease in peripheral vascular resistance. It shows initially that the systolic force drops sharply due to the increase in pump output as shown in Figure 6.31. At the $9^{th}$ beat the change in force is about zero because the pump output has dropped to the desired value. The steady state value of systolic force is about 31.41 N. Figure 6.31 shows the pump output of the system on a beat by beat basis which explains the sharp corners on the figure. The pump output is initially seen to rise which is corrected by a drop in systolic force. The drop in systolic force causes the pump output to gradually drop below the desired value which is corrected by an increase in systolic force which causes the observed oscillations seen in the systolic force of Figure 6.30. The outlet cannula pressure is seen in Figure 6.32 which shows a sharp drop in pressure and then a rise in pressure due to the systolic force correction. A steady state outlet cannula pressure of 73 mm Hg is attained at about the $25^{th}$ beat.

Figure 6.33 and Figure 6.34 show EDV and ESV from the simulation. The EDV is seen to initially rise and drop to a steady state value of about 80 ml from the effects of systolic force. While ESV initialy drops and then rises and attains a steady state value of about 0 ml. The estimated ESV is slightly higher than zero (1 ml). Figure 6.35 and Figure 6.36 show the errors in EDV and ESV respectively. The maximum error in EDV is seen during control and is about 2.1 ml and a steady state error of about 1.2 ml. While the ESV maximum error is also seen during active control which is 6 ml and an error at steady state of 1 ml. These errors do not impact the control action to any significant degree because the estimated pump output is very close to the actual value.

Figure 6.37 shows the pump output error which has a maximum value of $0.5\frac{L}{min}$ at the $9^{th}$ beat due to the ESV estimate error. The ejection fraction is shown in Figure 6.38 which shows initial increase and then a drop in the ejection fraction which explains the pressure-volume loop behaviour.

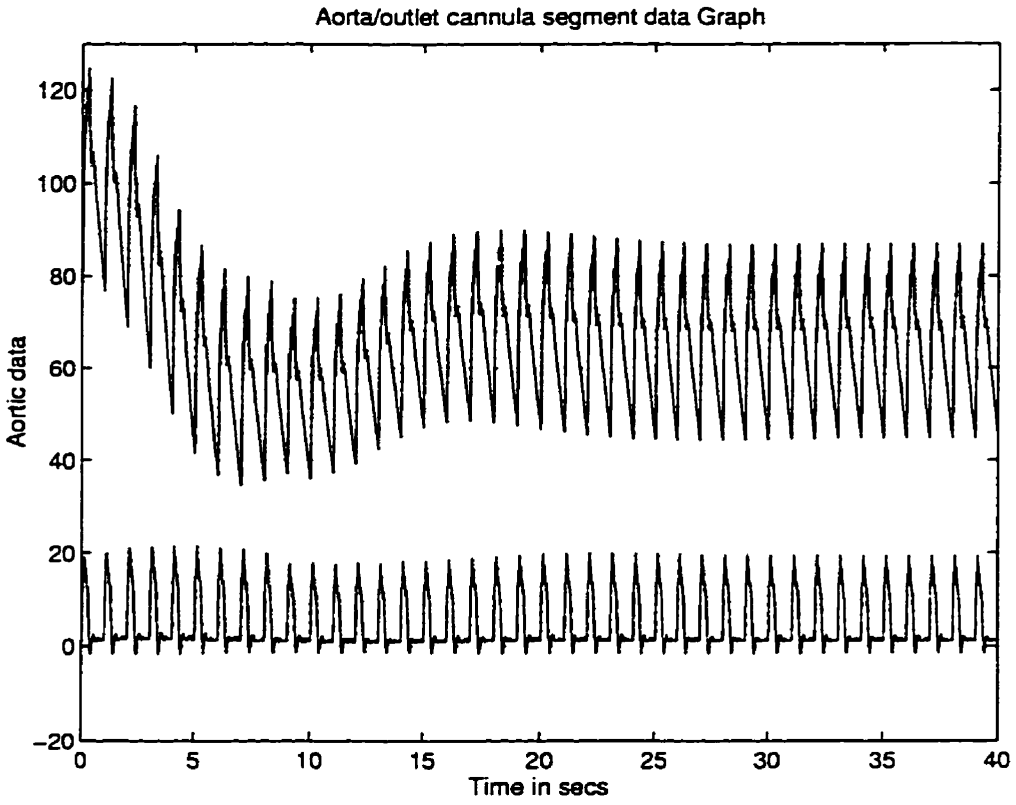


**Figure 6.27:** aorta/outlet cannula segment data for an decrease in peripherial resistance ($R_{pe} \times 0.5$) ( - aorta pressure [mm Hg], .. outlet cannula pressure [mm Hg], -.- aorta flow rate $[\frac{L}{min}]$, - outlet cannula flow rate (lower line) $[\frac{L}{min}]$)

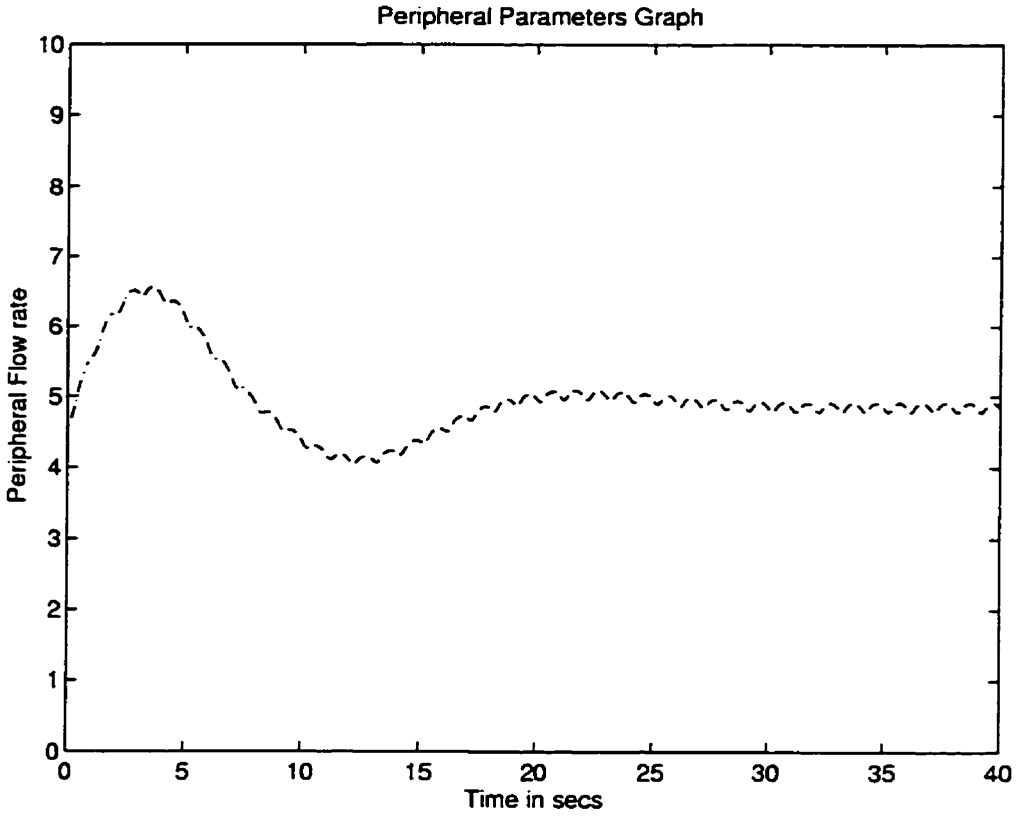


**Figure 6.28:** Peripheral flow $[\frac{L}{min}]$ for an decrease in peripherial resistance ($R_{pe} \times 0.5$).

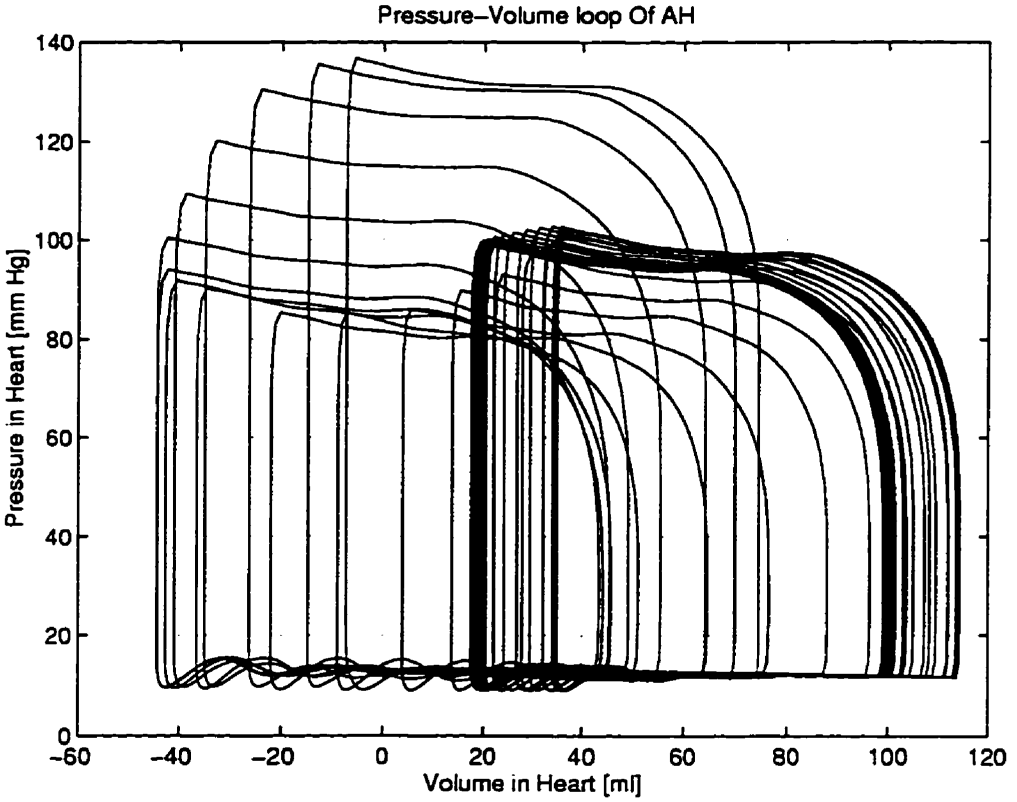


**Figure 6.29:** Pressure Volume Loop for an decrease in peripherial resistance ($R_{pe} \times 0.5$)

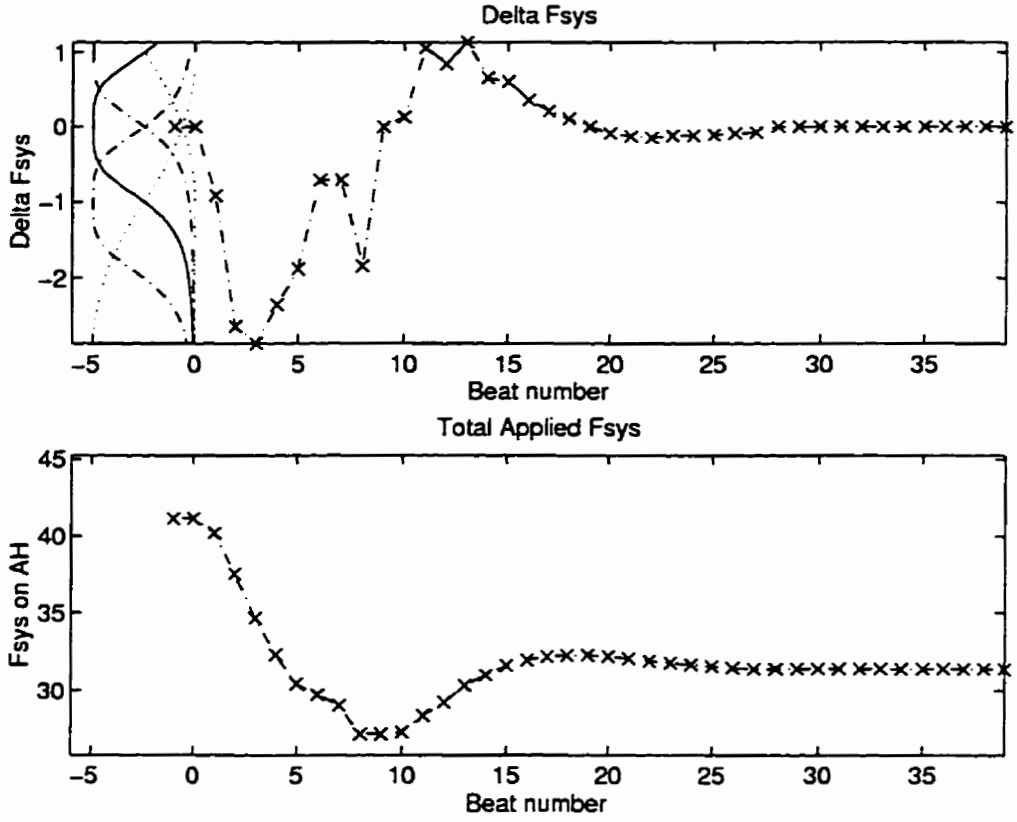


**Figure 6.30:** Control changes for an decrease in peripherial resistance ($R_{pe} \times 0.5$). Top: change in systolic force for each beat [N]. Bottom: The systolic force acting on the artificial heart from beat to beat [N].

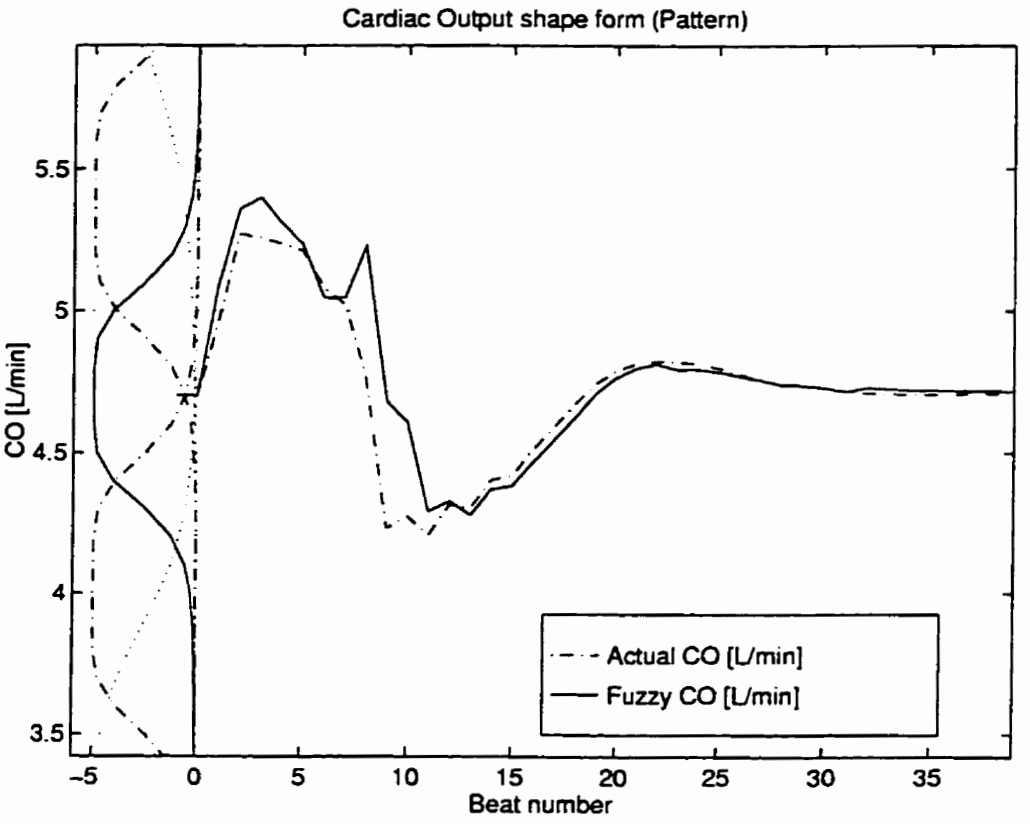


**Figure 6.31:** pump output for an decrease in peripherial resistance ($R_{pe} \times 2$). ( - Fuzzy infered pump output $[\frac{L}{min}]$, -.- Actual pump output $[\frac{L}{min}]$).

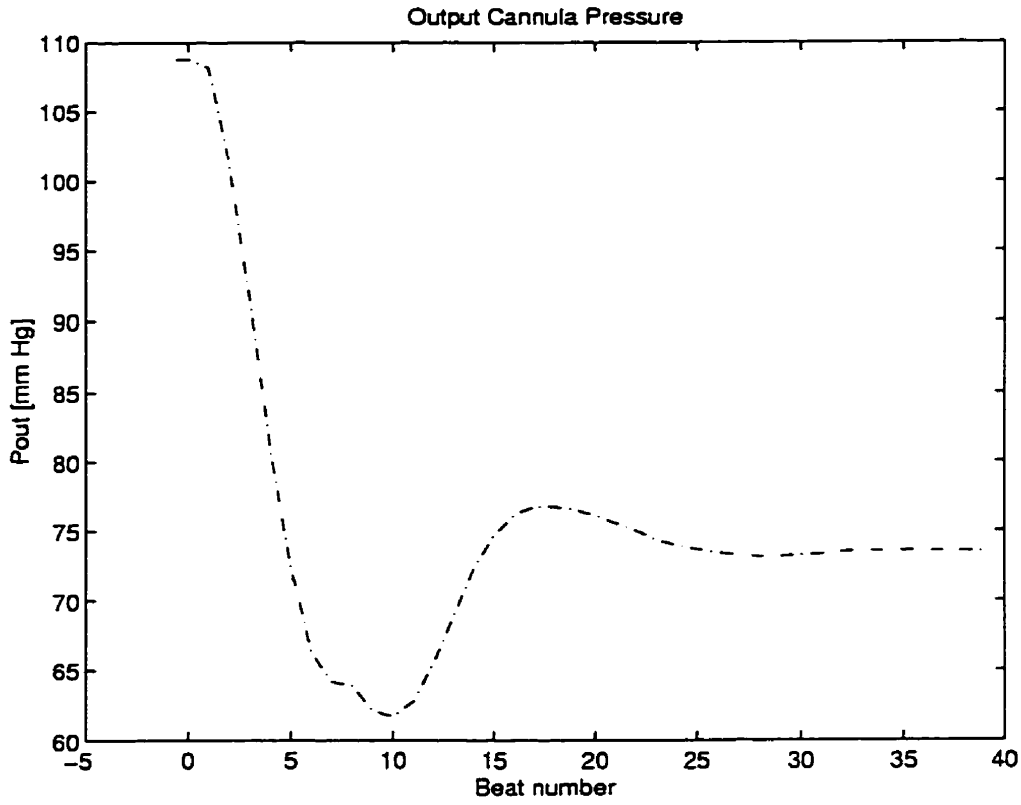


**Figure 6.32:** Average outlet cannula pressure over the systolic phase for an decrease in peripherial resistance ($R_{pe} \times 0.5$). ( -.- Output cannula pressure [mm Hg]).

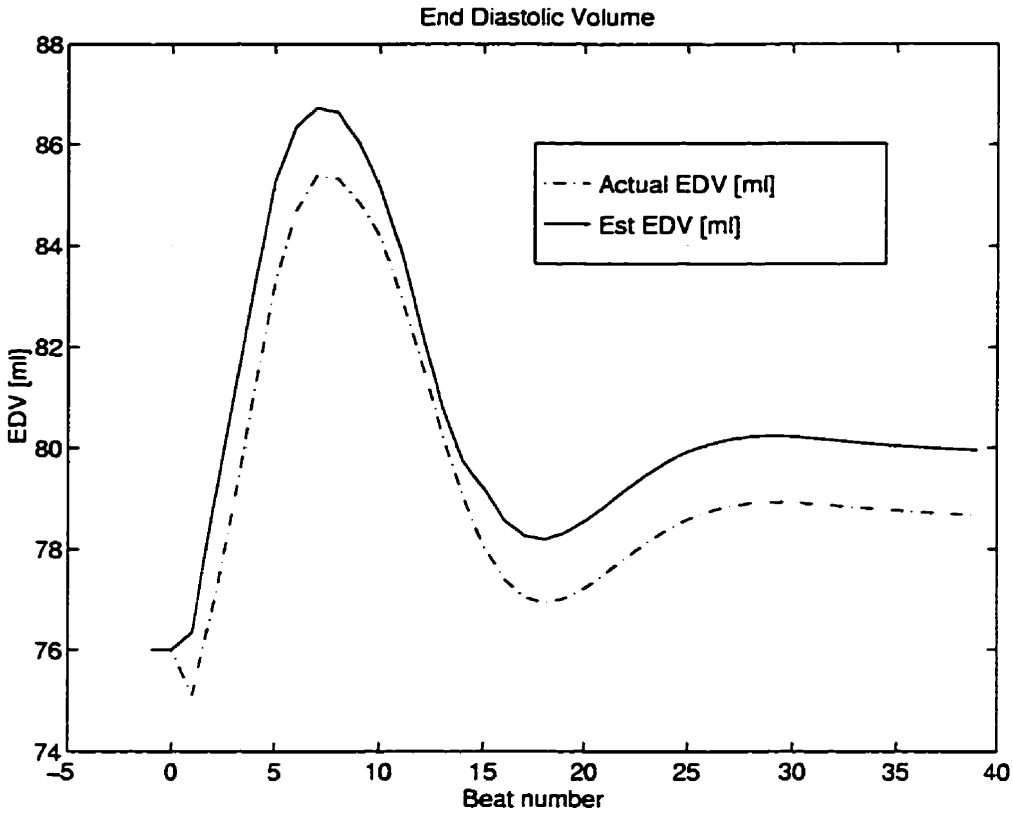


**Figure 6.33:** End diastolic volume for an decrease in peripherial resistance ($R_{pe} \times 0.5$). ( - Fuzzy infered EDV [ml], -.- Actual EDV [ml])

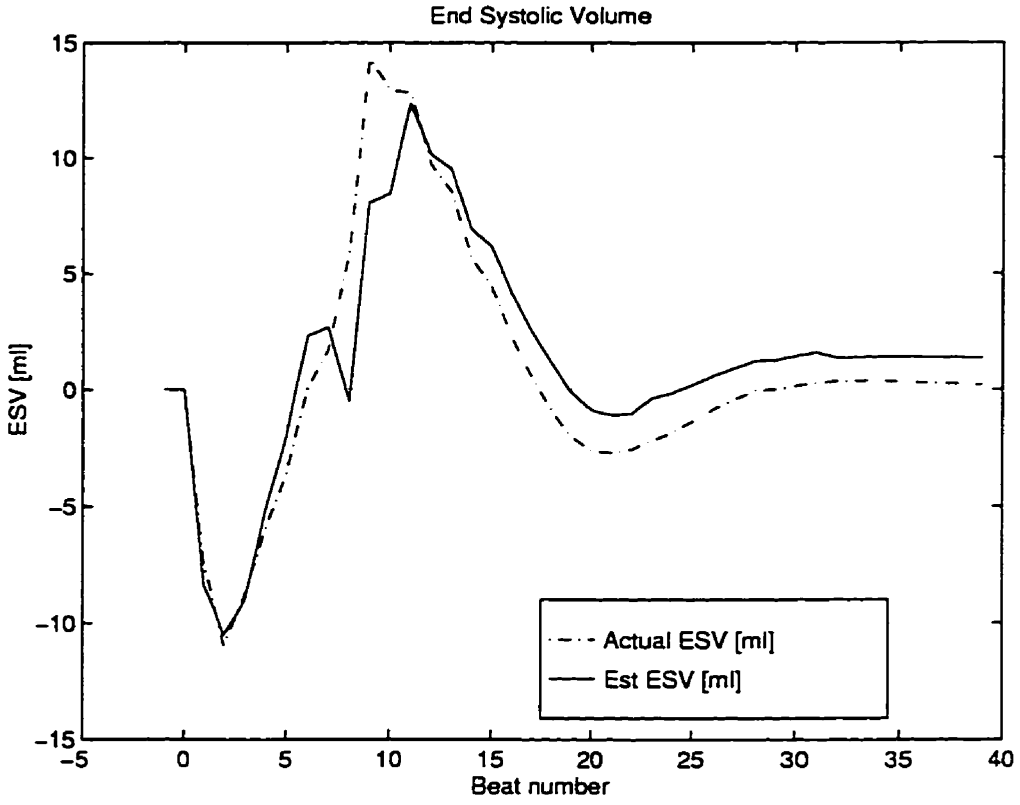


**Figure 6.34:** End systolic volume for an decrease in peripherial resistance ($R_{pe} \times 0.5$). ( - Fuzzy infered ESV [ml]. -.- Actual ESV [ml])

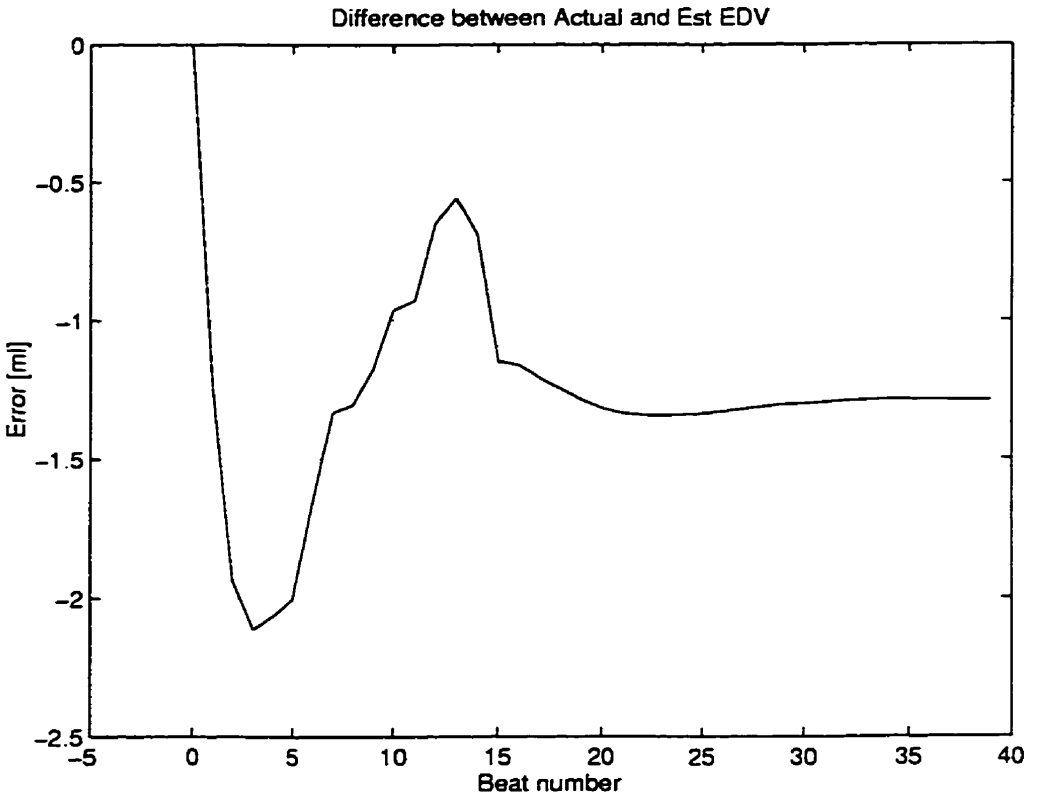


**Figure 6.35:** End diastolic volume [ml] error for a decrease in peripherial resistance ($R_{pe} \times 0.5$).

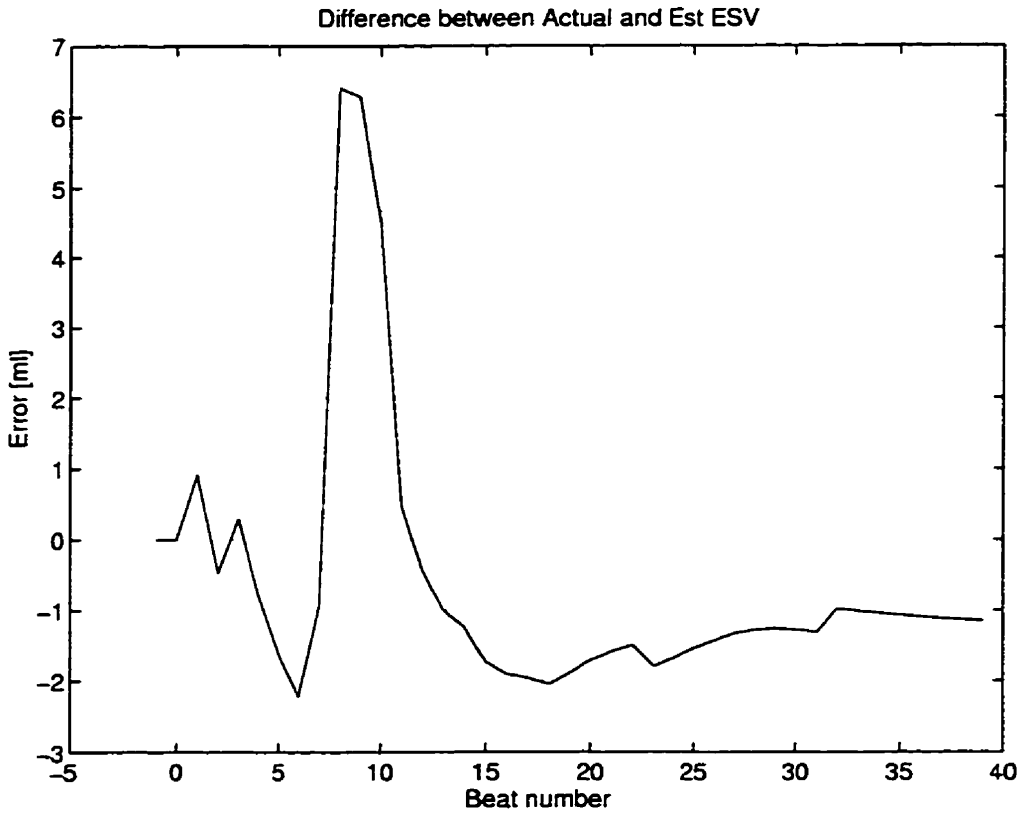


**Figure 6.36:** End systolic volume [ml] error for a decrease in peripherial resistance ($R_{pe} \times 0.5$).

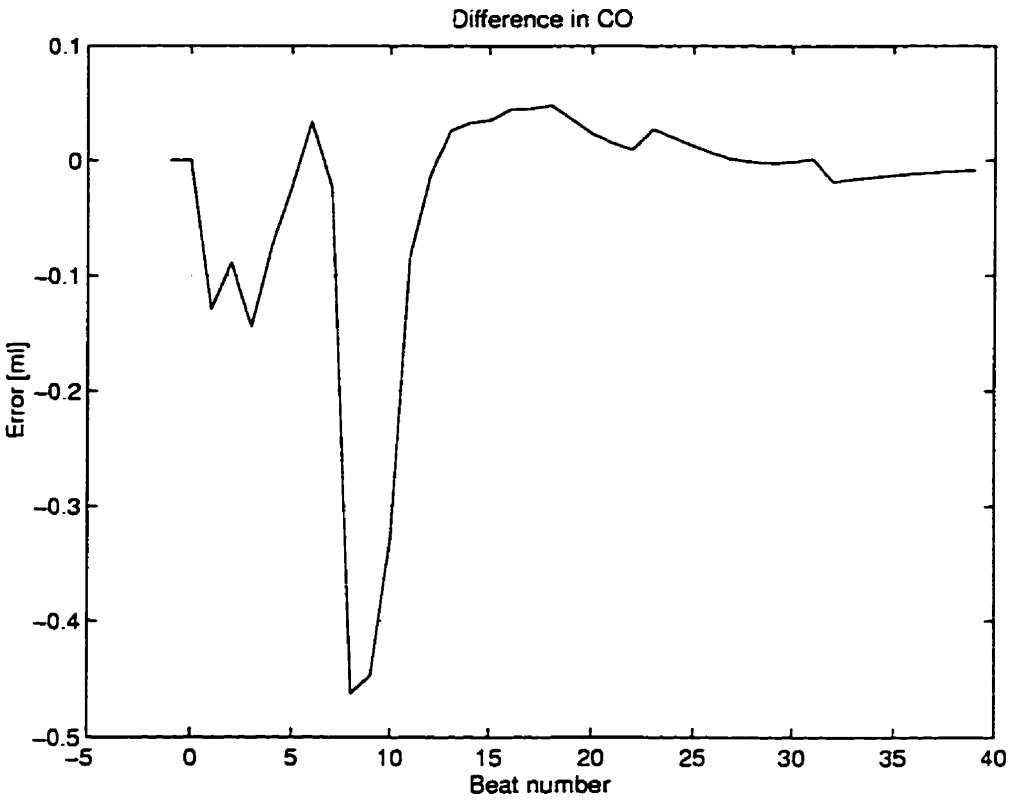


**Figure 6.37:** pump output $[\frac{L}{min}]$ error for a decrease in peripherial resistance ($R_{pe} \times 0.5$).

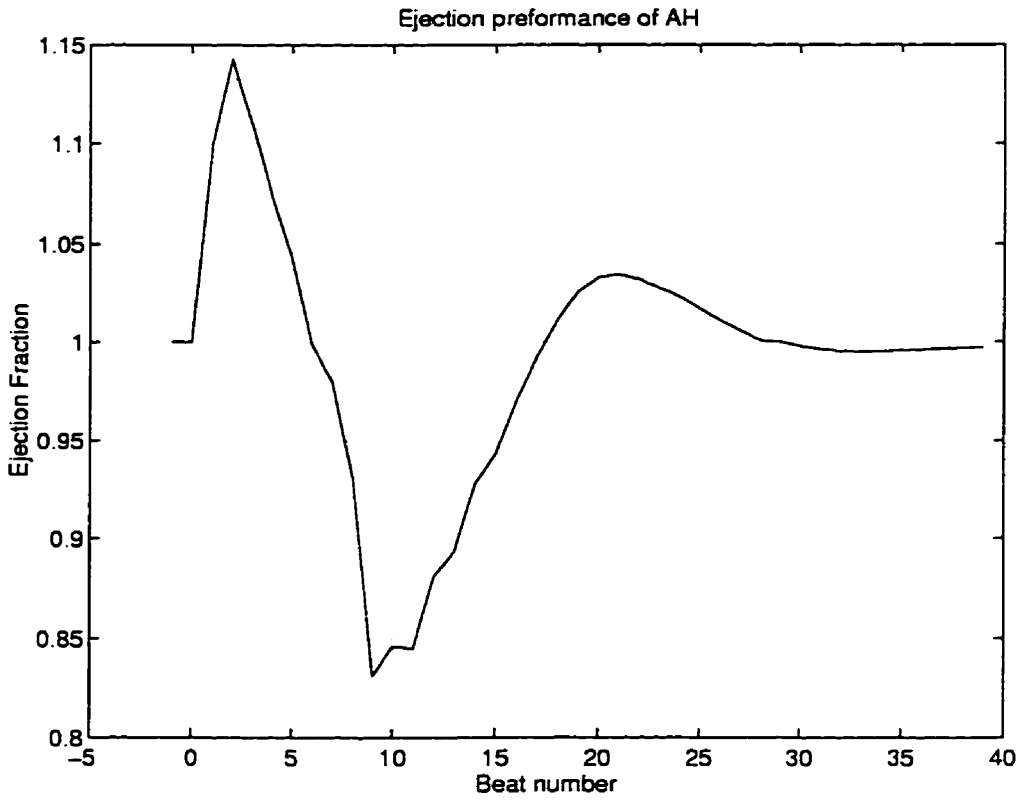


**Figure 6.38:** Ejection fraction for an decrease in peripherial resistance ($R_{pe} \times 0.5$).

## 6.14 Initial Condition Response

The initial conditions is the state vector used when the simulation is begun. These initial conditions include the volume of blood in each of the circulatory segments and the momentum of blood in these segments at startup.

### 6.14.1 Outlet cannula Volume

The outlet cannula volume initial conditions were changed to simulate lower and higher startup blood volumes with the aid of a multiplier less than one and greater than one respectively. The response of the system is very similar to the later discussed changes in the value of the outlet cannula compliance values ($C_{cnot}$).

When outlet cannula volume is increased or decreased it causes the outlet cannula pressure and flow rate to be very oscillator for the first few beats of the simulation. The oscillations dampen out due the the high stiffness of the model. The controller during this is very minimal and approaches its nominal systolic force after the few (5-7) beats with $F_{sys} = 41.8N$. The main changes in systolic force are during the first (2-4) beats of the simulation. At very large changes in the startup values of the outlet cannula volume the estimated stroke volume is not accurate because the input values of the $\Delta P_{in}$ and $\Delta P_{out}$ are outside their universe of discourse.

The effect of an increase in initial cannula blood volume is similar to the behavior during a decrease in the outlet cannula compliance. Figure 6.39 shows the control for an increase in the outlet cannula volume by a factor of 2 which shows that a steady state is achieved after the first few beats. Figure 6.40 shows the pump output during the first beat, the estimated pump output is off because of the estimation of the ESV. The outlet pressure gradient is 4.354 mm Hg which is outside the range of $\langle 8.5, 28.7 \rangle$ mm Hg for the ESV estimator. This shows that the estimator has failed for ESV.

The effect of the decrease in initial blood volume in the cannula is similar to the in-

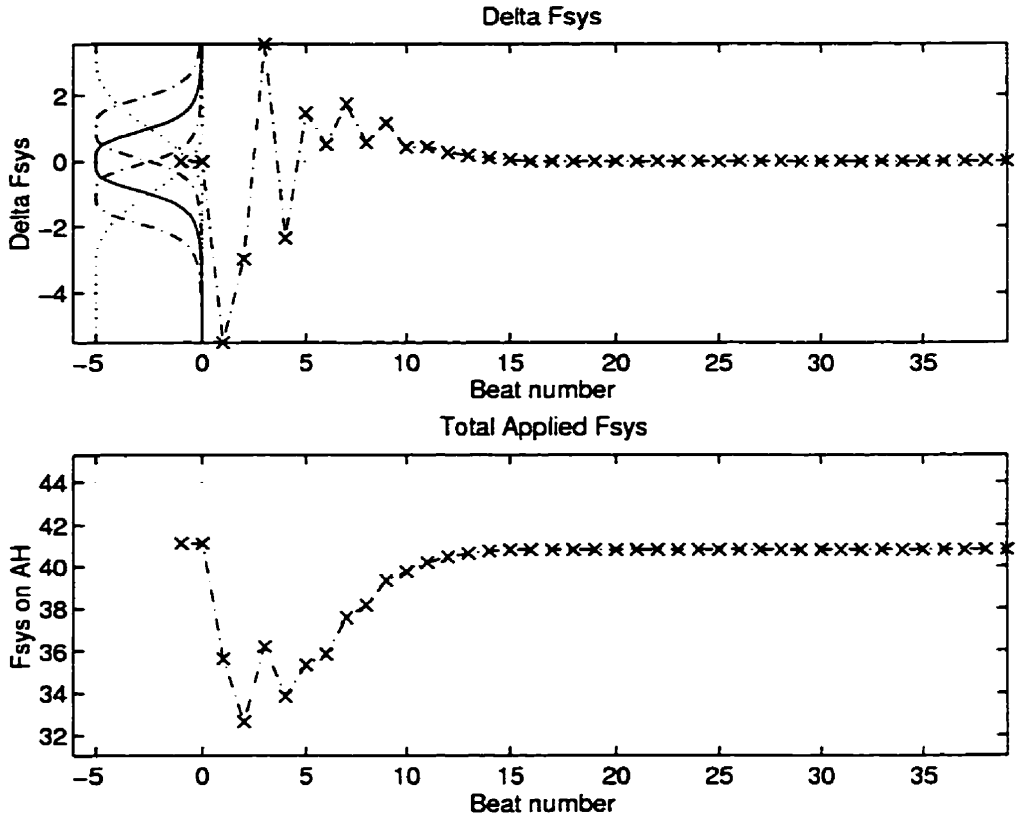


**Figure 6.39:** Control force for step change in initial outlet cannula volume by ×2.Top: Change in systolic force [N] ( -.- change in systolic force. x controller infered change in systolic force [N]) Bottom: Systolic force on model [N] ( -.- Systolic force trend. x controller infered systolic force acting on heart [N]).

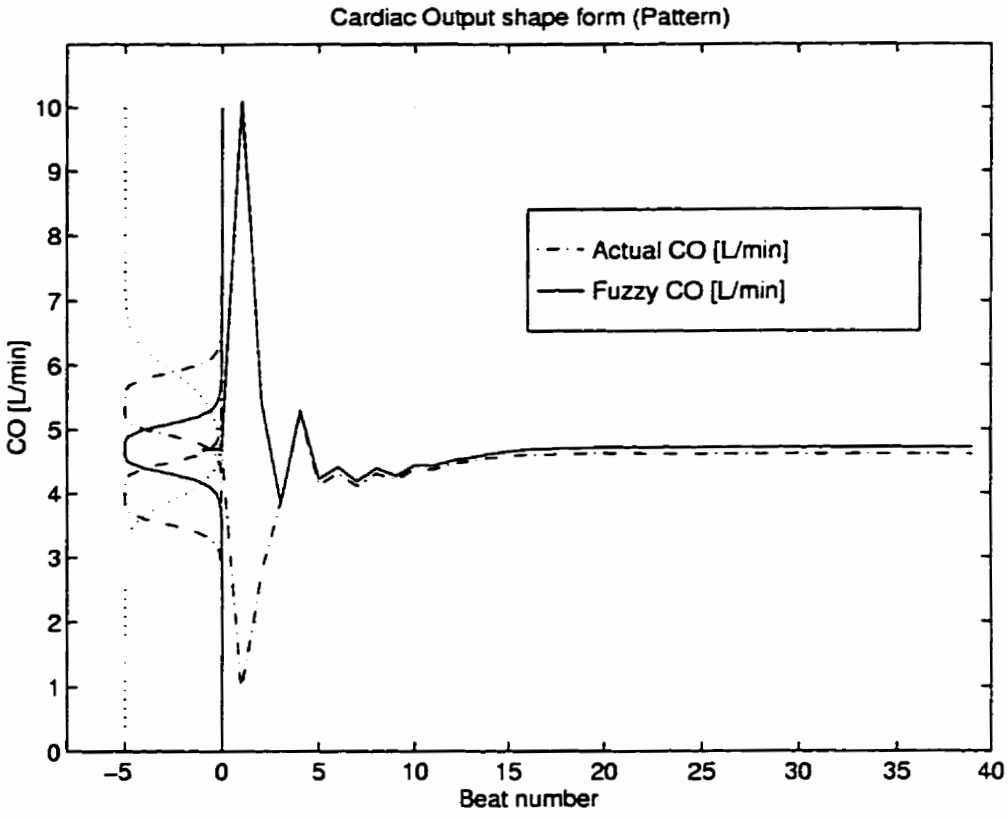


**Figure 6.40:** pump output for an increase in Initial Outlet cannula volume ×2. ( - Fuzzy infered pump output $[\frac{L}{min}]$. -.- Actual pump output $[\frac{L}{min}]$).

crease in outlet cannula compliance. Figure 6.41 shows that the force attains again steady state after the first few beats for a decrease in half of the nominal blood volume. It shows that the system is much more stable to a decrease in the volume than to a increase in the blood volume. Figure 6.42 shows the pump output. It shows that the pump output is estimated correctly. The first beat shows a pressure gradient over the outlet valve to be 20.42 mm Hg which is in the universe of discourse range.

The aorta segment volume was varied to produce a similar effect. Its response was similar to the reaction seen in the change in the outlet cannula volume. But the failure of the ESV was not observed at 4 times to 0.25 times the nominal blood volume in the aorta segment at startup. Changes in inlet cannula volume have a much smaller impact than that of outlet cannula.

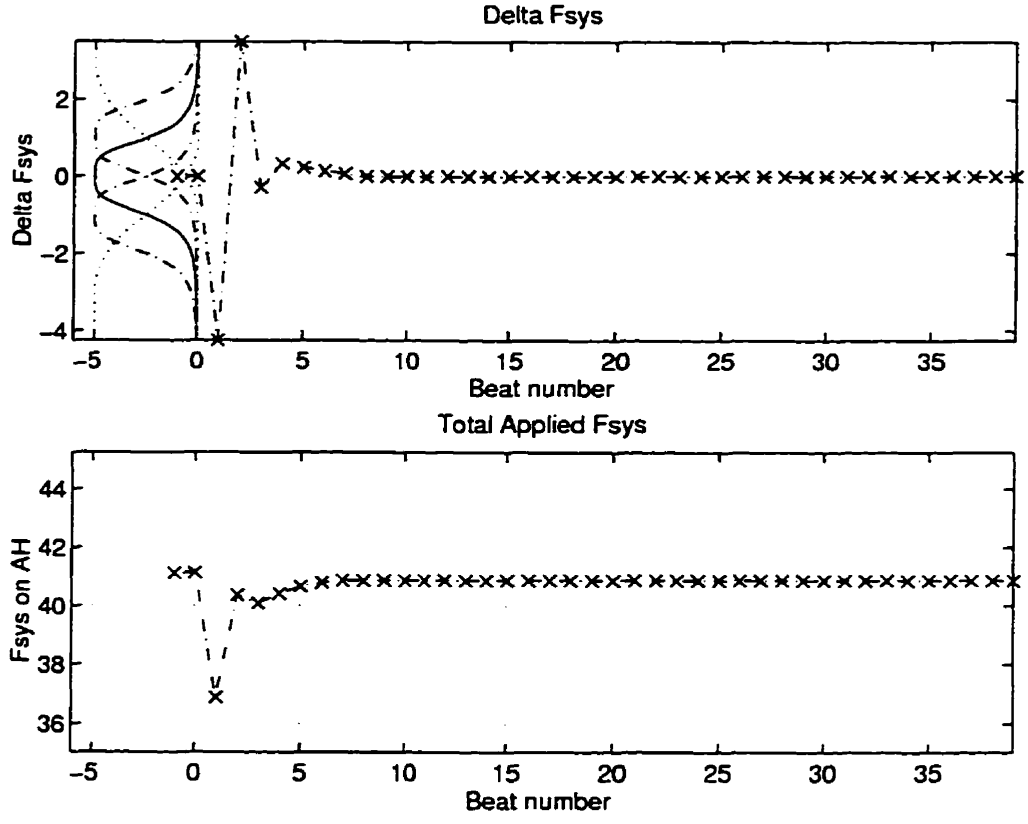


**Figure 6.41:** Control force for step change in initial outlet cannula volume by ×0.5.Top: Change in systolic force [N] ( -.- change in systolic force, x controller infered change in systolic force [N]) Bottom: Systolic force on model [N] ( -.- Systolic force trend, x controller infered systolic force acting on heart [N]).

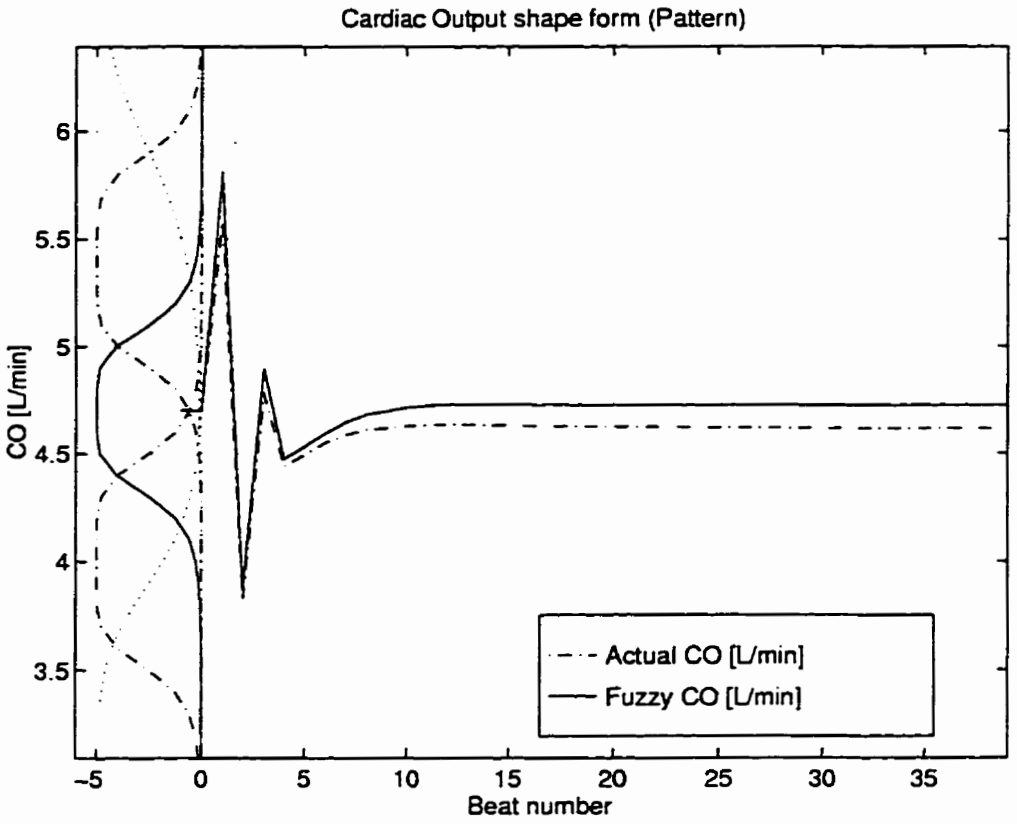


**Figure 6.42:** pump output for an decrease in Initial Outlet cannula volume $\times 0.5$.
( - Fuzzy infered pump output $[\frac{L}{min}]$, -.- Actual pump output $[\frac{L}{min}]$).

### 6.14.2 Peripheral Momentum

The peripheral momentum is varied at startup similar to the outlet cannula blood volume. The control for an increase in peripheral momentum by a factor of 2 is shown in Figure 6.43. The force shows drastic force correction for the first 3 beats and then a slow incremental changes to bring back the force to nominal. Similar behavior is also seen for a decrease in the peripheral momentum which has an initial increase in systolic force increment.

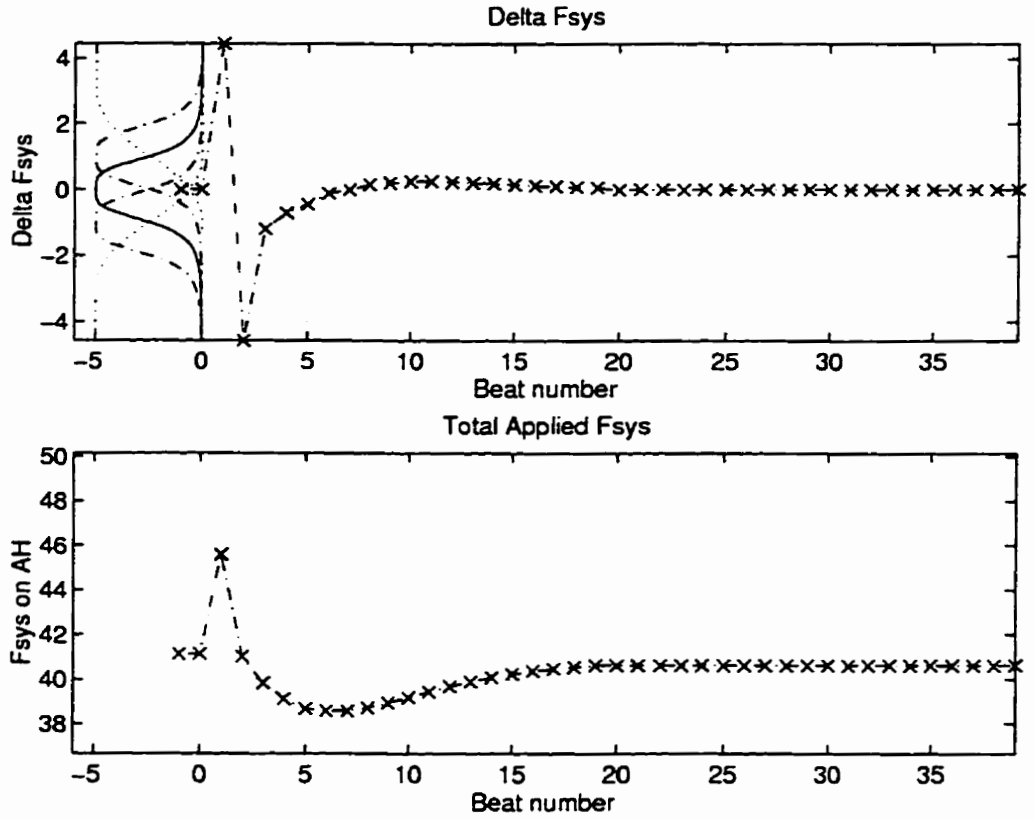


**Figure 6.43:** Control force for step change in initial peripheral momentum by ×2.Top: Change in systolic force [N] ( -.- change in systolic force. x controller infered change in systolic force [N]) Bottom: Systolic force on model [N] ( -.- Systolic force trend. x controller infered systolic force acting on heart [N]).

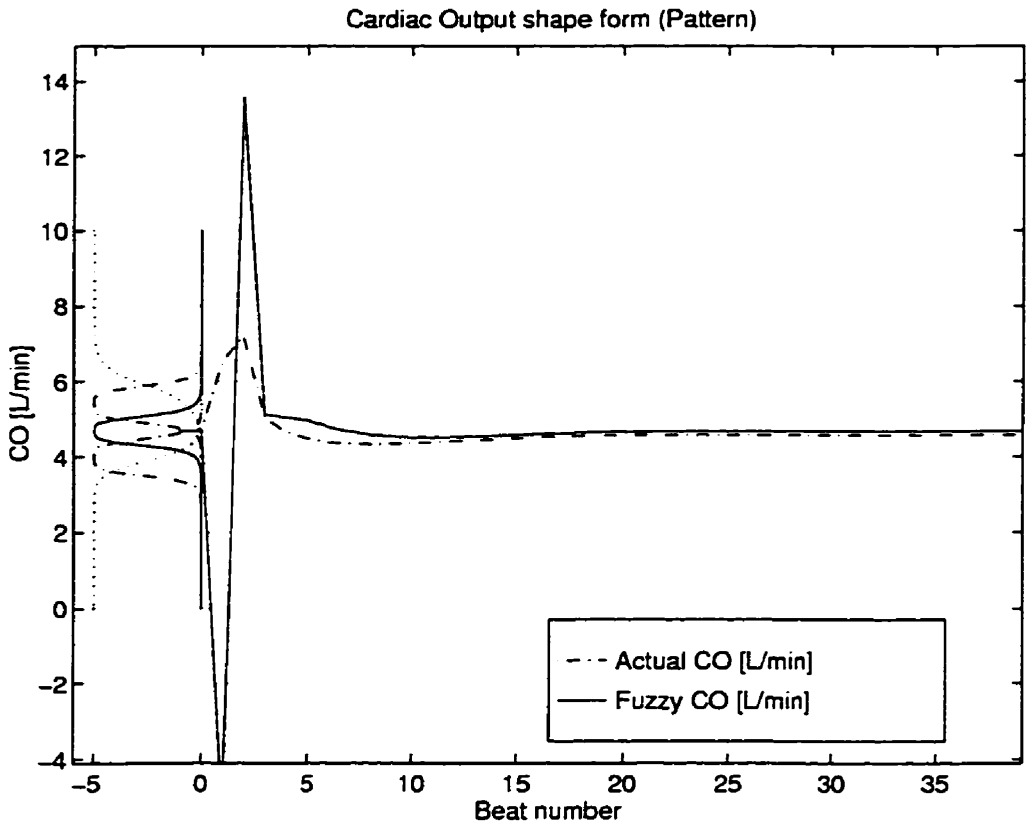


**Figure 6.44:** pump output for an decrease in Initial peripheral momentum $\times 2$. ( - Fuzzy infered pump output $[\frac{L}{min}]$. -.- Actual pump output $[\frac{L}{min}]$).

## 6.15 Sensitivity Study

The robustness of the controller is tested by observing the failures caused by changes in system parameters. These failure limits and modes are determined by running the simulation for various altered systemic values. These values are altered by the aid of a multiplier which is greater than one to show an increase in the specfic systemic variable and less than one to show a drop in that specific variable. During these simulations all other parameters of the system are held constant at their nominal values as in Table 5.4 and 5.5. The FLC holds the pump output at the required value by changing the systolic force.

| Parameter Study | | |
|---|---|---|
| **Variable** | **Multipler** | **Failure multipler/mode** |
| Aorta inertance (dec) | 0.1, 0.25, 0.5, 0.75 | < 0.1 - Aorta press. |
| Aorta inertance (inc) | 1.1, 1.5, 2, 4, 6, 8, 10 | > 10 - None |
| Inlet Can. Inertance (dec) | 0.1, 0.25, 0.5, 0.75 | 0.1 - Inlet can. Freq. |
| Inlet Can. Inertance (inc) | 1.1, 1.5, 2, 4, 6, 8, 10 | 8 - Inlet can. Ampl. |
| Outlet Can. Inertance (dec) | 0.1, 0.25, 0.5, 0.75 | 0.25 - Low Art. flow |
| Outlet Can. Inertance (inc) | 1.1, 1.5, 2, 4, 6, 8, 10 | 8 - High Art. flow |
| Inlet Compliance (dec) | 0.1, 0.25, 0.5, 0.75 | < 0.1 - Startup Inlet Press. |
| Inlet Compliance (inc) | 1.1, 1.5, 2, 4, 6, 8, 10 | > 10 - Startup Inlet Press. |
| Outlet Compliance (dec) | 0.1, 0.25, 0.5, 0.75 | < 0.1 - Startup Outlet Press. |
| Outlet Compliance (inc) | 1.1, 1.5, 2, 4, 6, 8, 10 | > 10 - Startup Outlet Press. |
| Heart Inertance (dec) | 0.1, 0.25, 0.5, 0.75 | 0.1 - ESV est. |
| Heart Inertance (inc) | 1.1, 1.5, 2, 4, 6, 8, 10 | 10 - ESV est. |

## 6.16 Aorta Inertance ($I_{ao}$)

The increase/decrease in inertance is representative of an increase in the length of the aorta segment that was modeled from the TEAM. Since the inertance is defined by the Equation (2.3), an increase/decrease in aorta inertance can be brought about

by various methods: a change in the cross sectional area, a change in the length of the aorta segment or a change in blood density. The increase and decrease in aorta cross section is common during pumping of blood (Windkessel effect). Some drugs induce dilaton or constriction of arteries in which case the cross sectional area is also changed. This causes a change in the inertance of the blood in the aorta. A decrease in the aorta cross-sectional area is also common in some patients when they are suffering from certain cardiovascular diseases (build up of fat tissue on the arterial walls).

### 6.16.1 Increase in $I_{ao}$

The pressure difference across the output cannula valve and the flow rate of blood from the artificial heart are very similar to the nominal case. A close inspection reveals that the pressure across the outlet valve during systole is slightly higher than the nominal case. This results in slightly more volume being pumped out for the duration of systole.

The aorta data shown in Figure 6.45 shows that the aorta pressure is seen to be more oscillatory than in the nominal case. The increase in the inertance of the aorta requires the blood to be pushed harder in order to flow. The periperal flow is still the same (about $4.7\frac{L}{min}$). The venous data and the artificial heart data are also nominal without any vast changes. The pressure volume loop is observed to drift slightly to the left (negative) region. The change in $I_{ao}$ seems to have only effected the aorta locally which effects the system very slightly.

### 6.16.2 Decrease in $I_{ao}$

The inertance was reduced to half its nominal value. The outlet pressure gradient and the flow rate of blood from the artificial heart are about nominal. Figure 6.46 shows the aorta preformance at a lower aorta inertance. The oscillations apparent in the aorta segment for the increased inertance is not apparent here. The pressures

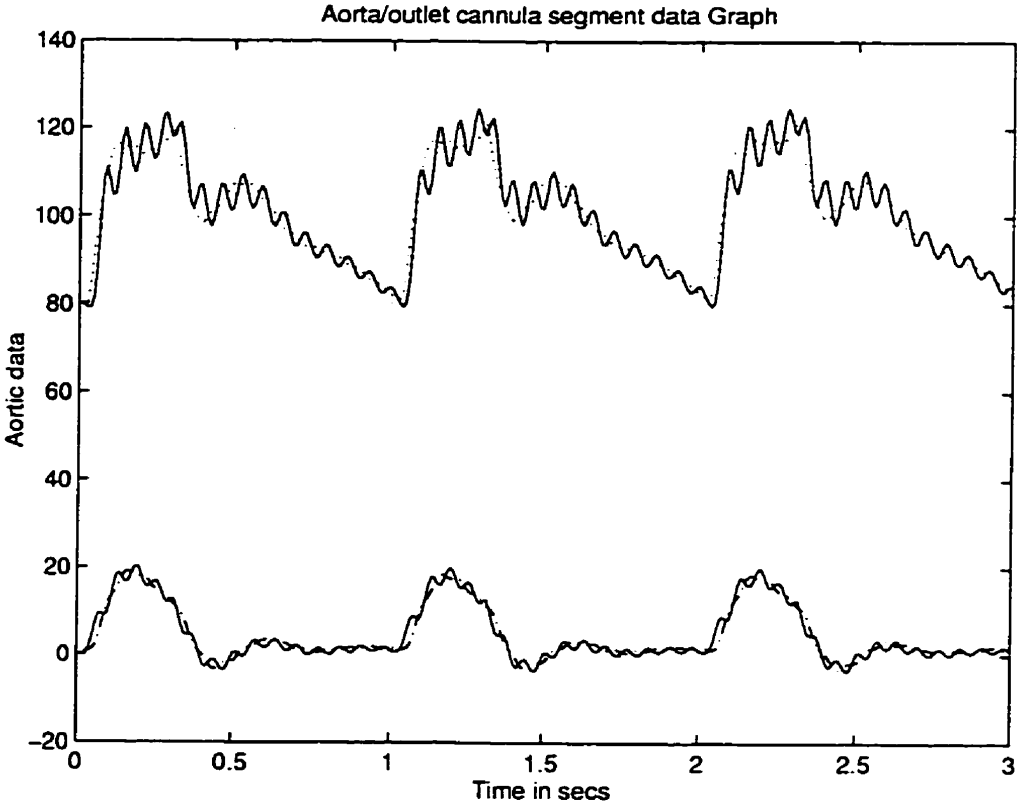


**Figure 6.45:** Aorta/outlet cannula segment data for an increase in aorta inertance ($I_{ao} \times 2$). ( - aorta pressure [mm Hg]. .. outlet cannula pressure [mm Hg]. -.- aorta flow rate $[\frac{L}{min}]$. - outlet cannula flow rate (lower line) $[\frac{L}{min}]$).

seem to be much smoother than nominal. This shows that lower values of inertance will cause less oscillations in the pressure and flow rate of blood through the aorta segment. The peripheral flow is the same as that of the increased aorta inertance at a value of about $4.7\frac{L}{min}$. The venous parameters, inlet parameters and artificial heart parameters are also similar to the increased inertance.

The pressure-volume was observed not to drift to the left as far as in the case of increased aorta inertance. This is because at lower inertance the pressure oscillations are lower and hence the mean value of pressure across the outlet valve is about nominal.

## 6.17 Cannula Inertance $I_{cnin}$

The inlet cannula inertance on the location of the artificial heart in the human body. The location of the artificial heart can vary from patient to patient and in such cases the length of the inlet cannula can either be extended or reduced. The change in inertance can also be brought about by changing the cross sectional area of the cannula as shown in the Equation (2.3). Therefore the response of the controller to such changes in inlet cannula length are important.

### 6.17.1 Increase in $I_{cnin}$

When $I_{cnin}$ is increased the venous segment pressure and flow rate become very oscillatory. The inlet cannula pressure is shown in Figure 6.47. The amplitude of the inlet cannula pressure can be seen to be very large with a lower frequency. The oscillations also persist into the diastolic phase of the beat causing the internal artificial heart pressure during diastole to osciliate. This is observed in the inlet flow rate as shown in Figure 6.48. The flow rate shows a large drop during diastole due to the pressure amplitude in the inlet cannula. This osciliation, if increased can cause the inlet valve to temporarily flutter (passive valves). Such valve flutter

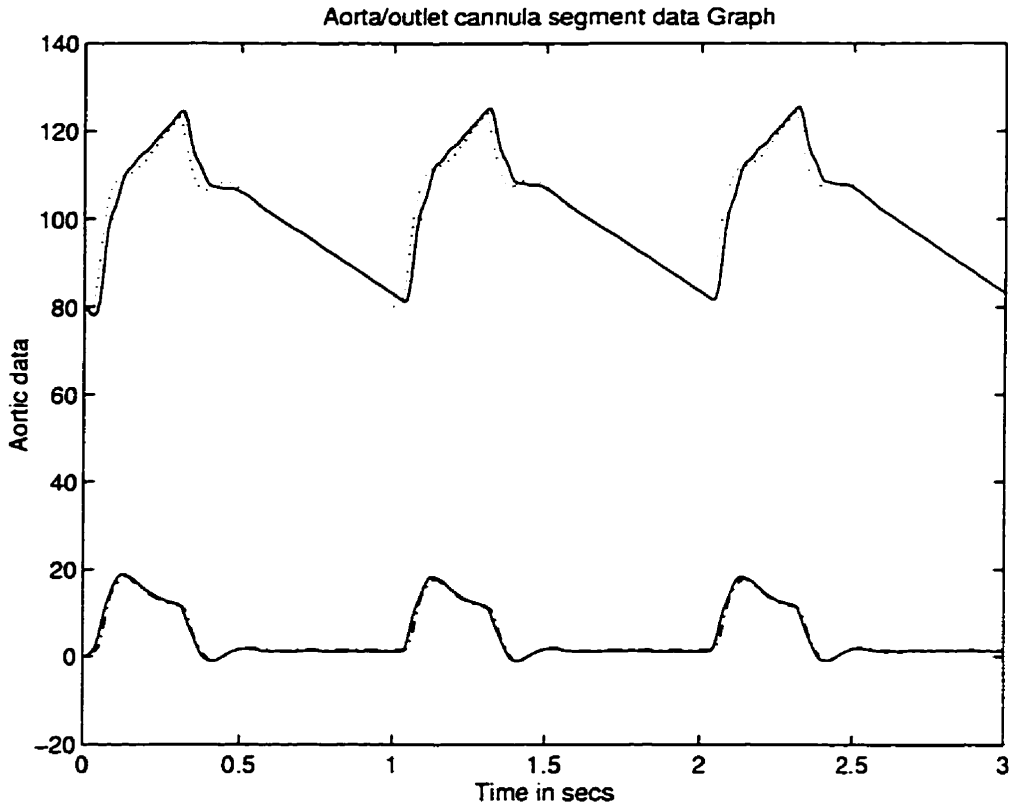


**Figure 6.46:** Aorta/outlet cannula segment data for an decrease in aorta inertance ($I_{ao} \times 0.5$). ( - aorta pressure [mm Hg], .. outlet cannula pressure [mm Hg], -.- aorta flow rate $[\frac{L}{min}]$, -.- outlet cannula flow rate $[\frac{L}{min}]$).

may cause damage to the valve or even cause thrombosis of blood due to turbulent flow produced from the flutter effect. The increase in pressure in the inlet cannula will also cause cyclic wear and eventual failure of the valve. Figure 6.49 shows the pressure-volume loop of the circulatory system. The pressure-volume loop shows a drift of the blood volume towards the negative region implying that ejection volume is higher.

The failure of the circulatory system occurs at the $Icnin \times 8$ as shown in Figure 6.50. The inlet cannula pressure is seen to become very ocillatory with a large amplitude. This causes a large pressure on the inlet valve (Similar to the water hammer effect). The cannula segment may not be able to maintain such high pressure oscillation for extended periods of time due to the cyclic loading of the segment.

### 6.17.2 Decrease in $I_{cnin}$

A decrease in $I_{cnin}$ shows no difference in the outlet cannula parameters, hence the flow rate and the pressure gradient across the outlet valve seem nominal. The steady state data show very minimal change in pressures. The aorta and the arterial segment also shows no variation in pressure or flow rate of blood. The periperial flow in the system is steady at the nominal value. The first observable change to the circulatory system is observed in the venous segment which shows that the inlet cannula pressure and the flow rate in the cannula segment have an increased frequency and lower amplitude of oscillation as shown in Figure 6.51. Another observable feature is that once the diastolic phase (inlet valve opens) begins, no oscilations are observed in the inlet cannula segment. This is also visible in the inlet flow rate when compared to that of the nominal simulation during diastolic phase.

The artificial heart blood volume is also seen not to be changed. The Figure 6.52 shows inlet/outlet flow rate in detail. The diastolic filling flow rate is seen to be much smoother than in the nominal case. The reduction of the cannula segment in a patient's artificial heart is shown to provide smoother flow into the artificial heart

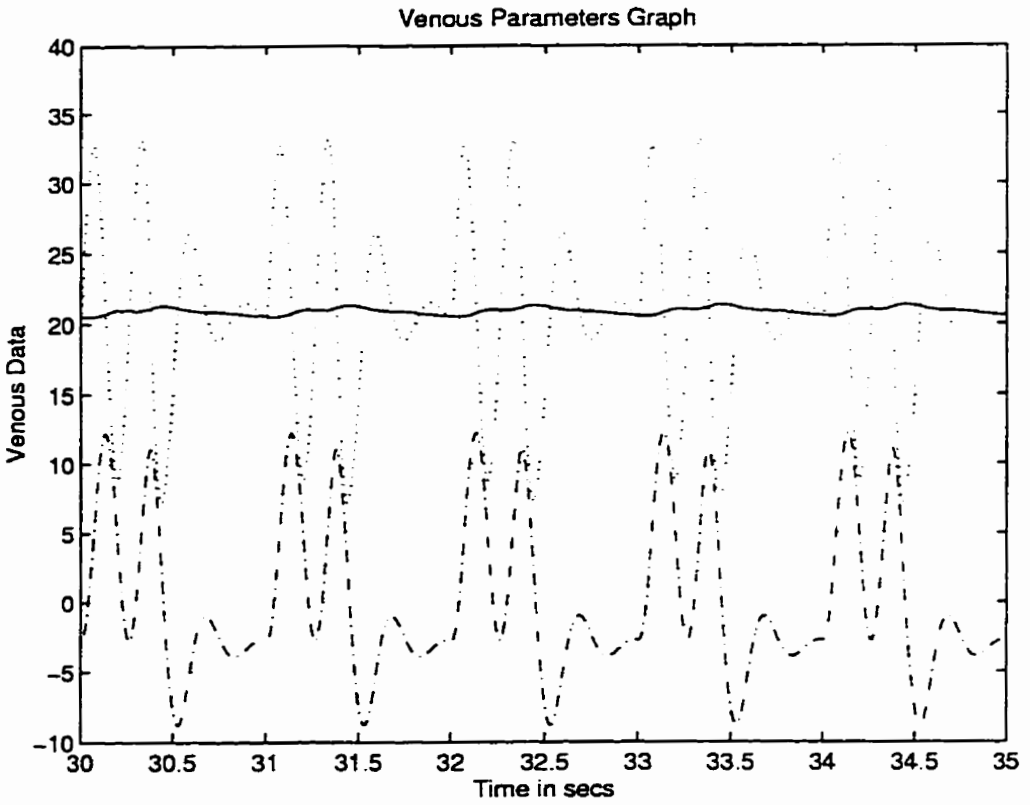


**Figure 6.47:** Venous/inlet cannula segment data for an increase in inlet cannula inertance ($I_{cnin} \times 4$). ( .. Inlet cannula pressure [mm Hg], - venous pressure [mm Hg], -.- inlet cannula flow rate $[\frac{L}{min}]$).

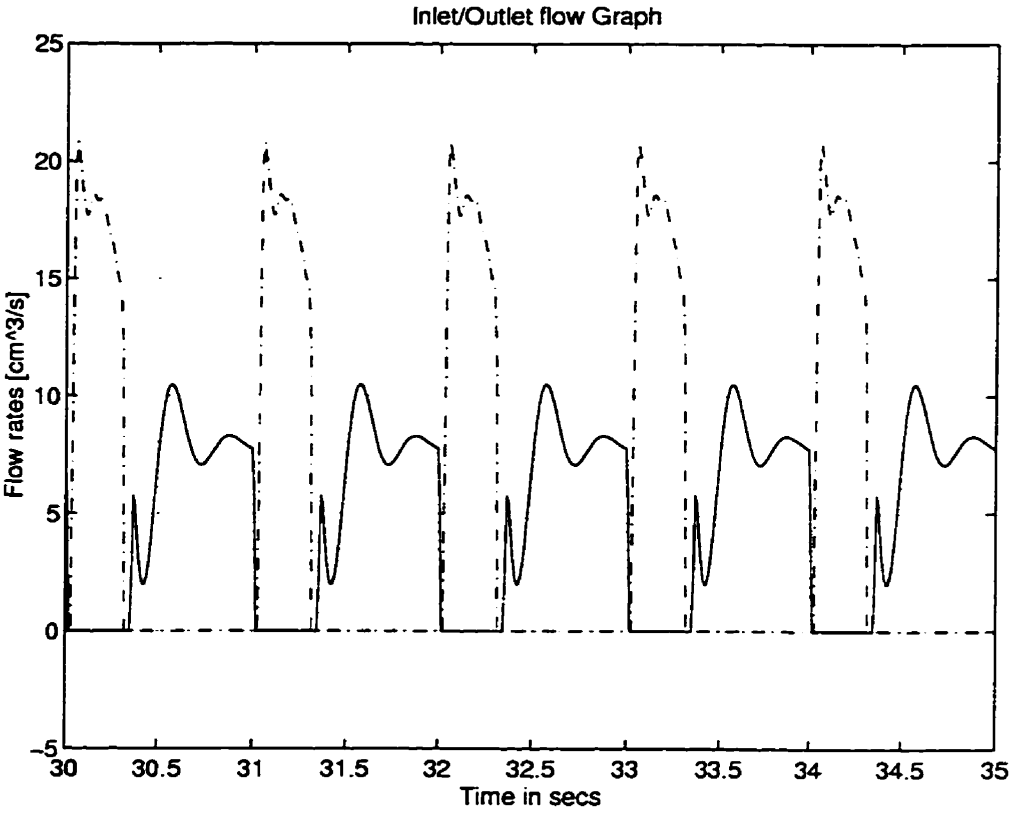


**Figure 6.48:** Inlet/Outlet flow rate of the artificial heart for an increase in inlet cannula inertance ($I_{cnin} \times 4$). ( -.- systolic flow rate $[\frac{L}{min}]$, - diastolic flow rate $[\frac{L}{min}]$).

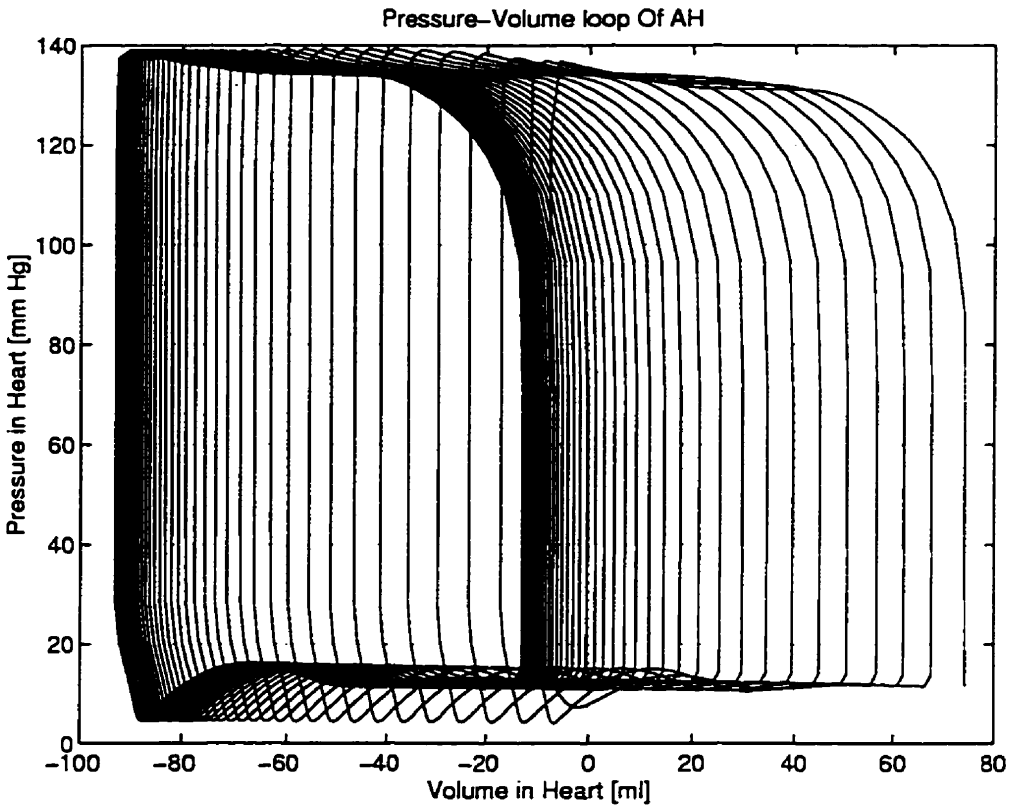


**Figure 6.49:** Pressure-Volume loop for an increase in inlet cannula inertance ($I_{cnin} \times 4$).

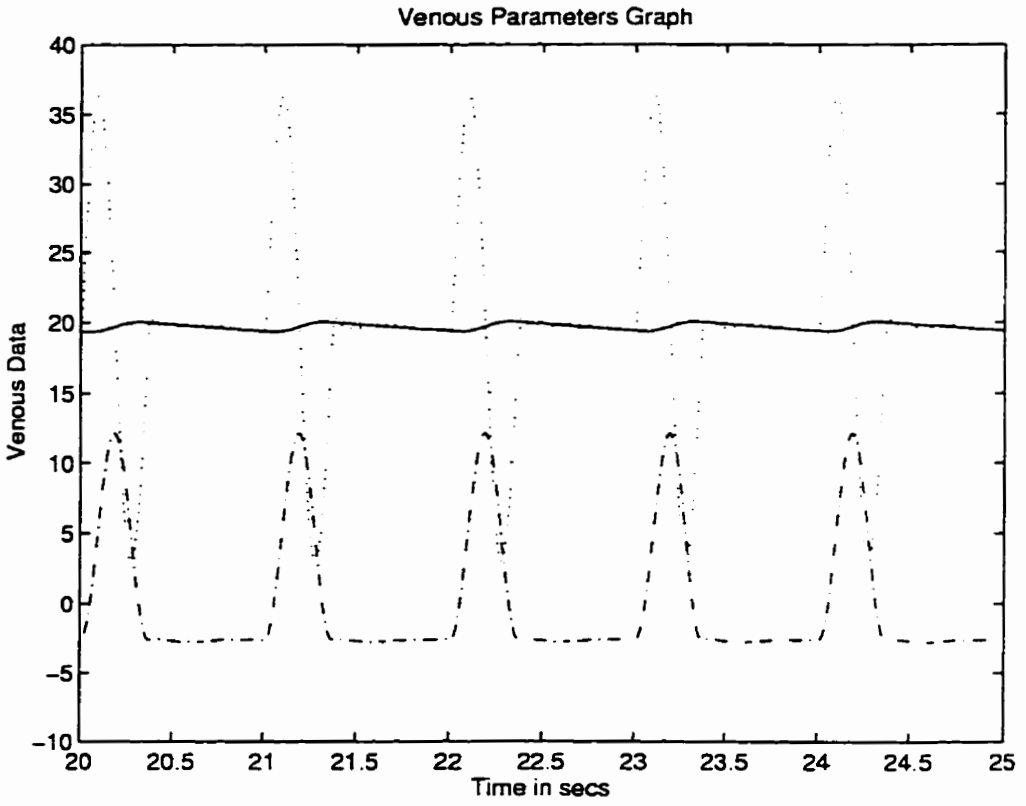


**Figure 6.50:** Venous/inlet cannula segment data for increased inlet cannula inertance and at possible failure point of circulatory model ($I_{cnin} \times 8$). ( .. Inlet cannula pressure [mm Hg]. - venous pressure [mm Hg]. -.- inlet cannula flow rate $[\frac{L}{min}]$).

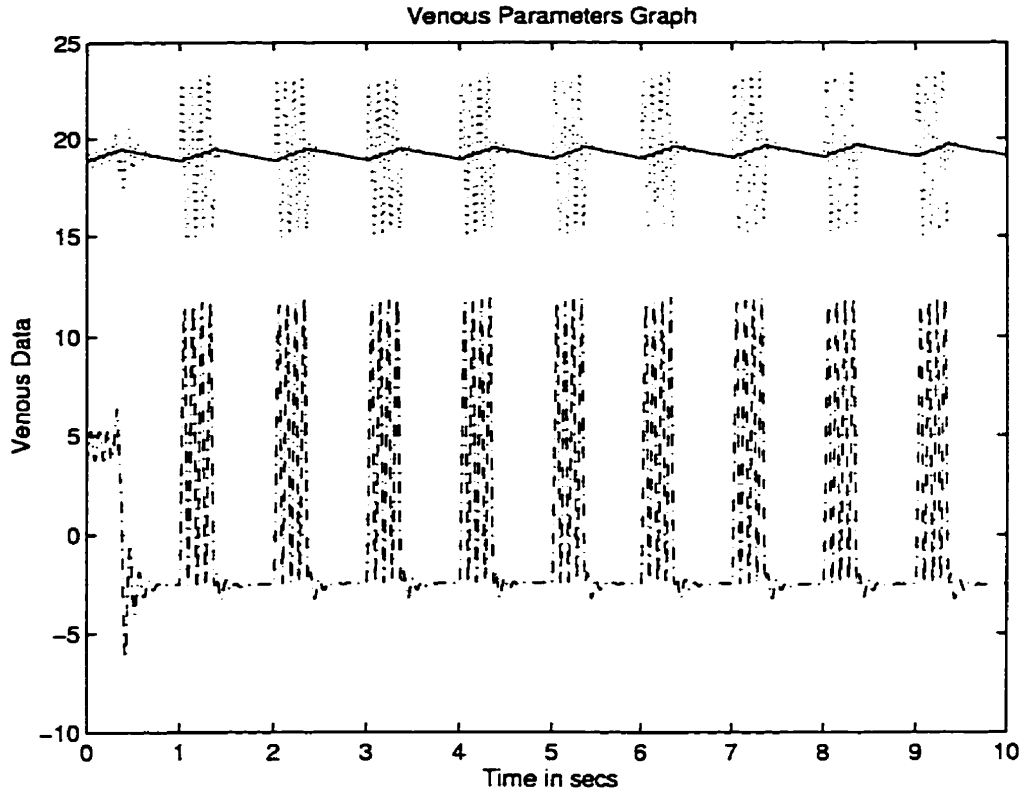


**Figure 6.51:** Venous/inlet cannula segment data for a decrease in inlet cannula inertance ($I_{cnin} \times 0.5$). ( .. Inlet cannula pressure [mm Hg]. - venous pressure [mm Hg]. -.- inlet cannula flow rate $[\frac{L}{min}]$).

during filling with very little oscillation produced from the cannula. But the high frequency oscillation may cause turbulent flood in the inlet cannula due to the water hammer on the inlet valve during systolic process.

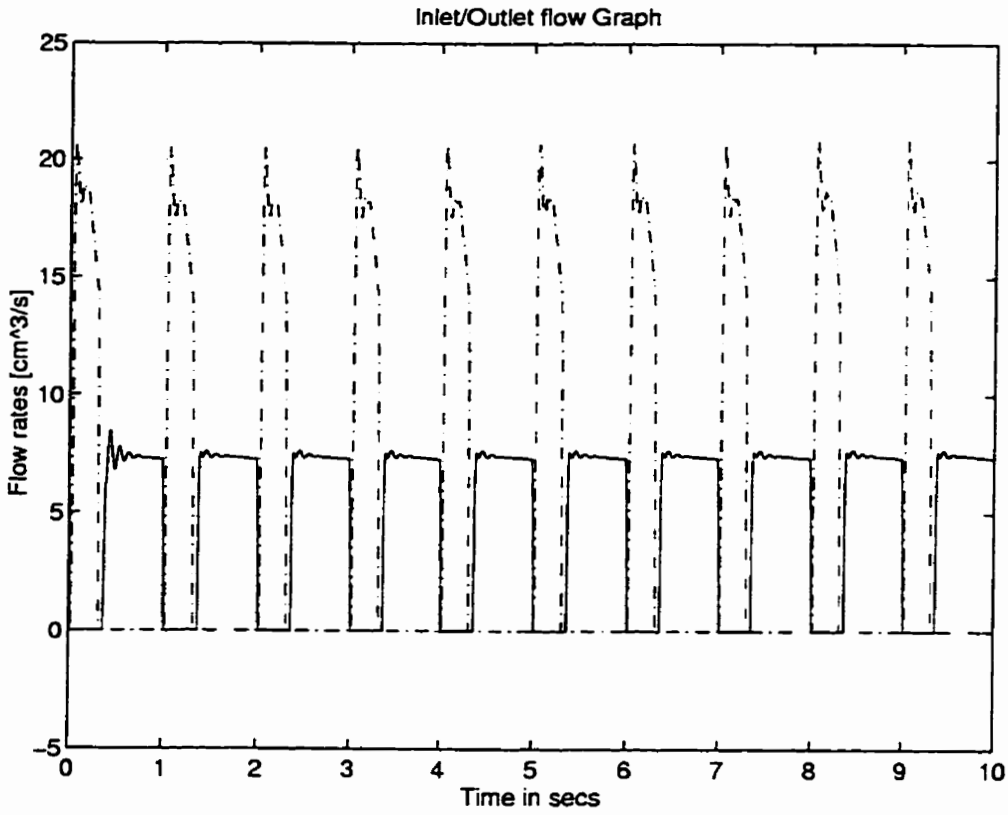


**Figure 6.52:** Inlet/Outlet flow rate of the artificial heart for a decrease in inlet cannula inertance ($I_{cnin} \times 0.5$). ( -.- systolic flow rate $[\frac{L}{min}]$. - diastolic flow rate $[\frac{L}{min}]$).

## 6.18 Cannula Inertance $I_{cnot}$

The varitation in the outlet cannula is similar to the change in inertance of the aorta segment and the inlet cannula. The outlet cannula is generally attached from the artificial heart to the aorta segment. Due to positioning of the the artificial heart the outlet cannula can vary from patient to patient as in the inlet cannula position depending on avaliability cavity space in the human body for implantation.

### 6.18.1 Increase in $I_{cnot}$

When $I_{cnot}$ is increase the outlet cannula parameters show very little change. The aorta segment which contains the parameters of the outlet cannula shows changes. The Figure 6.53 shows the pressure in the outlet cannula and can be seen to oscillate at a lower frequency. These oscillations are also evident in the aorta pressures which shows lower frequency oscillations than the nominal condition.

The arterial segment in Figure 6.54 shows that the arterial flow rate has increased. The arterial pressure has not changed from the nominal value but the aorta/outlet pressure oscillations are visible in the arterial segment. The peripheral flow is also nominal with little observable change. There is no observed change in the venous or the inlet cannula segments. All artificial heart parameters are observed to be nominal also. The artificial heart blood volume is seen to drop lower than the nominal case implying that more blood is pumped out of the artificial heart.

### 6.18.2 Decrease in $I_{cnot}$

When the $I_{cnot}$ is decreased the outlet cannula paramters show no visible differences from nominal case. The aorta data (Figure 6.55) shows that the cannula pressure has a high frequency oscillation with a low amplitude. This is also reflected in the aorta pressure seen in Figure 6.55. There is no change in the pressure range of either the aorta or the outlet cannula. The arterial segment flow rate shown in Figure 6.55 shows a decrease in the blood flow rate though the arterial segment. The peripheral

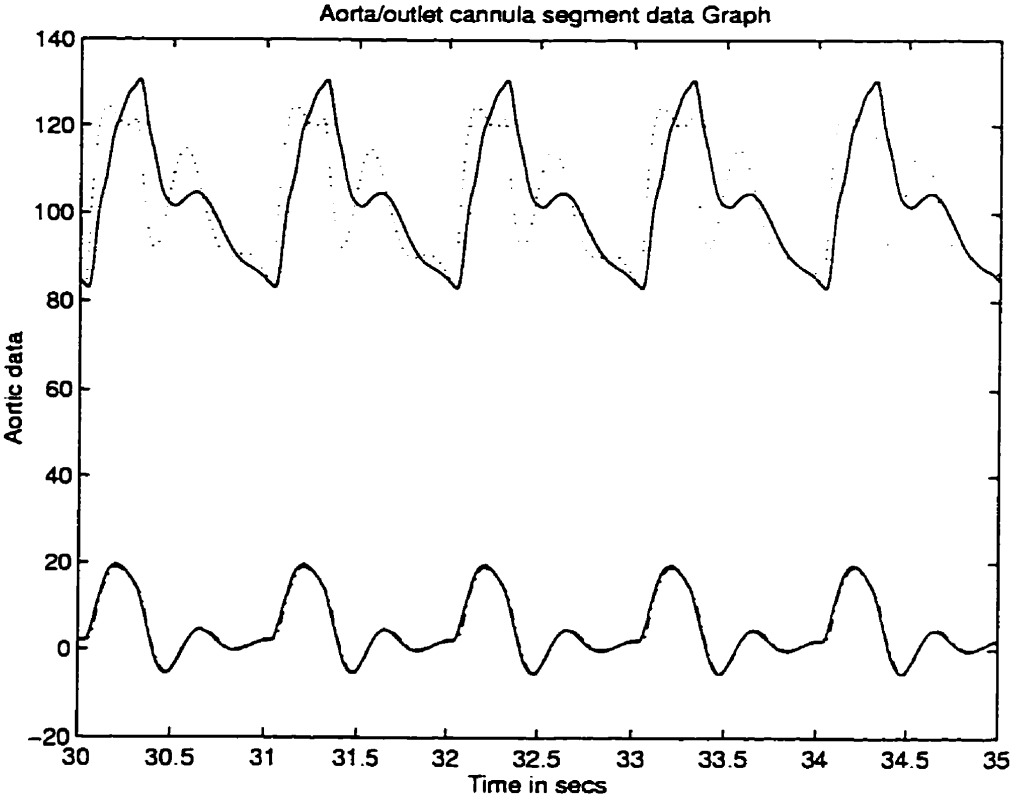


**Figure 6.53:** Aorta/outlet cannula segment data for an increase in outlet cannula inertance ($I_{cnot} \times 4$). ( - aorta pressure [mm Hg], .. outlet cannula pressure [mm Hg], -.- aorta flow rate $[\frac{L}{min}]$, - outlet cannula flow rate (lower line) $[\frac{L}{min}]$).

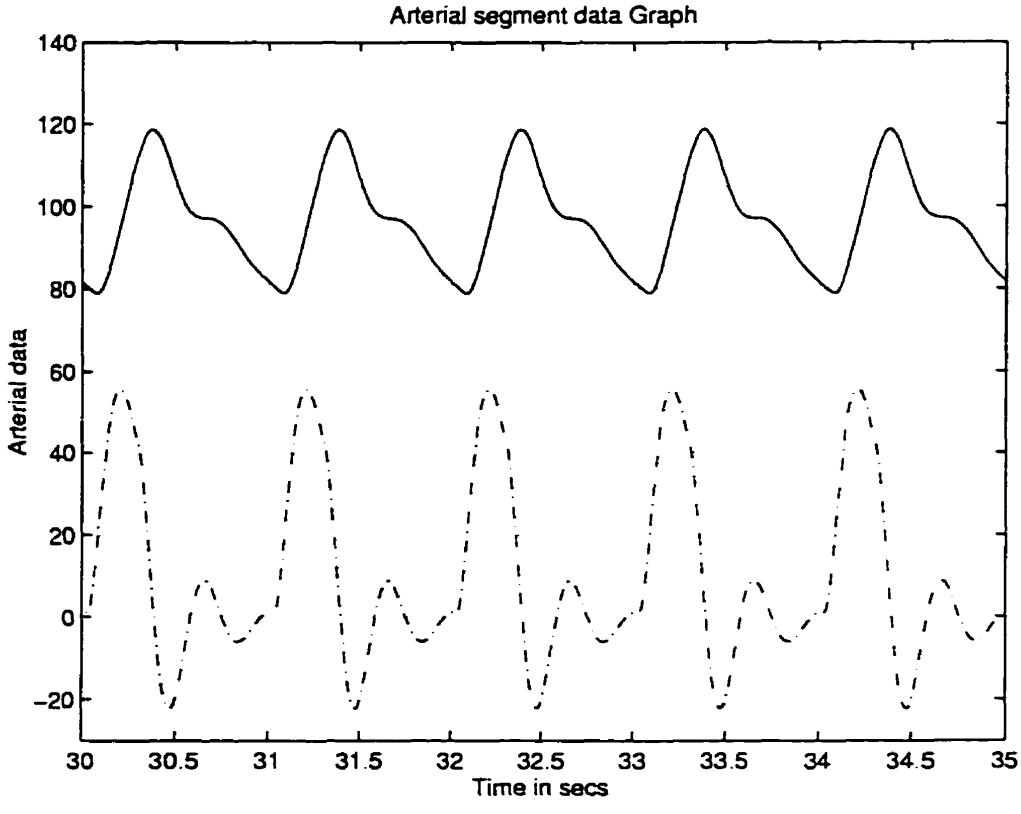


**Figure 6.54:** Arterial Segment data for an increase in outlet cannula inertance ($I_{cnot} \times 4$). ( - arterial pressure [mm Hg]. -.- arterial flow rate $[\frac{L}{min}]$).

flow, venous and inlet cannula segments are still nominal. Artificial heart volume seen on the pressure-volume loop shows no changes.

The failure of the decrease in outlet canula inertance was seen at 0.25 times the nominal value. This is shown in Figure 6.56. The flow rate in the arterial segment is seen to be very low and sometimes negative. This is the flow rate into and out of the compliance element as shown schematically in Figure 5.14.

## 6.19 Artificial Heart Inertia ($I_{ht}$)

The variation of the $I_{ht}$ changes the piston mass modeled in the artificial heart. An increase in $I_{ht}$ would imply that more force would be required to accelerate the piston while a decrease would require a lower force.

### 6.19.1 Increase in $I_{ht}$

The increase in the interia of the artificial heart piston is seen to effect the outlet flow rate as seen in Figure 6.57. The outlet flow rate is seen to have decreased. The aorta segment and outlet cannula show a slight increased flow rate. The artificial heart parameters shows that during the systolic phase the pressure in the artificial heart is higher than nominal. The Figure 6.58 shows the pressure-volume loop. The blood volume is seen to increase into the positive region which means blood is being left behind in the heart after each beat.

### 6.19.2 Decrease in $I_{ht}$

When the outlet cannula data are observed it can be seen that there is an increase in flow rate from the artificial heart. The periperal flow is seen to be nominal. The venous pressure has increased slightly. There is also an observable increase in the amplitude of oscillation in the inlet cannula pressure. The artificial heart blood volume is seen to drop to a negative value implying that more blood is ejected on each

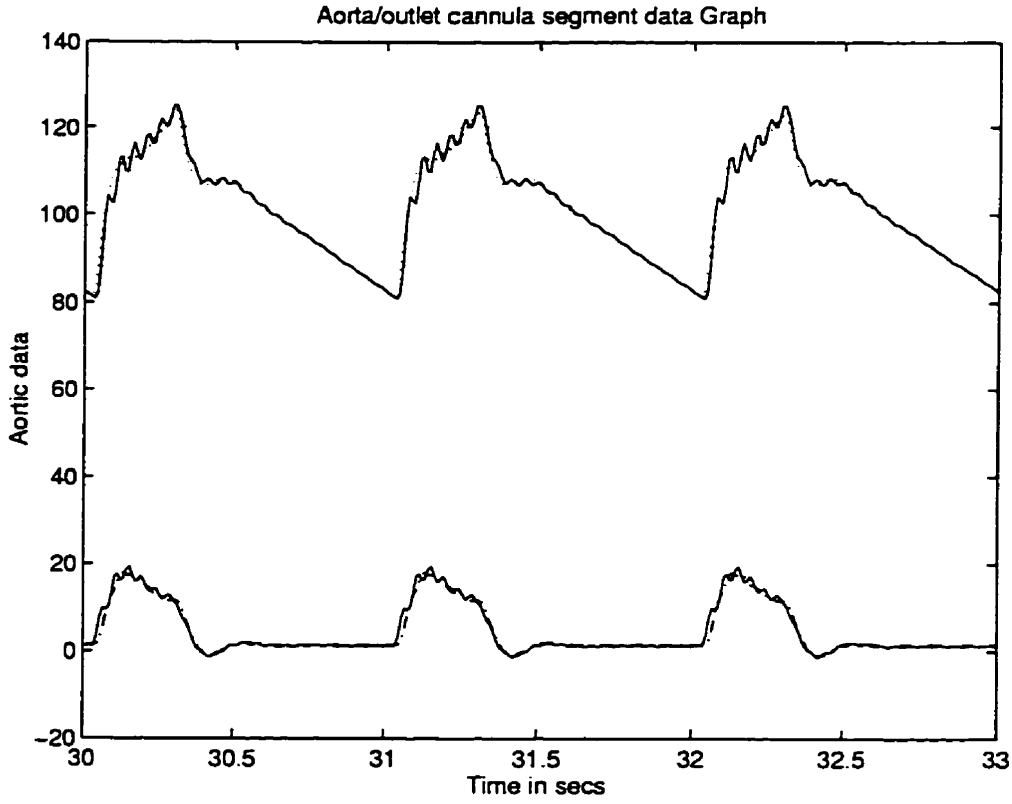


**Figure 6.55:** Aorta/Outlet cannula segment for a decrease in outlet cannula inertance ($I_{cnot} \times 0.5$). ( - aorta pressure [mm Hg], .. outlet cannula pressure [mm Hg], -.- aorta flow rate $[\frac{L}{min}]$, -.- outlet cannula flow rate $[\frac{L}{min}]$).

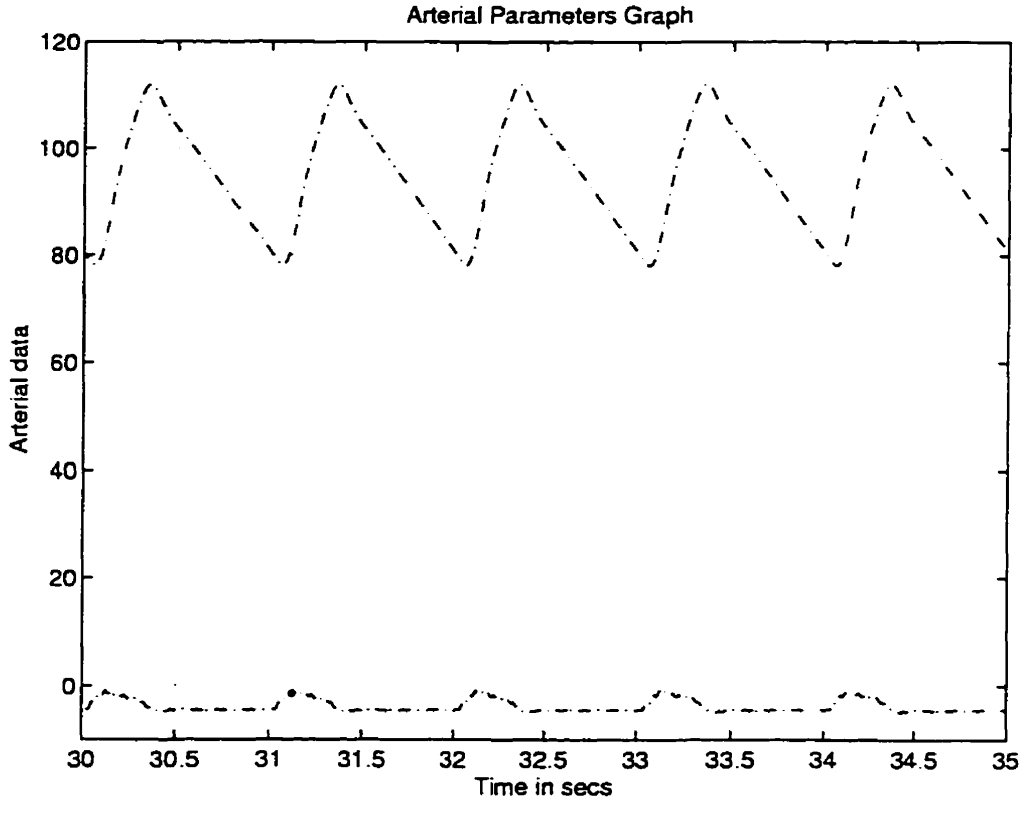


**Figure 6.56:** Arterial segment data for a decrease in outlet cannula inertance ($I_{cnot} \times 0.25$). ( -.- arterial pressure [mm Hg], -.- arterial flow rate (lower line) $[\frac{L}{min}]$).

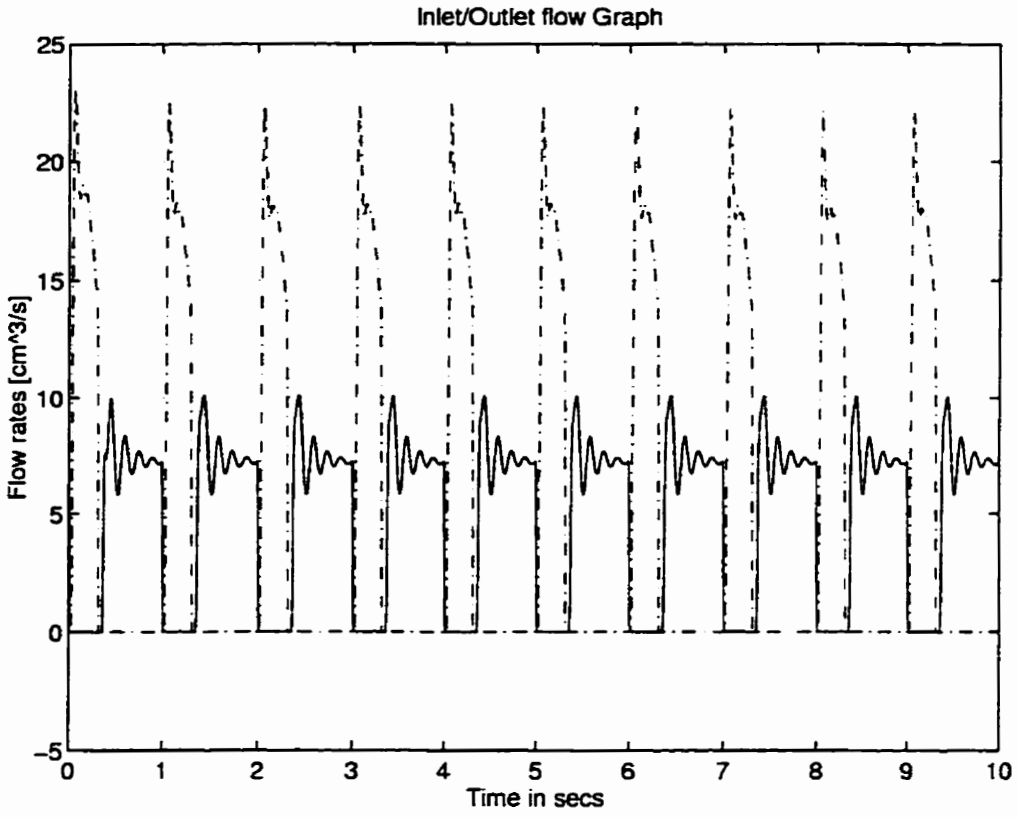


**Figure 6.57:** Inlet/Outlet Flow of artificial heart for an increase in heart inertia ($I_{ht} \times 2$). ( -.- systolic flow rate $[\frac{L}{min}]$, - diastolic flow rate $[\frac{L}{min}]$).

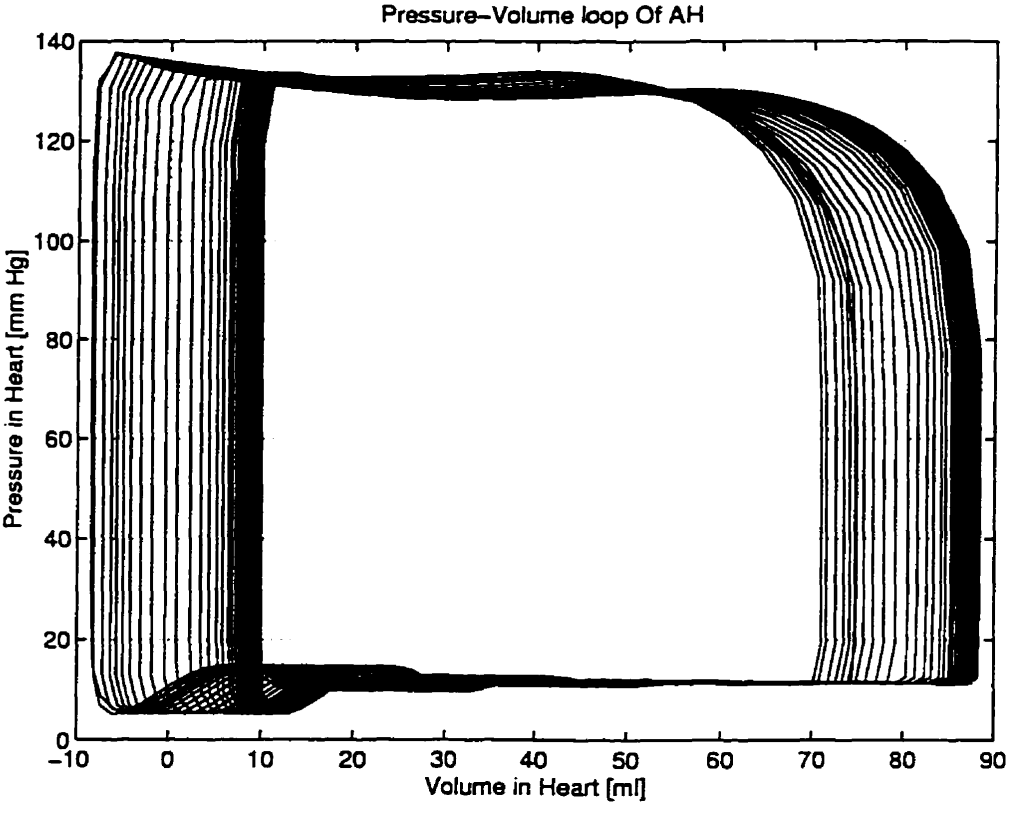


**Figure 6.58:** Pressure-Volume Loop for an increase in heart inertia ($I_{ht} \times 2$).

stroke of the heart as shown in Figure 6.59. Figure 6.60 shows the ejection fraction. It shows that the ejection is greater than one. The inlet flow when compared to the nominal case is about the same. An increase is obsevered in the outlet flow from the artificial heart.

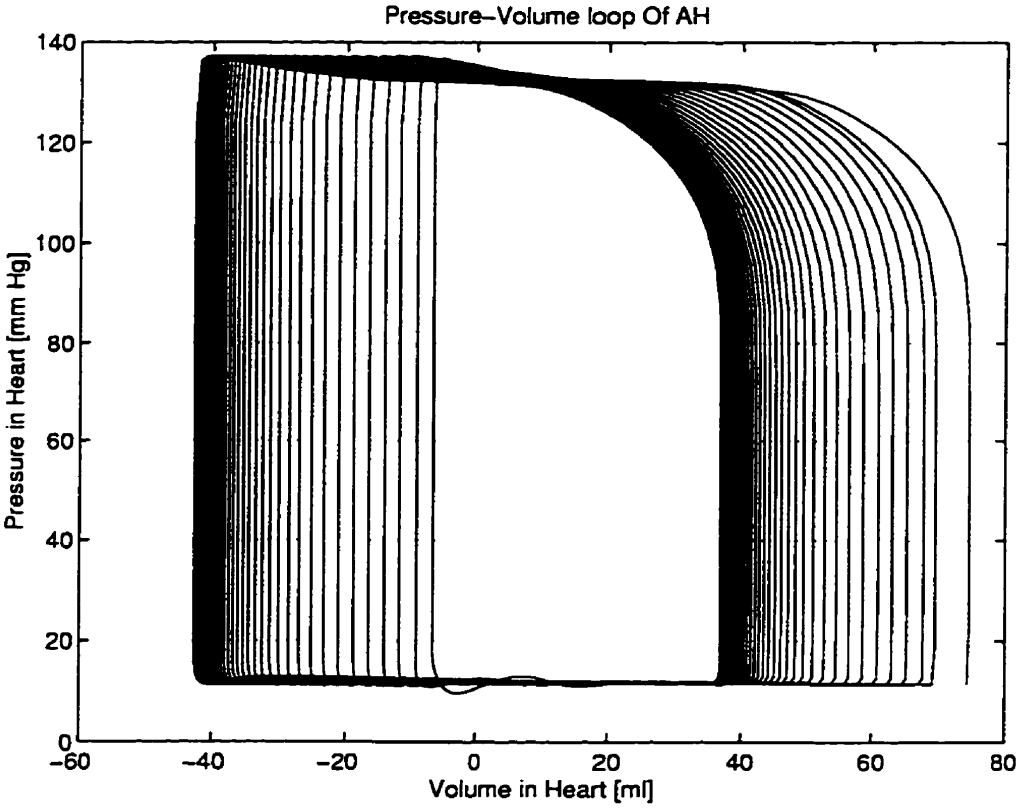


**Figure 6.59:** Pressure-Volume Loop for an decrease in heart inertia ($I_{ht} \times 0.5$).

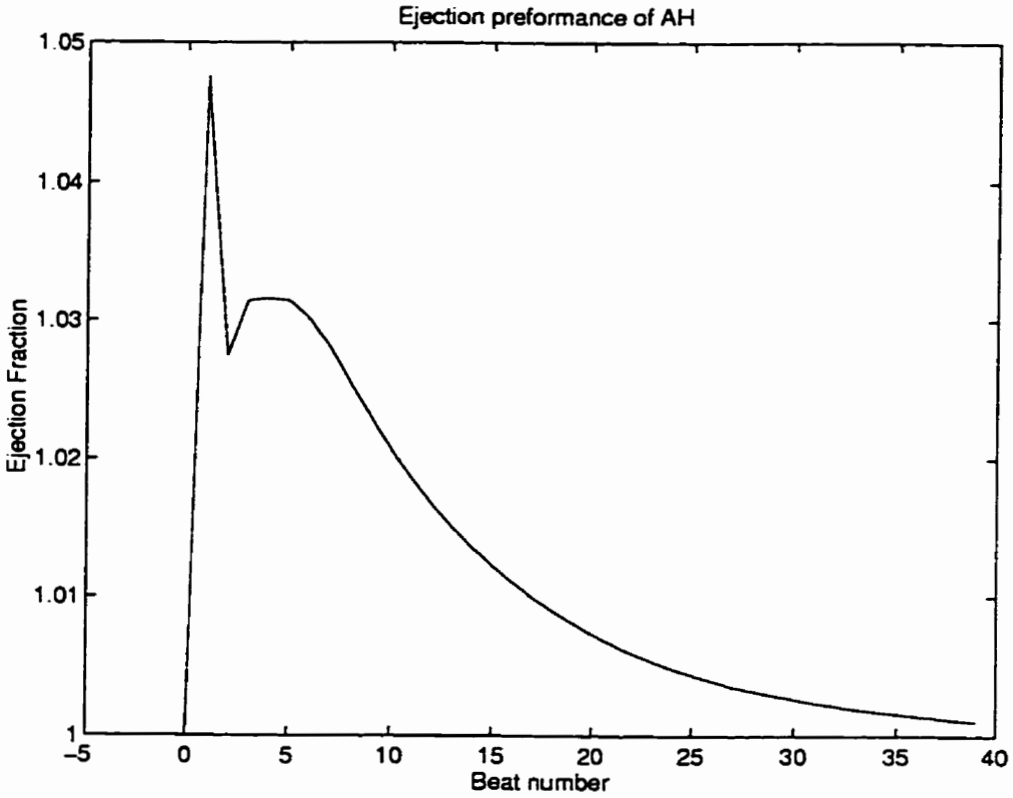


**Figure 6.60:** Ejection fraction for a decreased heart inertia ($I_{ht} \times 0.5$).

## 6.20 Inlet Cannula Compliance ($C_{cnin}$)

The change in the compliance is basically changing the pressure-volume relationship in the segment which is given in Equation (2.1). Any change in compliance in a segment would require either a change in the material elasticity of the segment or the change can occur due to wear and fatigue from prolonged use of the segment. At present the cannula segments are generally made up of low porosity woven Dacron whose compliance was attained from [1].

### 6.20.1 Increase in $C_{cnin}$

The increase in the inlet cannula compliance effect is mainly localized to the initial startup of the simulation where there is a sudden change to the system. Since the initial conditions are preset to nominal steady state conditions, this causes a sudden change in the circulatory system. This effect disappears after the first few beats when the volume in the segment is corrected. The effect is very similar to the initial conditions simulated above as in section 6.14.1. The main effect of the change in compliance is seen in the venous segment as shown in Figure 6.61. The startup cannula flow rate and pressure is seen to be very oscilatory for the first 2 beats of the simulation because of the initial volume in the segment is not at the models steady state value.

Initially the inlet cannula valve flutters for the first beat of the simulation before it becomes stabilized. The flutter of the valve can be seen in Figure 6.62 which shows the input valve parameters. The positive gradients show when the inlet valve will be open. The first beat shows rapid opening and closure of the valve. Such valve response can cause damage to the valve or clot blood due to turbulence.

### 6.20.2 Decrease in $C_{cnin}$

The decrease in cannula compliance by half causes the pressure to double for a unit increase in volume. This causes large pressure oscillations during startup just as in

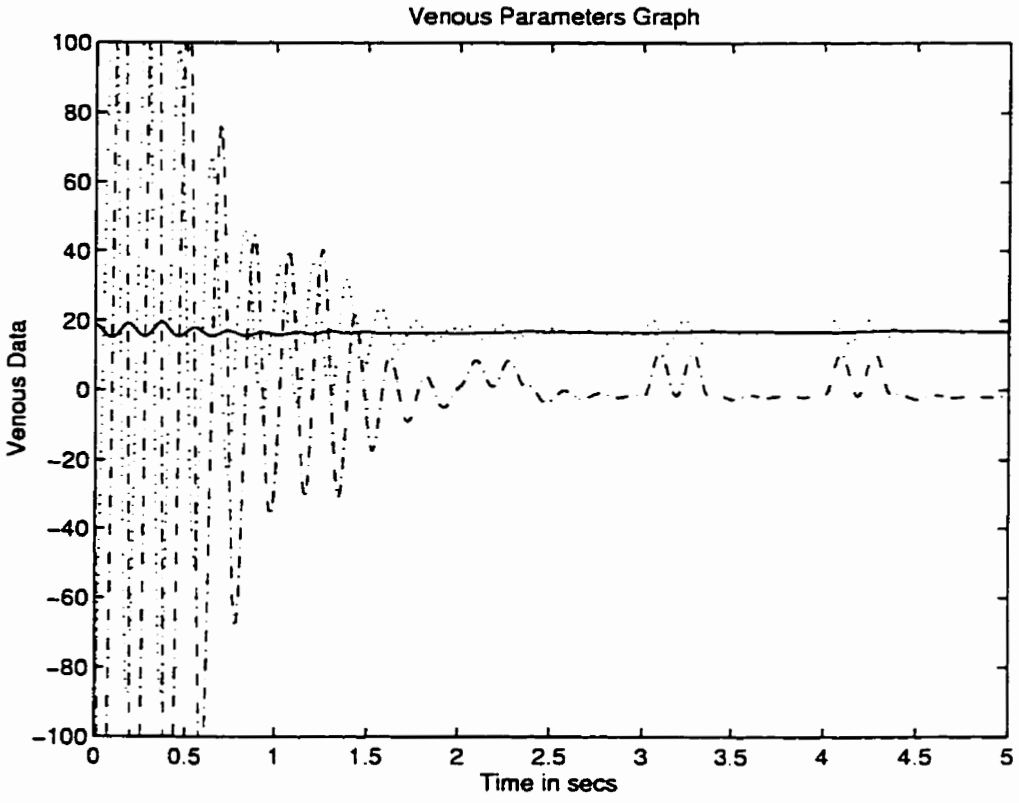


**Figure 6.61:** Venous/inlet cannula segment data for an increase in inlet cannula compliance ($C_{cnin} \times 2$). ( .. Inlet cannula pressure [mm Hg]. - venous pressure [mm Hg], -.- inlet cannula flow rate $[\frac{L}{min}]$).

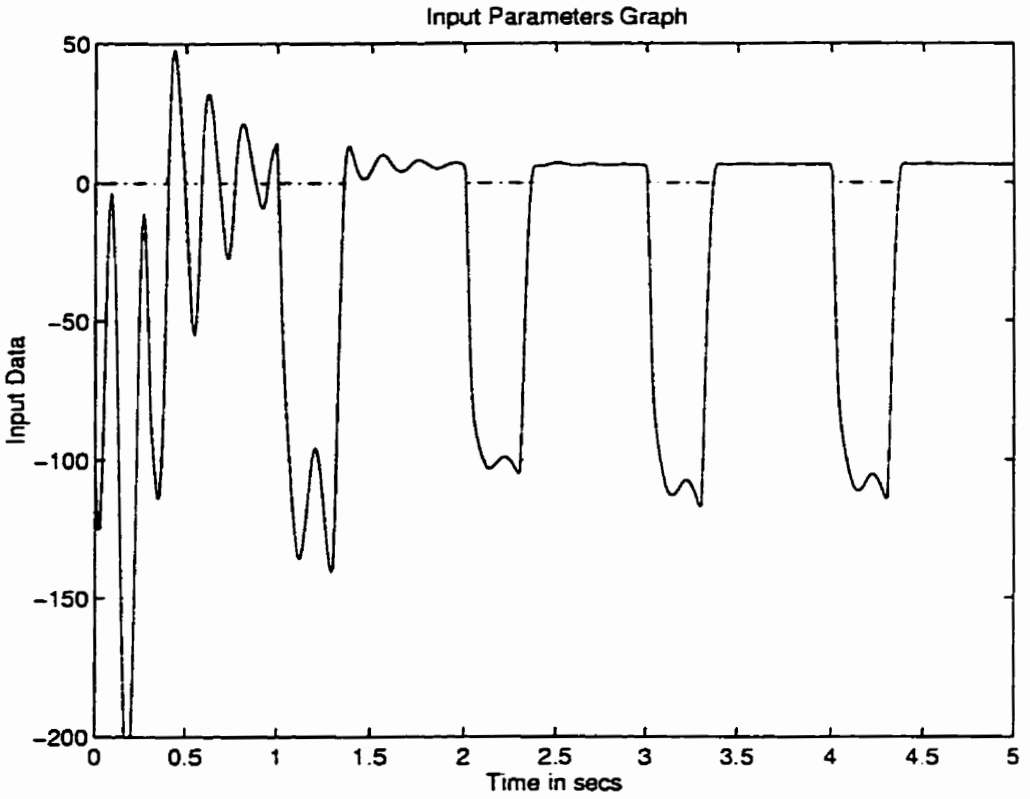


**Figure 6.62:** Input valve parameters for an increase in inlet cannula compliance ($C_{cnin} \times 2$). ( - pressure gradient across inlet valve [mm Hg]. -.- flow rate across the inlet valve $[\frac{L}{min}]$).

the increased compliance case due to the initial condition value. This is very visible in the inlet cannula pressure as shown in Figure 6.63. Figure 6.63 also shows an increase in amplitude of the inlet cannula pressure. The same effect of valve flutter is seen as in the case of an increase in inlet cannula compliance.

## 6.21 Outlet Cannula Compliance ($C_{cnot}$)

Similar to the inlet cannula compliance, the compliance of the oulet cannula was altered and simulated. The results are similar to the initial conditions done above in section 6.14.1.

### 6.21.1 Increase in $C_{cnot}$

The increase in the outlet cannula compliance is again reflected in the startup conditions (step change). The aorta and outlet cannula pressure rapidly change during the first 3 beats of the simulation implying drastic changes in volume reallocation in the circulatory system as shown in Figure 6.64. The flow rate is seen to change for the first beat. At steady state the aorta and outlet cannula pressure is higher than nominal. A similar behaviour is seen in the arterial segment with fewer oscillations in the pressure and flow rate. The peripheral flow in the system shows an initial decrease and a slight rise (oscillatory response) until steady state is reach at about the $15^{th}$ beat as shown in Figure 6.65. The venous segment also shows large amplitude oscillations in the pressure in the inlet cannula and flow rate for the first beat of the simulation. The pressure-volume loop shown in Figure 6.66 shows a rapid drop in volume to a negative value implying that ejection volume is larger than EDV for the first 3 beats because of the lower initial volume in the outlet cannula. This is verified in the flow rates from the artificial heart and the ejection fraction.

### 6.21.2 Decrease in $C_{cnot}$

Initial conditions of the outlet cannula flow rate and pressure, aorta pressure and flow and the arterial segment all show the same rapid changes for the first 2 beats

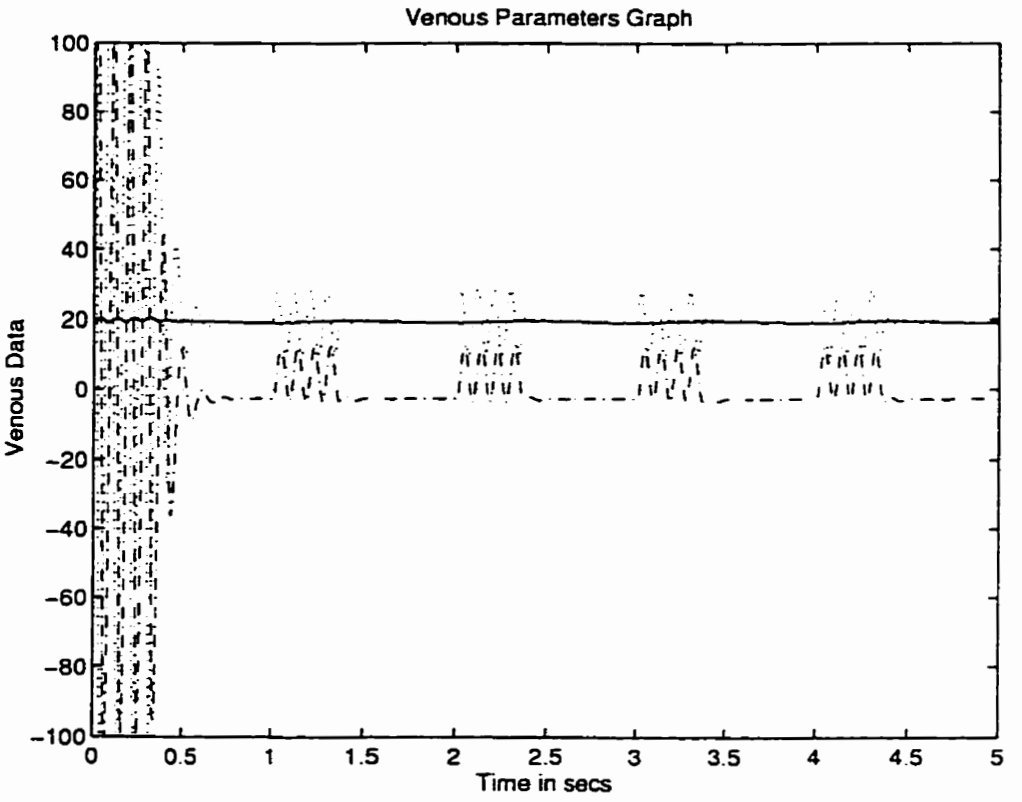


**Figure 6.63:** Venous/inlet cannula segment data for a decrease in inlet cannula compliance ($C_{cnin} \times 0.5$). ( .. Inlet cannula pressure [mm Hg], - venous pressure [mm Hg], -.- inlet cannula flow rate $[\frac{L}{min}]$).

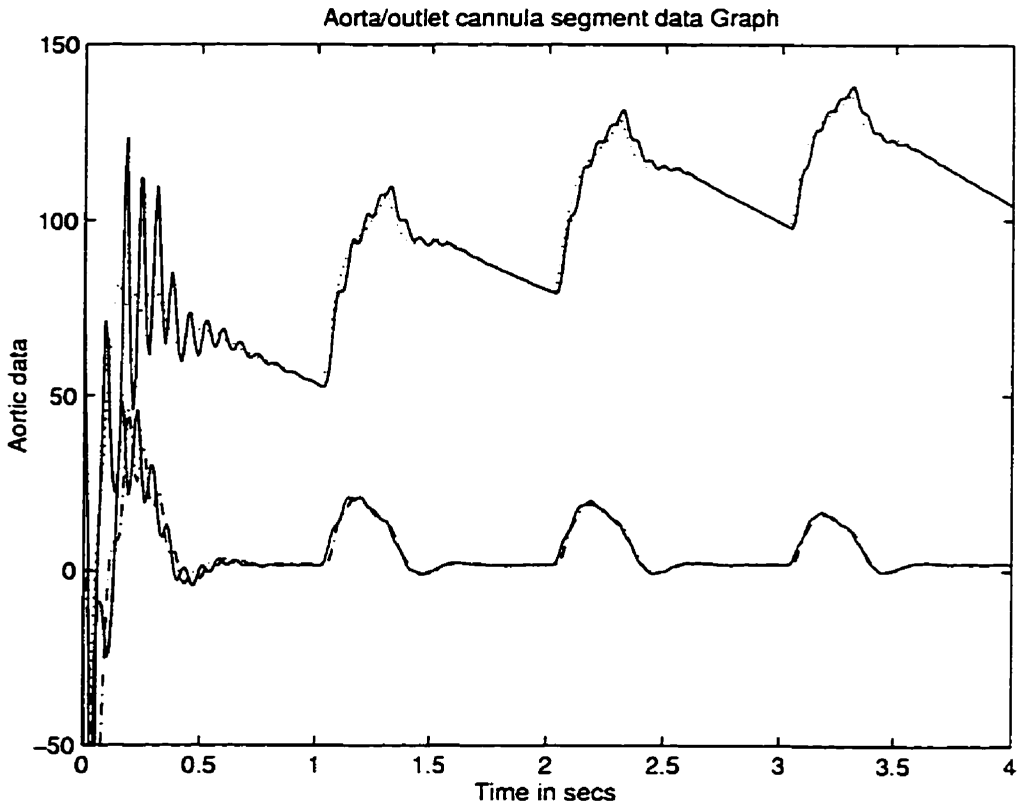


**Figure 6.64:** Aorta/outlet cannula segment for an increase in outlet cannula compliance ($C_{cnot} \times 2$). ( - aorta pressure [mm Hg], .. outlet cannula pressure [mm Hg], -.- aorta flow rate [$\frac{L}{min}$], - outlet cannula flow rate (lower line) [$\frac{L}{min}$]).

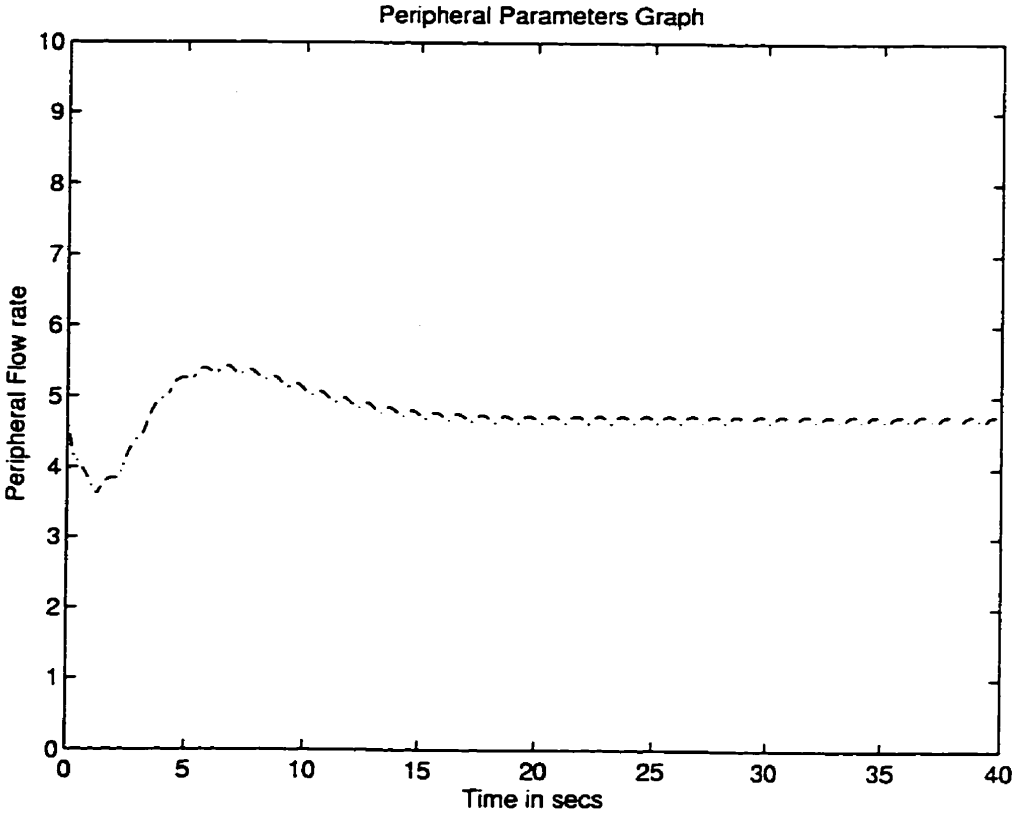


**Figure 6.65:** Peripheral flow for an increase in outlet cannula compliance ($C_{cnot} \times 2$).

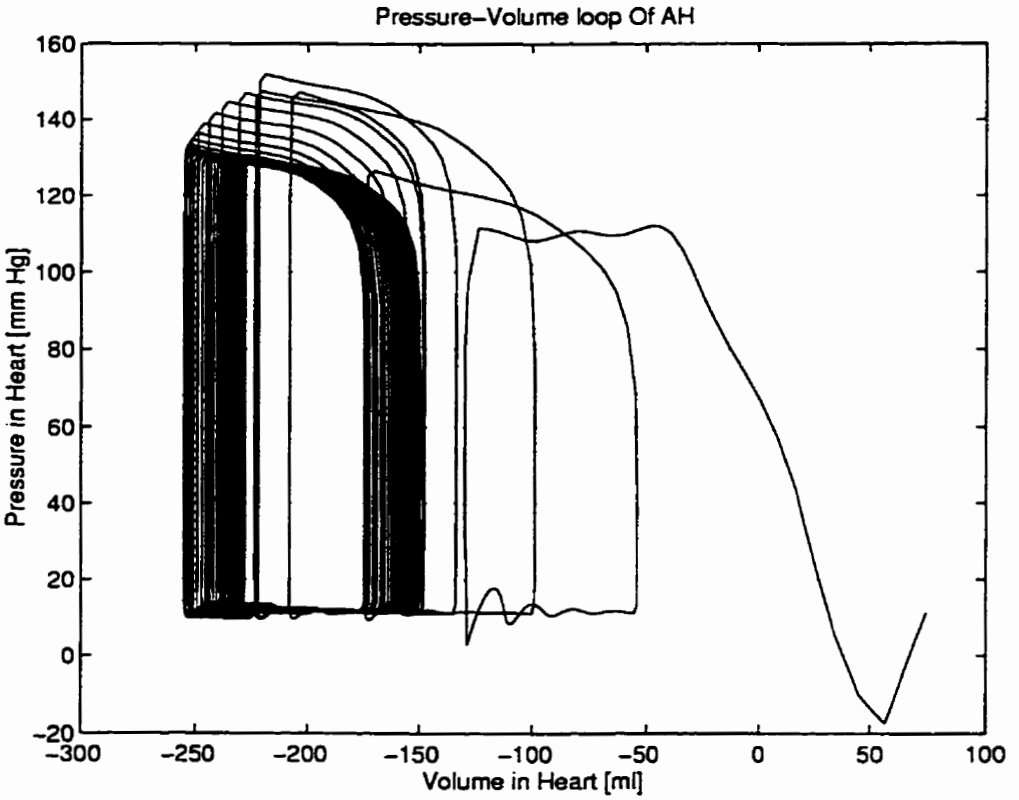


**Figure 6.66:** Pressure-Volume Loop for an increase in outlet cannula compliance($C_{cnot} \times 2$).

in the simulation which is seen in Figure 6.68. The peripheral flow initially shows a brief rise in flow for the first 5 beats then steady state is reached on the $6^{th}$ beat. There are little or no changes in the venous and inlet cannula parameters. A large drop in outlet flow rate is seen in the initial few beats which rises to nominal values by the $4^{th}$ beat. The pressure-volume loop shown in Figure 6.68 shows that the artificial heart volume drifts toward the positive region implying that less blood is ejected during systole and hence an ejection fraction less than one.

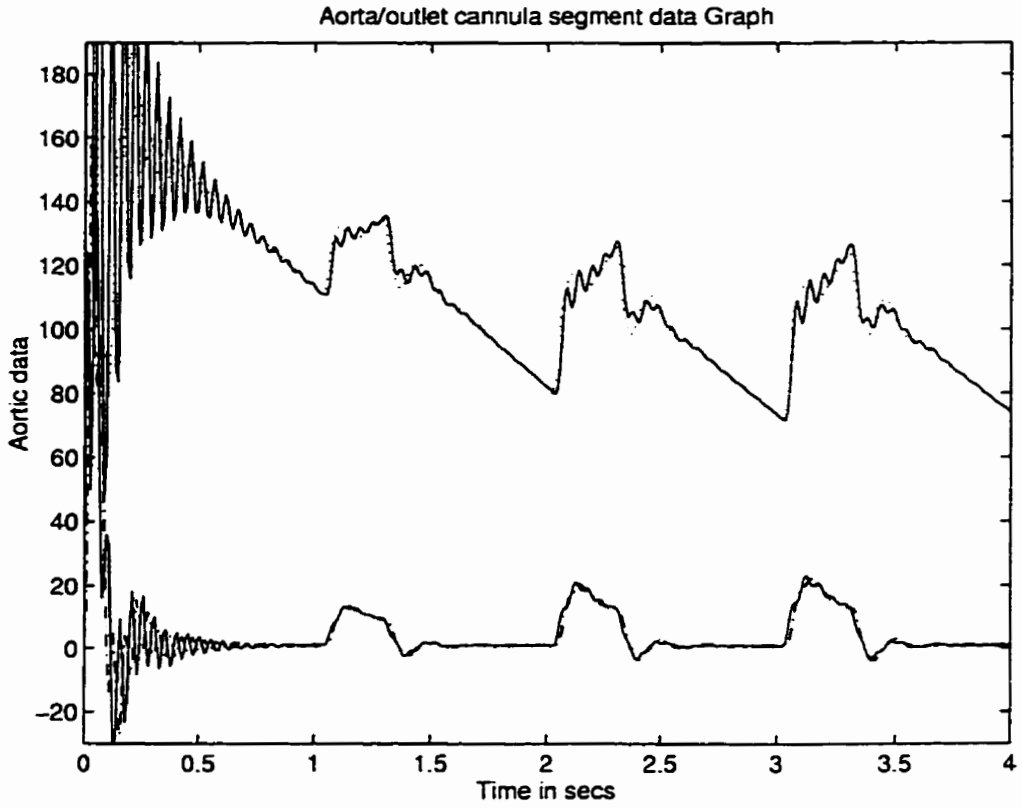


**Figure 6.67:** Aorta/Outlet segment data for a decrease in outlet cannula compliance ($C_{cnot} \times 0.5$). ( - aorta pressure [mm Hg], .. outlet cannula pressure [mm Hg], -.- aorta flow rate $[\frac{L}{min}]$. - outlet cannula flow rate (lower line) $[\frac{L}{min}]$).

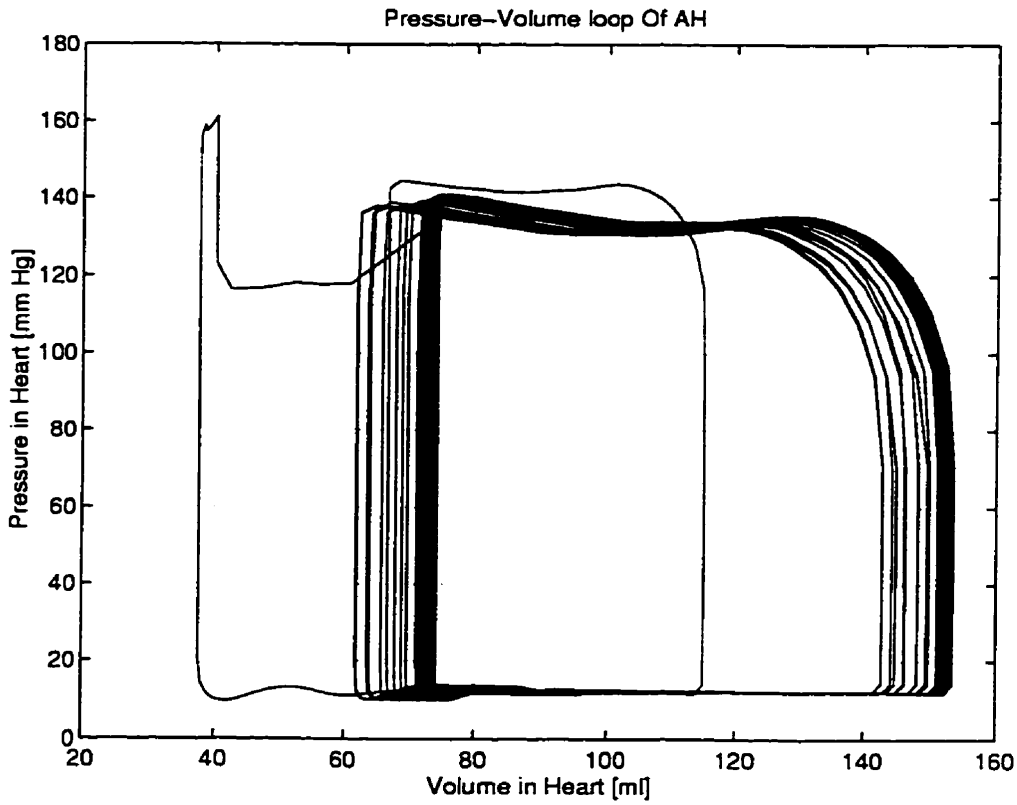


**Figure 6.68:** Pressure-Volume Loop for a decrease in outlet cannula compliance ($C_{cnot} \times 0.5$)

## 6.22 Peripheral Inertance ($I_{pe}$)

The change in peripheral inertance is similar to extending the number of blood vessels, capillaries, and venules in the musclar tissues and organs to provide adequate blood prefusion to supply oxygen, nutrients, remove waste and for temperature control. This parameter is vague and therefore this simulation shows the range over which the ciculatory model and control can be valid.

### 6.22.1 Increase in $I_{pe}$

The peripherial inertance was increased by 4 times. The effect of the increase shows oscillation on the systemic parameters of the model on a macro scale as shown in Figure 6.69. Figure 6.69 shows the venous segment and the effect of increased peripheral inertance. The aorta, arterial, venous inlet/outlet show similar behaviour as the aorta pressure drops. The peripheral flow in Figure 6.70 shows the oscillations. Initially the periperal flow is below $2\frac{L}{min}$ but this lasts for a duration of only the first 5 beats when the peripheral climbs to $4\frac{L}{min}$. The artificial heart pressures during systole are seen to increase initially. The Figure 6.71 shows the pressure volume loop of the artificial heart which shows the oscillations described above.

### 6.22.2 Decrease in $I_{pe}$

The simulation for a decrease in the peripheral inertance shows similar behaviour to an increase above. The aorta and outlet cannula pressures show a large drop. This causes the outlet flow rate to rise as shown in Figure 6.72. The aorta pressures rise again to stablize in the $4^{th}$ beat. The peripheral flow shows the flow rate to be very oscillatory as when peripheral inertance is decreased. This oscillations are shown in Figure 6.73. The venous segment shows that the inlet flow rate starts very high and becomes nominal after the first beat.

No significant change is seen in the inlet valve parameters. The artificial heart

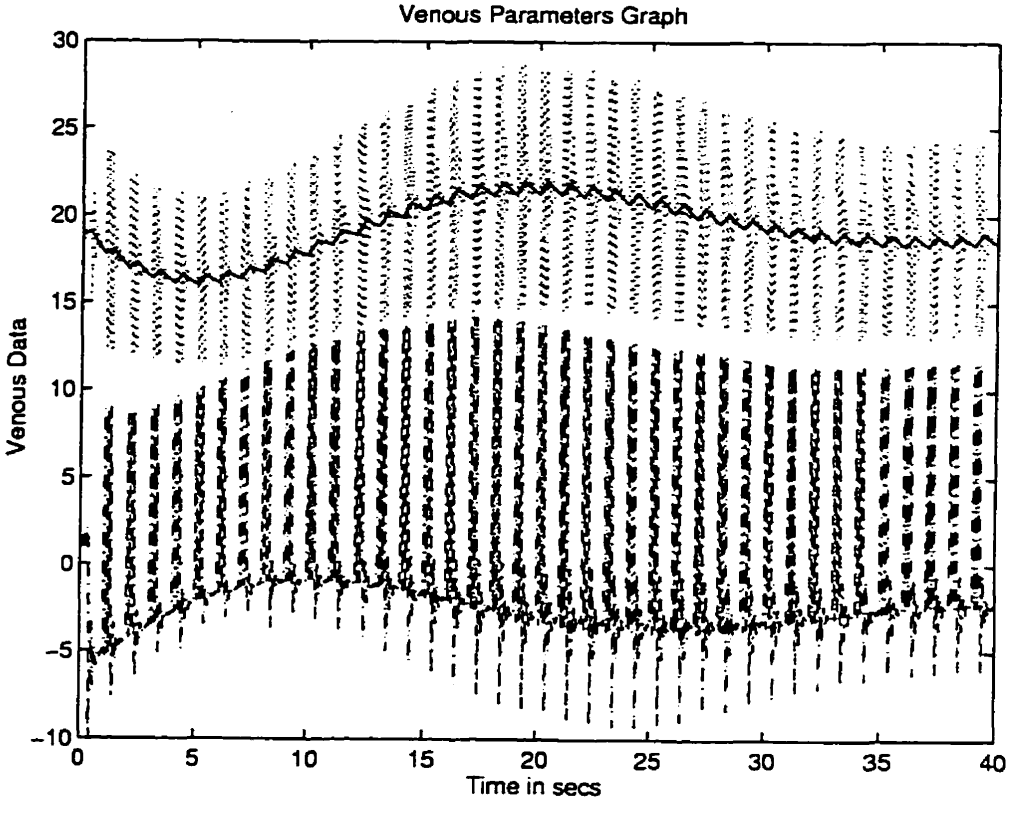


**Figure 6.69:** Venous/inlet cannula segment data for an increase in peripheral inertance ($I_{pe} \times 4$). ( .. Inlet cannula pressure [mm Hg], - venous pressure [mm Hg], -.- inlet cannula flow rate $[\frac{L}{min}]$).

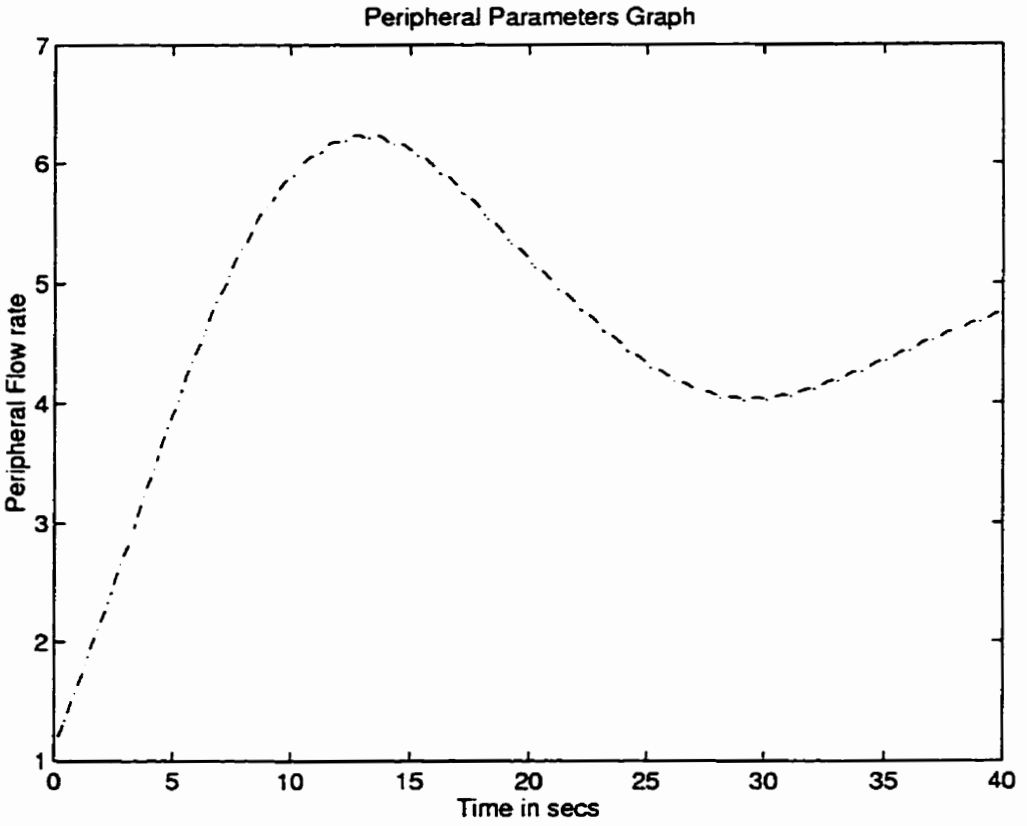


**Figure 6.70:** Peripheral Flow for an increase in peripheral inertance ($I_{pe} \times 4$).

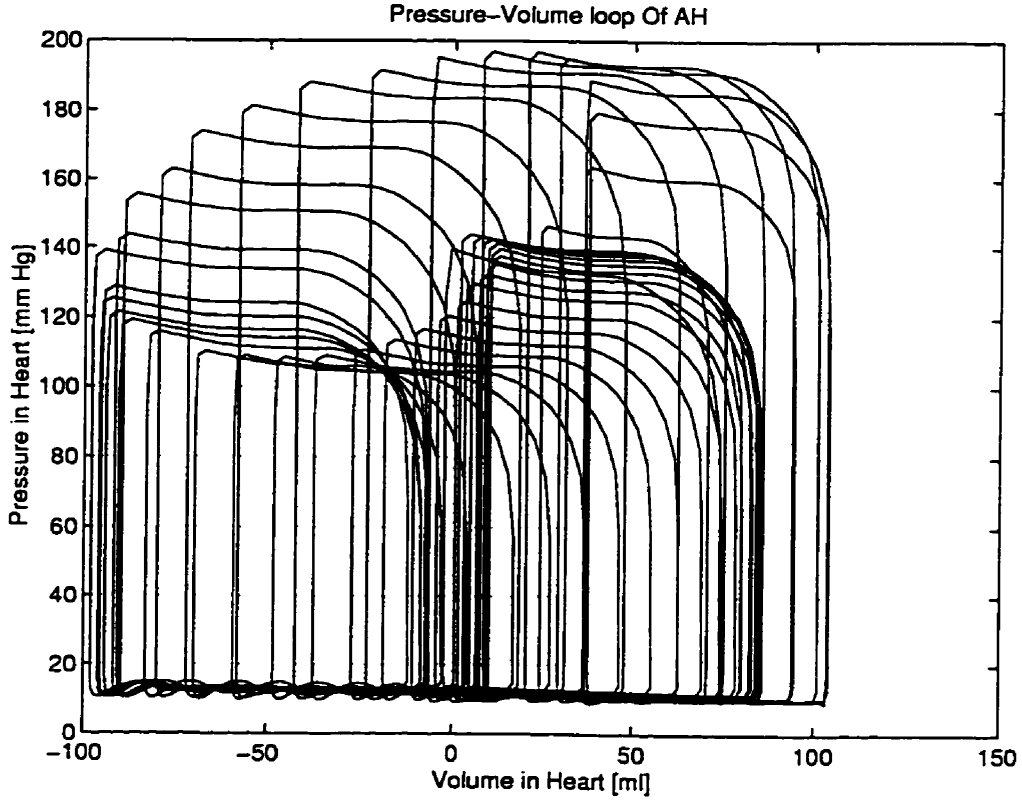


**Figure 6.71:** Pressure Volume loop for an increase in peripheral inertance ($I_{pe} \times 4$).

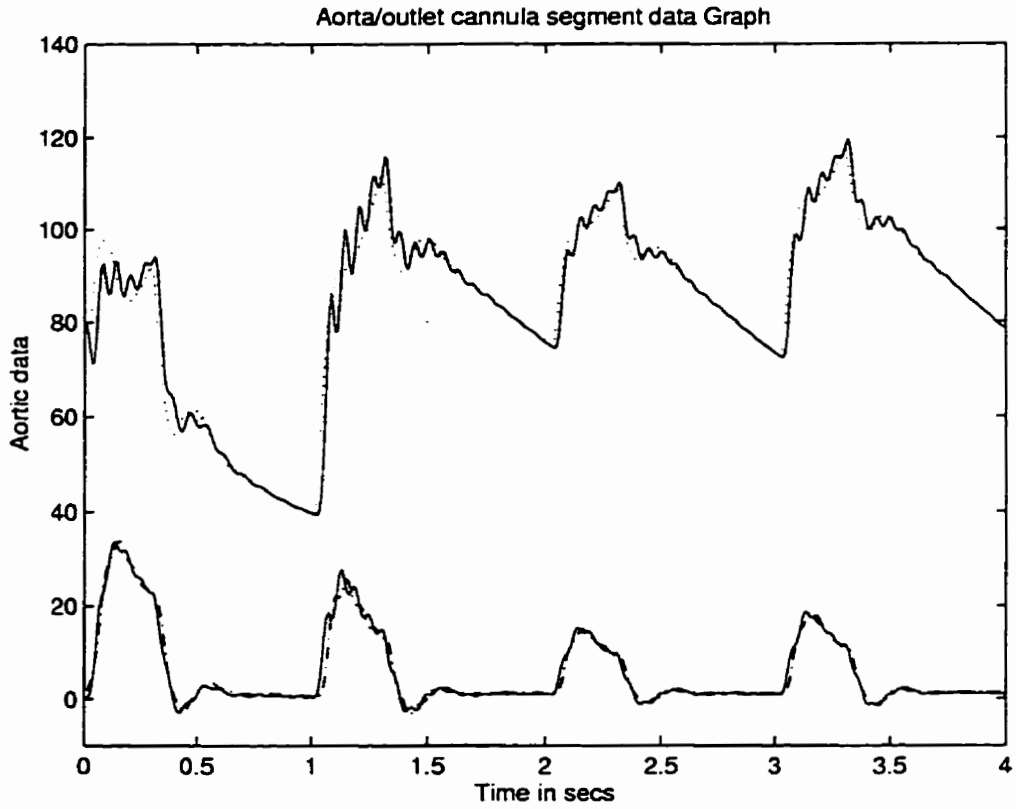


**Figure 6.72:** Aorta/outlet cannula segment data for a decrease in peripheral inertance ($I_{pe} \times 0.1$). ( - aorta pressure [mm Hg]. .. outlet cannula pressure [mm Hg], -.- aorta flow rate $[\frac{L}{min}]$. - outlet cannula flow rate (lower line) $[\frac{L}{min}]$).

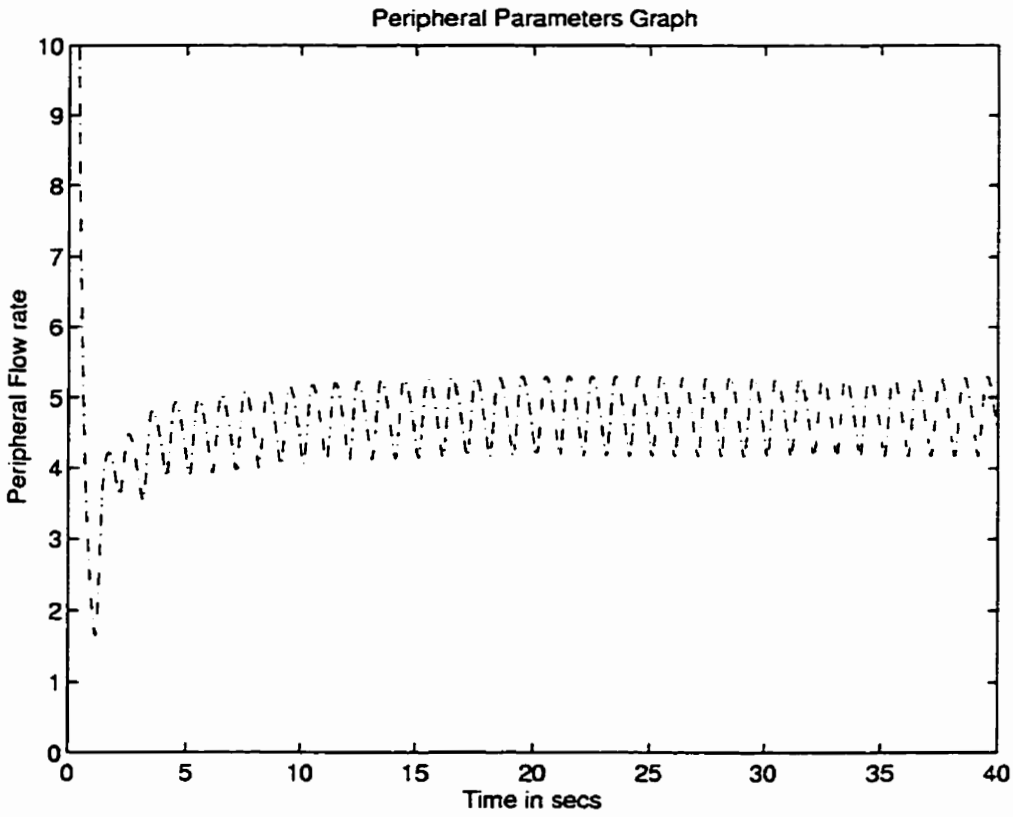


**Figure 6.73:** Peripheral Flow for a decrease in peripheral inertance ($I_{pe} \times 0.1$).

parameters show small changes in the systolic pressure. The outlet flow increased during the first 2 beats and returns. The Pressure-Volme loop moves towards the left (negative) during the first few beats. The loop then moves back toward the right to aproximately nominal values as shown in Figure 6.74.

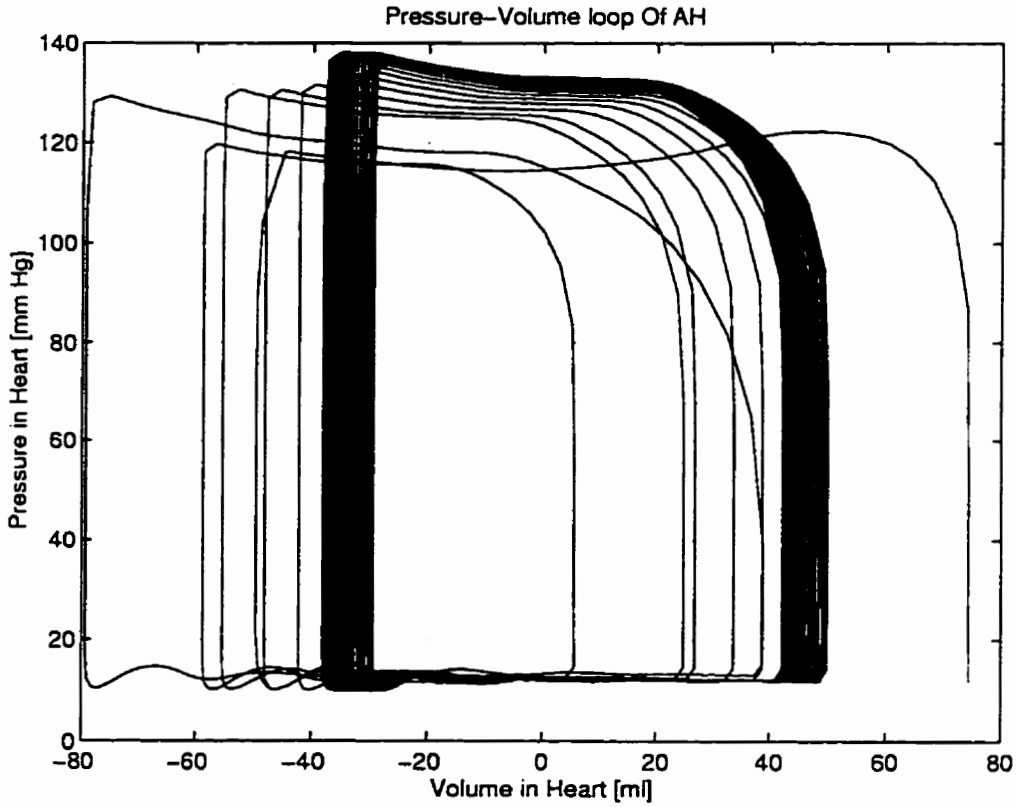


**Figure 6.74:** Pressure-Volume Loop for a decrease in peripheral inertance $I_{pe} \times 0.1$).

## 6.23 Heart Resistance and Compliance

The changes in heart parameters causes the trained EDV and ESV to be altered because the data used in training has been changed. This causing failure of the estimators to predict the stroke volume and pump output. Therefore the control action proposed by the FLC is misleading. The resistance of the heart, inlet/outlet valves and the heart complaince caused EDV and ESV estimates to have the same problem.

# Chapter 7

# Conclusion and Recommendations

## 7.1 Conclusion

The development of the aorta segment produces better results of the aorta behaviour during control. This is seen when the blood volume is lowered or raised during changes in the peripheral resistance or other model parameters and also from observation of the pressure waveform. The behaviour of the aorta is more representative of the human circulatory system.

The use of the estimator for EDV and ESV is seen to provide accurate estimation when the simulation is within the trained pressure gradient. The ANFIS presented shows that ESV errors are larger than the EDV errors due to the changes in the control force from beat to beat, but the ESV estimate is accurate enough to provide a good cardiac output estimate. The ESV estimator becomes less accurate as the simulation moves outside the universe of discourse for the inputs of the ANFIS. A side effect of trained data is that the estimator is specific to the system for which it has been trained. Hence changes in the circulatory models parameters that effect the trained data can produce errors in estimation of EDV and ESV. The present estimator model is robust for most of the systemic parameters, it accurately estimates the EDV and ESV for stablization of cardiac output in the model under study except in extreme conditions were the model parameters are changed to about 0.5 or 2 times its nominal value. Such values are assumed to be very extreme.

The use of adaptive neuro fuzzy inference systems can be used to provide important relationships between various parameters that are presently very hard to relate due to the complex interaction of multiple parameters. The EDV ANFIS shown in this simulation can be seen to be linear with respect to changes in inlet pressure gradient ($\Delta P_{in}$) to a fixed diastolic time ($t_{dia}$). The linear function can be used to provide a relationship between EDV and inlet pressure gradient. Therefore the use of ANFIS models provides a way to analyze data and provide a relationship between the input and output of complex and highly non-linear systems without a clear mathematical analysis of the various interactions involved.

The use of the systolic force as a control variable to maintain the required pump output is shown through simulation to be possible. The altered peripheral resistance causes a change in the pump output which is corrected within the first minute of the simulation. A side effect of increasing or decreasing the systolic force is the effect on the average outlet cannula pressure during systole. A drop in the systolic force causes a decrease in the average outlet cannula pressure during systole and vice versa. The pressure changes do not impact the system strongly and would be a function of the outlet cannula design parameters (compliance). Pump output is still maintained and such high/low pressures are assumed common in high blood pressure patients and patients under extreme physical activity.

## 7.2 Future Recommendations

The present model of the circulatory system is quite robust. It models the peripheral flow, aorta segment, arterial segment, venous segment, artificial heart and inlet/outlet cannula segment. These segments make up most of the major parts of the human circulatory system. Improvements can be made to better model the actual human circulatory system and to exercise better control of the artificial heart. The venous segment at present is modelled similarly to the previous lumped arterial model. Studies have shown that venous segment is prone to collapse when the pressure drops in the venous segment [18]. If the venous segment model is developed, the diastolic force $F_{dia}$ can also be used as a control variable. The alteration of the $F_{dia}$ will provide a method of altering the EDV directly which will provide the required volume in the heart for systole to maintain the required pump output. The venous segment is a slightly more complex segment to model since the collapse of the venous would affect the flow rate through the segment which would mean that the model would have to have coupling between the pressure in the venous segment and the resistive element in the venous segment [20].

The addition of the right ventricle model will allow a new group of studies on the use of two devices to work in a total artificial heart (TAH) configuration. The volume ejected from the right ventricle to the left side (balancing the left and right side blood volumes) would have to be maintained to provide continuous flow of blood. The first stage wold be to produce a full circulatory system model from the existing model. Studies of using paired ventricle assist devices (VADs) can also be studied for feasability as implantable artificial hearts.

Ventricular assist devices generally operate inline with the natural heart. The modeling the natural heart would be a key step in begining to do synchronization studies and optimization of control for the ventricular assist devices.

At present no pulmonary circulation is modelled. The modeling of the pulmonary

circulation may provide help in determing the effect of lower oxygenation or simulate respiratory failure in a patient and to model patients under physical activity who are suffering from lower oxygen saturation in the blood [6]. These studies will help in determining the required pump output to provide the required oxygen to the body.

A study of determining the required pump output by moitoring various parameters would be very good. Presently the fuzzy logic controller matches the desired pump output set by the user. If a robust model was developed to provide a required pump output estimate, it would replace the desired pump output. It could be based on the difference in venous oxygen saturation ($SvO_2$) and arterial oxygen saturation ($SaO_2$) and it would be a key step to provide active control of an artificial heart [59, 6, 12, 11].

The intelligent control provides a method to alter the systolic force used to drive the artificial heart which can be beneficial to save energy and for power conservation during rest. The fixed rate and Full-Fill Full-Eject controllers cannot at present do this without manual changes in the force control parameters. A combination of both the Full-Fill Full-Eject systolic/diastolic timing and the systolic/diastolic force acting on the heart maybe a promising method of control.

The tuning process is very tedious and time consuming. Hence a more research in the development of a method other than ANFIS or manual tuning of fuzzy logic controller behaviour would help in using fuzzy logic control and modeling in more engineering applications.

To reduce computational overhead the controller can be used to act with a preset number of beats. Hence the control action will only take place every preset $n^{th}$ beat. This will alow the system to adjust to the new control input before a new control input is suggested. Another method of control is to produce multiple control models to attain a picture of the circulatory system under different physiological conditions and expressing them as subsystems, then implimenting a fuzzy logic controller to non-linearly average the subsystems for any given control condition.

# References


[1] S Tan. *Development of a Dynamic Model of a Ventricular Assist Device for Investigation of Control Systems.* Carleton University. Ottawa. Ontario. Canada. 1996.

[2] Ghista D. N. Clinical cardiac assesment. interventions and assist technology. *Adv. Cardiovascular Physiology.* 7:1–25. 1990.

[3] Watson T. J. Heart replacement (artificial heart 5): Implantable artificial heart systems. $5^{th}$ *International Symposium on artificial hearts and assist devices.* pages 95–100. January 1995.

[4] Tatauya S. Takatani S. Shiono M. Sakuma I. Glueck J. Noon G. P. Nose Y. and DeBakey M. E. Development of totally implantable electromechanical artificial heart systems: Baylor ventricular assist system. *Artificial Organs.* 16(4):407–413. 1992.

[5] Mussivand T. Interview. *Fuzzy Logic Controller Presentation.* June 1997.

[6] Takatani S. Noda H. Takano H. and Akutsu T. Continuous in-line monitoring of oxygen delivery to control artificial heart output. *Artificial Organs.* 14(6):458–465, 1990.

[7] Yoshizawa M. Takeda H. Yambe T. and Nitta S. Assessing cardiovascular dynamics during ventricular assistance. *IEEE Engineering In Medicine And Biology*, pages 687–692, Nov/Dec 1994.

[8] Ghista D. N. Clinical cardiac assesment, interventions and assist technology. *Adv Cardiovascular Physiology*, 7:89–117, 1990.

[9] withington P. S. Graham T. R. Meikle R. J. Allan A. Marrinan M. T. and lewis C. T. In vitro evaluation of an implantable left ventricular assist device. *journal Of Medical Engineering & Technology*. 15(2):68–71, 1991.

[10] Gibbson J.H. Application of a mechanical heart-lung apparatus to cardiac surgery. *Minn. Med.*, 37:171, 1954.

[11] Schima H. Trubel W. Coriam F. Huber L. Muller M. R. Redl G. Losert U. Thoma H. and Wolner E. Control of the total artificial heart: New aspects in human versus animal experience. *Artificial Organs*. 13(6):545 552. 1989.

[12] C. S. Pearson P. T. Workman H. W. Howard H. E. Cholvin N. R. Swift and Al-Nakeeb S. Venous and arteriovenous difference in oxyhemoglobin concentrations as parameters to control stroke volume of an artificial heart. *Medical Research Engineering*. pages 25–29. Jan/Feb 1969.

[13] Y C Fung. *Biodynamics: Circulation*. Springer-Verlag. Berlin. 1984.

[14] Klimes F. Shorkovsky J. Zita J. Andreovsk F. Bednarik B. and Vasku J. Analysis and model of controlling system to control heart rate and stroke volumes of an artificial heart. *Medical And Biological Engineering*. pages 662–668. September 1975.

[15] Yu Clement et al. Multiple-model adaptive predictive control of mean arterial pressure and cardiac output. *IEEE Transactions On Biomedical Engineering*. 39(8):765–777, 1992.

[16] T. G. Coleman. Mathematical analysis of cardiovascular function. *IEEE Transactions On Biomedical Engineering*, BME-32(4):289–294. 1985.

[17] T. Ezzaher, A. El Ouazzani and B. Crozatier. Timing and velocity of ejection as major determinants of end-systolic pressure in isolated rabbit hearts. *Circulation*. 90:3055–3062. 1994.

[18] Melchior F.M. Srinivasan R.S. Charles J.B. Mathematical modeling of human cardiovascular system for simulation of orthostatic response. *Heart Circ. Physiol.*. 31:H1920–H1933. 1992.

[19] Rideout V. C and D. E. Dick. Difference-differential equations for fluid in distensible tubes. *IEEE Trans. Biomed. Eng.*. 14:171–177. 1967.

[20] Hiroyuki Suga. Incorporation of venous resistance in togawa's four quadrant diagram for guytons circulatory equilibrium. *Japanese Heart Journal*. 29:89–97. January 1988.

[21] Chuen Chien Lee. Fuzzy logic in control systems: Fuzzy logic controller part i. *IEEE Transactions On Systems, Man and Cybernetics*. 20(10):419–435. 1990.

[22] Chuen Chien Lee. Fuzzy logic in control systems: Fuzzy logic controller part ii. *IEEE Transactions On Systems, Man and Cybernetics*. 20(10):419–435. 1990.

[23] D. E. Thomas and B. Armstrong-Helouvry. Fuzzy logic control- a taxonomy of demonstrated benefits. *Proceedings Of The IEEE*. 83(3):407–421. 1995.

[24] Ying H. McEachern M. Eddleman D. W. and Sheppard L. Fuzzy control of mean arterial pressure in postsurgical patients with sodium nitoprusside infusuion. *IEEE Transactions On Biomedical Engineering*. 39(10):1060–1069. 1992.

[25] Hudson D. L. and Cohen M. E. Fuzzy logic in medical expert systems. *IEEE Transactions In Medicine And Biology*, pages 693–698. Nov/Dec 1994.

[26] Moore D Chiu S, Chand S and Chaudhary A. Fuzzy logic for control of roll and moment for a flexible wing aircraft. *IEEE control systems magazine*. 11(4):42–48, 1991.

[27] Luo J and Lan E. Fuzzy logic controller for aircraft flight control. *Fuzzy logic and Intelligent systems*. pages 85–115. 1995.

[28] Andreassen S. Decisions based on qualitative and quantitative reasoning. *Proceedings of the workshop "System Engineering In Medicine"*. 47:68–79. March 1989.

[29] Mira J. Otero R. P. Barro S. Barreiro A. Ruiz R. Marin R. Delgado A. E. Amaro A. and Jacket M. Knowledge based systems in ccu's: Monitoring and patients follow-up. *Proceedings of the workshop "System Engineering In Medicine"*. 47:174–192. March 1989.

[30] C. M Held and R. J Roy. Multiple drug hemodynamic control by means of a supervisory-fuzzy rule-based adaptive control system: Valiadtion on a model. *IEEE Transactions On Biomedical Engineering*. 42(4):371–385. 1995.

[31] Katayama Ryu. Special issue on fuzzy control. *Journal of robotics and mechatronics*. 7(1):2–8. Febuary 1995.

[32] Kaufmann A. *Introduction to the Theory Of Fuzzy Subsets Vol I*. Academic Press. 1975.

[33] R.and Filev P. D. Yager. *Essentials of fuzzy modelling and control*. John Wiley & Sons. Inc., 1994.

[34] Kruse Rudolf. *Foundations of fuzzy systems*. John-Wiley & Sons. New York. 1994.

[35] Zadeh L. A. Fuzzy sets. *Information and Control*. 8:338–353. 1965.

[36] Kandel A. and Langholz G. *Fuzzy control systems*. CRC press. Boca Raton. Florida, 1994.

[37] Driankov Dimiter. *An introduction Fuzzy control*. Springer. Berlin. 1993.

[38] J. Shing and R. Jang. Anfis: Adaptive-network-based fuzzy interence system. *IEEE Transactions On Systems, Man And Cybernetics*. 23(3):665–685. 1993.

[39] Kasabov N K. *Foundations of neural networks, fuzzy systems, and knowledge engineering.* Cambridge Press, MIT press, 1996.

[40] Margolis Donald L. Karnopp Dean C. and Rosenberg Ronald C. *System Dynamics: A Unified Approach.* John Wiley & Sons, New York, 1990.

[41] R. H. Stern and H. Rasmussen. Left ventricuar ejection: Model solution by collocation, an appoximate analytical method. *Computing Biological Medicine*, 26(3):255–261, 1996.

[42] Tsuruta H. Sato T. Shirataka M. and Ikeda N. Mathematical model of cardiovascular mechanics for diagnostic analysis and treatment of heart failure: Part 1 model description and theortical analysis. *Medical & Biological Engineering & Computing*, 32:3–11, 1994.

[43] A. L. King. Pressure-volume relation for cylinderical tubes with elastomeric walls: The human aorta. *Journal Of Applied Physics*, 17(6):501–505, 1946.

[44] K. P. Liu, Z. Brin and F. C. P. Yin. Estimation of total arterial compliance: an improved method and evaluation of current methods. *American Journal Of Physiology*, 251(20):H588–H600, 1986.

[45] Laskey W. K. Parker G. H. Ferrari V. A. Kussmaul W. G. and Noordergraaf. Estimation of total systemic arterial compliance in humans. *Journal Of Applied Physiology*, 69(1):112–119, 1990.

[46] Melchior F. M. Srinivasan R. S. Philippe H. T. and Clere J. M. Simulation of cardiovascular response to lower body negative pressure from 0 to -40mmhg. *Journal Of Applied Physiology*, 77(2):630–640, 1994.

[47] Oscasio W. C. Rigney D. R. Clark K. P. and Mark R. G. bpshape wk4: A computer program that implements a physiological model for analyzing the shape of blood pressure waveforms. *Computer Methods and Programs in Biomedicine*, 39:169–194, 1993.

[48] D. Burkhoff and J. V. Tyberg. Why does pulmonary venous pressure rise after onset of lv dysfunction: a theoretical analysis. *American Journal Of Physiology.* 265:H1819–H1828. 1993.

[49] Lazzari C. De. Ferrari G. Mimmo R. Tosti G. and Ambrisi D. A desk-top computer model of the circulatory system for heart assistance simulation: effect of an lvad on energetic relationships inside the left ventricle. *Medical Engineering In physics.* 16(3):97–103. 1994.

[50] Caro C. G. Pedley T. J. Schroter R. C. and Seed W. A. *The mechanics of circulation.* Oxford University Press. 1978.

[51] U. Klute. G. K. Tasch and D. B. Geselowitz. An optimal controller for an electric ventricular-assist device: Theory. implementation and testing. *IEEE Transactions On Biomedical Engineering.* 39(4):394–403. 1992.

[52] Rushmer F. Robert. *Cardiovascular Dynamics.* W. B. Saunders Company. 1976.

[53] Willard P. W and Beck H. R. A system for measurement of cardiovascular parameters. *Medical Research Engineering.* pages 33–36. May-june 1969.

[54] Lerner A.Y. Artificial blood circulation: Stabilization. physiological. control. and optimization. *Artif Organs*, 14:110–117, 1990.

[55] Masuzawa T. Taenaka Y. Nakatani T. Akagi H. and Takano H. Recent progress in automatic control of the total artificial heart in ncvc. *Department Of Artificial Organs, National Cardiovascular Center Research Institute.* Osaka. Japan:105–109, 1975.

[56] Yoshizawa M. Takeda H. Yambe T. Katahira Y. and Nitta S. Real-time cardiac output estimation of the circulatory system under left ventricular assistance. *IEEE Transactions On Biomedical Engineering.* 40(3):266–274. 1993.

[57] Akio S Hirokuni A. Tohru S. Automatic control and monitoring system for pneumatic vad. *Department of Thoracic and Cardiovascular surgery*. pages 75–79. 1991.

[58] Gulley Ned and Roger Jang J. S. *Fuzzy logic toolbox*. The Mathworks Inc. Natick. Mass., 1995.

[59] Baker N. A. A galavanic cell suitable for monitoring cortical oxygen in man. *Medical And Biological Engineering*. 1:443–449. May 1975.

# Appendix A

# Matlab Code

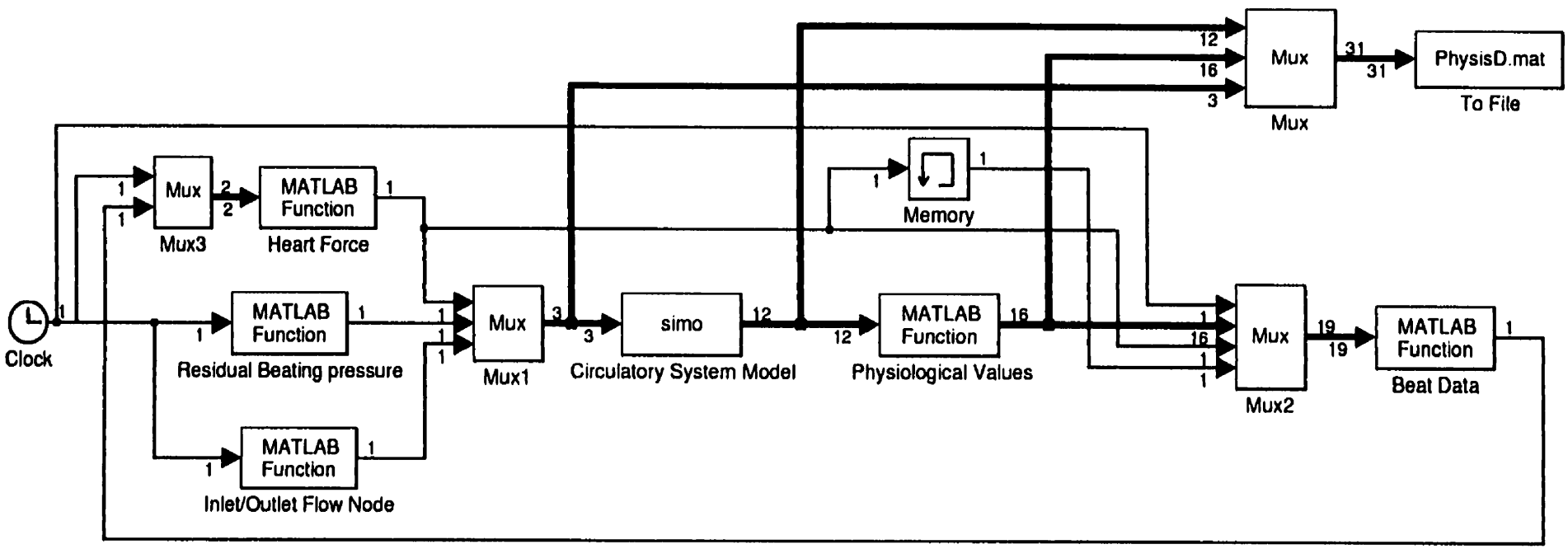
Clock
Mux
Mux3
MATLAB Function
Heart Force
MATLAB Function
Residual Beating pressure
MATLAB Function
Inlet/Outlet Flow Node
Mux
Mux1
simo
Circulatory System Model
Memory
MATLAB Function
Physiological Values
Mux
Mux
Mux2
MATLAB Function
Beat Data
PhysisD.mat
To File

```
function [sys,x0,str,ts] = sfuntmpl(t,x,u,flag)

global  rm w A Rht Iht Icnot Rcnot Rot Rotm Icnin Rcnin Rin Rinm Iao Rao Ipe Rpe
global  vnpvfis anfisedv anfisesv forcectrl Desired_CO Fsys_ctrl

%Revised on 2 Janurary 1998.

%SFUNTMPL General M-file S-function template
%   With M-file S-functions, you can define you own ordinary differential
%   equations (ODEs), discrete system equations, and/or just about
%   any type of algorithm to be used within a Simulink block diagram.
%
%   The general form of an M-File S-function syntax is:
%       [SYS,X0,STR,TS] = SFUNC(T,X,U,FLAG,P1,...,Pn)
%
%   What is returned by SFUNC at a given point in time, T, depends on the
%   value of the FLAG, the current state vector, X, and the current
%   input vector, U.
%
%   FLAG   RESULT             DESCRIPTION
%   -----  ------             -------------------------------------------
%   0      [SIZES,X0,STR,TS]  Initialization, return system sizes in SYS,
%                             initial state in X0, state ordering strings
%                             in STR, and sample times in TS.
%   1      DX                 Return continuous state derivatives in SYS.
%   2      DS                 Update discrete states SYS = X(n+1)
%   3      Y                  Return outputs in SYS.
%   4      TNEXT              Return next time hit for variable step sample
%                             time in SYS.
%   5                         Reserved for future (root finding).
%   9      []                 Termination, perform any cleanup SYS=[].
%
%
%   The state vectors, X and X0 consists of continuous states followed
%   by discrete states.
%
%   Optional parameters, P1,...,Pn can be provided to the S-function and
%   used during any FLAG operation.
%
%   When SFUNC is called with FLAG = 0, the following information
%   should be returned:
%
%      SYS(1) = Number of continuous states.
%      SYS(2) = Number of discrete states.
%      SYS(3) = Number of outputs.
%      SYS(4) = Number of inputs.
%               Any of the first four elements in SYS can be specified
%               as -1 indicating that they are dynamically sized. The
%               actual length for all other flags will be equal to the
%               length of the input, U.
%      SYS(5) = Reserved for root finding. Must be zero.
%      SYS(6) = Direct feedthrough flag (1=yes, 0=no). The s-function
%               has direct feedthrough if U is used during the FLAG=3
%               call. Setting this to 0 is akin to making a promise that
%               U will not be used during FLAG=3. If you break the promise
%               then unpredictable results will occur.
%      SYS(7) = Number of sample times. This is the number of rows in TS.
%
%
%      X0     = Initial state conditions or [] if no states.
%
%      STR    = State ordering strings which is generally specified as [].
%
%      TS     = An m-by-2 matrix containing the sample time
%               (period, offset) information. Where m = number of sample
%               times. The ordering of the sample times must be:
%
%               TS = [0      0,      : Continuous sample time.
```

```
%            0      1,       : Continuous, but fixed in minor step
%                               sample time.
%                  PERIOD OFFSET, : Discrete sample time where
%                               PERIOD > 0 & OFFSET < PERIOD.
%                  -2     0];     : Variable step discrete sample time
%                               were FLAG=4 is used to get time of
%                               next hit.
%
%            There can be more than one sample time providing
%            they are ordered such that they are monotonically
%            increasing. Only the needed sample times should be
%            specified in TS. When specifying than one
%            sample time, you must check for sample hits explicitly by
%            seeing if
%               abs(round((T-OFFSET)/PERIOD) - (T-OFFSET)/PERIOD)
%            is within a specified tolerance, generally 1e-8. This
%            tolerance is dependent upon your model's sampling times
%            and simulation time.
%
%            You can also specify that the sample time of the S-function
%            is inherited from the driving block. For functions which
%            change during minor steps, this is done by
%            specifying SYS(7) = 1 and TS = [-1 0]. For functions which
%            are held during minor steps, this is done by specifying
%            SYS(7) = 1 and TS = [-1 0].

%
% The following outlines the general structure of an S-function.
%

switch flag,
  % Initialization %
  case 0,
    [sys,x0,str,ts]=mdlInitializeSizes;
  % Derivatives %
  case 1,
    sys=mdlDerivatives(t,x,u);
  % Update %
  case 2,
    sys=mdlUpdate(t,x,u);
  % Outputs %
  case 3,
    sys=mdlOutputs(t,x,u);
  % GetTimeOfNextVarHit %
  case 4,
    sys=mdlGetTimeOfNextVarHit(t,x,u);
  % Terminate %
  case 9,
    sys=mdlTerminate(t,x,u);
  % Unexpected flags %
  otherwise
    error(['Unhandled flag = ',num2str(flag)]);
end

% end sfuntmpl

%
%=============================================================================
% mdlInitializeSizes
% Return the sizes, initial conditions, and sample times for the S-function.
%=============================================================================
%
function [sys,x0,str,ts]=mdlInitializeSizes

global rm w A Rht Iht Icnot Rcnot Rot Rotm Icnin Rcnin Rin Rinm Iao Rao Ipe Rpe vnpvfis
global N2Hg Cm2L cm2m Cat Cht Cbli Cblo Cvn atoff htoff icanoff ocanoff vnoff sw counter_0
global counter_1 num_beats prev_mode systole diastole anfisedv anfisesv forcectrl
global Desired_CO Fsys_ctrl
```

```
% call simsizes for a sizes structure, fill it in and convert it to a
% sizes array.
%
% Note that in this example, the values are hard coded.  This is not a
% recommended practice as the characteristics of the block are typically
% defined by the S-function parameters.

%*************************************************************************
%        Initialize variables for ODEs
%*************************************************************************

%FIXED RATE CONDITION
rm = 6;                 %VALVE RESISTANCE FACTOR
w = pi*2;               %Residual beat frequency

%DESIGN PARAMETERS FOR THE VAD (FIXED RATE MODE)
Rht = 0.47;             %VAD RESISTANCE TO MOTION[Ns/cm] Nominal: 0.47
Iht = 0.0038;           %INERTIA OF VAD MEMBRANE[*100kg] Nominal: 0.0038

%CANNULA INERTANCE PARAMETERS
Icnot = 0.0000263;    %INERTIA OF OUTLET CANNULA[Ns^2/cm^5] Nominal: 0.0000263
Icnin = 0.0000132;    %INERTIA OF INLET CANNULA [Ns^2/cm^5] Nominal: 0.0000132

%VALVE RESISTANCE
Rin = 0.0008;           %INLET VALVE RESISTANCE [Ns/cm^5] Nominal: 0.0008
Rot = 0.0008;           %OUTLET VALVE RESISTANCE[Ns/cm^5] Nominal: 0.0008

%AORTA PARAMETERS
Iao = 0.00003401;     %AORTA INERTANCE  [Ns^2/cm^5]

%PERIPHERAL CIRCULATION
Rpe = 0.0125;           %CIRCULATORY RESISTANCE        [Ns/cm^5]   Nominal: 0.0125
Ipe = 0.0275;      %INERTIA OF CIRCULATORY SYSTEM [Ns^2/cm^5] Nominal: 0.0275

%CHARACTERISTIC RESISTANCE AND TUNING PARAMETERS
Rcnot = 0;
Rao = 0.0011;           %Nominal:0.0011====[0.0014,0.0009]
Rcnin = 0;              %nominal:0.0001 But changes the EDV,ESV estimates.

%Compliance Elements
Cat    = 90;              %ARTERIAL COMPLIANCE              [cm^5/N] Nominal: 133 +100;
Cht    = 28;              %Heart COMPLIANCE                 [cm^5/N] Nominal: 28
Cbli   = 32;              %Input Cannula Compliance         [cm^5/N] Nominal: 32
Cblo   = 32;              %Output cannula compliance        [cm^5/N] Nominal: 32
Cvn    = 3500;            %VENOUS COMPIANCE                 [cm^5/N] Nominal: 3500

%Offset of Compliance Elements
atoff    = -4.13;         %Arterial Compliance offset       [N/cm^2] Nominal: -4.13
htoff    = -0.178;        %Heart Compliance offset          [N/cm^2] Nominal: -0.178
icanoff  = -2.62;         %Input Cannula Compliance offset  [N/cm^2] Nominal: -2.62
ocanoff  = -5.24;         %Output Cannula Compliance offset [N/cm^2] Nominal: -5.24
vnoff    = -0.4;          %Venous Compliance offset         [N/cm^2] Nominal: -0.4

%Operation modes
systole =1;
diastole = 0;

%Systolic force during startup (Nominal)
Fsys_ctrl = 41.13;

%Desired Pump output
Desired_CO = 4.7;

%*************************************************************************
%        CONVERSION UNITS
%*************************************************************************
```

```
%CONVERSION OF PRESSURE [N/cm^2] TO [mm Hg].
density_Hg = 0.0135;                    %[kg/cm^3]
Gravity = 9.81;                         %[m/s^2]
N2Hg = 10/(Gravity*density_Hg);         %Conversion factor

%CONVERSION OF FLOW RATE FROM [cm^3/s] TO [L/min].
%Assuming density of Blood is that of water.
Cm2L = 0.06;                            %Conversion factor

%CONVERSION OF POWER FROM [Ncm/s] TO [Watts].
%100cm = 1meter.
cm2m = 1/100;

%1000[cm^3] = 1 [litre]
%     1 [mL] = 1 [cm^3]

%*************************************************************************
%              Initialize varibales for simulation at t=0
%*************************************************************************

sw = 0;
counter_1 = 0;
counter_0 = 0;
num_beats = -1;
prev_mode = systole;

%Size of Values for simulation
sizes = simsizes;

sizes.NumContStates  = 12;
sizes.NumDiscStates  = 0;
sizes.NumOutputs     = 12;
sizes.NumInputs      = 3;
sizes.DirFeedthrough = 1;
sizes.NumSampleTimes = 1;

sys = simsizes(sizes);

% initialize the initial conditions
%x(1)  = Pump Momentum                          0.0     0.0
%x(2)  = VAD Chamber Volume          [cm^3]     46.0    9.1
%x(3)  = Output Canula Volume        [cm^3]     288.7   284.7
%x(4)  = Output Canula Momentum                 0.0     0.0
%x(5)  = Aorta volume                [cm^3]     20.0    24.6
%x(6)  = Aorta momentum                         0.0     0.0
%x(7)  = Arterial Volume             [cm^3]     714     705
%x(8)  = Peripheral Momentum                    2.3     2.2
%x(9)  = Venous Volume               [cm^3]     2493    2463
%x(10) = Input Canula Momentum                  0.0     0.0
%x(11) = Input Canula Volume         [cm^3]     126.9   126.9
%x(12) = Piston postion              [cm]

x0 = [0.0, 9.3, 201.7, 0.0, 24.6, 0.0, 464.9, 2.1, 2273.6, 0.0, 91.8, 0];

%Fuzzy FIS for Pressure-Volume Relationship of Venous Segment
vnpvfis=readfis('Fuzpvvn.fis');
anfisedv=readfis('anfisedv');
anfisesv=readfis('anfisesv');
forcectrl=readfis('hardcntr');

% str is always an empty matrix
str = [];

% initialize the array of sample times
ts  = [0 0];

% end mdlInitializeSizes
```

```
%=============================================================================
% mdlDerivatives
% Return the derivatives for the continuous states.
%=============================================================================

function sys=mdlDerivatives(t,x,u)

global  rm w A Rht Iht Icnot Rcnot Rot Rotm Icnin Rcnin Rin Rinm Iao Rao Ipe Rpe vnpvfis
global  N2Hg

dp_out = heartoff(x(2))-outcanof(x(3));   %PRESS DIFF ACROSS OUTPUT VALVE
dp_in = incanoff(x(11))-heartoff(x(2));   %PRESS DIFF ACROSS INLET VALVE

Rotm = Rot* 10^(rm*((dp_out)<0));         %RESISTANCE OF OUTLET VALVE
Rinm = Rin* 10^(rm*((dp_in)<0));          %RESISTANCE OF INLET VALVE

% CHARATERISTIC EQUATIONS

%Pump momentum (P_2)
sys(1) = -((Rht/Iht)*x(1)) -(A*heartoff(x(2))) + u(1);

%x(2)  = VAD Chamber Volume
sys(2) = ((A/Iht)*x(1)) - (((1/Rinm)+(1/Rotm))*heartoff(x(2)))...
     + ((1/Rotm)*outcanof(x(3))) + ((1/Rinm)*incanoff(x(11)));

%x(3)  = Output Cannula Volume
sys(3) = ((1/Rotm)*heartoff(x(2))) - ((1/Rotm)*outcanof(x(3)))...
     - ((1/Icnot)*x(4));

%x(4)  = Output Cannula Momentum
sys(4) = outcanof(x(3)) - aortapv(x(5)) - ((Rcnot/Icnot)*x(4));

%x(5)  = Aorta volume
sys(5) = ((1/Icnot)*x(4)) - ((1/Iao)*x(6));

%x(6)  = Aorta momentum
sys(6) = -artoff(x(7)) + aortapv(x(5)) - ((Rao/Iao)*x(6)) - (u(2)*cos(w*t));

%x(7)  = Arterial Volume
sys(7) = -((1/Ipe)*x(8)) + ((1/Iao)*x(6));

%x(8)  = Peripheral Momentum
sys(8) = artoff(x(7)) - ((Rpe/Ipe)*x(8)) - fuzpvn(x(9)) - (u(2)*cos(w*t));

%x(9)  = Venous volume
sys(9) = ((1/Ipe)*x(8)) - ((1/Icnin)*x(10)) + u(3);

%x(10) = Input cannula Momentum
sys(10) = fuzpvn(x(9)) - incanoff(x(11)) - ((Rvn(fuzpvn(x(9))*N2Hg)/Icnin)*x(10));

%x(11) = Input Cannula Volume
sys(11) = ((1/Icnin)*x(10)) + ((1/Rinm)*(heartoff(x(2))-incanoff(x(11))));

%x(12) = Piston position
sys(12) = ((1/Iht)*x(1));

% end mdlDerivatives

%=============================================================================
% mdlUpdate
% Handle discrete state updates, sample time hits, and major time step
% requirements.
%=============================================================================

function sys=mdlUpdate(t,x,u)

sys = [];
```

```
% end mdlUpdate

%=============================================================================
% mdlOutputs
% Return the block outputs.
%=============================================================================

function sys=mdlOutputs(t,x,u)

%STATES OF THE MODEL
%x(1)  = Pump momentum            [Ns]
%x(2)  = VAD Chamber Volume       [cm^3]
%x(3)  = Output Cannula Volume    [cm^3]
%x(4)  = Output Cannula Momentum  [Ns/cm^2]
%x(5)  = Aorta volume             [cm^3]
%x(6)  = Aorta momentum           [Ns/cm^3]
%x(7)  = Arterial Volume          [cm^3]
%x(8)  = Peripheral Momentum      [Ns/cm^2]
%x(9)  = Venous volume            [cm^3]
%x(10) = Input cannula Momentum   [Ns/cm^2]
%x(11) = Input Cannula Volume     [cm^3]
%x(12) = Piston position          [cm]

sys = [x(1);x(2);x(3);x(4);x(5);x(6);x(7);x(8);x(9);x(10);x(11);x(12)];

% end mdlOutputs

%=============================================================================
% mdlGetTimeOfNextVarHit
% Return the time of the next hit for this block.  Note that the result is
% absolute time.  Note that this function is only used when you specify a
% variable discrete-time sample time [-2 0] in the sample time array in
% mdlInitializeSizes.
%=============================================================================

function sys=mdlGetTimeOfNextVarHit(t,x,u)

sampleTime = 1;    %  Example, set the next hit to be one second later.
sys = t + sampleTime;

% end mdlGetTimeOfNextVarHit

%=============================================================================
% mdlTerminate
% Perform any end of simulation tasks.
%=============================================================================

function sys=mdlTerminate(t,x,u)

sys = [];

% end mdlTerminate
```

```
%Input vector is:
%x(1) = time
%x(2) = Output cannula pressure
%x(3) = Input cannula pressure
%x(4) = Heart pressure
%x(5) = Aorta pressures
%x(6) = Arterial pressure
%x(7) = Venous pressure
%x(8) = Pressure gradient across output valve
%x(9) = pressure gradient across input valve
%x(10) = Heart piston velocity
%x(11) = Peripheral flow rate
%x(12) = Outlet cannula flow rate
%x(13) = Aorta flow rate
%x(14) = Inlet cannula flow rate
%x(15) = Arterial flow rate
%x(16) = venous flowrate
%x(17) = Heart blood volume
%x(18) = Force on system
%x(19) = previous force on system last time step

%Output
%Fuzzy Systolic force (Fsys_cntrl)

function beat_dat = fxbeat(x)

global sw counter_0 counter_1 num_beats prev_mode systole diastole sys_beat_data
dia_beat_data
global beatdiaend beatstart Sys_force cur_end_dia_vol prev_end_sys_vol anfisedv anfisesv
forcectrl
global Desired_CO Fsys_ctrl

%Finds Switch between diastole to Systole
if (x(18) > 0)              %Beat sorted on Force on heart.
  Sys_force = x(18);

%Using only positive gradient or favourable gradient for flow throught
%the oulet valve.If non-favourable gradient valve is closed (Passive valve)

  if (x(8) > 0)                          %records +tive Delta P across outlet.
    counter_1 = counter_1 + 1;           %array counter.
    sys_beat_data(counter_1,1) = x(1);   %Data Storage for Sys.
    sys_beat_data(counter_1,2) = x(2);   %Outlet cannula pressure
    sys_beat_data(counter_1,3) = x(8);   %Pressure Gradient across outlet valve
    sys_beat_data(counter_1,4) = x(4);   %Heart Pressure
    sys_beat_data(counter_1,5) = x(8);
  end
%confirm Switch between Dia-->Sys.

  if ((prev_mode == diastole))
     if (x(19) > 0)               %Check tolerance
         disp(['Time is Dia --> Sys : ',num2str(x(1))]);
         cur_end_dia_vol = x(17);   %Vol in heart at end Dia.
         prev_mode = systole;       %set flag for next Sys-->Dia.
         beatdiaend = x(1);         %End of Dia time.
     end
  end
end

%Finds switch between systole to diastole
if (x(18) == 0)             %Beat sorted on Force on heart.
  Dia_force = x(18);

%Using only positive gradient or favourable gradient for flow throught
%the oulet valve.If non-favourable gradient valve is closed (Passive valve)

  if (x(9) > 0)             %records +tive Delta P across inlet
    counter_0 = counter_0 + 1;         %array counter.
```

```
    dia_beat_data(counter_0,1) = x(1);     %Data Storage for Dia.
    dia_beat_data(counter_0,2) = x(3);     %Inlet cannula pressure
    dia_beat_data(counter_0,3) = x(9);     %Pressure gradient across inlet valve
    dia_beat_data(counter_0,4) = x(4);     %heart Pressure
    dia_beat_data(counter_0,5) = x(8);
  end
%confirm Switch between Sys-->Dia.

  if ((prev_mode == systole))
     if (x(19) == 0)                  %Check tolerance
        disp(['Time is Sys --> Dia : ',num2str(x(1))]);
        sw = 2;                       %Beat flag found (Sys-->Dia).
        cur_end_sys_vol = x(17);      %Vol in Heart at end of Sys.
        prev_mode = diastole;         %Set flag for next Dia-->Sys.
        beatend = x(1);               %End of beat time.
        num_beats = num_beats + 1;    %beat counter.
        if (num_beats > 0)            %dummy beat due to systole start.
           disp(['BEAT #:',num2str(num_beats)]);
        elseif (num_beats == 0)       %If dummy beat new beatstart & Beat#1.
           beatstart = beatend;
        end
     end
  end
end

%removes the first systole part of the simulation to make a beat
%contain diastole and then followed by systole for a complete beat cycle.

if (sw == 2)&(num_beats == 0)             %For first systolic condition no
  prev_end_sys_vol = cur_end_sys_vol;     %processing of data required.
  sys_beat_data = [];
  dia_beat_data = [];
  counter_0 = 0;
  counter_1 = 0;
  sw = 0;
  disp('   ');
  disp(['Initial systole push phase has been Cut Off']);
  disp(['Begining to count Heart Beats on basis of Filling-->Ejection']);
  disp('   ');

%if two switches are detected then one beat cycle is up Diastole followed by Systole.
%processes the cycle data and outputs it to user.

elseif (sw == 2)

%***********FIND AVERAGE INLET AND OUTLET CANNULA PRESSURE**********
  avg_inlet_press_dia = intavg(dia_beat_data(:,1),dia_beat_data(:,2));
  avg_outlet_press_sys = intavg(sys_beat_data(:,1),sys_beat_data(:,2));
  disp(['Average inlet press during diastole : ',num2str(avg_inlet_press_dia)]);
  disp(['Average outlet press during systole : ',num2str(avg_outlet_press_sys)]);

%*************FIND AVERAGE INLET AND OUTLET VAD PRESSURE************
  avg_VAD_press_dia = intavg(dia_beat_data(:,1),dia_beat_data(:,4));
  avg_VAD_press_sys = intavg(sys_beat_data(:,1),sys_beat_data(:,4));
  disp(['Average VAD press during diastole   : ',num2str(avg_VAD_press_dia)]);
  disp(['Average VAD press during systole    : ',num2str(avg_VAD_press_sys)]);

%*********FIND AVERAGE INLET AND OUTLET CANNULA PRESSURE DIFF********
  avg_inlet_press_diff_dia = intavg(dia_beat_data(:,1),dia_beat_data(:,3));
  avg_outlet_press_diff_sys = intavg(sys_beat_data(:,1),sys_beat_data(:,3));
  disp(['Average inlet press diff @ diastole : ',num2str(avg_inlet_press_diff_dia)]);
  disp(['Average outlet press diff @ systole : ',num2str(avg_outlet_press_diff_sys)]);

%****************FIND SYS/DIA FRACTION AND CYCLE TIME**************
  sys_fraction = beatend - beatdiaend;
  dia_fraction = beatdiaend - beatstart;
  cycle_time = beatend - beatstart;
  disp(['Systole data   : ',num2str(sys_fraction),'s @ ',num2str(Sys_force),' N']);
```

```
  disp(['Diastole data  : ',num2str(dia_fraction),'s @ ',num2str(Dia_force),' N']);
  disp(['Cycle time     : ',num2str(cycle_time),'s']);
  disp('    ');

%***************Volume of blood in VAD after diastole**************
  EDV = cur_end_dia_vol - prev_end_sys_vol;
  disp(['Actual End Diastolic Volume (Per beat): ',num2str(EDV),' ml']);
  EDV_est = evalfis([avg_inlet_press_diff_dia(1,1) round(dia_fraction*10)/10],anfisedv);
  EDV_est = evalfis([avg_inlet_press_diff_dia dia_fraction],anfisedv);
  disp(['Fuzzy estimated End Diastolic Volume   : ',num2str(EDV_est),' ml']);

%***************Volume of blood left in VAD after systole************
  ESV = cur_end_sys_vol - prev_end_sys_vol;  %may need the end dia volume not sys volume.
  stroke_volume = EDV - ESV;
  disp(['Actual End Systolic Volume (/beat)     : ',num2str(ESV),' ml']);
  ESV_est = evalfis([avg_inlet_press_diff_dia(1,1)
avg_outlet_press_diff_sys(1,1)],anfisesv);
  disp(['Fuzzy estimate End Systolic Volume     : ',num2str(ESV_est),' ml']);

%*************************CARDIOVASCULAR OUTPUT*********************
  beats_pm = (60/cycle_time);
  SV_est = EDV_est - ESV_est;
  disp(['Actual Stroke Volume (/beat)           : ',num2str(stroke_volume),' ml']);
  disp(['Fuzzy estimate Stroke Volume (/beat)   : ',num2str(SV_est),' ml']);
  Actual_cardiac_output = (beats_pm*stroke_volume)/1000;
  Fuzzy_cardiac_output = (beats_pm*SV_est)/1000;
  disp(['Actual Cardiac output                  : ',num2str(Actual_cardiac_output),'
L/min']);
  disp(['Fuzzy estimate Cardiac output          : ',num2str(Fuzzy_cardiac_output),'
L/min']);
  disp('    ');

%*****************Relative Error on CO estimate*******************
  CO_error = abs(Actual_cardiac_output - Fuzzy_cardiac_output);
  disp(['CO error : ',num2str(CO_error)]);

%********************Steady state Error on CO***********************

  SSerrCO = abs(Desired_CO - Fuzzy_cardiac_output);
  disp(['Desired CO Error (Find SS): ',num2str(SSerrCO),' L/min']);

%*************************CONTROLLER FORCE OUTPUT******************

  dFsys_ctrl = evalfis([Fuzzy_cardiac_output],forcectrl);
  if (abs(dFsys_ctrl) <= 0.05)
    dFsys_ctrl = 0;
  end
  disp(['Fuzzy Change in Control Force : ',num2str(dFsys_ctrl),' N']);
  Fsys_ctrl = Fsys_ctrl + dFsys_ctrl;
  %set_prev_Fsys = Fsys_ctrl + dFsys_ctrl;
  disp(['Fuzzy Control Force(CO cntrl) : ',num2str(Fsys_ctrl),' N']);

%************************Heart Preformance*************************
  Ej_frac = (stroke_volume/EDV);
  disp(['VAD preformance Ejection frac  : ',num2str(Ej_frac)]);

  disp('    ');
  %prev_avg_outlet_press_sys = avg_outlet_press_sys;
  %prev_avg_VAD_press_sys = avg_VAD_press_sys;
  prev_end_sys_vol = cur_end_sys_vol;
  sys_beat_data = [];
  dia_beat_data = [];
  counter_0 = 0;
  counter_1 = 0;
  sw = 0;
  beatstart = beatend;
end
```

```
%*******************************************************************************
%Revised on 28 march 1998
%To process the parameters in MAT file
%INPUT: data file
%OUTPUT:
%none
%*******************************************************************************
clear
disp('    ')
load PhysisD.mat

t = data(1,:);
disp('    ');

%Info on the data file in workspace.
Data_size = size(data);
Data_pts = Data_size(1,1);
Data_vec = Data_size(1,2);

disp(['Number of Data time pts are = ',num2str(Data_pts)]);
disp(['Data vector is              = ',num2str(Data_vec)]);

%*******************************************************************************
%      Plots to print and Data analysis after Simulation is run
%
%The plots will be created and appended to the graph*.eps file
%After generation  of graphs the data is processed for var ious mean values
%*******************************************************************************

%Heart Parameter Graph
figure(1);
plot(t,data(16,:),'r-',t,data(22,:),'g-',t,data(30,:),'b-');
title('Heart Parameters Graph');
xlabel('Time in secs');
ylabel('Heart Data');grid;
legend('Heart Pressure [mm Hg]','Diaphgram velocity [cm/s]','Force [N]',-1);

%Outlet Cannula Parameters Graphs
figure(2);
plot(t,data(14,:),'r-.',t,data(24,:),'g-');
title('Output Parameters Graph');
xlabel('Time in secs');
ylabel('Data');grid
legend('Outlet Pressure [mm Hg]','Outlet Flowrate [L/min]',-1);

%Aorta Parameter Graph
figure(2);
plot(t,data(17,:),'r-',t,data(25,:),'g-');
title('Aorta Parameters Graph');
xlabel('Time in secs');
ylabel('Data');grid;
legend('Aorta Pressure [mm Hg]','Aorta Flowrate [L/min]',-1);

%Arterial Parameter Graph
figure(3);
plot(t,data(18,:),'r-',t,data(27,:),'g-');
title('Arterial Parameters Graph');
xlabel('Time in secs');
ylabel('Data');grid;
legend('Arterial Pressure [mm Hg]','Arterial Flowrate [L/min]',-1);

%Peripheral Parameter Graph
figure(5);
plot(t,data(23,:),'r-');
title('Peripheral Flow');
xlabel('Time in secs');
ylabel('Data');grid;
legend('Peripheral Flow [L/min]',-1);
```

```
%Venous Parameter Graph
figure(6);
plot(t,data(19,:),'r-',t,data(28,:),'g-');
title('Venous Parameters Graph');
xlabel('Time in secs');
ylabel('Data');grid;
legend('Venous Pressure [mm Hg]','Venous Flowrate [L/min]',-1);

%Inlet Cannula Parameters Graphs
figure(7);
plot(t,data(15,:),'r-',t,data(26,:),'g-');
title('Input Parameters Graph');
xlabel('Time in secs');
ylabel('Data');grid;
legend('Inlet Pressure [mm Hg]','Inlet Flowrate [L/min]',-1);
```

```
%*************************************************************************
%     Controller Preformance (Fuzzy Logic controller)
%*************************************************************************
clear
disp(['****Analyzing Controller Data and plotting****']);

load Fixed_Beat_analysis.mat

sizev = size(Beat_data,1);
disp(['The Size of the data vector is ',num2str(sizev)]);

scale = -5;

%run simulation results into graphics
dof1 = 0:0.1:10;
imf1 = scale*gbellmf(dof1,[2.9 8 1]);
imf2 = scale*gbellmf(dof1,[0.5 3 4]);
imf3 = scale*gbellmf(dof1,[0.4 2.5 4.7]);
imf4 = scale*gbellmf(dof1,[0.5 3 5.4]);
imf5 = scale*gbellmf(dof1,[3.5 6.5 9.4]);

dof2 = -10:0.1:10;
omf1 = scale*zmf(dof2,[-3 1 0 0]);
omf2 = scale*gbellmf(dof2,[1 2 -1]);
omf3 = scale*gbellmf(dof2,[1 2 0]);
omf4 = scale*gbellmf(dof2,[1 2 1]);
omf5 = scale*smf(dof2,[-1 3]);

dof2 = dof2;
dof1 = dof1;

Max_beats = max(Beat_data(:,1));
Min_beats = min(Beat_data(:,1)) + scale;
Max_dFsys = max(Beat_data(:,6))*1;
Min_dFsys = min(Beat_data(:,6))*1;
Max_Fsys = max(Beat_data(:,7))*1.1;
Min_Fsys = min(Beat_data(:,7))*0.95;
Max_CO = max(Beat_data(:,9))*1.1;
Min_CO = min(Beat_data(:,9))*0.8;
Max_Out_Can = max(Beat_data(:,5))*1.1;
Min_Out_Can = min(Beat_data(:,5))*0.9;

error_edv = Beat_data(:,10) - Beat_data(:,11);
error_esv = Beat_data(:,12) - Beat_data(:,13);
error_co = Beat_data(:,8) - Beat_data(:,9);

num = Beat_data(:,10);
dem = (Beat_data(:,10)-Beat_data(:,12));
size(num,1);
size(dem,1);

for i = 1:sizev
ej_frac(i,1) = dem(i,1)/num(i,1);
end

figure(1);
subplot(2,1,1),plot(Beat_data(:,1),Beat_data(:,6),'g-
.',Beat_data(:,1),Beat_data(:,6),'rx');
hold;
plot(omf1,dof2,'r:',omf2,dof2,'y-.',omf3,dof2,'w-',omf4,dof2,'y-.',omf5,dof2,'r:');
title('Delta Fsys');
axis([Min_beats Max_beats Min_dFsys Max_dFsys]);
xlabel('Beat number');
ylabel('Delta Fsys');grid;
%legend('Systolic Flow [L/min]','Press diff Out valve [mm Hg]',-1);

subplot(2,1,2),plot(Beat_data(:,1),Beat_data(:,7),'g-
.',Beat_data(:,1),Beat_data(:,7),'rx');
```

```
axis([Min_beats Max_beats Min_Fsys Max_Fsys]);
title('Total Applied Fsys');
xlabel('Beat number');
ylabel('Fsys on AH');grid;
%legend('Systolic Flow [L/min]','Press diff Out valve [mm Hg]',-1);
print -deps graph10.eps

figure(2);
plot(Beat_data(:,1),Beat_data(:,8),'g-.',Beat_data(:,1),Beat_data(:,9),'y-');
hold;
plot(imf1,dof1,'r:',imf2,dof1,'y-.',imf3,dof1,'w-',imf4,dof1,'y-.',imf5,dof1,'r:');
axis([Min_beats Max_beats Min_CO Max_CO]);
title('Cardiac Output shape form (Pattern)');
xlabel('Beat number');
ylabel('CO [L/min]');grid;
legend('Actual CO [L/min]','Fuzzy CO [L/min]');
print -deps graph11.eps

figure(3);
plot(Beat_data(:,1),Beat_data(:,8),'c+',Beat_data(:,1),Beat_data(:,9),'r*');
hold;
plot(imf1,dof1,'r:',imf2,dof1,'y-.',imf3,dof1,'w-',imf4,dof1,'y-.',imf5,dof1,'r:');
axis([Min_beats Max_beats Min_CO Max_CO]);
title('Cardiac Output for each Beat');
xlabel('Beat number');
ylabel('CO [L/min]');grid;
legend('Actual CO [L/min]','Fuzzy CO [L/min]');
print -deps graph12.eps

figure(4);
plot(Beat_data(:,1),Beat_data(:,5),'g-.');
%axis([Min_beats Max_beats Min_Out_Can Max_Out_Can]);
title('Output Cannula Pressure');
xlabel('Beat number');
ylabel('Pout [mm Hg]');grid;
%legend('Systolic Flow [L/min]','Press diff Out valve [mm Hg]',-1);
print -deps graph13.eps

figure(5);
plot(Beat_data(:,1),Beat_data(:,10),'g-.',Beat_data(:,1),Beat_data(:,11),'y-');
title('End Diastolic Volume');
xlabel('Beat number');
ylabel('EDV [ml]');grid;
legend('Actual EDV [ml]','Est EDV [ml]');
print -deps graph14.eps

figure(6);
plot(Beat_data(:,1),Beat_data(:,12),'g-.',Beat_data(:,1),Beat_data(:,13),'y-');
title('End Systolic Volume ');
xlabel('Beat number');
ylabel('ESV [ml]');grid;
legend('Actual ESV [ml]','Est ESV [ml]');
print -deps graph15.eps

figure(7);
plot(Beat_data(:,1),error_edv,'r-');
title('Difference between Actual and Est EDV');
xlabel('Beat number');
ylabel('Error [ml]');grid;
print -deps graph16.eps

figure(8);
plot(Beat_data(:,1),error_esv,'r-');
title('Difference between Actual and Est ESV');
xlabel('Beat number');
ylabel('Error [ml]');grid;
print -deps graph17.eps
```

```
figure(9);
plot(Beat_data(:,1),error_co,'r-');
title('Difference in CO');
xlabel('Beat number');
ylabel('Error [ml]');grid;
print -deps graph18.eps

figure(10);
plot(Beat_data(:,1),ej_frac(:,1),'r-');
title('Ejection preformance of AH');
xlabel('Beat number');
ylabel('Ejection Fraction');grid;
print -deps graph19.eps

disp(['****Analysis of Control data over****']);
```

```
[System]
Name='HardCntrl'
Type='mamdani'
NumInputs=1
NumOutputs=1
NumRules=5
AndMethod='min'
OrMethod='max'
ImpMethod='min'
AggMethod='max'
DefuzzMethod='centroid'

[Input1]
Name='Cardiac_Output'
Range=[0 9.4]
NumMFs=5
MF1='VLow':'gbellmf',[2.9 8 1]
MF2='MLow':'gbellmf',[0.5 3 4]
MF3='Norm':'gbellmf',[0.4 2.5 4.7]
MF4='MHigh':'gbellmf',[0.5 3 5.4]
MF5='VHigh':'gbellmf',[2.9 8 8.4]

[Output1]
Name='Force'
Range=[-10 10]
NumMFs=5
MF1='Low':'zmf',[-3 1 0 0]
MF2='MLow':'gbellmf',[1 2 -1]
MF3='Norm':'gbellmf',[1 2 0]
MF4='MHigh':'gbellmf',[1 2 1]
MF5='High':'smf',[-1 3]

[Rules]
1, 5 (1) : 1
2, 2 (1) : 1
3, 3 (1) : 1
4, 4 (1) : 1
5, 1 (1) : 1
```

```
[System]
Name='EDV Estimate'
Type='sugeno'
NumInputs=2
NumOutputs=1
NumRules=15
AndMethod='prod'
OrMethod='max'
ImpMethod='prod'
AggMethod='max'
DefuzzMethod='wtaver'

[Input1]
Name='input1'
Range=[5.028 9.692]
NumMFs=5
MF1='in1mf1':'dsigmf',[10.7204123799575 4.44497516361772 10.753478169026 5.793591359606681
MF2='in1mf2':'dsigmf',[10.7149078415644 5.29340156120852 10.7238988852937
6.47795521162185]
MF3='in1mf3':'dsigmf',[10.7244775871072 6.75363696018776 10.7354507752198
7.59457239980095]
MF4='in1mf4':'dsigmf',[10.7307698575443 8.08726670915512 10.7227433976863
9.02996446583085]
MF5='in1mf5':'dsigmf',[10.7237407419064 9.22252468800864 10.7204116905417
10.2750003462932]

[Input2]
Name='input2'
Range=[0.6974 0.7]
NumMFs=3
MF1='in2mf1':'dsigmf',[11538.4615384618 0.696750088684508 11538.4615384618
0.697923367170194]
MF2='in2mf2':'dsigmf',[11538.4615384618 0.697890460726483 11538.4615384613
0.709349309324434]
MF3='in2mf3':'dsigmf',[11538.4615384614 0.706701439531846 11538.4615384622
0.707389599151592]

[Output1]
Name='output'
Range=[52.78 102.7]
NumMFs=15
MF1='out1mf1':'linear',[9.86893779587489 1.24128955449647 1.77988155959838]
MF2='out1mf2':'linear',[9.98440605157702 -24.2968449395736 19.5663132053103]
MF3='out1mf3':'linear',[-2.68877470388354e-028 -3.2733593885328e-029 -4.6760606238298e-
029]
MF4='out1mf4':'linear',[10.0924345484366 1.26665263060021 1.81624919157236]
MF5='out1mf5':'linear',[10.4474332711135 -93.5823011880693 66.0272170674791]
MF6='out1mf6':'linear',[-1.26732402266453e-027 -1.4625867411704e-028 -2.0892996205591Se-
028]
MF7='out1mf7':'linear',[8.84879586232728e-005 1.01918413227191e-005 1.4589965563718e-005]
MF8='out1mf8':'linear',[10.23212126294 -4.48744668107252 5.06115882553467]
MF9='out1mf9':'linear',[-9.44521128618133e-029 -1.00797358478015e-029 -1.4398675063488Ae-
029]
MF10='out1mf10':'linear',[4.74719038870638e-010 -6.4148843986018Se-012 -9.1457249621490Ge-
012]
MF11='out1mf11':'linear',[10.6301104220777 -0.331374845738066 -0.473384680891504]
MF12='out1mf12':'linear',[2.71972824640669e-033 -9.381540804425lle-035 -1.340213544115Ge-
034]
MF13='out1mf13':'linear',[4.3231687915055e-010 -7.442673208158e-011 -1.06323902874761e-
010]
MF14='out1mf14':'linear',[11.0153253151362 -1.89637660811816 -2.7091094400774]
MF15='out1mf15':'linear',[2.88618918707514e-033 -4.96880714330486e-034 -7.0982959188875Be-
034]

[Rules]
1 1, 1 (1) : 1
1 2, 2 (1) : 1
1 3, 3 (1) : 1
```

```
2 1, 4 (1) : 1
2 2, 5 (1) : 1
2 3, 6 (1) : 1
3 1, 7 (1) : 1
3 2, 8 (1) : 1
3 3, 9 (1) : 1
4 1, 10 (1) : 1
4 2, 11 (1) : 1
4 3, 12 (1) : 1
5 1, 13 (1) : 1
5 2, 14 (1) : 1
5 3, 15 (1) : 1
```

```
[System]
Name='ESV Estimate'
Type='sugeno'
NumInputs=2
NumOutputs=1
NumRules=25
AndMethod='prod'
OrMethod='max'
ImpMethod='prod'
AggMethod='max'
DefuzzMethod='wtaver'

[Input1]
Name='input1'
Range=[3.694 12]
NumMFs=5
MF1='in1mf1':'dsigmf',[6.01974477068277 2.65575042364372 6.06588167697261
4.94717344176673]
MF2='in1mf2':'dsigmf',[6.01385512781399 5.21045801440679 6.0263207697667 7.3192410903269
MF3='in1mf3':'dsigmf',[6.01556431530901 6.61175956505242 5.93207246375706
8.78879601409124]
MF4='in1mf4':'dsigmf',[5.97976444190927 8.35101021459536 6.0600420047695
10.7319827661988]
MF5='in1mf5':'dsigmf',[5.88322971449428 10.1968442997019 6.0197465241292 13.1382559994496

[Input2]
Name='input2'
Range=[8.466 28.66]
NumMFs=5
MF1='in2mf1':'dsigmf',[2.47598681720722 5.9417489165314 2.57283986951904 11.1092552875127
MF2='in2mf2':'dsigmf',[2.54023179349031 11.4355761931862 2.52965650624656
16.0952030597586]
MF3='in2mf3':'dsigmf',[2.50397247106774 16.1722324122685 2.48704863935056
21.1834532485284]
MF4='in2mf4':'dsigmf',[2.49691218619921 21.2076940662715 2.49604073079762
25.9313220718792]
MF5='in2mf5':'dsigmf',[2.43234470600307 25.8304828757647 2.47598677479526
31.1842508841033]

[Output1]
Name='output'
Range=[-38.52 27.94]
NumMFs=25
MF1='out1mf1':'linear',[10.2504847268394 -4.59080102375182 3.38135108619101]
MF2='out1mf2':'linear',[12.5962918241749 -4.61315074512367 -7.50735646175191]
MF3='out1mf3':'linear',[-12.6867576506603 -30.3025875563405 -2.46806029840524]
MF4='out1mf4':'linear',[-7.12518362956298e-005 7.86816374111275e-006 -9.8903089637690
006]
MF5='out1mf5':'linear',[-4.37213435101421e-006 -1.24290873628162e-005 -5.1614859383739
007]
MF6='out1mf6':'linear',[10.1812156301908 -4.58480989206612 4.2249450512711]
MF7='out1mf7':'linear',[11.0107941562329 -5.15551924668648 6.33550808168639]
MF8='out1mf8':'linear',[10.7276390218218 -3.68664949219074 -7.008215881396]
MF9='out1mf9':'linear',[-113.928552424904 41.0516229583896 -10.6305565073753]
MF10='out1mf10':'linear',[-8.11044433535312 -23.053896828434 -0.957731102341722]
MF11='out1mf11':'linear',[0.230099848029772 -3.9422784496852 64.6497492116991]
MF12='out1mf12':'linear',[10.8738137693773 -4.8736779429171 2.45517659642618]
MF13='out1mf13':'linear',[18.6097364961149 -5.49280652596518 -47.479533458064]
MF14='out1mf14':'linear',[9.33317898196166 -5.70559131301073 32.0532027313435]
MF15='out1mf15':'linear',[-44.6648353648655 18.1081748658553 -97.8314479629321]
MF16='out1mf16':'linear',[1.16986409176397 2.2306784726271 0.174869864392892]
MF17='out1mf17':'linear',[-10.1322607756243 -14.4936742714462 -1.41585184605577]
MF18='out1mf18':'linear',[19.242364392951 -5.3883827474188 -66.5657437098831]
MF19='out1mf19':'linear',[9.81538838680726 -5.68921692582631 28.9287825675528]
MF20='out1mf20':'linear',[12.410861754904 -5.39070483114989 -2.31820815710918]
MF21='out1mf21':'linear',[2.62982625768954e-005 4.96385428691344e-005 3.94458095278972e-
006]
MF22='out1mf22':'linear',[-0.0212729187974714 -0.0465907220913332 -0.0023804677200397]
```

```
MF23='outlmf23':'linear',[-40.8520521036573 16.2471532663854 8.11108859852543]
MF24='outlmf24':'linear',[11.1352407004239 -6.25454984513026 29.1894184616601]
MF25='outlmf25':'linear',[7.10023890189582 -11.6107782847776 223.890081303787]

[Rules]
1 1, 1 (1) : 1
1 2, 2 (1) : 1
1 3, 3 (1) : 1
1 4, 4 (1) : 1
1 5, 5 (1) : 1
2 1, 6 (1) : 1
2 2, 7 (1) : 1
2 3, 8 (1) : 1
2 4, 9 (1) : 1
2 5, 10 (1) : 1
3 1, 11 (1) : 1
3 2, 12 (1) : 1
3 3, 13 (1) : 1
3 4, 14 (1) : 1
3 5, 15 (1) : 1
4 1, 16 (1) : 1
4 2, 17 (1) : 1
4 3, 18 (1) : 1
4 4, 19 (1) : 1
4 5, 20 (1) : 1
5 1, 21 (1) : 1
5 2, 22 (1) : 1
5 3, 23 (1) : 1
5 4, 24 (1) : 1
5 5, 25 (1) : 1
```

```
clear
%Nominal condition

EDV_N = [7.409  0.7  77.75;7.403  0.7  77.67;7.404  0.7  77.67; ...
   7.404  0.7  77.67;7.404  0.7  77.67;7.404  0.7  77.67; ...
   7.403  0.7  77.66;7.403  0.7  77.65;7.402  0.7  77.65; ...
   7.402  0.7  77.65;7.402  0.7  77.64;7.402  0.7  77.64; ...
   7.401  0.7  77.64;7.401  0.7  77.64];

%Rpe decreased by *0.9
EDV_L09_Rpe = [7.5 0.7 78.61;7.53 0.7 78.92;7.557 0.7 79.2;7.58 0.7 79.44; ...
      7.601 0.7 79.66;7.619 0.7 79.85;7.629 0.7 80.03;7.643 0.7 80.18; ...
      7.656 0.7 80.32;7.668 0.7 80.45;7.679 0.7 80.56;7.689 0.7 80.67; ...
      7.698 0.7 80.76;7.706 0.7 80.85;7.713 0.7 80.92;7.726 0.7 81.06; ...
      7.736 0.7 81.16;7.744 0.7 81.25;7.751 0.7 81.32;7.756 0.7 81.38; ...
      7.761 0.7 81.43;7.764 0.7 81.47;7.767 0.7 81.5;7.77 0.7 81.52; ...
      7.772 0.7 81.55;7.773 0.7 81.56;7.774 0.7 81.58;7.776 0.7 81.59; ...
      7.776 0.7 81.6;7.777 0.7 81.6];

%Rpe decreased by *0.8
EDV_L08_Rpe = [7.597 0.7 79.63;7.661 0.7 80.29;7.719 0.7 80.89;7.769 0.7 81.42; ...
      7.813 0.7 81.88;7.852 0.7 82.3;7.886 0.7 82.67;7.918 0.7 83.01; ...
      7.897 0.7 83.31;7.923 0.7 83.58;7.946 0.7 83.83;7.967 0.7 84.05; ...
      7.987 0.7 84.25;8.004 0.7 84.44;8.019 0.7 84.6;8.033 0.7 84.75; ...
      8.046 0.7 84.88;8.057 0.7 85;8.077 0.7 85.2;8.093 0.7 85.37; ...
      8.106 0.7 85.51;8.116 0.7 85.62;8.125 0.7 85.71;8.132 0.7 85.78; ...
      8.137 0.7 85.84;8.142 0.7 85.89;8.146 0.7 85.93;8.149 0.7 85.96; ...
      8.151 0.7 85.98;8.153 0.7 86;8.155 0.7 86.02;8.156 0.7 86.03];

%Rpe decreased by *0.75
EDV_L075_Rpe = [7.488  0.7  78.52;7.569  0.7  79.28;7.652  0.7  80.17; ...
      7.735  0.7  81.03;7.809  0.7  81.80;7.825  0.7  82.49; ...
      7.883  0.7  83.10;7.934  0.7  83.64;7.980  0.7  84.12; ...
      8.021  0.7  84.56;8.058  0.7  84.95;8.092  0.7  85.30; ...
      8.122  0.7  85.62;8.149  0.7  85.90;8.174  0.7  86.16; ...
      8.196  0.7  86.39;8.216  0.7  86.60;8.234  0.7  86.79; ...
      8.250  0.7  86.96;8.265  0.7  87.12;8.278  0.7  87.25; ...
      8.290  0.7  87.38;8.300  0.7  87.49;8.310  0.7  87.59; ...
      8.319  0.7  87.68;8.327  0.7  87.77;8.334  0.7  87.84; ...
      8.340  0.7  87.91];

%Rpe decreased by *0.7
EDV_L07_Rpe = [7.709 0.7 80.74;7.813 0.7 81.8;7.857 0.7 82.77;7.94 0.7 83.63; ...
      8.012 0.7 84.39;8.076 0.7 85.06;8.133 0.7 85.66;8.184 0.7 86.2; ...
      8.23 0.7 86.68;8.271 0.7 87.12;8.309 0.7 87.51;8.326 0.7 87.87; ...
      8.383 0.7 88.47;8.428 0.7 88.96;8.465 0.7 89.36;8.496 0.7 89.69; ...
      8.52 0.7 89.95;8.54 0.7 90.16;8.556 0.7 90.33;8.569 0.7 90.47; ...
      8.579 0.7 90.59;8.588 0.7 90.68;8.595 0.7 90.75;8.601 0.7 90.81; ...
      8.605 0.7 90.86;8.609 0.7 90.9;8.612 0.7 90.93;8.614 0.7 90.96; ...
      8.616 0.7 90.98];

%Rpe decreased by *0.6
EDV_L06_Rpe = [7.783 0.7  81.95;7.935 0.7  83.48;8.071 0.7  84.88;8.175 0.7  86.12; ...
      8.277 0.7  87.22;8.368 0.7  88.19;8.448 0.7  89.05;8.519 0.7  89.82; ...
      8.583 0.7  90.51;8.641 0.7  91.13;8.693 0.7  91.69;8.74 0.7  92.2; ...
      8.782 0.7  92.65;8.82 0.7  93.06;8.854 0.7  93.42;8.885 0.7  93.75; ...
      8.936 0.7  94.31;8.978 0.7  94.75;9.011 0.7  95.11;9.039 0.7  95.4; ...
      9.06 0.7  95.64;9.078 0.7  95.83;9.092 0.7  95.98;9.103 0.7  96.1; ...
      9.117 0.7  96.24;9.126 0.7  96.34;9.133 0.7  96.42;9.138 0.7  96.47; ...
      9.14 0.7  96.5];

%Rpe decreased by *0.5
EDV_L05_Rpe = [8.11 0.7  85.34;8.291 0.7  87.24;8.45 0.7  88.94;8.589 0.7  90.43; ...
      8.712 0.7  91.76;8.821 0.7  92.93;8.917 0.7  93.97;9.003 0.7  94.89; ...
      9.048 0.7  95.71;9.116 0.7  96.45;9.178 0.7  97.11;9.234 0.7  97.7; ...
      9.284 0.7  98.23;9.329 0.7  98.71;9.369 0.7  99.14;9.405 0.7  99.52; ...
      9.438 0.7  99.87;9.467 0.7  100.2;9.505 0.7  100.7;9.544 0.7  101.1; ...
      9.576 0.7  101.5;9.601 0.7  101.7;9.622 0.7  102;9.638 0.7  102.1; ...
```

```
      9.651 0.7  102.3;9.662 0.7  102.4;9.67 0.7  102.5;9.677 0.7  102.5; ...
      9.682 0.7  102.6;9.687 0.7  102.7;9.69 0.7  102.7;9.692 0.7  102.7];

%Rpe decreased by *1.2
EDV_H12_Rpe = [7.183 0.7 75.48;7.139 0.7 75.01;7.1 0.7 74.6;7.065 0.7 74.23;7.034 0.7
73.9; ...
      7.005 0.7 73.6;6.98 0.7 73.33;6.957 0.7 73.08;6.936 0.7 72.86;6.917 0.7  72.66; ...
      6.899 0.7 72.48;6.884 0.7 72.31;6.869 0.7 72.16;6.857 0.7 72.03;6.845 0.7  71.9; ...
      6.835 0.7 71.79;6.825 0.7 71.69;6.809 0.7 71.52;6.795 0.7 71.38;6.784 0.7  71.26;
...
      6.775 0.7 71.17;6.768 0.7 71.09;6.762 0.7 71.02;6.757 0.7 70.97;6.753 0.7  70.93;
...
      6.75 0.7 70.89;6.747 0.7 70.87;6.745 0.7 70.84;6.743 0.7 70.82;6.741 0.7  70.81; ...
      6.74 0.7 70.79];

%Rpe decreased by *1.4
EDV_H14_Rpe = [6.997 0.7 73.62;6.917 0.7 72.79;6.847 0.7 72.05;6.784 0.7 71.38;6.727 0.7
70.78; ...
      6.676 0.7 70.23;6.629 0.7 69.74;6.587 0.7 69.3;6.549 0.7 68.9;6.515 0.7 68.53; ...
      6.484 0.7 68.2;6.455 0.7 67.9;6.43 0.7 67.63;6.407 0.7 67.39;6.367 0.7 66.97; ...
      6.334 0.7 66.62;6.307 0.7 66.34;6.285 0.7 66.1;6.267 0.7 65.91;6.252 0.7 65.76; ...
      6.24 0.7 65.63;6.23 0.7 65.52;6.222 0.7 65.44;6.215 0.7 65.37;6.21 0.7 65.31; ...
      6.205 0.7 65.26;6.202 0.7 65.22;6.199 0.7 65.19;6.196 0.7 65.17;6.195 0.7 65.15];

%Rpe decreased by *1.6
EDV_H16_Rpe = [6.96 0.7 73.3;6.837 0.7 72.03;6.729 0.7 70.9;6.633 0.7 69.88;6.548 0.7
68.98; ...
      6.47 0.7 68.16;6.4 0.7 67.42;6.337 0.7 66.75;6.279 0.7 66.14;6.227 0.7 65.59; ...
      6.179 0.7 65.09;6.143 0.7 64.63;6.104 0.7 64.23;6.069 0.7 63.86;6.036 0.7 63.52; ...
      6.007 0.7 63.21;5.981 0.7 62.94;5.935 0.7 62.46;5.898 0.7 62.07;5.867 0.7 61.75; ...
      5.842 0.7 61.48;5.842 0.7 61.26;5.825 0.7 61.08;5.811 0.7 60.94;5.799 0.7 60.81; ...
      5.79 0.7 60.71;5.782 0.7 60.63;5.776 0.7 60.56;5.77 0.7 60.51;5.766 0.7 60.46; ...
      5.762 0.7 60.43;5.761 0.7 60.41];

%Rpe decreased by *1.8
EDV_H18_Rpe = [6.849 0.7 72.21;6.7 0.7 70.66;6.568 0.7 69.28;6.451 0.7  68.04;6.346 0.7
66.93; ...
      6.251 0.7 65.93;6.172 0.7 65.02;6.093 0.7 64.19;6.021 0.7  63.45;5.957 0.7 62.77;
...
      5.898 0.6999 62.16;5.866 0.6999 61.6;5.818 0.6999 61.09;5.775 0.6999 60.63; ...
      5.735 0.6999 60.22;5.699 0.6999 59.84;5.667 0.6999 59.49;5.611 0.6999 58.9; ...
      5.564 0.6999 58.41;5.526 0.6999 58.01;5.484 0.6974 57.38;5.466 0.6999 57.37; ...
      5.445 0.6999 57.15;5.428 0.6999 56.97;5.414 0.6999 56.82;5.403 0.6999 56.7; ...
      5.393 0.6999 56.6;5.385 0.6999 56.52;5.379 0.6999 56.45;5.373 0.6999 56.39; ...
      5.369 0.6999 56.34;5.367 0.6999 56.32];

%Rpe decreased by *2
EDV_H2_Rpe = [6.948 0.7  73.24;6.752 0.7  71.25;6.579 0.6999  69.46;6.428 0.6999  67.86;
...
      6.3 0.6999  66.44;6.178 0.6999  65.16;6.067 0.6999  64;5.967 0.6998  62.95; ...
      5.897 0.6998  62;5.815 0.6998  61.13;5.663 0.6974  59.26;5.608 0.6998  58.94; ...
      5.552 0.6998  58.35;5.502 0.6998  57.82;5.456 0.6998  57.33;5.415 0.6998  56.89; ...
      5.377 0.6998  56.49;5.343 0.6998  56.13;5.292 0.6998  55.5;5.242 0.6998  54.98; ...
      5.201 0.6998  54.56;5.167 0.6998  54.2;5.138 0.6998  53.91;5.093 0.6998  53.44; ...
      5.077 0.6998  53.29;5.065 0.6998  53.16;5.055 0.6998  53.05;5.046 0.6998  52.96; ...
      5.039 0.6998  52.89;5.033 0.6998  52.83;5.028 0.6998  52.78];

%From EDV_H2_Rpe unusal data from simulation
%4.283 0.6992  53.76;5.086 0.6993  60.42;


% setup training and checking matrix (variable is "data").
data_EDV = [EDV_N;EDV_L09_Rpe;EDV_L08_Rpe;EDV_L075_Rpe;EDV_L07_Rpe;EDV_L06_Rpe; ...
      EDV_L05_Rpe;EDV_H12_Rpe;EDV_H14_Rpe;EDV_H16_Rpe;EDV_H18_Rpe; ...
         EDV_H2_Rpe];

data_size = size(data_EDV);
disp(['The size of the EDV data is : ',num2str(data_size)]);
```

```
%Nominal condition

ESV_N = [7.404 17.05 0.07174;7.404 17.06 0.02372;7.404 17.07 0.01448;7.404 17.06 0.01798;
...
   7.402 17.06 0.008337;7.402 17.06 0.006813;7.401 17.06 0.003037;7.401 17.06 0.0009999;
...
   7.401 17.06 0.0005455;7.401 17.06 0.0004931];

%Rpe decreased by *0.9
ESV_L09_Rpe = [7.53 17.83 -3.177;7.58 17.83 -2.624;7.619 17.79 -2.083; ...
      7.643 17.77 -1.679;7.668 17.76 -1.368;7.689 17.76 -1.116;7.706 17.75 -0.9108; ...
      7.72 17.74 -0.7427;7.736 17.74 -0.5468;7.747 17.73 -0.4027;7.756 17.73 -0.2965; ...
      7.761 17.73 -0.2418;7.764 17.72 -0.1971;7.768 17.72 -0.1452;7.771 17.72 -0.1184; ...
      7.773 17.72 -0.08716;7.774 17.72 -0.07107;7.776 17.72 -0.04725;7.777 17.72 -
0.03853];

%Rpe decreased by *0.8
ESV_L08_Rpe = [7.661 18.8 -6.798;7.719 18.81 -6.281;7.769 18.79 -5.644; ...
      7.813 18.76 -5.026;7.852 18.73 -4.478;7.886 18.7 -4.005;7.918 18.69 -3.597; ...
      7.897 18.68 -3.238;7.923 18.66 -2.919;7.946 18.66 -2.633;7.967 18.65 -2.375; ...
      7.987 18.64 -2.142;8.004 18.63 -1.932;8.033 18.62 -1.571;8.068 18.61 -1.151; ...
      8.085 18.6 -0.936;8.1 18.6 -0.7609;8.111 18.59 -0.6186;8.121 18.59 -0.5029; ...
      8.128 18.58 -0.4088;8.135 18.58 -0.3323;8.14 18.58 -0.2702;8.144 18.58 -0.2196; ...
      8.147 18.58 -0.1785;8.151 18.57 -0.1309;8.154 18.57 -0.09593;8.156 18.57 -0.07031];

%Rpe decreased by *0.7
ESV_L07_Rpe = [7.813 19.82 -10.91;7.857 19.85 -10.12;7.94 19.82 -9.109; ...
      8.076 19.71 -7.205;8.184 19.64 -5.754;8.271 19.59 -4.652;8.326 19.56 -3.776; ...
      8.383 19.54 -3.065;8.428 19.52 -2.486;8.465 19.5 -2.016;8.496 19.49 -1.635; ...
      8.52 19.47 -1.326;8.556 19.46 -0.872;8.574 19.45 -0.6368;8.592 19.44 -0.4188; ...
      8.601 19.44 -0.3059;8.609 19.43 -0.2012;8.614 19.43 -0.1323;8.616 19.43 -0.1073];

%Rpe decreased by *0.6
ESV_L06_Rpe = [7.935 21.1 -15.6;8.071 21.17 -14.56;8.175 21.13 -13.14; ...
      8.277 21.05 -11.7;8.368 20.97 -10.38;8.448 20.91 -9.233;8.519 20.86 -8.244; ...
      8.641 20.79 -6.633;8.74 20.74 -5.366;8.782 20.72 -4.828;8.854 20.69 -3.904; ...
      8.912 20.66 -3.146;8.958 20.65 -2.535;8.996 20.63 -2.043;9.026 20.61 -1.647; ...
      9.05 20.6 -1.328;9.07 20.59 -1.07;9.085 20.59 -0.8626;9.098 20.58 -0.6954; ...
      9.108 20.57 -0.5605;9.117 20.57 -0.4518;9.123 20.57 -0.3642;9.131 20.56 -0.2636; ...
      9.136 20.56 -0.1908;9.14 20.56 -0.1381];

%Rpe decreased by *0.5
ESV_L05_Rpe = [8.291 22.73 -19.73;8.589 22.59 -15.94;8.821 22.39 -12.53; ...
      8.917 22.32 -11.13;9.003 22.26 -9.921;9.048 22.21 -8.871;9.116 22.17 -7.947; ...
      9.178 22.14 -7.126;9.234 22.11 -6.392;9.284 22.09 -5.733;9.329 22.06 -5.141; ...
      9.369 22.04 -4.61;9.405 22.02 -4.133;9.438 22.01 -3.706;9.467 21.99 -3.322; ...
      9.493 21.98 -2.978;9.505 21.97 -2.669;9.526 21.95 -2.391;9.544 21.94 -2.143; ...
      9.576 21.93 -1.72;9.589 21.92 -1.541;9.612 21.91 -1.238;9.63 21.9 -0.9937; ...
      9.645 21.89 -0.7978;9.657 21.88 -0.6406;9.666 21.88 -0.5143;9.674 21.88 -0.4129; ...
      9.68 21.87 -0.3316;9.685 21.87 -0.2662;9.689 21.87 -0.2137;9.692 21.87 -0.1716];

%Rpe decreased by *0.4
ESV_L04_Rpe = [8.552 24.19 -25.82;8.762 24.18 -23.53;8.916 24.12 -20.98; ...
      9.077 23.97 -18.55;9.219 23.83 -16.39;9.334 23.72 -14.5;9.445 23.63 -12.88; ...
      9.545 23.56 -11.47;9.633 23.5 -10.24;9.713 23.45 -9.152;9.784 23.41 -8.186; ...
      9.847 23.37 -7.323;9.904 23.34 -6.551;9.955 23.31 -5.859;10 23.28 -5.24; ...
      10.08 23.23 -4.189;10.14 23.2 -3.349;10.19 23.17 -2.677;10.23 23.14 -2.14; ...
      10.26 23.12 -1.711;10.28 23.11 -1.368;10.3 23.1 -1.093;10.32 23.09 -0.874; ...
      10.33 23.08 -0.6987;10.34 23.07 -0.5586;10.35 23.07 -0.4466;10.36 23.07 -0.357; ...
      10.36 23.06 -0.2854;10.37 23.06 -0.2281];

%Rpe decreased by *0.3
ESV_L03_Rpe = [9.081 26.05 -30.28;9.319 25.93 -27.1; ...
      9.528 25.75 -23.98;9.71 25.77 -21.14;9.871 25.62 -18.64;10.01 25.49 -16.48; ...
      10.14 25.39 -14.62;10.25 25.31 -12.99;10.35 25.24 -11.57;10.44 25.19 -10.31; ...
      10.52 25.14 -9.201;10.59 25.09 -8.208;10.66 25.05 -7.323;10.71 25.02 -6.532; ...
      10.81 24.95 -5.196;10.88 24.91 -4.132;10.94 24.87 -3.286;10.99 24.84 -2.613; ...
      11.03 24.81 -2.077;11.06 24.79 -1.652;11.09 24.78 -1.314;11.1 24.76 -1.045; ...
```

```
      11.12 24.76 -0.8307;11.13 24.75 -0.6605;11.14 24.74 -0.5253;11.15 24.74 -0.4177; ...
      11.16 24.73 -0.3322;11.16 24.73 -0.2641];

%Rpe decreased by *0.2
ESV_L02_Rpe = [9.494 28.66 -38.52;9.8 28.55 -34.7; ...
      10.07 28.28 -30.79;10.3 28.06 -27.13;10.51 27.91 -23.86;10.69 27.73 -21; ...
      10.85 27.57 -18.52;10.99 27.44 -16.37;11.11 27.34 -14.5;11.22 27.25 -12.86; ...
      11.32 27.17 -11.42;11.41 27.11 -10.15;11.48 27.05 -9.019;11.48 27 -8.013; ...
      11.59 26.91 -6.323;11.69 26.84 -4.988;11.76 26.79 -3.934;11.82 26.74 -3.102; ...
      11.86 26.71 -2.447;11.9 26.68 -1.93;11.93 26.66 -1.522;11.95 26.64 -1.201; ...
      11.97 26.63 -0.947;11.98 26.62 -0.7469;11.99 26.62 -0.6634;12 26.61 -0.5232; ...
      12 26.6 -0.4127;11.99 26.6 -0.3255;11.99 26.6 -0.2568];
%above 0.2:8.769 27.95 -42.91;9.147 28.47 -41.59;

%Rpe decreased by *1.2
ESV_H12_Rpe = [7.233 15.51 5.707;7.183 15.47 5.395;7.139 15.48 4.915;7.1 15.5 4.42;7.065
15.52 3.967; ...
      7.034 15.53 3.57;7.005 15.54 3.222;6.98 15.55 2.913;6.957 15.56 2.637;6.936 15.57
2.388; ...
      6.899 15.58 1.957;6.884 15.58 1.772;6.857 15.59 1.452;6.835 15.6 1.19;6.817 15.61
0.9753; ...
      6.802 15.61 0.7992;6.79 15.61 0.6549;6.784 15.62 0.5929;6.775 15.62 0.4859;6.768
15.62 0.3982; ...
      6.762 15.62 0.3263;6.757 15.63 0.2674;6.753 15.63 0.2191;6.75 15.63 0.1796;6.747
15.63 0.1472; ...
      6.745 15.63 0.1206;6.743 15.63 0.09882;6.741 15.63 0.07331;6.74 15.63 0.06637];

%Rpe decreased by *1.4
ESV_H14_Rpe = [7.087 14.24 10.33;6.997 14.17 9.724;6.917 14.18 8.847;6.847 14.22
7.963;6.784 14.25 7.164; ...
      6.727 14.28 6.463;6.676 14.3 5.844;6.629 14.31 5.285;6.549 14.34 4.334;6.484 14.36
3.553; ...
      6.43 14.37 2.913;6.407 14.38 2.638;6.386 14.39 2.388;6.367 14.39 2.162;6.349 14.4
1.958; ...
      6.334 14.4 1.773;6.32 14.41 1.605;6.307 14.41 1.453;6.295 14.41 1.316;6.285 14.42
1.191; ...
      6.267 14.42 0.9767;6.252 14.43 0.8007;6.24 14.43 0.6564;6.23 14.43 0.5381;6.222
14.44 0.4411; ...
      6.215 14.44 0.3616;6.21 14.44 0.2965;6.205 14.44 0.243;6.202 14.44 0.1992;6.197
14.44 0.1479; ...
      6.195 14.45 0.1212];

%Rpe decreased by *1.6
ESV_H16_Rpe = [6.96 13.25 14.15;6.837 13.17 13.26;6.729 13.19 12.06;6.633 13.24
10.86;6.548 13.27 9.782; ...
      6.47 13.3 8.833;6.4 13.32 7.993;6.337 13.34 7.24;6.279 13.36 6.562;6.227 13.37
5.948; ...
      6.179 13.38 5.391;6.143 13.39 4.887;6.104 13.4 4.432;6.069 13.41 4.019;6.036 13.42
3.644; ...
      6.007 13.43 3.304;5.981 13.44 2.996;5.957 13.44 2.717;5.935 13.45 2.463;5.898 13.46
2.026; ...
      5.867 13.47 1.666;5.842 13.47 1.37;5.842 13.48 1.127;5.825 13.48 0.9264;5.811 13.49
0.7616; ...
      5.799 13.49 0.6261;5.79 13.49 0.5147;5.782 13.5 0.4231;5.776 13.5 0.3478;5.77 13.5
0.2859; ...
      5.766 13.5 0.2351;5.762 13.5 0.1932;5.761 13.5 0.1752];

%Rpe decreased by *1.8
ESV_H18_Rpe = [6.7 12.27 16.22;6.568 12.3 14.73;6.451 12.35 13.28;6.346 12.39 11.99; ...
      6.251 12.42 10.84;6.172 12.45 9.828;6.093 12.47 8.916;6.021 12.49 8.091;5.957 12.51
7.343; ...
      5.898 12.52 6.665;5.866 12.54 6.048;5.818 12.55 5.488;5.775 12.56 4.979;5.735 12.57
4.518; ...
      5.667 12.59 3.72;5.611 12.6 3.062;5.564 12.62 2.521;5.526 12.63 2.076;5.484 12.65
1.367; ...
      5.466 12.64 1.379;5.445 12.65 1.132;5.428 12.65 0.9302;5.414 12.66 0.7656;5.403
12.66 0.6304; ...
      5.393 12.66 0.519;5.385 12.66 0.4273;5.379 12.67 0.3518;5.373 12.67 0.2896;5.369
```

```
12.67 0.2384; ...
      5.367 12.67 0.2164];

%Rpe decreased by *2
ESV_H2_Rpe = [6.579 11.63 18.68;6.428 11.65 16.97;6.3 11.7 15.34;6.178 11.74 13.88; ...
      6.067 11.77 12.58;5.967 11.8 11.41;5.897 11.82 10.36;5.815 11.84 9.408; ...
      5.663 11.87 7.399;5.608 11.89 7.017;5.552 11.9 6.366;5.502 11.91 5.778;5.456 11.93
5.245; ...
      5.415 11.94 4.762;5.377 11.94 4.324;5.343 11.92 3.926;5.292 11.93 3.237;5.242 11.95
2.668; ...
      5.201 11.96 2.2;5.167 11.96 1.814;5.138 11.97 1.495;5.093 11.98 0.9849; ...
      5.077 11.98 0.8087;5.065 11.99 0.6649;5.055 11.99 0.548;5.046 11.99 0.4518;5.039
11.99 0.3725; ...
      5.033 11.99 0.3071;5.028 11.99 0.2532];

%Rpe decreased by *2.2
ESV_H22_Rpe = [6.474 10.92 20.79;6.312 10.94 18.91;6.161 10.99 17.13;6.046 11.03 15.52;
...
      5.804 11.08 12.4;5.707 11.11 11.59;5.615 11.13 10.52;5.531 11.15 9.554; ...
      5.456 11.17 8.679;5.387 11.18 7.885;5.333 11.2 7.164;5.275 11.21 6.508;5.222 11.22
5.913; ...
      5.174 11.23 5.372;5.13 11.24 4.881;5.09 11.25 4.434;5.021 11.26 3.66;4.973 11.27
2.646; ...
      4.946 11.29 2.471;4.909 11.29 2.038;4.878 11.3 1.684;4.852 11.31 1.391;4.831 11.31
1.15; ...
      4.8 11.31 0.5612;4.796 11.32 0.759;4.79 11.32 0.6233;4.78 11.32 0.515;4.769 11.33
0.387; ...
      4.741 11.32 -0.101];

%Rpe decreased by *2.4
ESV_H24_Rpe = [6.384 10.28 22.6;6.208 10.3 20.59;6.042 10.35 18.68; ...
      5.915 10.39 16.95;5.78 10.42 15.39;5.658 10.45 13.98;5.547 10.47 12.71;5.446 10.49
11.55; ...
      5.354 10.51 10.5;5.282 10.66 10.29;5.203 10.54 8.323;5.126 10.56 7.869;5.062 10.58
7.141; ...
      4.983 10.6 5.901;4.893 10.62 4.883;4.818 10.64 4.04;4.761 10.65 3.343;4.71 10.66
2.766; ...
      4.646 10.66 1.901;4.63 10.68 1.871;4.602 10.68 1.543;4.578 10.69 1.277;4.558 10.69
1.057; ...
      4.542 10.7 0.8745;4.534 10.69 0.3278;4.515 10.7 0.5774;4.507 10.7 0.4732;4.499 10.7
0.3916; ...
      4.493 10.71 0.3242];
%above 2.4:6.827 10.84 24.73;

%Rpe decreased by *2.6
ESV_H26_Rpe = [6.31 9.737 24.17;6.112 9.749 22.05;5.957 9.791 20.04; ...
      5.798 9.832 18.2;5.654 9.867 16.54;5.523 9.897 15.04;5.403 9.923 13.68;5.295 9.946
12.44; ...
      5.203 9.939 11.31;5.111 9.957 10.29;5.027 9.974 9.358;4.951 9.989 8.51;4.912 10
7.744; ...
      4.85 10.01 7.047;4.794 10.03 6.412;4.701 10.05 5.31;4.619 10.06 4.397;4.552 10.08
3.641; ...
      4.496 10.09 3.015;4.453 10.22 3.152;4.409 10.1 2.05;4.378 10.11 1.689;4.352 10.12
1.398; ...
      4.331 10.12 1.157;4.313 10.12 0.9584;4.298 10.13 0.7937;4.286 10.13 0.6572;4.276
10.13 0.5443; ...
      4.267 10.13 0.4507;4.261 10.13 0.3732];
%above 2.6:6.774 10.31 26.62;

%Rpe decreased by *2.8
ESV_H28_Rpe = [6.236 9.302 25.56;6.028 9.309 23.35;5.863 9.345 21.24; ...
      5.694 9.381 19.31;5.541 9.413 17.56;5.401 9.441 15.97;5.284 9.466 14.53;5.165 9.488
13.22; ...
      5.057 9.508 12.03;4.959 9.526 10.94;4.901 9.543 9.962;4.821 9.558 9.07;4.749 9.571
8.257; ...
      4.688 9.584 7.517;4.627 9.595 6.844;4.573 9.606 6.23;4.477 9.624 5.164;4.398 9.639
4.28; ...
      4.332 9.651 3.548;4.278 9.661 2.941;4.233 9.67 2.437;4.196 9.677 2.02;4.165 9.683
```

```
1.674; ...
      4.139 9.688 1.388;4.118 9.692 1.15;4.108 9.693 1.047;4.092 9.696 0.8681;4.079 9.699
0.7195; ...
      4.068 9.701 0.5964;4.059 9.703 0.4943;4.051 9.704 0.4097];

%Rpe decreased by *3
ESV_H3_Rpe = [6.17 8.861 26.81;5.973 8.862 24.52;5.777 8.893 22.32; ...
      5.6 8.928 20.31;5.439 8.959 18.48;5.302 8.986 16.81;5.164 9.011 15.3;5.039 9.033
13.93; ...
      4.956 9.053 12.68;4.854 9.071 11.54;4.762 9.088 10.51;4.683 9.103 9.574;4.606 9.117
8.719; ...
      4.536 9.129 7.94;4.472 9.141 7.231;4.414 9.151 6.586;4.313 9.169 5.462;4.23 9.184
4.53; ...
      4.16 9.197 3.757;4.103 9.207 3.116;4.055 9.215 2.585;4.015 9.222 2.144;3.982 9.228
1.778; ...
      3.955 9.233 1.475;3.932 9.237 1.223;3.914 9.241 1.014;3.898 9.243 0.8413;3.885 9.246
0.6978; ...
      3.874 9.248 0.5788;3.866 9.249 0.48];

%Rpe decreased by *3.2
ESV_H32_Rpe = [6.11 8.475 27.94;5.905 8.466 25.57;5.7 8.496 23.3; ...
      5.515 8.531 21.21;5.346 8.563 19.31;5.2 8.592 17.57;5.056 8.619 16;4.956 8.643
14.57; ...
      4.839 8.664 13.27;4.733 8.684 12.09;4.641 8.702 11.01;4.553 8.718 10.03;4.472 8.733
9.139; ...
      4.399 8.746 8.325;4.332 8.759 7.584;4.271 8.77 6.909;4.165 8.789 5.733;4.077 8.806
4.758; ...
      4.004 8.819 3.949;3.943 8.83 3.277;3.893 8.84 2.719;3.851 8.847 2.257;3.817 8.854
1.873; ...
      3.788 8.859 1.554;3.764 8.863 1.29;3.744 8.867 1.07;3.728 8.87 0.8883;3.714 8.873
0.7372; ...
      3.703 8.875 0.6118;3.694 8.876 0.5077];

% setup training and checking matrix (variable is "data").
data_ESV = [ESV_N;ESV_L09_Rpe;ESV_L08_Rpe;ESV_L07_Rpe;ESV_L06_Rpe;ESV_L05_Rpe;ESV_L04_Rpe;
...
      ESV_L03_Rpe;ESV_L02_Rpe;ESV_H12_Rpe;ESV_H14_Rpe;ESV_H16_Rpe;ESV_H18_Rpe;ESV_H2_Rpe;
...
         ESV_H22_Rpe;ESV_H24_Rpe;ESV_H26_Rpe;ESV_H28_Rpe;ESV_H3_Rpe;ESV_H32_Rpe];

data_size = size(data_ESV);
disp(['The size of the ESV data is : ',num2str(data_size)]);

gph_ESV
```

```
%*******************************************************************************
%Revised on 20 march 1998
%Train a FIS for estimating the EDV based on the change
%in pressure across the inlet valve and based on the diastole duration.
%*******************************************************************************

%training data generated from I/O model
%Training Data Stored in : trndata
%Checking Data Stored in : chkdata

%reads in the data pts for training the fuzzy estimator
%the data are held in workspace variable "data"

dat_EDV

%Divides the data into training pts and checking pts
%All pts are "training"
%even pts are used also for "checking"

numpts = length(data_EDV);
trndata = data_EDV(1:1:numpts,:);
chkdata = data_EDV(2:2:numpts,:);

%Initial membership functions for inputs to be trained.

nummfs = [5 3];
mftype = str2mat('dsigmf','dsigmf');
fismat = genfis1(trndata,nummfs,mftype);

%Input 1: "delta pressure across the inlet valve"

[x1,mf1] = plotmf(fismat,'input',1);
figure(5);
plot(x1,mf1);
xlabel('Degree of Membership');
ylabel('Difference In pressure across input valve [mm Hg]');
title('Initial membership for Pressure Differnece across Inlet');
print -dps Iinledv.eps

%Input 2: "Diastole timing" set at ~0.7 sec

[x2,mf2] = plotmf(fismat,'input',2);
figure(6);
plot(x2,mf2);
xlabel('Degree of Membership');
ylabel('Diastolic time [sec]');
title('Initial membership for Diastole timing (0.7s)');
print -dps Iin2edv.eps

%number of batch times to train the data samples.

numepochs = 100;         %nominal: 100
[fismat1,trnerr,ss,fismat2,chkerr]=anfis(trndata,fismat,numepochs,NaN,chkdata);

%Training results

trnout = evalfis([trndata(:,1) trndata(:,2)],fismat1);
trnRMSE = norm(trnout -trndata(:,3))/sqrt(length(trnout));

disp(['***Generating Plots for training Routine***']);

%Ploting error curves
epoch = 1:numepochs;
figure(7);
plot(epoch,trnerr,'o',epoch,chkerr,'x'); hold on;
plot(epoch,[trnerr,chkerr]); hold off;
title('Training Error');
xlabel('Epoch number');
```

```
ylabel('Error');
legend('Training error','Checking error');
print -dps erredv.eps

[x1,mf1] = plotmf(fismat1,'input',1);
figure(8);
plot(x1,mf1);
xlabel('Degree of Membership');
ylabel('Difference In pressure across input valve [mm Hg]');
title('Final membership for Change in press');
print -dps Finledv.eps

[x2,mf2] = plotmf(fismat1,'input',2);
figure(9);
plot(x2,mf2);
xlabel('Degree of Membership');
ylabel('Diastolic time [sec]');
title('Final membership for Diastole timing');
print -dps Fin2edv.eps

anfis_y = evalfis([trndata(:,1) trndata(:,2)],fismat1);

figure(10);
gensurf(fismat1);
xlabel('Press across inlet [mm Hg]');
ylabel('Diastole Time [sec]');
zlabel('End Diastolic Volume [ml]');
title('Fuzzy Surface plot after Training');
print -dps SPedv.eps
```

```
%*************************************************************************
%Revised on 20 march 1998
%Train a FIS for estimating the ESV based on the change
%in pressure across the outlet valve.
%*************************************************************************

%training data generated from I/O model
%Training Data Stored in : trndata
%Checking Data Stored in : chkdata

%reads in the data pts for training the fuzzy estimator
%the data are held in workspace variable "data"
dat_ESV

%Divides the data into training pts and checking pts
%odd pts are "training"
%even pts are "checking"
numpts = length(data_ESV);
trndata = data_ESV(1:1:numpts,:);
chkdata = data_ESV(2:2:numpts,:);

%Initial membership functions to be trained.
nummfs = [5 5];       %[5 5] = 0.14 error
mftype = str2mat('dsigmf','dsigmf');
fismat = genfis1(trndata,nummfs,mftype);

%Input 1: "delta pressure across the outlet valve"
[x1,mf1] = plotmf(fismat,'input',1);
figure(5);
plot(x1,mf1);
title('Intial membership for dP across inlet');
print -dps Iinlesv.eps

%Input 2: "Systole timing" set at ~~0.7 sec
[x2,mf2] = plotmf(fismat,'input',2);
figure(6);
plot(x2,mf2);
title('Intial membership for dP across outlet');
print -dps Iin2esv.eps

%number of batch time to train the data samples.
numepochs = 100;      %nominal=100
[fismat1,trnerr,ss,fismat2,chkerr]=anfis(trndata,fismat,numepochs,NaN,chkdata);

%Training results
trnout = evalfis([trndata(:,1) trndata(:,2)],fismat1);
trnRMSE = norm(trnout -trndata(:,3))/sqrt(length(trnout));

%Ploting error curves
epoch = 1:numepochs;
figure(7);
plot(epoch,trnerr,'o',epoch,chkerr,'x')
hold on;
plot(epoch,[trnerr,chkerr]);
hold off;
print -dps erresv.eps

[x1,mf1] = plotmf(fismat1,'input',1);
figure(8);
plot(x1,mf1);
title('Final membership for dP across inlet');
print -dps Finlesv.eps

[x2,mf2] = plotmf(fismat1,'input',2);
figure(9);
plot(x2,mf2);
title('Final membership for dP across outlet');
print -dps Fin2esv.eps
```

```
anfis_y = evalfis([trndata(:,1) trndata(:,2)],fismat1);

figure(10);
gensurf(fismat1);
xlabel('Pressure across inlet valve [mm Hg]');
ylabel('Pressure across outlet valve [mm Hg]');
zlabel('End Systolic Volume [ml]');
title('Input/Output Surface plot Trained');
print -dps SPesv.eps
```

# IMAGE EVALUATION
# TEST TARGET (QA-3)

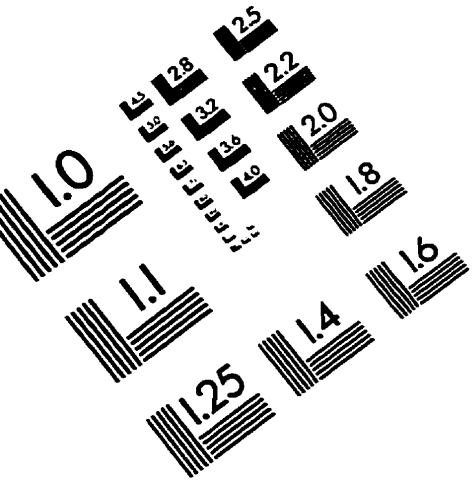


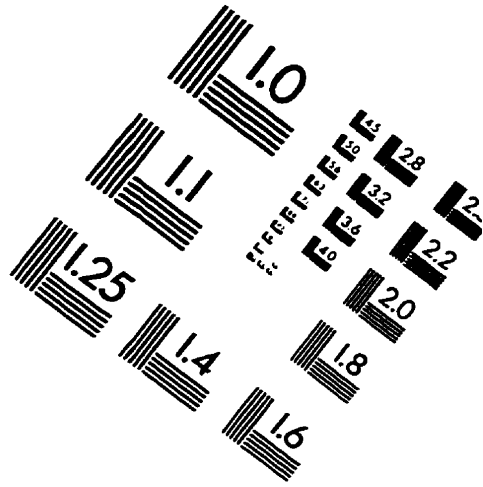


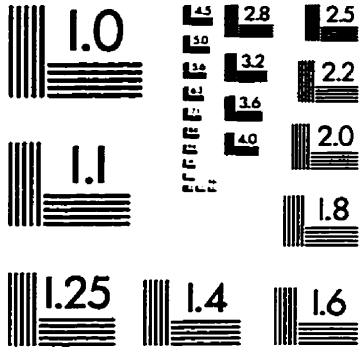


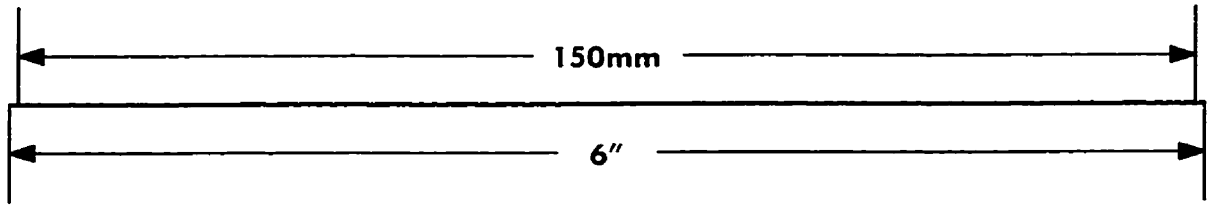


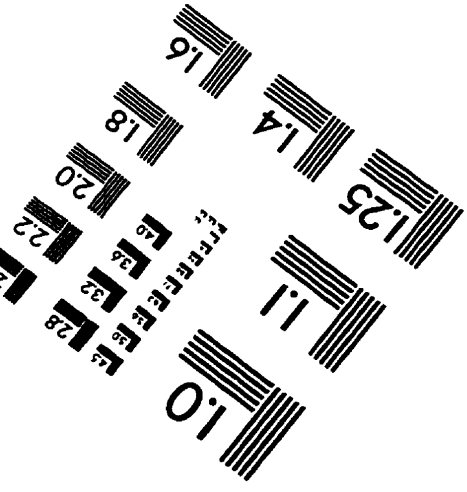


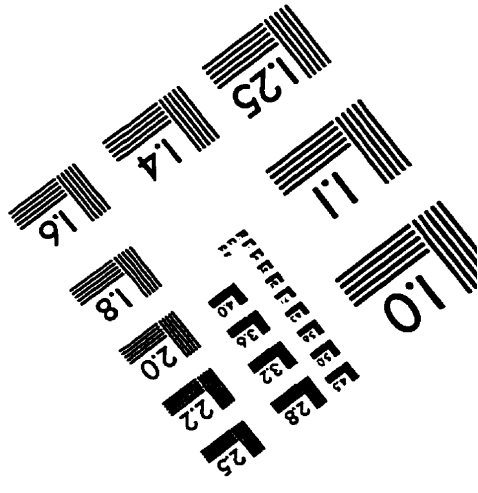


APPLIED IMAGE, Inc
1653 East Main Street
Rochester, NY 14609 USA
Phone: 716/482-0300
Fax: 716/288-5989